NON CHIRAL BOSONIZATION OF A LUTTINGER LIQUID

A thesis
submitted for the degree of
Doctor of Philosophy

Joy Prakash Das

Under the guidance of
Prof. Girish. S. Setlur

Department of Physics
Indian Institute of Technology Guwahati
Guwahati 781 039, Assam, India

NON CHIRAL BOSONIZATION OF A LUTTINGER LIQUID

A thesis
submitted for the degree of
Doctor of Philosophy

Joy Prakash Das
Roll No. 146121021

Under the guidance of
Prof. Girish. S. Setlur

Department of Physics
Indian Institute of Technology Guwahati
Guwahati 781 039, Assam, India

January 2019

In matters of science, a thousand proclamations by so-called experts are outweighed by the humble reasoning of a single individual.

- Galileo Galilei

Dedicated to my family

Declaration

The work in this thesis entitled "Non chiral bosonization of a Luttinger liquid" has been carried out by me under the supervision of Prof. Girish S. Setlur, Department of Physics, Indian Institute of Technology Guwahati. No part of this thesis has been submitted elsewhere for award of any other degree or qualification. The research works have been carried out in the period from January, 2015 to December, 2018.

In keeping with general practice of reporting scientific observations, due acknowledgments have been made wherever the work described is based on the findings of other investigations.

Place: IIT Guwahati
Date:

Joy Prakash Das
Roll No. 146121021

भारतीय प्रौद्योगिकी संस्थान गुवाहाटी
Indian Institute of Technology Guwahati

Certificate

This is to certify that the research work contained in this thesis entitled "Non chiral bosonization of a Luttinger liquid" by Mr. Joy Prakash Das, a PhD student of the Department of Physics, IIT Guwahati was carried out under my supervision. This work is original and has not been submitted elsewhere for award of any degree.

Place: IIT Guwahati
Date:

Prof. Girish S. Setlur
Department of Physics,
IIT Guwahati.
Email: gsetlur@iitg.ac.in

भारतीय प्रौद्योगिकी संस्थान गुवाहाटी
Indian Institute of Technology Guwahati

Acknowledgements

I will forever be grateful to my supervisor Prof. Girish S. Setlur for introducing me to this challenging yet interesting field of research. His intelligent ideas and constant guidance have always helped me in moving forward with my thesis work. I have always admired his courage to challenge the conventional notion of a subject which has prevailed for a long time among a huge number of popular figures. If I am sent four years back in time to the day of choosing a supervisor, I will again approach him with the better version of me - more sincere and more hardworking.

I extend my sincere gratitude to my doctoral committee members - Prof. P. Poulose, Prof. Amarendra Sarma and Dr. P.A.S. Sree Krishna for reviewing my progress every year and sharing their invaluable comments, suggestions and feedback that have enabled me to improve and present my work in the shape that it is today.

I would like to express my heartfelt thanks to all the faculties of the Physics department of IIT Guwahati for building my foundation of Physics when I was an undergraduate student in the same institute, which has tremendously influenced me to build a career in Physics. I would also like to thank all the staff members of the department for their support, co-operation and friendly behavior. My special thanks to the H.O.D's of the Physics department Prof. Basu, Prof. Poulose and Prof. Ghosh for all the facilities in the department and the timely meetings with the research scholars, addressing their concerns.

I would like to thank my friends of IIT Guwahati from the bottom of my heart, especially the 2014 batch. I am grateful to the Art of living and the Hare Krishna Movement for teaching me yoga and imparting me spiritual knowledge that have helped in transcending the good and not so good times of my Ph.D. life.

I am also highly grateful to Dr. Uma Dutta of Cotton University for her moral support and words of encouragement. I am also thankful to my seniors Dr. Enamullah, Dr. Vipin Kumar, Dr. Upendra Kumar for their supportive and helping nature. It was a lovely group of us.

My deepest gratitude to my mother for shaping me for life and taking a lot of pains for my career. I have always felt the blessings of my father from the unseen world. I am thankful to all the members of my family for constant moral support and help. No amount of acknowledgment will ever be enough to do justice to the kind of support, love and encouragement I have received from my family and this thesis is dedicated to them.

I thank all the people who have been in direct or indirect association with me for my research work and have helped me in even the slightest possible manner.

Above all I thank the Divine for everything - just everything.

भारतीय प्रौद्योगिकी संस्थान गुवाहाटी
Indian Institute of Technology Guwahati

Abstract

In this work, the powerful Non-chiral bosonization technique (NCBT) is introduced, which is a non-trivial modification of the standard Fermi-Bose correspondence in one spatial dimension made in order to facilitate the study of strongly inhomogeneous Luttinger liquids (LL) where the properties of free fermions plus the source of inhomogeneities are reproduced exactly. The formalism is applied to obtain the correlation functions of translationally non-invariant systems like LL with a cluster of impurities (barriers/wells) around an origin, a one step fermionic ladder, slowly moving impurities in a Luttinger liquid, etc. The obtained correlation functions are used to study various physical phenomena like Friedel oscillations, resonant tunneling, dynamical density of states, conductance, mobility (in case of mobile impurities) and so on. The results are validated using the Schwinger Dyson equation and perturbative methods. The present method is superior to the conventional bosonization methods (g-ology methods) which requires additional tools like re-normalization, etc. to deal with impurities.

भारतीय प्रौद्योगिकी संस्थान गुवाहाटी
Indian Institute of Technology Guwahati

Contents

List of Figures

List of Tables

Chapter 1

Introduction

The subject matter of many body physics revolves around the study of mutual interactions between the constituent particles of a given system. The study of interactions provides insights into various physical phenomena going on in the real life systems, which otherwise can't be explained using the non-interacting theory. The best way to quantify the study of interactions is to compute the correlation functions of the mutually interacting particles of a given system in the thermodynamic limit. An analytical approach for achieving this goal is often formidable as interactions make the exact solutions impractical or rather impossible. Hence various approximations are adopted so that the mathematics becomes doable keeping the physics substantially intact. When it comes to fermionic systems, the well established Fermi liquid theory is used to successfully deal with interactions, e.g. in metallic systems at sufficiently low temperatures. But this theory breaks down for systems where the motion of electrons is restricted to one dimension. In fact, the physics of one dimensional systems is drastically but wonderfully different from that of the higher dimensions. This has led to an increasing interest among the theoretical physicists in the one dimensional world. It is true that one dimensional systems are taken as examples to illustrate some fundamental concepts like a harmonic oscillator and particle in a box as one can get a deeper insight into the physics involved using relatively easier mathematics. But those are all for a single particle system. When it comes to many particle systems with mutual interaction between the particles, 1D systems are no more the easier versions of the higher dimensional systems, but are rather a distinct class of systems altogether. On the other hand, with the advent of nano-fabrication techniques, physical realizations of such 1D systems has been made possible such as carbon nano-tubes, semi-conducting quantum wire, cold atoms, etc. which hold a promising future in terms of technology due to their fantastic properties. Hence 1D systems are no more mere toys for theorists to play with. They indeed are a class of systems whose properties need to be understood better and the present work is an attempt to do the same.

The study of strongly correlated electrons in one dimension has fascinated condensed matter physicists since the middle of the last century. Due to the breakdown of the Fermi liquid

theory in such systems, an alternative was proposed which was developed in the pioneering works of Tomonaga [1], Luttinger [2], Mattis and Lieb [3] and many more and finally given a proper shape by Duncan Haldane [4] who coined the term 'Luttinger liquid' in analogy with 'Fermi liquid'. The Luttinger liquid (LL) model is based on the linearization of the energy momentum dispersion relation near the Fermi level so that the Hamiltonian can be exactly solvable. The objective is to calculate the N-point Green functions of the given fermionic system. Once these are obtained, one can use them to study a plethora of physical phenomena going on in such systems.

The N-point particle (hole) Green function is the quantum overlap between two states of a system where each state has N particles added (removed) at various locations and times. An analytical study (as against a numerical one) of mutually interacting quantum particles is beset with intimidate technical difficulties and various approximation techniques are used to mitigate these problems. The obvious method that springs to mind is to expand in powers of the interaction potential between the quantum particles. In one dimension, each term in this perturbation series carried out in momentum space, diverges logarithmically at low momenta (known as infra-red divergences). Moreover calculating the series up to a certain order of the interaction potential and neglecting the higher order will be a controlled approximation only when the interaction term is much smaller in magnitude then the rest of the terms in the Hamiltonian (kinetic and potential energy terms). But this is not necessarily the case for strongly correlated systems. Hence a "non-perturbative" method is called for where a fermion field operator is expressed as a function of bosonic fields and hence called 'bosonization'. For translationally invariant systems, this method is well established (see e.g. Giamarchi [5]). However the introduction of an impurity into the otherwise homogeneous system makes this formalism, also known as 'g-ology' insufficient and one has to depend on renormalization and/or numerical techniques for the computation of the correlation functions. In this work, an alternative has been proposed which is able to provide closed formulas for Green functions of translationally non-invariant systems without adhering to renormalization and other techniques. We call this technique as 'Non chiral bosonization technique' or NCBT and it is discussed elaborately in the second chapter. The present chapter is a general introduction to this fascinating field of one dimensional physics and the theoretical tools employed for such systems leading to the necessity of NCBT.

1.1 One dimensional systems

It has been known from Moore's law [6] that the number of components in an integrated chip doubles about every two years, which has led to the pursuit of finer and finer materials and finally leading to the realization of systems which has one or more dimensions of the order of the electron wavelength. One important category of such systems are 1D systems or nano-wires. From the theoretical point of view, this reduced dimensionality offers interesting

Physics leading to some unique properties of the 1D systems. Novel theoretical tools and techniques have been developed to understand these 1D systems, since the second half of the last century. Physical realization also started appearing towards the end of the last century which triggered the theorists to dig deeper into the physics of such wonderful systems.

1.1.1 Failure of the Fermi Liquid theory

The effect of interactions in high-dimensional (2D and 3D) fermionic systems is explained by Landau's Fermi liquid theory [7] which has been the centerpiece of our understanding of interacting Fermi systems. Let us consider a system of electrons without mutual interactions. In such a case, if an electron has to move to a different position, it can do it without any obstruction. But if mutual interactions are introduced, then the movement of an electron will be affected by the density of other electrons around its position. Now let us consider electrons dressed with the density fluctuation around them and call these individual objects as quasiparticles. The interactions preserve the total particle number, spin and momentum. Moreover, the addition of density fluctuations around an electron are not going to affect the fermion commutation rules. Hence the excitations which are made up of electron and density fluctuations are also fermions with the same charge, spin and momentum. But certain other quantities like mass, magnetic moment, etc. are renormalized to new values. In higher dimensions, these quasiparticles can move more or less freely (see figure 1.1 (a)). This is the essence of the Fermi liquid theory that the properties of the interacting fermions remain essentially similar to those of free fermionic particles. This is however a very superficial explanation of the theory and the actual situation is much more complicated. There exists residual interactions between the quasiparticles. However, it will serve the purpose of understanding why this theory breaks down in one dimension.

(a) (b)

FIGURE 1.1: (a) Quasiparticles in 2D and 3D systems which can move nearly freely. (b) Quasiparticles in 1D which can move only collectively.

The above scenario gets completely changed in one dimension. In this case, if a quasiparticle has to move, it has to push all the quasiparticles in front of it (figure 1.1 (b)) and thus any individual movement is prohibited. This collectivization of excitations is the key difference between one-dimensional and higher dimensional systems. Due to such collectivization, Fermi

liquid theory does not work in one dimensional systems [5]. For fermions with spin, this scenario is worse. Since only collective excitations can exist, a single fermionic excitation has to split itself into a collective excitation carrying charge and another collective excitation carrying spin. These excitations has to travel with different velocities and thus an electron has to break into two elementary excitations namely holon (carrying charge) and spinon (carrying spin). This phenomenon is called spin-charge separation and is a signature of 1D systems. These properties are very different from those of the quasiparticles in the Fermi liquid theory.

The other alternative is to adopt a perturbative approach and expand the correlation functions in powers of the interaction potential between the quantum particles. But in one dimension, each term in this perturbation series carried out in momentum space, diverges logarithmically at low momenta (known as infra-red divergences). Hence perturbative approach is also not suitable to deal with interactions in such systems. Hence a non-perturbative technique is called for which expresses a fermionic Hamiltonian in terms of bosonic operators to deal with interactions in such systems.

1.1.2 Tomonaga model

Because of the failure of the Fermi liquid theory and the perturbative approach to deal with the interactions prevailing in 1D systems, it was a challenging task at hand to solve the Hamiltonian of such 1D correlated systems. Way back in the 1950's Nobel laureate S. Tomonaga suggested some approximations so that the Hamiltonian might be solvable [8].

The one dimensional fermionic Hamiltonian in presence of mutual interactions is not exactly solvable. Consider the excitations in 1D fermionic systems. The basic approximation of this model is that the particle hole excitations in such systems, consisting of two particle states, are approximated as bosons based on the assertion that the wave-function of the two fermion states has bosonic properties. This approximation is however criticized in the present work as the the particle-hole excitations of the Fermi system that make the kinetic energy of the Hamiltonian diagonal in these operators are not bosons even 'approximately' [9]. The following Hamiltonian was considered in this model.

$$H = v_F \sum_{k,s} |k| a^\dagger_{k,s} a_{k,s} + \frac{1}{2L} \sum_k V_k \ \rho(k)\rho(-k) \tag{1.1}$$

where

$$\rho(k) = \sum_{p,s} a^\dagger_{p-\frac{k}{2},s} a_{p+\frac{k}{2},s}$$

where L is the length of the system and v_F is the Fermi velocity. The other important assumption, as can be seen from the Hamiltonian, is the linear dispersion relation where energy $\sim |k|\ v_F$. The label s $(= \pm 1)$ denotes spin, $\rho(k)$ denotes the density operator and V_k represents the mutual interactions between the particles. The basic step in the Tomonaga

model was the division of the density operator into two parts.

$$\rho(k) = \rho_1(k) + \rho_2(k)$$

where

$$\rho_1(k) = \sum_{p>0,s} a^\dagger_{p-\frac{k}{2},s} a_{p+\frac{k}{2},s}$$
$$\rho_2(k) = \sum_{p<0,s} a^\dagger_{p-\frac{k}{2},s} a_{p+\frac{k}{2},s}$$

The full density operator $\rho(k)$ commutes with other density operators $\rho(k')$ but the parts ρ_1 and ρ_2 do not commute with the same parts for different wave vectors. For an important special case of $k' = -k$, the commutation relations for $k < 2k_F$ come out to be the following.

$$\begin{aligned} [\rho_1(k), \rho_1(-k)] &= \left(\frac{kL}{\pi}\right) \\ [\rho_2(k), \rho_2(-k)] &= -\left(\frac{kL}{\pi}\right) \\ [\rho_1(k), \rho_2(-k)] &= 0 \end{aligned} \tag{1.2}$$

The central approximation of this model is that these density operators obey the exact commutation relations given as follows.

$$\begin{aligned} [\rho_1(k), \rho_1(-k')] &= \delta_{k,k'}\left(\frac{kL}{\pi}\right) \\ [\rho_2(k), \rho_2(-k')] &= -\delta_{k,k'}\left(\frac{kL}{\pi}\right) \\ [\rho_1(k), \rho_2(-k')] &= 0 \end{aligned} \tag{1.3}$$

Although the above relations are not exact, the expectation values of these commutators are given exactly, which makes the approximation reasonable. Now the density operators $\rho_1(\pm k)$ and $\rho_2(\pm k)$ can be expressed in terms of bosonic creation and annihilation operators such that the commutation relations in equation (1.3) are obeyed. For positive k, they are as follows.

$$\begin{aligned} \rho_1(k) &= b_k\sqrt{\frac{kL}{\pi}} \;\; ; \;\; \rho_1(-k) = b^\dagger_k\sqrt{\frac{kL}{\pi}} \\ \rho_2(k) &= b^\dagger_{-k}\sqrt{\frac{kL}{\pi}} \;\; ; \;\; \rho_2(-k) = b_{-k}\sqrt{\frac{kL}{\pi}} \end{aligned} \tag{1.4}$$

where $[b_k, b^\dagger_{k'}] = \delta_{k,k'}$. Hence the interaction term in the Hamiltonian given in equation (1.1) can now be written in terms of these boson operators as follows.

$$\frac{1}{2L}\sum_k V_k\ \rho(k)\rho(-k) = \sum_k \bar{V}_k(b_k + b^\dagger_{-k})(b^\dagger_k + b_{-k}) \tag{1.5}$$

where $\bar{V}_k = \frac{|k|V_k}{2\pi}$. Hence the electron electron interaction terms has been represented in terms of bosonic excitations of the electron gas. The kinetic energy term is also expressed in terms of boson operators so that the necessary commutation relations are preserved approximately.

$$H_0 = v_F \sum_{k,s} |k| a^\dagger_{k,s} a_{k,s} \approx \sum_k \omega_k b^\dagger_k b_k \tag{1.6}$$

where $\omega_k = kv_F$. Hence the Hamiltonian tooks the following form.

$$H = \sum_k \left(\omega_k b^\dagger_k b_k + \bar{V}_k(b_k + b^\dagger_{-k})(b^\dagger_k + b_{-k})\right) \tag{1.7}$$

Thus the Hamiltonian which was quartic in the fermion basic becomes a quadratic one in the boson basic and is exactly solvable. This is the basic idea of the Tomonaga model which was a breakthrough in the subject of 1D interacting systems.

1.1.3 Luttinger model

A decade later after Tomonaga has proposed his model, Luttinger revived interest in the subject and proposed his alternative model in 1963. His model is similar to the Tomonaga model in some of its essential properties. However it has the advantage of being exactly solvable using lesser number of approximations as compared to the Tomonaga model. The major difference lies in the basic feature of the Luttinger model, viz. the system has two types of fermions - right movers (having an energy spectrum given by $\epsilon_k = kv_F$) and left movers (having an energy spectrum given by $\epsilon_k = -kv_F$). They are shown in figure 1.2 (a) by the solid and dashed lines. On the other hand, in the Tomonaga model, the same kind of particle is represented throughout the band of states. In the Luttinger model, the occupied energy states stretches to negative infinity and hence there is an infinite number of each kind of particles.

Designating the fermionic operator as $a_{i,k,s}$ where $i = 1$ for $\epsilon_k = kv_F$ and $i = 2$ for $\epsilon_k = -kv_F$, k and s are the same as those in the Tomonaga model. The two bands are quite independent which results in the fermion operators to anti-commute.

$$\{a_{i,k,s}, a^\dagger_{j,k',s'}\} = \delta_{i,j}\delta_{k,k'}\delta_{s,s'} \tag{1.8}$$

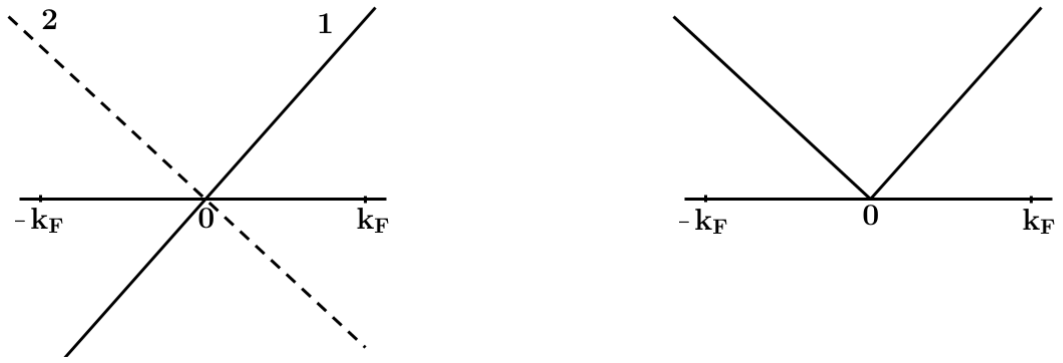

(a) (b)

FIGURE 1.2: (a) Luttinger liquid model having two distinct particles with separate energy bands. (b) Tomonaga model having one particle whose energy band is $v_F|k|$.

The density and spin operators are defined as in the Tomonaga model as follows.

$$\rho_i(p) = \sum_{k,s} a^\dagger_{i,k+p,s} a_{i,k,s}$$
$$\rho_i(-p) = \sum_{k,s} a^\dagger_{i,k,s} a_{i,k+p,s}$$

$$\sigma_i(p) = \sum_{k,s} s a^\dagger_{i,k+p,s} a_{i,k,s}$$
$$\sigma_i(-p) = \sum_{k,s} s a^\dagger_{i,k,s} a_{i,k+p,s}$$

Hence

$$\rho_i(-p) = \rho_i^\dagger(p) \ ; \ \sigma_i(-p) = \sigma_i^\dagger(p)$$

The Luttinger model has the same kind of commutation relations as the Tomonaga model given in equation (1.3) but now they are valid for all values of p (unlike $p < 2k_F$ in the earlier model).

$$\begin{aligned} [\rho_1(-p), \rho_1(p')] &= \delta_{p,p'} \left(\frac{pL}{\pi}\right) \\ [\rho_2(p), \rho_2(-p')] &= \delta_{k,k'} \left(\frac{pL}{\pi}\right) \\ [\rho_1(p), \rho_2(p')] &= 0 \end{aligned} \tag{1.9}$$

$$
\begin{aligned}
[\sigma_1(-p), \sigma_1(p')] &= \delta_{p,p'} \left(\frac{pL}{\pi}\right) \\
[\sigma_2(-p), \sigma_2(p')] &= -\delta_{p,p'} \left(\frac{pL}{\pi}\right) \\
[\sigma_1(p), \sigma_2(p')] &= 0
\end{aligned} \tag{1.10}
$$

$$
[\sigma_i(p), \rho_j(p')] = 0 \tag{1.11}
$$

But these commutation relations are valid under the assumption that there is an infinite number of negative energy particles. The kinetic energy term of the Luttinger model in terms of the fermion operators is as follows.

$$
H_0 = v_F \sum_{k,s} k(a^\dagger_{1,k,s} a_{1,k,s} - a^\dagger_{2,k,s} a_{2,k,s}) \tag{1.12}
$$

This Hamiltonian has the following commutation relations with the density and spin operators ($p > 0$).

$$
\begin{aligned}
[H_0, \rho_1(p)] &= v_F p \rho_1(p) \; ; \quad [H_0, \rho_2(p)] = -v_F p \rho_2(p) \\
[H_0, \sigma_1(p)] &= v_F p \sigma_1(p) \; ; \quad [H_0, \sigma_2(p)] = -v_F p \sigma_2(p)
\end{aligned}
$$

Using these, the kinetic energy term can be exactly represented by the operators as follows.

$$
H_0 = \frac{\pi v_F}{L} \sum_{p>0} [\rho_1(p)\rho_1(-p) + \rho_2(-p)\rho_2(p) + \sigma_1(p)\sigma_1(-p) + \sigma_2(-p)\sigma_2(p)] \tag{1.13}
$$

The major advancement of the Luttinger model is that the restriction that the boson approximation applies only for excitations with small k is removed. The transformation to the bosonic representation is however similar to the Tomonaga model.

$$
\begin{aligned}
\rho_1(-p) &= b_{1p} \sqrt{\frac{pL}{\pi}} \; ; \quad \rho_1(p) = b^\dagger_{1p} \sqrt{\frac{pL}{\pi}} \\
\rho_2(-p) &= b^\dagger_{2,-p} \sqrt{\frac{pL}{\pi}} \; ; \; \rho_2(p) = b_{2,-p} \sqrt{\frac{pL}{\pi}}
\end{aligned} \tag{1.14}
$$

$$
\begin{aligned}
\sigma_1(-p) &= c_{1p} \sqrt{\frac{pL}{\pi}} \; ; \quad \sigma_1(p) = c^\dagger_{1p} \sqrt{\frac{pL}{\pi}} \\
\sigma_2(-p) &= c^\dagger_{2,-p} \sqrt{\frac{pL}{\pi}} \; ; \; \sigma_2(p) = c_{2,-p} \sqrt{\frac{pL}{\pi}}
\end{aligned} \tag{1.15}
$$

The Hamiltonian (kinetic energy term) finally becomes the following.

$$
H_0 = \sum_{p>0} p v_F (b^\dagger_{1,p} b_{1,p} + b^\dagger_{2,-p} b_{2,-p} + c^\dagger_{1,p} c_{1,p} + c^\dagger_{2,-p} c_{2,-p}) \tag{1.16}
$$

The density operator $\rho_1(p)$ $(p > 0)$ represents a particle getting annihilated with momentum k and created with momentum $k + p$. This operation leads to the generation of an electron hole pair when $k < k_F$ and $k + p > k_F$. The bosonic operator $b^\dagger_{1p}$ represents the summation over all such electron hole pairs. On the other hand $\rho_2(p)$ $(p > 0)$ takes a particle from the occupied state $k + p > k_F$ (where k is negative) to the unoccupied state $k < -k_F$. The bosonic operator $b^\dagger_{2,-p}$ represents the summation over all such electron hole pairs.

Interaction terms, which are expressed as the product of four fermion operators or two density operators, are dealt similar to the earlier model by using this bosonic representation and thus converting the Hamiltonian from from quartic to quadrtic. Although the Luttinger model has the advantage of being exactly solvable, it has the disadvantage of being unphysical since it contains an infinite number of negative energy particles.

Mattis and Lieb [3] took the first step towards a correct solution of this model of interacting 1D fermions proposed by Luttinger [2]. This was followed by the contributions from Schotte and Schotte [10], Luther and Peschel [11], Heidenreich [12], Haldane [4] and many more and finally nurtured to maturity by Haldane [4, 13].

1.1.4 Physical realizations

One dimensional systems started gaining interests among the researchers because of its unique properties which are drastically different from those of higher dimensional systems. From the theoretical point of view, it was definitely an interesting problem to solve the 1D interacting Hamiltonian by transforming it from the fermionic basis to a bosonic one. But it did not remain merely of theoretical interest for long. With the advent of nano-fabrication techniques, physical realizations of one dimensional systems were made possible. In the recent decades, we have witnessed an explosion in the realization of real 1D systems.

Ishii et al. [14] have shown that at low temperatures single walled carbon nanotubes shows Tomonaga-Luttinger liquid behavior. Auslaender et al. [15] measured the collective excitation spectrum of interaction electrons in 1D by controlling the energy and momentum of electrons tunneling between two closely spaced, parallel quantum wires thereby measuring the conductance. Besides there are other examples of physical realizations of isolated one dimensional systems like Josephson junction arrays [16], edge states in quantum hall systems [17] and ultra cold atoms in 1D [18]. Besides with the progress of material science, it has been possible to realize bulk materials with 1D structures inside. The prominent examples in this regard are organic super-conductors [19] and spin ladder sytems [20]. The Luttinger liquid model plays a crucial role in the study of these systems.

Hence 1D systems are no more mere toys for the theoreticians to play with. They hold a promising future in terms of technology and it is of extreme importance to understand the

underlying physics of these systems and an attempt to do the same has been done in the present work.

1.2 Bosonization

In the previous section, we have seen how transforming a Hamiltonian from the fermion basis to a bosonic one makes it exactly solvable. This is because of the fact that the interaction term, which is quartic in terms of fermionic operators, becomes quadratic when expressed in terms of bosonic operators and is trivial to diagonalize. Bosonization refers to the process of expressing a fermion operator in terms of bosonic operators. Over the years, it has become the most prevalent method to tackle strongly correlated electrons in 1D systems. In this section we provide a detailed history of the subject of 1D many body physics in general and bosonization in particular. This will be followed by a brief description of the formalism of standard bosonization.

1.2.1 History of bosonization

The idea of Bosonization was comprehended somewhere around the later part of the 20th century by particle physicists Sidney Coleman and Stanley Mandelstam and also independently by the condensed matter physicists Daniel Mattis and Alan Luther. Coleman has drawn a parallel between the massive Thirring model and the Sine Gordon theory by showing that the fermion Green's function has an independent description in terms of bosonic variables [21]. On the other hand, authors like Luther and Mandelstam took another step in this regard by remarking that the Fermi field operator itself can be expressed in terms of bosonic variables. The subject line of bosonization started somewhere along these lines.

The present work aims to apply bosonization techniques to deal with different types of one dimensional systems with interacting fermions, or better called as the 'Luttinger liquid'. The subject has a long history of wide variety of work done and it is of utmost importance to have a note of the related work done so that one can appreciate the importance and novelty of the current research.

Before 1990

One dimensional systems grabbed a lot of attention in the second half of the last century owing to its peculiar properties. As early as 1950, S. Tomonaga was able to show that an assembly of Fermi particles in one dimension can be described by a quantized field of sound waves in the Fermi gas, where the sound waves obey Bose statistics [1]. Later in 1963, essential achievements to this model was reflected in the work of Luttinger [2] and a couple

of years later, Mattis and Lieb provided an exact solution to this model [3]. A few years later, Schotte and Schotte [10] first introduced a bosonic representation of a fermion field at a single point ($\psi_\eta(x=0) \sim e^{-i\phi_\eta(x=0)}$) to calculate x-ray transition rates. In the year 1974, this bosonic representation was extended from a single point to arbitrary x ($\psi_\eta(x) \sim e^{-i\phi_\eta(x)}$) simultaneously by Mattis [22] and by Luther and Peschel [11]. A year later, Heidenreich et al. [12] made this description complete by introducing the number-lowering Klein factors. However, the explicit construction of the Klein factors in terms of bare fermionic operators was described by Haldane in the year 1979 [13].

On the other hand, there were others like Dzyaloshinskii and Larkin [23] who tackled the problem directly in the fermionic representation, which is considered a remarkable calculation in dealing with the divergences of the perturbative approach. Similarly, there were other works in the 70's carried out by Anderson, Zawadowski and Solyom. [24, 25] who tackled the problem in the fermionic representation and used renormalization group methods to extract the main singularities from the perturbation theory and sum them. These approaches are much more difficult as compared to bosonization, which is the easier alternative to do the same.

Efetov and Larkin in the year 1975 [26] found the correlation functions of a 1D Fermi gas with an infinitely strong attraction and showed that acoustic excitations make the major contribution to the formation of the singularities of these correlation functions. On the other hand, in the year 1979, the classical reviews by Emery [27] and Solyom [28] discussed the use of renormalization group (RG) to treat the singularities that occurs when treating the 1D interaction problem perturbatively. Finally in the year 1981, Haldane laid the foundation of modern bosonization in his famous work [4] where the term 'Luttinger liquid' was coined. Erik and Herman in 1987 studied the bosonization of chiral fermion theories on arbitrary compact Riemann surfaces and expressed the fermionic and bosonic correlation functions in terms of theta functions and proved their equality [29]. In 1988, Lee and Chen applied a new bosonization procedure, based on an exact method of functional integration, to one dimensional Tomonaga-Luttinger model with forward scattering and got around the conventional procedure where the fermion field operator is represented by charge and spin density(bosonic) fields [30].

1990-2000

Kane and Fisher in 1992 dealt with the problem of transport in a one-channel Luttinger liquid through a weak link where they discussed that the sign of interactions between the particles (attractive or repulsive) has a role to play in their transport [31]. The same authors in the same year studied resonant tunneling in an interacting one dimensional electron gas through a double barrier structure, where they found some striking differences in terms of temperature dependence on resonance as compared to the non-interacting case [32]. S. Eggert

et al. in the same year studied how an isolated impurity affects the low energy properties of a half-odd-integer-spin Heisenberg anti-ferromagnetic chain and tried to bring analogies with the Kondo effect [33]. A year later, Matveev et al. [34] used a simple renormalization group method to study conductance of a weakly interacting electron gas in 1D in the presence of an impurity of arbitrary strength. Fabrizio and Gogolin in 1995 extended the Haldane's Luttinger liquid description to a one dimensional interacting electrons with open boundary conditions and analyzed how presence of boundaries modifies various correlation functions [35]. Whereas Leclair et al. showed that a single impurity in the one dimensional Luttinger model creates a local modification of the charge density analogous to the Friedel oscillations [36]. In the same year Schmitteckert et al. studied spinless fermions on a ring with near-est neighbor interactions along with a disorder using density matrix renormalization group algorithm [37]. The theoretical prediction of Kane and Fisher (1992) was later confirmed in 1997 by Qin, Fabrizio and Yu by analyzing the finite size scaling behavior of low energy spectrum. In this paper, they numerically investigated the behavior of a single impurity in a one-dimensional Luttinger liquid by means of density matrix renormalization group [38]. Furusaki in 1997 revisited the orthogonality catastrophe in a Tomonaga Luttinger liquid with an impurity where the dimensionless conductance or interaction parameter, g=1/2 [39].

Mattsson et al. used Bosonization techniques to calculate the exact finite temperature single electron Green's function of a spinful Luttinger liquid confined by open boundaries, besides constructing and analyzing the corresponding local spectral density [40]. A. Komnik et al. calculated the Fermi edge singularity exponent for correlated electrons in one dimension in addition to studying a dynamic k-channel Kondo impurity via Abelian bosonization [41]. M. Bockrath et al. in 1998 studied the Luttinger liquid behavior in carbon nano-tubes and found that the conductance and differential conductance scale as power laws with respect to temperature and power voltage respectively [42]. V. Fernandez et al. in 1999 extended the non local version of Coleman's equivalence between the Thirring and sine-Gordon models to the case in which the original fermion fields interact with fixed impurities [43]. Y. L. Liu in 2000 treated backscattering of electrons on an impurity in a one dimensional interacting spinless electronic system using bosonization and phase shift representation, where they showed that the correlation exponents of the system depend on a phase shift induced by back scattering [44]. Whereas Schönhammer et al. in the same year studied the boundary effects on one particle spectra of Luttinger liquids using variety of models [45].

2000-2010

Fernandez and Na'on in 2001 introduced a path integral approach that permits the calculation charge density oscillations in a Luttinger liquid with impurities and obtained an explicit expression for the envelope of Friedel oscillations in the presence of arbitrary electron-electron

potentials [46]. Meden et al. computed the flow of renormalized impurity potential for a single impurity in a Luttinger liquid over the entire energy range from the microscopic scale of a lattice fermion model down to low energy limit [47]. Cazalilla in 2002 put an effort to study the ground state properties and low lying excitations of longitudinally confined interacting bosons by extending Haldane's harmonic fluid description to open boundary conditions. He obtained the momentum distribution, boson density and one particle density matrix for finite size and boundary effects, besides finding Friedel oscillations in the density [48]. In the same year, Meden et al. presented the influence exerted by an impurity in the electronic properties of a Luttinger liquid by using fermionic renormalization. They concluded that for large systems the low energy properties close to the impurity are as if the chain is cut into two pieces with open boundary conditions at the ends [49]. A year later, the same authors coupled an interacting nano-wire containing an impurity to non interacting semi infinite leads and studied the conductance G using a functional renormalization group method. Their results have shown excellent agreement with the analytically known scaling function at Luttinger liquid parameter K=1/2 and numerical density matrix renormalization group data [50]. Anfuso and Eggert in 2003 studied Luttinger liquid in a finite one-dimensional wire with box like boundary conditions by considering local distribution of a single particle spectral weight. They remarked that for the non-interacting case, the probability of extracting a single electron at a given place and energy can be interpreted as the square of the electron-wavefunction, whereas for the interacting case the wavefunctions obtain additional structure with sharp depletion near the edges and modulations throughout the wire [51]. In the same year, T. Stauber studied the Tomonaga Luttinger model with impurity by means of flow equations for Hamiltonians, where he formulated the system within collective density fluctuations, restricting himself from the use of bosonization formulas [52]. In 2004, Andergassen et al. improved the functional renormalization group (fRG) for impurities and boundaries in Luttinger liquids by including renormalization of the two particle interaction, in addition to renormalization of the impurity potential. Besides these, they also derived explicit flow equations for spinless lattice fermions with nearest neighbor interaction at zero temperature and also presented a fast algorithm to solve the same [53]. Grishin et al. used a functional integral formalism to find the exact representation of the electron Green function of the Luttinger liquid in the presence of a back-scattering impurity in the low-temperature limit, which allowed them to reproduce results for the suppression of electron local density of states at the position of impurity and for the Friedel oscillations at finite temperature [54]. In the same year, Nishimoto and Jeckelmann presented a dynamic density matrix renormalization group approach to the spectral properties of the quantum impurity problems [55].

In 2005, Enss et al. studied transport through a one dimensional quantum wire of correlated fermions connected to semi infinite leads. The wire contains either a single impurity or two barriers, the latter allowing for resonant tunneling and using functional renormalization group they calculated the linear conductance of wires of mesoscopic length and for all relevant

temperature scales [56]. The same group in the same year studied resonant tunneling in a Luttinger liquid with a double barrier enclosing a dot region.They showed the variation of the conductance G as a function of temperature T within a microscopic model calculation [57]. A year later, K. Kamide et al. studied the scaling of a single impurity potential in a Tomonaga-Luttinger liquid for arbitrary impurity strength and introduced the boson representation for the electron field operator including a phase shift by the impurity scattering [58]. R.Gezzi et al. in 2007 extended the concept of functional renormalization for quantum many body problems to non-equilibrium systems. They handled both stationary and time-dependent situations by using suitable generating functional based on the Keldysh approach and thus deriving a system of coupled differential equations for the m-particle vertex functions [59]. Jacobs et al. proposed a non-equilibrium version of functional renormalization within the Keldysh formalism by introducing a complex valued flow parameter in the Fermi or Bose functions of each reservoir and applied to non equilibrium transport through an interacting quantum wire [60]. Trushin et al. calculated the tunneling density of states for a Tomonaga-Luttinger liquid placed under a strong bias voltage and calculated both equilibrium and non-equilibrium tunneling exponents and observed their differences [61]. The single impurity problem in a spinful Tomonaga-Luttinger liquid is studied numerically by Hamamoto et al. using Monte Carlo methods through which they could analyze charge and spin conductance in the non perturbative regime [62]. In 2009, Kamide et al. developed a bosonization technique to treat an impurity which can not only connect the ones for the strong and weak impurity limits but reproduce exact scaling equation for the transmission probability in the weak two body interaction limit [63].

2010 onwards

Gutman et al. in 2010 developed a Bosonization technique for one dimensional fermions out of equilibrium in the framework of Keldysh action formalism. They employed the technique to study an interacting quantum wire attached to two electrodes with arbitrary energy distributions [64]. Galda et al. took into account the influence of electron phonon coupling on electron transport through a Luttinger liquid with an embedded weak scatterer or weak link [65]. The Luttinger liquid theory which has served as the paradigm for one dimensional systems in presence of interactions is based on linearization of the dispersion relations of the constituent particles. Beyond the low energy limit, the non linearity becomes essential and Imambekov et al. in 2012 used novel methods to tackle these systems which includes ideas from Fermi edge singularity and Fermi liquid theory, perturbation theory, etc and thus studied 1D quantum fluids beyond the Luttinger paradigm [66]. On the other hand, Rozhkov in 2014 demonstrated that a suitable fine tuning of the interaction between the fermions can stabilize a state in one dimension, which is neither similar to Fermi liquid nor to Luttinger liquid, which they called quasi Fermi liquid [67]. In 2012, Atland et al. presented a paradigmatic picture of an impurity in a Luttinger model, alternative to Kane and Fisher [31] picture. They

addressed the problem of a Luttinger liquid with a scatterer the allows for both coherent and incoherent scattering channels [68]. The same group in 2015 found that this model is qualitatively different from the elastic impurity set-up analyzed by Kane and Fisher [31] and also from the inelastic scattering studied by Furusaki and Matveev [69]. Thus they proposed a paradigmatic picture of Luttinger liquid where they extensively studied the renormalization group flows for this problem, the fixed point landscape, and scaling near those points [70]. More recently in 2015, Protopopov et al. explored the weak-strong-coupling Bose-Fermi duality in a chiral Luttinger liquid with non linear dispersion of bosonic and fermionic excitations. They used bosonization, a unitary transformation and a refermionization to map the system onto that of weakly interacting bosons at high temperatures and weakly interacting fermions at low temperatures [71]. Besides quantum impurity problems, another class of interesting problems in 1D constitutes the disordered systems where if the degree of randomness is sufficient, it leads to Anderson localization [161–165]. Enormous work has been done on these subjects of 'Luttinger liquids' and 'bosonization' and our survey of the literature is in no way exhaustive. Nevertheless it manages to give an idea of how the subject was started as well as its progress in the last seventy years or so.

1.2.2 Formalism

Bosonization, as the name suggests, is an attempt to recast theories involving entities which are not bosons in terms of bosons. It is generally used for fermionic fields (it is also possible to recast bosons in terms of other bosons) which are expressed as functions of bosonic fields that are typically bilinears of the original fields. This is not merely a scrupulous activity, but has proven to be extremely useful in studying intercting fermions in a 1D system, which is otherwise intractable when formulated in terms of fermions. The Fermi field ψ_η is expressed as an exponential of a bosonic field ϕ_η as $\psi_\eta \sim F_\eta\, e^{-i\phi_\eta}$. This is analogous to the polar representation of a complex number. Here F_η is the Klein factor which maintains the number-conservation rule. The formalism of bosonization is user-friendly once the bosonization rules are understood. More than half a century of progress made on this subject, including works of Tomonaga [1], Luttinger [2], Mattis and Lieb [3], Luther and Peschel [11], Heidenreich [12], Haldane [4] and many others, has resulted in a bifurcation of bosonization into two somewhat different approaches which has been discussed in the elaborate paper by Delft et al. [72]. Both these approaches, viz., constructive bosonization and field theoretical bosonization, has been briefly discussed here.

1.2.2.1 Field theoretical bosonization

This has become the most widely used approach to bosonization because of its simplicity, one famous example using this approach is that of Kane and Fisher [31]. One starts by defining the boson fields $\phi_\eta(x)$ which obeys a set of prescribed properties. Using field theoretical tools,

the commutation relations are calculated for these bosonic fields which are usually defined for a system of infinite size. This is followed by the calculation of Green's functions of $e^{-i\phi_\eta(x)}$ and $e^{i\phi_\eta(x)}$, which turns out to be identical to those of the fermion fields $\psi_\eta(x)$ and $\psi_\eta^\dagger(x)$. Hence a formal correspondence between the two was suggested of the form given as follows.

$$\psi_\eta(x) \sim F_\eta e^{-i\phi_\eta(x)} \tag{1.17}$$

The factor F_η is the so-called Klein factors which ensures that appropriate commutation rules are obeyed by the Fermi fields expressed in terms of bosonic fields ($\{\psi_\eta, \psi_{\eta'}^\dagger\} = \delta_{\eta,\eta'}$). The field theoretical approach, which is also adopted in the present work, demonstrates sufficiently well that bosonization can be used to study interacting 1D systems. However, there is no clarification as to why it works. The answer to this is provided by the more rigorous approach to bosonization called the 'constructive' approach which is briefly discussed in the next subsection. The bosonic field $\phi_\eta(x)$ and the Klein factor F_η do not appear naturally from first principle. They rather seem to be mere auxiliary quantities introduced and their properties fine tuned to get things done. In other words, the way of expressing a Fermi field operator in terms of bosonic variable as shown in equation (1.17) appear to be somewhat an arbitrary co-incidence though demonstrably true and useful. Hence for a better understanding it is necessary to dive deep into the more fundamental way of doing bosonization which is the constructive approach [72].

1.2.2.2 Constructive bosonization

The constructive approach to bosonization is more rigorous as compared to the field theoretical approach and it justifies the fundamentals of the latter approach. It was used in the remarkable works of Mattis and Lieb [3], Luther and Peschel [11], Emery [27], while Haldane gave a proper shape to it in his famous work [4]. The formalism starts with the second quantized expression of the Fermi field as follows.

$$\psi_\eta(x) = \sqrt{\frac{2\pi}{L}} \sum_k e^{-ikx} c_{k,\eta} \tag{1.18}$$

Here L is the size of the finite system which quantizes the momenta. Thus the Hilbert space consists of a countable set of states which is crucial in this approach. All further operators and fields are *constructed* explicitly and naturally in terms of these initially given $c_{k,\eta}$-operators. This approach is described in details in the excellent article by Delft et al. [72]. It is possible to derive the entire formalism of bosonization at a most elementary level as a set of operator identities in Fock space using standard operator identities (e.g. Baker-Hausdorff lemma) to manipulate functions of the $c_{k,\eta}$-operators. Since all the ingredients of this approach are constructed explicitly from the $c_{k,\eta}$'s, their physical meaning is clear. For example, $\partial\phi_\eta(x)$ represents local density fluctuations of the Fermi sea for a fixed total fermion number and

F_η lowers the total number of η-fermions by one. On the other hand, in the field theoretical approach, the Fock space of states being not explicitly defined, the relation given in equation (1.17) merely has the status of a Fermi Bose correspondence. For example, the Klein factors F_η is considered merely as a tool to ensure anti-commutation rules ignoring the fact that it also lowers the number of η-electrons. This is necessary to balance the number of particles on both sides of the equation (1.17) as the LHS is an annihilation operator and the exponential term of the RHS is number conserving.

Most importantly the constructive approach also explains why it is possible at all to represent a fermionic field in terms of bosonic fields - which is the essence of any kind of bosonization. Consider the Fermi ground state $|\vec{0}\rangle_0$. The state $\psi_\eta|\vec{0}\rangle_0$ turns out to be an eigenstate of the bosonic operators $b_{q\eta}$ from which the bosonic field $\phi = -\sum_{q>0}\sqrt{\frac{2\pi}{qL}}(e^{-q(ix+a/2)}b_{q\eta} + h.c)$ is constructed. Hence the Fermi state $\psi_\eta|\vec{0}\rangle_0$ must have a coherent state representation in terms of these bosonic operators $b^\dagger_{q\eta}$'s and this turns out to be $\sim F_\eta e^{-i\phi_\eta(x)}|\vec{0}\rangle_0$. Hence the constructive approach reveals the trick that makes bosonization works [72]. However for practical usage, one can adopt the field theoretical approach to yield correct results and rely on the constructive approach for connecting the dots.

1.3 Impurity in a Luttinger liquid

While the peculiar nature of mutual interaction makes one dimensional systems unique, this specialty is further enhanced by the response to an external impurity introduced into such systems. It turns out that the relevance of a local impurity depends on the sign of interaction (attractive or repulsive) between the constituent particles of a one dimensional system. This was discussed in the seminal paper by Kane and Fisher [31]. As has been emphasized in the present work that the standard bosonization methods are not sufficient in the study of impurities in 1D systems, although they are necessary. They require additional field theoretical techniques like renormalization group or numerical techniques like DMRG, Monte-Carlo, etc. These are briefly described below. The main advantage of non chiral bosonization technique is that it can easily tackle certain classes of impurities in 1D systems without adhering to such additional methods.

1.3.1 Renormalization group

Renormalization group or RG methods has been used extensively in the last few decades to study fundamental interactions at the microscopic scale, whose otherwise straightforward quantum field theoretical treatment would result in infinities. The perturbative treatment of interacting electrons in 1D is one such example which is plagued with divergences. The RG approach aims to extract the main singularities from the perturbative expansion and sum

them. The basic idea of this approach is to formulate an effective Hamiltonian (or action) which would capture the low energy physics of a system. In other words, it relates the original problem to another which will be easier to solve, provided the low energy physics of both are identical [5].

If one adopts the Kadanoff and Wilson formulation [73, 74], one starts by writing the partition function of the system.

$$Z = \sum_{all\ \ states} e^{-\beta H} = \sum_{all\ \ states} e^{-S}$$

where H is the Hamiltonian, β is inverse temperature and S is the action which typically contains degrees of freedom at wave-vectors up to certain cutoff Λ. As described above, the goal is to reformulate this action and retain only those degrees of freedom which are in the vicinity of $|k| = k_F$. Consider a cut-off dependent action $S(\Lambda)$. The first task is to eliminate all degrees of freedom between Λ and Λ/s where $s > 1$ and obtain a new action $S(\Lambda = \Lambda/s)$. This is followed by a "scale change" $k \rightarrow sk$ which brings the cut-off back to its original value and a new action $S(\Lambda)$ is obtained. The coupling constants are now changed because of the degrees of freedom being integrated out. A value of s infinitesimally close to unity is chosen and the first two steps are performed iteratively. This eventually leads to differential equations for the couplings, which may be integrated in favorable situations until all non-interesting degrees of freedom (high momentum modes) have been eliminated [75].

The RG approach has been crucial in dealing with impurities in a Luttinger liquid. The famous examples in this regard will be Kane and Fisher [31], Matveev et al. [34], Andergasses et al. [53], etc. Kane and Fisher adopted an RG transformation which integrated out higher frequencies from the action of a Luttinger liquid with an impurity and then rescaling the frequency, leaving the action invariant. They treated the impurity as a perturbation in two extreme limits - weak barrier and weak link and predicted the two famous phenomena - 'cutting the chain' and 'healing the chain' [31]. These phenomena are also endorsed by NCBT without using any RG techniques. Matveev et al. [34] used a simple renormalization technique to study conductance of a Luttinger liquid in presence of an impurity of arbitrary strength. Their formalism could take into account backward scattering as well but it could only deal with weak mutual interactions. Andergassen et al. [53] improved the functional renormalization group (fRG) for impurities and boundaries in Luttinger liquids by considering renormalization of both the two-particle interaction and the impurity potential. These studies lead to really intricate calculations which are beyond the scope of the present work - whose sole aim is to promulgate an easier alternative which is described in the next chapter.

1.3.2 Numerical methods

While analytical methods used to study Luttinger liquids confronts technical difficulties, which are taken care by adopting various approximation schemes, there were others who tried to

study the same problem using numerical methods. Prominent among them are density matrix renormalization group, Monte Carlo, finite size scaling, etc.

Density matrix renormalization has been the method of choice for the numerical studies in 1D systems. When it comes to calculation of the correlation functions, there are some fundamental differences owing to the energy band structures of the systems. For gapped systems, the correlation functions decay exponentially with the distance while correlation functions of gapless models decay algebraically with distance [76]. DMRG is used to optimize the ansatz wavefunctions called as Matrix Product States (MPS) and thus obtaining the correlation functions. But matrix product states are proven useful only for describing the ground states of gapped local Hamiltonians [77–79]. Every ground state of a gapped Hamiltonian in 1D can be approximated by a tensor network state to arbitrary precision [80]. But M. Andersson et al. investigated the convergence of DMRG for gapless systems in thermodynamic limit [81]. They concluded that when DMRG is used to study a gapless systems of free fermions it gives the wrong particle-hole and density density correlation functions. The expected correlation functions must decay algebraically but the ones obtained from DMRG decay exponentially. The difficulty in studying gapless systems using DMRG is that convergence is tough to achieve. Some remedies such as increasing the number of DMRG sweeps, working with finite sized systems are adopted to mitigate the problems.

The other numerical method frequently used to study Luttinger liquid is Monte Carlo. The conductance of Luttinger liquids with impurities has been studied using Monte Carlo simulations [62, 82, 83]. On the other hand, the finite size scaling method is a way of extracting values for certain exponents (like correlation function exponents) by observing how measured quantities vary as the size L of the system studied changes. Kawakami et al. [84] used this method in a 1D fermionic system and studied the low energy behavior, thereby obtaining exact formulas for correlation exponents. Qin et al. [85] analyzed the finite-size scaling behavior of the low energy spectrum of a Luttinger liquid with an impurity and confirmed the theoretical prediction of Kane and Fisher [31] both for attractive and repulsive interactions.

1.4 Summary

In this chapter, a general introduction to the field of one dimensional fermionic systems is given. Due to the collective nature of excitations in these systems the Fermi liquid theory fails, which led to an alternative that goes by the name ‘Luttinger liquid theory’. The basic idea was to express a fermionic Hamiltonian in terms of bosonic variables - a process called bosonization which started with the path breaking works of Tomonaga, Luttinger, Mattis and Lieb, Luther and Peschel, etc. and given a final shape by Haldane. A detailed history of bosonization is provided along with a brief description of the formalism. The physical realizations of such 1D systems have triggered interests among the researchers and various numerical

and analytical approaches are developed in the recent decades to explain the physical properties of such systems. On the other hand, the introduction of impurities into these systems leads to interesting physics described in the seminal work of Kane and Fisher. However, the conventional bosonization methods are insufficient to yield the full Green functions of such inhomogeneous 1D systems with an impurity of arbitrary strength without adhering to other methods like renomalization group. Hence we demonstrate a new way of doing bosonization which can provide the Green functions of a certain class of strongly inhomogeneous systems without using additional methods.

Chapter 2

Methodology

This chapter describes the technical aspects of the non chiral bosonization technique (NCBT) which has been introduced and used throughout the work. NCBT uses a field theoretical approach of doing bosonization where a fermion field operator is expressed as an exponential of a bosonic field. The basic necessity for the development of NCBT is that the non-local Fermi-Bose correspondence used in the standard bosonization techniques (also known as 'g-ology' methods) is suitable to study only homogeneous systems or a half line. For anything in between these two extremes, the g-ology techniques become insufficient and have to rely on other techniques like renormalization group or other numerical techniques like Density matrix renormalization group (DMRG) or Monte Carlo (MC), etc. But NCBT uses a version of field operator which is ideally suited to study the inhomogeneous Luttinger liquids and can produce the asymptotic Green functions of such systems. Before going to the formalism of NCBT in details, it is important to illustrate the shortcomings of the g-ology methods so that one can appreciate the necessity of a novel formalism.

2.1 Critique to g-ology based chiral bosonization

The conventional approach to bosonization (which is discussed in Giamarchi's book [5]) invokes the Dirac equation in 1+1 dimension with chiral 'right -movers' and 'left-movers'. It uses the plane wave basis to study one dimensional systems with translational symmetries. It is undoubtedly a remarkable achievement in calculating the N-point correlation functions of one dimensional interacting systems, where the well established Fermi liquid theory and perturbation theory fails.

But difficulties arise when we use the same approach to deal with systems that are translationally non invariant, e.g. systems with a boundary or a system with an impurity in it. The conventional bosonization technique requires a combination of renormalization group along with bosonization/refermionization techniques, but unable to obtain a closed formula for the

Green's functions for such systems. Moreover there are certain other aspects of this technique which needs to be rectified and this is exactly what NCBT does.

Coleman, way back in the 70's [21] , showed that the fermion Green function of the Thirring model has an independent description in terms of bosonic variables. On the other hand, physicists like Luther and Mandelstam [86] asserted that the Fermi field operator itself can be expressed in terms of bosonic variables. This assertion is quite stronger and is used by researchers in condensed matter physics to generate Hamiltonians of fermions in one dimensional systems. They claim this to be advantageous as the interaction Hamiltonian remains quadratic in the boson basis (unlike quartic in the fermion basis) and is thus trivial to diagonalize. But as a matter of fact, the particle hole excitations of the Fermi system that make the kinetic energy diagonal in these operators are not bosons, thus making the term bosonization a misnomer. The conventional bosonization treats the kinetic energy ($K = \sum_k \epsilon_k c_k^\dagger c_k = \sum_{p>0} v_F\ p\ b_{p,R}^\dagger b_{p,R} + \sum_{p>0} v_F\ p\ b_{p,L}^\dagger b_{p,L}\ +$ constant) as an operator identity whereas it is just a mnemonic for generating the correlation functions. To overcome these issues, an alternative was proposed (in the book 'Dynamics of classical and quantum fields' [9]) involving an action for fermions in terms of hydrodynamic variables and a prescription for generating the propagator of fermions that potentially also allows one to go beyond the linear dispersion approximation and also the random phase approximation.

T. Giamarchy in his book 'Quantum Physics in one dimension' [5] proposes the following formula for the field operator (Luther Haldane construction).

$$\psi_r^\dagger(x) = \lim_{\epsilon\to 0} \psi_r^\dagger(x;\epsilon) = \lim_{\epsilon\to 0} \frac{1}{\sqrt{2\epsilon L}} e^{-ir(k_F - \frac{\pi}{L})x} e^{i\phi_r^\dagger(x,\epsilon) + i\phi_r(x,\epsilon)} U_r^\dagger \tag{2.1}$$

where $r = \pm$ corresponding to right and left movers, and

$$\phi_r(x,\epsilon) = -\frac{\pi r x}{L} N_r + i \sum_{p\neq 0} \left(\frac{2\pi}{L|p|}\right)^{\frac{1}{2}} e^{-\frac{L\epsilon|p|}{2\pi}} Y(rp) b_p e^{ipx}$$

In equation (2.1), the matrix elements of the right-hand side is not equal to those of the field operator. Although Coleman in his paper on the equivalence of the massive Thirring model and Sine Gordon equation [21] has shown that the Green's functions comes out right in both the cases, no such remark has been made on the correctness of the Field operator. Thus the g-ology program which involves a literal interpretation of the Luther construction is not supported very well. Replacing the operator description by a path integral version based on Hubbard-Stratanovich transformation, as preached in some literature, may make things appear admissible, but it leads to the manipulation of infinities under the name of 'normal ordering'. Moreover, Coleman's assertion that $\bar{\psi}\gamma^\mu\psi \equiv -\frac{\beta}{2\pi}\epsilon^{\mu\nu}\partial_\nu\phi$ is a mere analogy because the left hand side is a Grassman number and the right hand side is a real number and they can at most be equivalent to each other.

The central point of all the above discussion lies in the assertion that the Luther Haldane construction given by equation (2.1), which is the backbone of standard bosonization, is not necessarily an operator identity but rather a mnemonic for generating the correlation functions. This distinction may seem scrupulous at first glance but its consequences are far reaching. An operator identity is universal and absolute (model independent) whereas a mnemonic can be model dependent and ad-hoc. Moreover a mnemonic can be modified under certain circumstances, which gives the liberty of inserting additional terms into the bosonic representation of the field operator and this is at the heart of the present work. After all, the field operator in itself does not make much of physical sense, but it is rather a means to obtain the correlation functions of the given system - which is the goal of this work.

Using Haldane's harmonic analysis (HHA) of the field operator, the density operator can be expressed in terms of the slow and rapidly varying parts as follows.

$$\rho(x,t) = \rho_0 + \tilde{\rho}_s(x,t) + \rho_0\ e^{2ik_F x}\ e^{2\pi i \int_{-\infty}^{x} dy\ \tilde{\rho}_s(y,t)} + \rho_0\ e^{-2ik_F x}\ e^{-2\pi i \int_{-\infty}^{x} dy\ \tilde{\rho}_s(y,t)} \tag{2.2}$$

Here $\tilde{\rho}_s(x,t)$ is the slowly varying part of the density fluctuation while the rapidly oscillating parts are given as follows.

$$\begin{aligned} \rho_f(x,t) &= \rho_0\ e^{2\pi i \int_{-\infty}^{x} dy\ \tilde{\rho}_s(y,t)} \\ \rho_f^*(x,t) &= \rho_0\ e^{-2\pi i \int_{-\infty}^{x} dy\ \tilde{\rho}_s(y,t)} \end{aligned} \tag{2.3}$$

Consider the fast part of the density density correlation function that oscillates as $e^{2ik_F(x-x')}$.

$$< \rho_f(x,t)\rho_f^*(x',t') >_{HHA} = e^{2ik_F(x-x')} < e^{2\pi i \int_{-\infty}^{x} dy\ \tilde{\rho}_s(y,t)} e^{-2\pi i \int_{-\infty}^{x'} dy'\ \tilde{\rho}_s(y',t')} > \tag{2.4}$$

This quantity can be trivially calculated using the Wick's theorem as follows.

$$< \rho_f(x,t)\rho_f^*(x',t') >_{Wick's} = - < \psi_L(x',t')\psi_L^\dagger(x,t) >< \psi_R(x,t)\psi_R^\dagger(x',t') > \tag{2.5}$$

In absence of mutual interactions all the quantities present in the RHS of equations (2.4) and (2.5) can be obtained trivially using Fermi algebra. It is observed that for a homogeneous system, both these equations give the same results. But the introduction an impurity (let's say a delta potential) leads to non-trivial exponents in the RHS of equation (2.4) while those of (2.5) continue to be trivial. This tells conclusively that this harmonic analysis is not suitable to study inhomogeneous systems. Moreover, the assertion in equation (2.2) can't be declared as an operator identity either, because the associated algebra makes sense in the limit $\rho_0 \to \infty$ and in this limit none of the operators are meaningful. Thus it can be said that both Luther's construction and Haldane's harmonic analysis of the field operator are at best only mnemonics for the correlation functions and it should be forbidden to use them as operators to construct Hamiltonians. So in summary, the critique to the conventional schemes of bosonization can be presented as the the following set of judgemental characterizations in

order.

1. Preposterous: Although the Fermi field operator has an expression in terms of bosons constructed out of Fermi bilinears and Klein factors, we are unable to find a proof in the existing literature that the matrix elements of the non-local combination of bosons is equal to the corresponding matrix elements of the field operator.

2. Plausible but still untrue: It was never been proven that equal-time number conserving products of Fermi fields can be expressed in terms of Fermi bilinears that are bosonic in character. Merely showing that the propagator comes out right is not enough, but instead all the matrix elements must come out right.

3. Possible fact: N-point functions have a non local integral representation involving commuting variables that may be simply related to Fermi bilinears such as current and densities [9].

To circumvent the problems associated with the conventional chiral bosonization, it is mandatory to declare the bosonization formulas as mnemonics to generate the N-point correlation functions rather than treating them as operator identities. Mnemonics are not mandated to be universal, unique and model independent. This gives the freedom to modify the field operator, expressed in terms of currents and densities, accordingly so that the Green functions of free fermions plus impurities comes out correctly - a quantity which is not obtainable using the standard chiral bosonization alone. This is the essence of Non chiral bosonization technique - a novel way of doing bosonization. In the next section, this whole procedure of this method, from writing the Hamiltonian to obtaining the correlation functions is discussed.

2.2 Working procedure

The central goal of this work is to obtain closed analytical expressions of the correlation functions of one dimensional system of electrons in the presence of certain sources of inhomogeneities like a cluster of impurities. This is done using the powerful tool, namely Non chiral bosonization, which explicitly makes use of the translationally non-invariant single particle wave functions. In this section the whole procedure of doing the same has been discussed, giving due importance to the formalism of NCBT. To provide a bird-eye view of the procedure a flow chart has been provided in the figure 2.1.

2.2.1 Single particle Green's functions

Consider a one dimensional system of length L ($L \to \infty$) which extends from $-L$ to L with an impurity (lets say a delta potential) at the origin. A more general version of this potential, viz. a cluster of impurities consisting of delta potentials, potential barriers/wells, etc. is taken

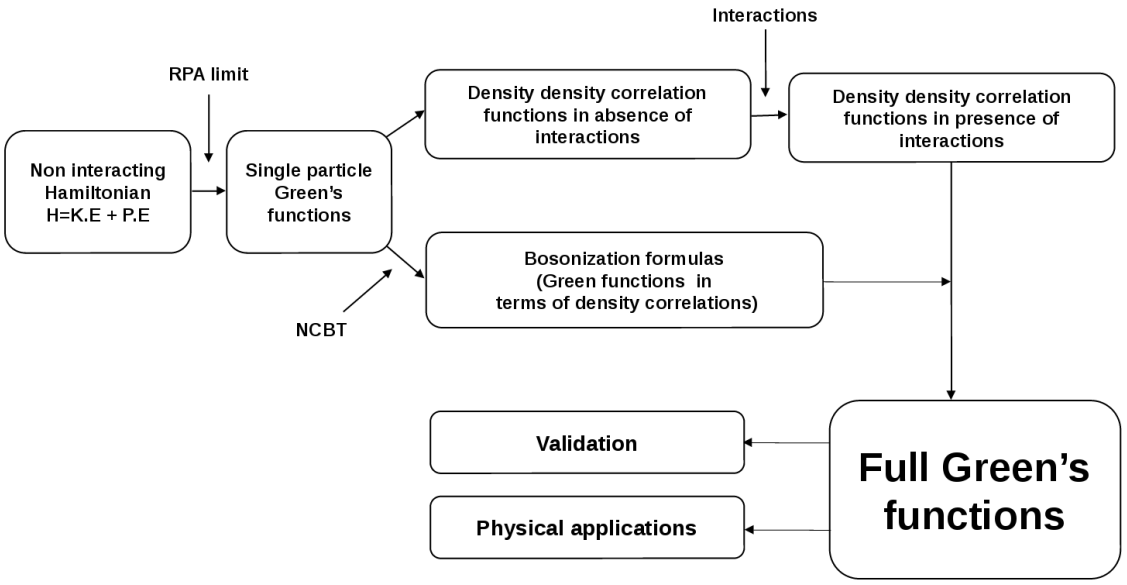

FIGURE 2.1: NCBT flow-chart: Schematic diagram showing the different steps of the present work from starting to end.

into account in the next chapter. The first task is to calculate the two point Green function of this system in absence of mutual interactions using the standard Fermi algebra.

Calculating the wavefunctions

Considering an impurity in a 1D system [31, 34, 52] modelled as delta potential of strength V_0, the Schrödinger equation reads as follows (note that Ψ represents wavefunction and ψ represents fermionic opertor).

$$-\frac{\hbar^2}{2m}\frac{d}{dx}\Psi(x) + V_0\delta(x)\Psi(x) = E\Psi(x) \tag{2.6}$$

This can be solved using elementary knowledge of quantum mechanics, which leads to two normalized sets of wave-functions, one with the propagation starting from the left and moving towards right (Ψ_R) while the other with that starting from the right and moving towards left (Ψ_L) .

$$\Psi_R(x) = \begin{cases} A_1 e^{ikx} + B_1 e^{-ikx} & -L/2 < x < 0 \\ A_2\ e^{ikx} & 0 < x < L/2 \end{cases} \tag{2.7}$$

$$\Psi_L(x) = \begin{cases} D_1\ e^{-ikx} & -L/2 < x < 0 \\ C_2 e^{ikx} + D_2 e^{-ikx} & 0 < x < L/2 \end{cases} \tag{2.8}$$

where,

$$A_1 = D_2 = \sqrt{\frac{1}{L}}$$
$$B_1 = C_2 = \sqrt{\frac{1}{L}} \frac{-\frac{imV_0}{k\hbar^2}}{\left(1+\frac{imV_0}{k\hbar^2}\right)}$$
$$A_2 = D_1 = \sqrt{\frac{1}{L}} \frac{1}{\left(1+\frac{imV_0}{k\hbar^2}\right)}$$

Random Phase Approximation

For an analytical solution to be feasible when mutual interactions are included, it is necessary to confine the study to the so-called random phase approximation (RPA). Under this approximation we linearize the energy momentum curve near the fermi level.

$$E = \frac{1}{2} m v_F^2 + p v_F = E_F + p v_F$$

where E_F is the Fermi energy and pv_F is the fluctuation around the Fermi energy. This is similar in spirit to the Tomonaga and Luttinger models which are also based on linearization of the energy momentum dispersion relations. Under the RPA limit [87], the Fermi momentum and the mass of the fermion are allowed to diverge in such a way that their ratio is finite (i.e. $k_F, m \to \infty$ but $k_F/m = v_F < \infty$). Units are chosen such that $\hbar = 1$, so that k_F is both the Fermi momentum as well as a wavenumber. Imposing the RPA limit to the wavefunctions in equations (2.7) and (2.8) leads to the following.

$$\Psi_R(x) = \begin{cases} A_1 e^{i(k_F+p)x} + B_1 e^{-i(k_F+p)x} & -L/2 < x < 0 \\ A_2 \ e^{i(k_F+p)x} & 0 < x < L/2 \end{cases} \tag{2.9}$$

$$\Psi_L(x) = \begin{cases} D_1 \ e^{-i(k_F+p)x} & -L/2 < x < 0 \\ C_2 e^{i(k_F+p)x} + D_2 e^{-i(k_F+p)x} & 0 < x < L/2 \end{cases} \tag{2.10}$$

$$A_1 = D_2 = \sqrt{\frac{1}{L}}$$
$$B_1 = C_2 = \sqrt{\frac{1}{L}} \frac{-\frac{iV_0}{v_F}}{\left(1+\frac{iV_0}{v_F}\right)}$$
$$A_2 = D_1 = \sqrt{\frac{1}{L}} \frac{1}{\left(1+\frac{iV_0}{v_F}\right)} \tag{2.11}$$

Calculating the Green functions

Green functions are calculated using three different methods [88] which are as follows.

a) Solving the Green function differential equation.

$$(E - \hat{H}(x))G(x, y; E) = \delta(x - y)$$

b) Summing up the spectral representation.

$$G(x, y; E) = \sum_n \frac{\Psi_n(x)\Psi_n^*(y)}{E - E_n}$$

c) Performing the Feynman path integral expansion of the Green function [89].

In this work, we adopt the second method for which we need a complete set of orthonormal states. Now, we know from quantum mechanics that for different values of momentum k, any two states of Ψ_R (or Ψ_L) will be orthogonal. The test is to check whether for the same value of k, $\Psi_R(k)$ and $\Psi_L(k)$ are mutually orthogonal.

$$\begin{aligned}
< \Psi_L(k)|\Psi_R(k) > &= \int_{-\frac{L}{2}}^{\frac{L}{2}} \Psi_L^*(x)\Psi_R(x)dx \\
&= \int_{-\frac{L}{2}}^{0} \Big(D_1^* e^{ikx}\Big)\Big(A_1 e^{ikx} + B_1 e^{-ikx}\Big)dx + \int_0^{\frac{L}{2}} \Big(C_2^* e^{-ikx} + D_2^* e^{ikx}\Big)\Big(A_2 e^{ikx}\Big)dx \\
&= \Big[D_1^* B_1 + C_2^* A_2\Big]\frac{L}{2} + \text{smaller terms}
\end{aligned}$$

Using equation (2.11) we have $[D_1^* B_1 + C_2^* A_2] = 0$ and hence $< \psi_L(k)|\psi_R(k) > \approx 0$. Thus they are already already orthogonal to each other. In some other examples, ψ_R and ψ_L need not be orthogonal. In those cases we can use Gram Schmidt orthogonalization as follows.

$$\begin{aligned}
\Psi_1 &= \Psi_R \\
\Psi_2 &= \Psi_L - < \Psi_1|\Psi_L > \Psi_1
\end{aligned}$$

Here Ψ_R and Ψ_L are normalized. Now Ψ_1 and Ψ_2 are orthogonal to each other as can be seen.

$$\begin{aligned}
< \Psi_1|\Psi_2 > &= \Big\langle \Psi_1 \Big| \Big(\Psi_L - < \Psi_1|\Psi_L > \Psi_1\Big) \Big\rangle \\
&= < \Psi_1|\Psi_L > - < \Psi_1|\Psi_L >< \Psi_1|\Psi_1 > \\
&= < \Psi_1|\Psi_L > - < \Psi_1|\Psi_L > \\
&= 0
\end{aligned}$$

We can calculate the Green's function from them as follows.

$$\begin{aligned}
G(x, x', E) = \sum_n \frac{\Psi(x)\Psi^*(x')}{E - E_n} &= \frac{L}{2\pi}\int \frac{\Psi(x)\Psi^*(x')}{\hbar\omega + i\epsilon - pv_F}dE \\
= \frac{L}{2\pi}\int \frac{\Psi(x)\Psi^*(x')}{v_F(\frac{\hbar\omega + i\epsilon}{v_F} - p)}v_F dp &= \frac{L}{2\pi}\int \frac{\Psi(x)\Psi^*(x')}{(\frac{\hbar\omega + i\epsilon}{v_F} - p)}dp
\end{aligned}$$

We have a pole at $p_0 = \frac{\hbar\omega + i\epsilon}{v_F}$. Hence

$$G(x, x', E) = \frac{L}{2\pi} 2\pi i \Psi(x, p_0)\Psi^*(x', p_0) = iL\Psi(x, p_0)\Psi^*(x', p_0)$$

In this case, we have two orthogonal states for the same energy level, viz, Ψ_R and Ψ_L. Thus the Green's functions will be of the following form.

$$G(x, x', E) = iL\Big[\Psi_L(x, p_0)\Psi_L^*(x', p_0) + \Psi_R(x, p_0)\Psi_R^*(x', p_0)\Big]$$

The time dependent green's function can be obtained by a simple Fourier transform of the energy dependent one.

$$\begin{aligned} G(x, x', t - t') &= \frac{1}{2\pi}\int G(x, x', E)e^{-i\omega(t-t')}d\omega \\ &= \frac{iL}{2\pi}\int \Big[\Psi_L(x, p_0)\Psi_L^*(x', p_0) + \Psi_R(x, p_0)\Psi_R^*(x', p_0)\Big]e^{-i\omega(t-t')}d\omega \end{aligned}$$

Now let us denote this full two-point Green function (also known as single particle Green function) of the system before taking the RPA limit (i.e. with parabolic energy-momentum relation) as $< T\ \psi(x, \sigma, t)\psi^\dagger(x', \sigma', t') >$, where the time ordering decides whether it is particle or hole Green function that is being studied and σ is the spin projection of the individual fermions. In terms of this, the asymptotic or RPA Green function is defined by "smearing out" the positions and times over the scale of the Fermi wavelength and Fermi times as follows,

$$\langle T\ \psi_\nu(x, \sigma, t)\psi_{\nu'}^\dagger(x', \sigma', t')\rangle = \lim_{m\to\infty} \ll \langle T\psi(y, \sigma, \tau)\psi^\dagger(y', \sigma', \tau')\rangle e^{-ik_F(\nu y - \nu' y')}e^{iE_F(\tau - \tau')} \gg \tag{2.12}$$

where,

$$\begin{aligned} \ll f(t) \gg &= \frac{1}{2T_F}\int_{t-T_F}^{t+T_F} d\tau\ f(\tau) \\ \ll g(x) \gg &= \frac{1}{2\lambda_F}\int_{x-\lambda_F}^{x+\lambda_F} dy\ g(y) \end{aligned} \tag{2.13}$$

with $\lambda_F = 2\pi/k_F$ and $T_F = 2\pi/E_F$, $k_F = mv_F$ and $E_F = (1/2)mv_F^2$ with $v_F < \infty$ being held fixed. Also, here $\nu, \nu' = \pm 1$ correspond to the right and left Fermi points. The full Green function is a linear combination of different rapidly oscillating parts as follows.

$$\begin{aligned} \Big\langle T\psi(x, \sigma, t)\psi^\dagger(x', \sigma', t')\Big\rangle = &\Big\langle T\psi_R(x, \sigma, t)\psi_R^\dagger(x', \sigma', t')\Big\rangle e^{ik_F(x-x')} + \Big\langle T\psi_L(x, \sigma, t)\psi_L^\dagger(x', \sigma', t')\Big\rangle e^{-ik_F(x-x')} \\ &+ \Big\langle T\psi_R(x, \sigma, t)\psi_L^\dagger(x', \sigma', t')\Big\rangle e^{ik_F(x+x')} + \Big\langle T\psi_L(x, \sigma, t)\psi_R^\dagger(x', \sigma', t')\Big\rangle e^{-ik_F(x+x')} \end{aligned} \tag{2.14}$$

The activity described in equation (2.12) simply extracts the envelope of a particular type of rapidly oscillating term from the full Green function (e.g. $< \psi_R\psi_R >$ from $< \psi\psi >$). The various envelopes of the Green functions in absence of mutual interactions are obtained as follows.

$$
\begin{aligned}
\Big\langle T\psi_R(x,\sigma,t)\psi_R^\dagger(x',\sigma',t')\Big\rangle =& \frac{\delta_{\sigma,\sigma'}}{(x-x')-v_F(t-t')}\left(\frac{i}{2\pi}-\frac{V_0}{2\pi v_F}\left(\frac{\theta(x')\theta(-x)}{\left(1-V_0\frac{i}{v_F}\right)}-\frac{\theta(x)\theta(-x')}{\left(1+V_0\frac{i}{v_F}\right)}\right)\right)\\
\Big\langle T\psi_L(x,\sigma,t)\psi_L^\dagger(x',\sigma',t')\Big\rangle =& \frac{\delta_{\sigma,\sigma'}}{-(x-x')-v_F(t-t')}\left(\frac{i}{2\pi}-\frac{V_0}{2\pi v_F}\left(\frac{\theta(-x')\theta(x)}{\left(1-V_0\frac{i}{v_F}\right)}-\frac{\theta(-x)\theta(x')}{\left(1+V_0\frac{i}{v_F}\right)}\right)\right)\\
\Big\langle T\psi_R(x,\sigma,t)\psi_L^\dagger(x',\sigma',t')\Big\rangle =& \frac{\delta_{\sigma,\sigma'}}{-(x+x')+v_F(t-t')}\frac{V_0}{2\pi v_F}\left(\frac{\theta(-x')\theta(-x)}{\left(1-V_0\frac{i}{v_F}\right)}-\frac{\theta(x)\theta(x')}{\left(1+V_0\frac{i}{v_F}\right)}\right)\\
\Big\langle T\psi_L(x,\sigma,t)\psi_R^\dagger(x',\sigma',t')\Big\rangle =& \frac{\delta_{\sigma,\sigma'}}{(x+x')+v_F(t-t')}\frac{V_0}{2\pi v_F}\left(\frac{\theta(x')\theta(x)}{\left(1-V_0\frac{i}{v_F}\right)}-\frac{\theta(-x)\theta(-x')}{\left(1+V_0\frac{i}{v_F}\right)}\right)
\end{aligned}
\tag{2.15}
$$

2.2.2 Density density correlation functions

The density density correlation function (DDCF) is a special case of four point function which is a crucial quantity in this approach. In absence of mutual interactions one can use the Wick's theorem to write the DDCF as follows.

$$
\begin{aligned}
\big\langle T\rho(x,\sigma,t)\rho(x',\sigma',t')\big\rangle =& \big\langle T\psi^\dagger(x,\sigma,t)\psi(x,\sigma,t)\psi^\dagger(x',\sigma',t')\psi(x',\sigma',t')\big\rangle\\
=& \big\langle T\psi^\dagger(x,\sigma,t)\psi(x,\sigma,t)\big\rangle\big\langle T\psi^\dagger(x',\sigma',t')\psi(x',\sigma',t')\big\rangle\\
&-\big\langle T\psi(x,\sigma,t)\psi^\dagger(x',\sigma',t')\big\rangle\big\langle T\psi(x',\sigma',t')\psi^\dagger(x,\sigma,t)\big\rangle\\
=& \big\langle\rho(x,\sigma,t)\big\rangle\big\langle\rho(x',\sigma',t')\big\rangle-\big\langle T\psi(x,\sigma,t)\psi^\dagger(x',\sigma',t')\big\rangle\big\langle T\psi(x',\sigma',t')\psi^\dagger(x,\sigma,t)\big\rangle
\end{aligned}
$$

Subtracting the average density terms (so that this is really the deviation) the density density correlation functions can be redefined as follows.

$$
\begin{aligned}
\big\langle T\tilde{\rho}(x,\sigma,t)\tilde{\rho}(x',\sigma',t')\big\rangle =& \big\langle T\rho(x,\sigma,t)\rho(x',\sigma',t')\big\rangle-\big\langle\rho(x,\sigma,t)\big\rangle\big\langle\rho(x',\sigma',t')\big\rangle\\
=& -\big\langle T\psi(x,\sigma,t)\psi^\dagger(x',\sigma',t')\big\rangle\big\langle T\psi(x',\sigma',t')\psi^\dagger(x,\sigma,t)\big\rangle
\end{aligned}
\tag{2.16}
$$

In the RPA sense, the density $\rho(x,t)$ may be "harmonically analyzed" as follows.

$$
\rho(x,\sigma,t)=\rho_s(x,\sigma,t)+e^{2ik_Fx}\ \rho_f(x,\sigma,t)+e^{-2ik_Fx}\ \rho_f^*(x,\sigma,t) \tag{2.17}
$$

where

$$
\begin{aligned}
\rho_s(x,\sigma,t)&=\psi_R^\dagger(x,\sigma,t)\psi_R(x,\sigma,t)+\psi_L^\dagger(x,\sigma,t)\psi_L(x,\sigma,t)\\
\rho_f(x,\sigma,t)&=\psi_R^\dagger(x,\sigma,t)\psi_L(x,\sigma,t)\\
\rho_f^*(x,\sigma,t)&=\psi_L^\dagger(x,\sigma,t)\psi_R(x,\sigma,t)
\end{aligned}
\tag{2.18}
$$

The density density correlation function (DDCF) contains both slowly varying (ρ_s) and rapidly oscillating (ρ_f) terms. Out of these only the slowly varying part of the density density correlation function is of importance to us. Using equations (2.16) and (2.18), we have the slowly varying part of the DDCF of a single impurity system as follows:

$$\begin{aligned} < T\tilde{\rho}_s(x,\sigma,t)\tilde{\rho}_s(x',\sigma,t') >= & \frac{1}{((x-x')+v_F(t-t'))^2}\left(-\frac{\theta(xx')}{(2\pi)^2} - \frac{\theta(-xx')}{(2\pi)^2}\frac{v_F^2}{v_F^2+V_0^2}\right) \\ & - \frac{1}{(2\pi)^2}\frac{V_0^2}{v_F^2+V_0^2}\left(\frac{\theta(xx')}{((x+x')-v_F(t-t'))^2} + \frac{\theta(xx')}{((x+x')+v_F(t-t'))^2}\right) \\ & + \frac{1}{((x-x')-v_F(t-t'))^2}\left(-\frac{\theta(xx')}{(2\pi)^2} - \frac{\theta(-xx')}{(2\pi)^2}\frac{v_F^2}{v_F^2+V_0^2}\right) \end{aligned} \tag{2.19}$$

Here $\theta(xx') = \theta(x)\theta(x') + \theta(-x)\theta(-x')$ and $\theta(-xx') = \theta(x)\theta(-x') + \theta(x)\theta(-x')$ where θ's represent Heaviside step functions. It is easy to see that on setting $V_0 = 0$ (no impurity), then the same side ($\theta(xx')$) and opposite sides ($\theta(-xx')$) have the same functional forms which is that of the homogeneous case, which is a necessary cross check.

2.2.3 Field operator reconstruction (Bosonization)

Having both the two point functions and the density density correlation functions in hand (in absence of mutual interactions), the next task is to reconstruct the field operator and express it explicitly in terms of currents and densities. Now the currents and densities are bilinears in the field operator ψ as follows.

$$\begin{aligned} \rho(x) &= \psi^\dagger(x)\psi(x) \\ J(x) &= Im[\psi^\dagger(x)\partial_x\psi(x)] \end{aligned} \tag{2.20}$$

Bosonization is inverting these relations and expressing ψ in terms of J and ρ. This inversion is accomplished by introducing the conjugate to the density $\pi(x)$ through the following relation.

$$J(x) = -\rho(x)\ \partial_x\pi(x) \tag{2.21}$$

Hence the conjugate to the density can be expressed explicitly as follows.

$$\pi(x) = -\int_{-\infty}^{x} dy \frac{J(y)}{\rho(y)} \tag{2.22}$$

To avoid singularities, it is assumed that $\rho(x) = \rho_0 + \tilde{\rho}(x)$ where $\rho_0 \neq 0$ is the uniform average density and expanded in powers of $\tilde{\rho}(x)$. In standard bosonization [5], the field operator is

expressed in terms of currents and densities as follows.

$$\psi_\nu(x,\sigma,t) \sim e^{i\theta_\nu(x,\sigma,t)} \tag{2.23}$$

Here $\nu = R\ (+1)$ for right movers and $\nu = L\ (-1)$ for left movers[1]. The currents can be expressed in terms of the densities using the continuity equation and hence the local phase can be expressed as a function of densities alone as follows.

$$\theta_\nu(x,\sigma,t) = \pi \int_{sgn(x)\infty}^{x} dy \left(\nu\ \rho_s(y,\sigma,t) - \int_{sgn(y)\infty}^{y} dy^{'}\ \partial_{v_F t}\ \rho_s(y^{'},\sigma,t) \right) \tag{2.24}$$

The prescription given by equation (2.23) is valid to obtain correlation functions only for homogeneous systems ($|R| = 0$) and a half-line (no tunneling, $|R| = 1$). This is done by clubbing together one annihilation and one creation field operator as follows (e.g. consider $< \psi_R \psi_R^\dagger >$).

$$< \psi_R(x,\sigma,t)\psi_R^\dagger(x',\sigma,t') \ \sim \ < e^{i\theta_R(x,\sigma,t)} e^{-i\theta_R(x',\sigma,t')} > \tag{2.25}$$

The symbol '$\sim$' has been used instead of equal sign because there are prefactors associated to the Green functions which are not obtainable using bosonization techniques. These model dependent pre-factors have to be fixed by a comparison with the non-interacting Green functions obtained using Fermi algebra. The bosonization formulas are for calculating the dynamics of the system (the part of the Green functions which are functions of both position x and time t) and not for the pre-factors. Using a version of cumulant expansion (Baker-Campbell-Hausdorff formula) equation (2.25) can be written as follows.

$$< \psi_R(x,\sigma,t)\psi_R^\dagger(x',\sigma,t') > \ \sim \ e^{\frac{1}{2}<(i\theta_R(x,\sigma,t))^2>} e^{\frac{1}{2}<(-i\theta_R(x',\sigma,t'))^2>} e^{<(i\theta_R(x,\sigma,t))(-i\theta_R(x',\sigma,t'))>} \tag{2.26}$$

The third term in the above equation will lead to the correct term corresponding to the Green function (see equation (2.15)).

$$e^{<\theta_R(x,\sigma,t)\theta_R(x',\sigma,t')>} = \frac{1}{x - x' - v_F(t-t')}$$

while the first two terms (of the type $< \theta_R >^2$) become independent of time after proper calculation and are incorporated into the pre-factors. Now the form of field operator prescribed in equation (2.23) when applied to a system with an impurity, where there will be reflectional terms like $< \psi_R \psi_L^\dagger >$ and $< \psi_L \psi_R^\dagger >$ along with translational terms like $< \psi_R \psi_R^\dagger >$ and $< \psi_R \psi_R^\dagger >$, will yield the following.

$$< \psi_R(x,\sigma,t)\psi_L^\dagger(x',\sigma,t') > \ \sim \ e^{<\theta_R(x,\sigma,t)\theta_L(x',\sigma,t')>} = \frac{1}{(x + x' - v_F(t-t'))^{|R|^2}}$$

[1]When R appears as a subscript (as ψ_R or θ_R) it means a right mover. And in all other cases it means the reflection amplitude.

But from equation (2.15) we can see that for a system with an impurity, the Green function for RL (x and x' on the same side of the impurity) goes as follows.

$$< \psi_R(x,\sigma,t)\psi_L^\dagger(x',\sigma,t') > \quad \sim \quad \frac{1}{(x+x'-v_F(t-t'))}$$

Hence the standard way of defining the field operator given by equation (2.23) is applicable for system with an impurity only for the extreme case of $|R| = 1$. For all other cases ($0 < |R| < 1$), it leads to a non-trivial exponent ($|R|^2$) which is not acceptable. Hence the expression for the field operator given in equation (2.23) needs to be modified so that the non-interacting Green functions are reproduced correctly.

In NCBT, the field operator is modified to include the effect of back-scattering by impurities making it suitable to study translationally non-invariant systems such as the case of an impurity in a 1D system. The modified field operator of NCBT may be written as follows [90].

$$\psi_\nu(x,\sigma,t) \sim C_{\lambda,\nu,\gamma}\ e^{i\theta_\nu(x,\sigma,t)+2\pi i\lambda\nu\int_{sgn(x)\infty}^{x}\ \rho_s(-y,\sigma,t)dy} \tag{2.27}$$

Here θ_ν is the familiar local phase given by equation (2.24). NCBT differs by the addition of the optional term $\rho_s(-y,\sigma,t)$ to this local phase that ensures the necessary trivial exponents for the single particle Green functions for a system of otherwise free fermions with impurities (which may also be obtained using standard Fermi algebra). The adjustable parameter λ can take values either 1 or 0, which decides the presence or absence of the new term. In other words, setting $\lambda = 0$ reduces the NCBT operator to standard bosonization operator given in equation (2.23). The factor $2\pi i$ ensures that the field operator obeys the necessary fermion commutation rules since this term does not change the statistics of the field operator. $C_{\lambda,\nu,\gamma}$ are pre-factors (discussed earlier) which are fixed by comparison with the non-interacting Green functions obtained from Fermi algebra. The field operator as given in equation (2.27) is to be treated as a mnemonic to obtain the Green functions rather than an operator identity, which avoids the necessity of the Klein factors that are conventionally used. The RHS of equation (2.27) is a function of currents and densities. The current and density operators contain one one annihilation and one creation operators and are hence number conserving in nature. Hence the RHS, only comprising of such operators, is also number conserving. But as we can see from equation (2.27) that the LHS is an annihilation operator. Since the traditional bosonization calls this relation an operator identity, they have to ensure number conservation and for this they introduce something called as Klein factors to settle this issue. But the final Green functions or propagators, which are of physical significance and are to be calculated, contain equal number of annihilation and creation operators. Hence the Klein factors eventually cancel out. The field operators are merely an intermediate tool and hence one can avoid using the Klein factors in them provided one does not call them as operator identities. Hence the field operator given in equation (2.27) is a treated as a mnemonic and not as an operator identity.

Now using this new version of Fermi Bose correspondence given in equation (2.27) the Green function for RL (x and x' on the same side of the impurity) is given as follows.

$$< \psi_R(x,\sigma,t)\psi_L^{\dagger}(x',\sigma,t') > \\ \sim e^{<\left(\theta_R(x,\sigma,t)+2\pi\lambda\int_{sgn(x)\infty}^{x}\ \rho_s(-y,\sigma,t)dy\right)\left(\theta_L(x',\sigma,t')-2\pi\lambda'\int_{sgn(x)\infty}^{x}\ \rho_s(-y,\sigma,t)dy\right)>} \tag{2.28}$$

Choosing $(\lambda,\lambda') = (0,1)$ (or $(1,0)$) (in accordance with equation (3.19)) we have

$$e^{<\left(\theta_R(x,\sigma,t)+2\pi\int_{sgn(x)\infty}^{x}\ \rho_s(-y,\sigma,t)dy\right)(\theta_L(x',\sigma,t'))>} = \frac{1}{(x+x'-v_F(t-t'))} \tag{2.29}$$

which matches with that obtained from the standard Fermi algebra. Hence using the Fermi Bose corresponce prescribed by NCBT and given in equation (2.27), the two-point functions for free fermions in presence of an impurity of arbitrary strength can be obtained correctly.

2.2.4 Including interactions

Using the explicit form of the field operator prescribed by NCBT, the two point functions can be written in terms of the slow part of the density density correlation functions, called the bosonized version of the Green functions. This has to be verified for the non-interacting case by comparing with the Green functions obtained using standard Fermi algebra. Once this is done, the only thing left is to replace the DDCFs with their interacting version. For this the DDCF given in equation (2.19) has to be modified to include interactions. Now the interaction part of the Hamiltonian can be written as follows.

$$H_{int} = \frac{1}{2}\int_{-\infty}^{\infty} dx \int_{-\infty}^{\infty} dx^{'}\ v(x-x^{'})\ \rho(x)\rho(x^{'}) \tag{2.30}$$

Here $v(x-x^{'}) = \frac{1}{L}\sum_q v_q \exp\left[-iq(x-x^{'})\right]$ (where $v_q = 0$ if $|q| > \Lambda$ for some fixed bandwidth $\Lambda \ll k_F$ and $v_q = v_0$ is a constant, otherwise) is the forward scattering mutual interaction. In the present work, the temperature is assumed to be much less compared to the bandwidth 'Λv_F' of the Luttinger liquid, which is equivalent to saying that we are dealing with the infinite bandwidth case. In presence of this short ranged forward scattering mutual interaction, the DDCF is obtained to be the following (derived in Appendix C).

$$< T\ \rho_s(x_1,\sigma_1,t_1)\rho_s(x_2,\sigma_2,t_2) >= \frac{1}{4}\Big(< T\ \rho_h(x_1,t_1)\rho_h(x_2,t_2) > +\sigma_1\sigma_2 < T\ \rho_n(x_1,t_1)\rho_n(x_2,t_2) > \Big) \tag{2.31}$$

where

$$< T\ \rho_h(x_1,t_1)\rho_h(x_2,t_2) >= \frac{v_F}{2\pi^2 v_h}\sum_{\nu=\pm1}\Bigg(-\frac{1}{(x_1-x_2+\nu v_h(t_1-t_2))^2} - \frac{|R|^2}{\left(1-\frac{(v_h-v_F)}{v_h}|R|^2\right)}\frac{\frac{v_F}{v_h}\ \mathrm{sgn}(x_1)\mathrm{sgn}(x_2)}{(|x_1|+|x_2|+\nu v_h(t_1-t_2))^2}\Bigg)$$

$$< T\ \rho_n(x_1,t_1)\rho_n(x_2,t_2) >= \frac{1}{2\pi^2}\sum_{\nu=\pm1}\Bigg(-\frac{1}{(x_1-x_2+\nu v_F(t_1-t_2))^2} - \frac{\mathrm{sgn}(x_1)\mathrm{sgn}(x_2)\ |R|^2}{(|x_1|+|x_2|+\nu v_F(t_1-t_2))^2}\Bigg) \tag{2.32}$$

Here $\rho_h(x,t) = \rho_s(x,\uparrow,t)+\rho_s(x,\downarrow,t)$ is the "holon" density and $\rho_n(x,t) = \rho_s(x,\uparrow,t)-\rho_s(x,\downarrow,t)$ is the "spinon" density. The holon velocity is given by $v_h = \sqrt{v_F^2+2v_F v_0/\pi}$ (v_0 is the strength of mutual interaction) whereas the spinon velocity is the same as the Fermi velocity v_F since it is the total density that couples to the short range potential. The presence of two different velocities is a signature of spin charge separation which is typical to 1D systems.

2.2.5 Many body Green functions

The full Green functions of the system in presence of both impurity and mutual interaction is obtaining by replacing the density density correlation functions in the bosonization formulas with their interacting version given by equations (2.31) and (2.32). The full Green function is the sum of all the parts (**Notation:** $X_i \equiv (x_i,\sigma_i,t_i)$ and $\tau_{12} = t_1 - t_2$).

$$\begin{aligned} < T\ \psi(X_1)\psi^\dagger(X_2) >= &< T\ \psi_R(X_1)\psi_R^\dagger(X_2) > + < T\ \psi_L(X_1)\psi_L^\dagger(X_2) > \\ &+ < T\ \psi_R(X_1)\psi_L^\dagger(X_2) > + < T\ \psi_L(X_1)\psi_R^\dagger(X_2) > \end{aligned} \tag{2.33}$$

and each part is a power law and takes the following form ($\nu_i = \pm1$).

$$< T\ \psi_{\nu_1}(X_1)\psi_{\nu_2}^\dagger(X_2) > \ \sim\ \frac{1}{(x_1-x_2-v_h\tau_{12})^A(-x_1+x_2-v_h\tau_{12})^B(x_1+x_2-v_h\tau_{12})^C} \frac{1}{(-x_1-x_2-v_h\tau_{12})^D(\nu_1x_1-\nu_2x_2-v_F\tau_{12})^{0.5}} \tag{2.34}$$

where A, B, C and D are system dependent exponents which are functions of the strength of interaction v_0 and the strength of impurity V_0 (and also the Fermi velocity v_F). On setting $v_0 = 0$, these Green functions takes the exact same form of the non interacting ones obtainable using Fermi algebra (equation (2.15)). The above Green functions is for zero temperature. The finite temperature versions of the formulas below can be obtained by replacing Z by $[\frac{\beta v_F}{\pi}Sinh[\frac{\pi Z}{\beta v_F}]]$ where Z represents terms having the form $[(\nu_1x_1-\nu_2x_2)-v_a(t_1-t_2)]$ (which

are present in the denominator of equation (2.34)) and v_a can be either v_h or v_F signifying holon or spinon velocity respectively.

2.3 Summary

In this chapter, the formalism of Non chiral bosonization technique is discussed. A few drawbacks of the conventional bosonization technique are pointed out which highlights the need of rectifying the technical aspects of g-ology based bosonization techniques by adopting NCBT. The step by step procedure of calculating the correlation functions was discussed, which can be summarized as follows. **a)** First the single particle two point functions is calculated in the RPA limit in presence of the external impurity potential. **b)** From the two point functions, the slow part of the density density correlation functions (DDCF) is calculated. **c)** The two point functions in (a) is expressed in terms of the densities calculated in (b), which is now called the bosonized version of the Green function. **d)** The DDCFs in (b) is modified to include interactions. **e)** In the bosonized version of the Green function obtained in (c), all the densities are replaced by their interacting versions obtained in (d) to get the Green function in presence of interactions as well as impurities.

Chapter 3

The quantum steeplechase

The quantum steeplechase is the study of a Luttinger liquid in one dimension in the presence of a finite number of barriers and wells clustered around an origin (figure 3.1). The powerful non-chiral bosonization technique (NCBT) is used to write down closed formulas for the two-point function of these systems in the sense of the random phase approximation (RPA). Unlike g-ology based methods [5] that are tied to the translationally invariant, free particle basis, the NCBT explicitly makes use of the translationally non-invariant single particle wavefunctions. The present approach, which amounts to constructing the 'restricted Hilbert space of states' not for free fermions but for free fermions plus these barriers/wells or weak links, is able to study the problem of Luttinger liquids in the presence of these imperfections more easily and is able to provide analytical expressions for the most singular part of the Green functions and so on that interpolate between the weak barrier and weak link cases.

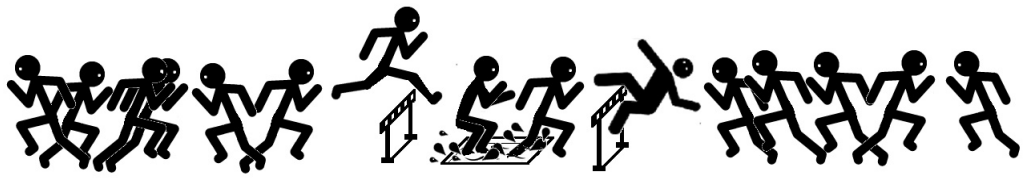

FIGURE 3.1: The Quantum Steeplechase: Athletes (representing electrons) crossing/bouncing off hurdles (potential barriers) and water-jumps (potential wells) while moving in both directions with the fastest athlete possessing the Fermi momentum and rubbing shoulders with each other (representing forward scattering short-range interactions)

The study of the effect of impurities in Luttinger liquids constitutes an important area of theoretical condensed matter physics, especially during the last few decades. The detailed study of transport in Luttinger liquid (LL) in the presence of a weak link was started by Kane and Fisher [31] followed by the study of a LL near a double barrier [32]. Since then a number of papers have appeared that have generalized these ideas using a variety of approaches which include fermionic renormalization [49], path integral approaches [46], functional renormalization [50, 53, 56, 59, 60], flow equations for Hamiltonians [52], functional integral formalism

[54], Monte Carlo methods [62] and so on. Different physical phenomena are also studied in Luttinger liquids with impurities: Friedel oscillations [91], conductance [92, 93], Kondo effect [94, 95], etc. Experimental realizations of 1D systems give a motivational boost to study quantum physics in one dimension. In this regard, Luttinger liquid behavior in carbon nano-tubes [42, 96], experimental evidences of resonant tunneling in a Luttinger liquid [97] are worth mentioning. But what is missing in the existing literature are explicit expressions of the correlation functions of a Luttinger liquid with localized potentials of arbitrary strengths in terms of elementary functions of positions and times. The best available are limiting cases for a weak barrier [5] and an infinite barrier [40] which can be obtained using conventional bosonization schemes.

In the present chapter [90, 98], we use the non chiral bosonization technique to provide the most singular part of the asymptotically exact Green functions of a Luttinger liquid with a cluster of impurities (of arbitrary strengths) and with the short-range forward scattering between the fermions. The obtained two point functions are used to study the dynamical density of states (DDOS) of the system which is a power law in case of a Luttinger liquid and thereby calculating the DDOS exponent. The non standard harmonic analysis used in NCBT is used to obtain the four point functions relevant to the study of Friedel oscillations.

3.1 System description

Consider a Luttinger liquid in one dimension with forward scattering short-range mutual interactions [5] in the presence of a scalar potential V(x) that is localized near an origin. The full generic-Hamiltonian of the system(s) under study (before taking the RPA limit) is (are),

$$H = \int_{-\infty}^{\infty} dx\ \psi^{\dagger}(x) \left(-\frac{1}{2m}\partial_x^2 + V(x) \right) \psi(x) + \frac{1}{2} \int_{-\infty}^{\infty} dx \int_{-\infty}^{\infty} dx'\ v(x-x')\ \rho(x)\rho(x') \tag{3.1}$$

where $v(x-x') = \frac{1}{L}\sum_q v_q \exp\left[-iq(x-x')\right]$ (where $v_q = 0$ if $|q| > \Lambda$ for some fixed bandwidth $\Lambda \ll k_F$ and $v_q = v_0$ is a constant, otherwise) is the forward scattering mutual interaction, L being the size of the system. Also, $V(x)$ is the external potential which represents the cluster of impurities around a fixed point. This potential is denoted by a black box indicating that it can be any finite sequence of barriers and wells. It can be as simple as a single delta potential or rather complicated like three delta potentials lying close to each other. The situation is described in figure 3.2 using playing cards. Assume that the cluster of potentials around the origin is unknown to us and thus represented by the black box in the unflipped card. Let the reflection and transmission amplitudes be called "R" and "T" respectively. The final Green functions will be a function of these Rs and Ts. At the end, one can replace the Rs and Ts with their explicit expressions for which one need to know the actual form of the potentials. This is done by flipping the card and calculating T and R in terms of the potential of that particular card.

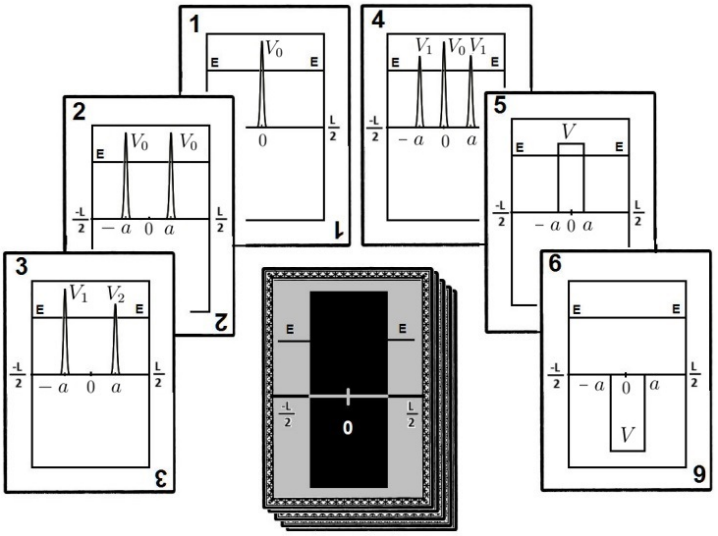

FIGURE 3.2: The black box: The back of each of the cards contains the black box (shown in the central deck) and when they are flipped, the contents of the black box are revealed as any one of the cluster of potentials near an origin. The formulas for the revealed potentials are as follows: (1) $V(x) = V_0\delta(x)$; (2) $V(x) = V_0(\delta(x+a)+\delta(x-a))$; (3) $V(x) = V_1\delta(x+a)+V_2\delta(x-a)$; (4) $V(x) = V_0\delta(x) + V_1(\delta(x \pm a))$; (5)$V(x) = V\theta(x+a)\theta(a-x)$; (6) $V(x) = -V\theta(x+a)\theta(a-x)$

The following potentials have been considered.

$$V(x) = \begin{cases} V_0\delta(x) & \text{(single delta)} \\ V_0(\delta(x+a)+\delta(x-a)) & \text{(symmetric double delta)} \\ V_1\delta(x+a)+V_2\delta(x-a) & \text{(asymmetric double delta)} \\ V_0\delta(x)+V_1(\delta(x\pm a)) & \text{(symmetric triple delta)} \\ V\theta(x+a)\theta(a-x) & \text{(finite barrier)} \\ -V\theta(x+a)\theta(a-x) & \text{(finite well)} \end{cases} \tag{3.2}$$

Here $\theta(x)$ is the Heaviside step function. The density is given by $\rho(x,t) = \psi^\dagger(x,t)\psi(x,t) - \rho_0$ (no point splitting is required before taking RPA limit). The central goal of this chapter is to write down the Green functions of these systems at zero and at finite temperature in the presence of the potentials described in equation (3.2) . For an analytical solution to be feasible when mutual interactions are included, it is necessary to confine the study to the so-called RPA limit which means, among other things, working in the limit where the Fermi momentum and the mass of the fermion diverge in such a way that their ratio is finite (i.e. $k_F, m \to \infty$ but $k_F/m = v_F < \infty$: units that make $\hbar = 1$, so that k_F is both the Fermi momentum as well as a wavenumber, are used) [87]. This amounts to linearizing the energy momentum dispersion near the Fermi surface ($E = E_F + pv_F$ instead of $E = p^2/(2m)$). Furthermore, if 'w' is the width of the cluster, it is then imperative to define how w scales in the RPA limit. The assertion made is that in the RPA limit $k_F w < \infty$ as $k_F \to \infty$. Similarly the heights and depths of the various barriers are assumed to be in fixed ratios with the Fermi energy

$E_F = \frac{1}{2}mv_F^2$ even as $m \to \infty$ with $v_F < \infty$. The systematic procedure for calculating the Green functions has been described in the previous chapter.

3.2 Green's functions of free fermions

Denote the full two-point Green function (also known as single particle Green function) of the system before taking the RPA limit (i.e. with parabolic energy-momentum relation) as $< T\ \psi(x,\sigma,t)\psi^\dagger(x',\sigma',t') >$ where the time ordering decides whether it is particle or hole Green function that is being studied and σ is the spin projection of the individual fermions. In terms of this, the asymptotic or RPA Green function is defined by "smearing out" the positions and times over the scale of the Fermi wavelength and Fermi times as follows,

$$\langle T\ \psi_\nu(x,\sigma,t)\psi^\dagger_{\nu'}(x',\sigma',t')\rangle = \lim_{m\to\infty} \ll \langle T\psi(y,\sigma,\tau)\psi^\dagger(y',\sigma',\tau')\rangle e^{-ik_F(\nu y-\nu' y')} e^{iE_F(\tau-\tau')} \gg \tag{3.3}$$

where,

$$\begin{aligned} \ll f(t) \gg &= \frac{1}{2T_F}\int_{t-T_F}^{t+T_F} d\tau\ f(\tau) \\ \ll g(x) \gg &= \frac{1}{2\lambda_F}\int_{x-\lambda_F}^{x+\lambda_F} dy\ g(y) \end{aligned} \tag{3.4}$$

with $\lambda_F = 2\pi/k_F$ and $T_F = 2\pi/E_F$, $k_F = mv_F$ and $E_F = (1/2)mv_F^2$ with $v_F < \infty$ being held fixed. Also, here $\nu, \nu^{'} = \pm 1$ correspond to the right and left Fermi points.

We start with the non-interacting Hamiltonian (after dropping the last term of equation (3.1)) and calculate the two orthonormal set of wavefunctions, one with the propagation starting from the left and the other with that starting from the right. The wavefunctions are subjected to the RPA limit discussed in the previous section. Using the spectral decomposition method [99, 100] the two-point Green function is obtained in position and energy coordinates, which undergoes a Fourier transform to yield the space-time two-point functions which has the following form (at zero temperature),

$$\langle T\ \psi_\nu(x,\sigma,t)\psi^\dagger_{\nu'}(x',\sigma',t')\rangle_0 = \sum_{\gamma,\gamma'=\pm1} \frac{\theta(\gamma x)\theta(\gamma' x')\ g_{\gamma,\gamma'}(\nu,\nu')}{(\nu x - \nu' x') - v_F(t-t')}\delta_{\sigma,\sigma'} \tag{3.5}$$

where $\theta(x)$ is Heaviside's step function and the expressions for $g_{\gamma,\gamma'}(\nu,\nu')$'s are given in table 3.1. Thus the above equation expresses the general Green functions of all the sub-cases in figure 3.2 in terms of their reflection (R) and transmission (T) amplitudes such that $|T|^2 + |R|^2 = 1$.

The next task is to calculate the values of the transmission (T) and reflection (R) amplitudes for all the sub-cases of equation (3.2) which can be done using elementary knowledge of quantum mechanics and are given below.

TABLE 3.1: Values of $g_{\gamma,\gamma'}(\nu,\nu')$ for the general case.

$g_{(\gamma,\gamma')}(\nu,\nu')$	γ=1,γ'=1	γ=−1,γ'=−1	γ=1,γ'=−1	γ=−1,γ'=1
$(\nu,\nu')=(1,1)$	$\frac{i}{2\pi}$	$\frac{i}{2\pi}$	$\frac{i}{2\pi}T$	$\frac{i}{2\pi}T^*$
$(\nu,\nu')=(-1,-1)$	$\frac{i}{2\pi}$	$\frac{i}{2\pi}$	$\frac{i}{2\pi}T^*$	$\frac{i}{2\pi}T$
$(\nu,\nu')=(1,-1)$	$\frac{i}{2\pi}R$	$\frac{i}{2\pi}R^*$	0	0
$(\nu,\nu')=(-1,1)$	$\frac{i}{2\pi}R^*$	$\frac{i}{2\pi}R$	0	0

(a) Single delta-function

$$T=\frac{1}{\left(1+V_0\frac{i}{v_F}\right)}\;;\;R=-\frac{iV_0}{v_F\left(1+V_0\frac{i}{v_F}\right)} \tag{3.6}$$

(b) Symmetric double delta-function

$$T=\frac{1}{\left(1+V_0\frac{i}{v_F}\right)^2-\left(\frac{iV_0}{v_F}e^{i\xi_0}\right)^2}\;;\;R=-\frac{2i\frac{V_0^2}{v_F^2}\sin[\xi_0]+\frac{2iV_0}{v_F}\cos[\xi_0]}{\left(1+V_0\frac{i}{v_F}\right)^2-\left(\frac{iV_0}{v_F}e^{i\xi_0}\right)^2} \tag{3.7}$$

(c) Asymmetric double delta-function

$$T=\frac{1}{\left(1+i\frac{V_1+V_2}{v_F}+\frac{i^2V_1V_2}{v_F^2}\right)+\frac{V_1V_2}{v_F^2}e^{2i\xi_0}}\;;\;R=-\frac{2i\frac{V_1V_2}{v_F^2}\sin[\xi_0]+\frac{2i}{v_F}\left(\frac{V_1e^{i\xi_0}+V_2e^{-i\xi_0}}{2}\right)}{\left(1+i\frac{V_1+V_2}{v_F}+\frac{i^2V_1V_2}{v_F^2}\right)+\frac{V_1V_2}{v_F^2}e^{2i\xi_0}} \tag{3.8}$$

(d) Symmetric triple delta-function

$$T=\frac{1}{\left(1-i\frac{V_0V_1^2}{v_F^3}-2\frac{V_0V_1}{v_F^2}-\frac{V_1^2}{v_F^2}+i\frac{V_0}{v_F}+2i\frac{V_1}{v_F}\right)+\frac{e^{i\xi_0}}{v_F^2}\left(2i\frac{V_0V_1^2}{v_F}-ie^{i\xi_0}\frac{V_0V_1^2}{v_F}+2V_0V_1+e^{i\xi_0}V_1^2\right)}$$

$$R=-\frac{2i\frac{V_0V_1^2}{v_F^3}-2i\frac{V_0V_1^2}{v_F^3}\cos[\xi_0]+2i\frac{V_0V_1}{v_F^2}\sin[\xi_0]+2i\frac{V_1^2}{v_F^2}\sin[\xi_0]+i\frac{V_0}{v_F}+2i\frac{V_1}{v_F}\cos[\xi_0]}{\left(1-i\frac{V_0V_1^2}{v_F^3}-2\frac{V_0V_1}{v_F^2}-\frac{V_1^2}{v_F^2}+i\frac{V_0}{v_F}+2i\frac{V_1}{v_F}\right)+\frac{e^{i\xi_0}}{v_F^2}\left(2i\frac{V_0V_1^2}{v_F}-ie^{i\xi_0}\frac{V_0V_1^2}{v_F}+2V_0V_1+e^{i\xi_0}V_1^2\right)} \tag{3.9}$$

Note: The expressions are derived in Appendix H. For the cases below $\lambda=\frac{V}{E_F}$ is fixed while taking the RPA limit. V is the well depth or barrier height. $E_F=\frac{1}{2}mv_F^2$ is the Fermi energy. $\xi_0=2k_Fa$ where k_F is the Fermi momentum and the barrier (or well) goes from '$-a$' to 'a'.

(e) Finite barrier tunneling

$$\begin{aligned}T&=\frac{4ie^{-i\xi_0}\sqrt{\lambda-1}}{4i\sqrt{\lambda-1}\cosh[\xi_0\sqrt{(\lambda-1)}]+2(2-\lambda)\sinh[\xi_0\sqrt{(\lambda-1)}]}\\R&=\frac{e^{-i\xi_0}2\lambda\sinh[\xi_0\sqrt{(\lambda-1)}]}{4i\sqrt{\lambda-1}\cosh[\xi_0\sqrt{(\lambda-1)}]+2(2-\lambda)\sinh[\xi_0\sqrt{(\lambda-1)}]}\end{aligned} \tag{3.10}$$

(f) Finite well scattering $(E > 0)$

$$
\begin{aligned}
T =& \frac{4e^{-i\xi_0}\sqrt{\lambda+1}}{4\sqrt{\lambda+1}\cos\left[\xi_0\sqrt{(\lambda+1)}\right] - 2i(2+\lambda)\sin\left[\xi_0\sqrt{(\lambda+1)}\right]} \\
R =& \frac{e^{-i\xi_0}2i\lambda\sin\left[\xi_0\sqrt{(\lambda+1)}\right]}{4\sqrt{\lambda+1}\cos\left[\xi_0\sqrt{(\lambda+1)}\right] - 2i(2+\lambda)\sin\left[\xi_0\sqrt{(\lambda+1)}\right]}
\end{aligned}
\tag{3.11}
$$

It can be shown that on taking proper limiting conditions, one can obtain one case from another, for example, from finite barrier to singe delta, from asymmetric double delta to symmetric double delta and so on. For potentials which lack inversion symmetry about any chosen point, (e.g. asymmetric double deltas) the presence of nontrivial phases in T and R contribute to the expected lack of inversion symmetry in the Green's functions.

Note that in equation (3.5), the term $[(\nu x - \nu' x') - v_F(t-t')]$ appears in the denominator. In general, in a Luttinger liquid with mutual interactions, this term appears with a non-trivial system dependent exponent viz. as $[(\nu x - \nu' x') - v_F(t-t')]^g$. Listing these g's and other similar exponents is one of the main goals of this work since $g = 1$ is only when mutual interaction between fermions are absent. It is easy to generalize these results to finite temperature since for this a simple replacement, viz., $\frac{1}{X} \to \frac{\pi}{\beta v_F}\ csch[\frac{\pi X}{\beta v_F}]$ is sufficient where e.g. $X \equiv [(\nu x - \nu' x') - v_F(t-t')]$ and β is inverse temperature.

3.2.1 Density density correlation function

The other main goal of this work to write down the density-density correlation function (DDCF) of the system which is a special case of a 4-point function. In the RPA sense, the density $\rho(x,t)$ may be "harmonically analyzed" as follows.

$$
\rho(x,t) = \rho_s(x,t) + e^{2ik_F x}\ \rho_f(x,t) + e^{-2ik_F x}\ \rho_f^*(x,t) \tag{3.12}
$$

The slowly varying part of the density ρ_s (the average density is subtracted out, so this is really the deviation) has an auto-correlation function which when mutual interactions are absent, may be written down using Wick's theorem as follows,

$$
\langle T\ \rho_s(x,t)\rho_s(x^{'},t^{'})\rangle_0 = -\sum_{\substack{\gamma,\gamma^{'}\\=\pm 1}}\ \sum_{\substack{\nu,\nu^{'}\\=\pm 1}} \frac{|g_{\gamma,\gamma'}(\nu,\nu')|^2\ \theta(\gamma x)\theta(\gamma' x')}{[(\nu x - \nu' x') - v_F(t-t')]^2} \tag{3.13}
$$

where $g_{\gamma,\gamma'}(\nu,\nu')$ are given in table 3.1. These three relations viz. equation (3.5), equation (3.12) and equation (3.13) shall be used in the subsequent sections as input to the NCBT scheme in order to enable an explicit evaluation of the Green functions.

3.3 Bosonized version of the N-point Green's functions

Just as the density may be harmonically analyzed, the field may also be harmonically analyzed so that $\psi(x) = e^{ik_F x}\ \psi_R(x) + e^{-ik_F x}\ \psi_L(x)$. Bosonization involves inverting the defining formulas for current and number densities viz. $j(x) = Im[\psi^\dagger(x)\partial_x\psi(x)]$ and $\rho(x) = \psi^\dagger(x)\psi(x)$ and rewriting $\psi(x)$ in terms of j and ρ. Then the continuity equation $\partial_t\rho + \partial_x j = 0$ is invoked to write $\psi(x)$ purely as a (non-local) function of ρ and $\partial_t\rho$. It follows therefore, that the the N-point function is some combination of the correlations of the density field with itself. Bosonization may be thought of as the "inverse of Wick's theorem". While Wick's theorem - which is valid only for systems with no mutual interactions - seeks to express higher order correlations in terms of lower order ones, bosonization seeks to express the single particle Green function in terms of the higher order density-density correlations. The inversion of the defining relation between current and densities in the standard bosonization scheme that goes by the name g-ology (see the book by Giamarchi [5]) yields the following relation between $\psi_\nu(x,\sigma,t)$ (where $\nu = R(+1)\ or\ L(-1)$) and the slowly varying part of the density (this is a mnemonic for generating the N-point functions),

$$\psi_\nu(x,\sigma,t) \sim \exp\left[i\theta_\nu(x,\sigma,t)\right] \tag{3.14}$$

with the local phase given by the formula,

$$\theta_\nu(x,\sigma,t) = \pi \int_{sgn(x)\infty}^{x} dy \left(\nu\ \rho_s(y,\sigma,t) - \int_{sgn(y)\infty}^{y} dy'\ \partial_{v_F t}\ \rho_s(y',\sigma,t) \right) \tag{3.15}$$

The above prescription in equation (3.14) is valid for nearly translationally invariant systems (i.e. with possible external potentials with Fourier components small compared to the Fermi momentum) and for systems with a half line (no tunneling across the barrier). In the present approach, a modification of the correspondence of equation (3.14) is introduced wherein the correlation functions of a system of free fermions plus barriers and wells with arbitrary heights (depths) can be as easily computed in the bosonized language as it is in the original Fermi language.

$$\psi_{\nu_i}(x_i,\sigma_i,t_i) \rightarrow \sum_{\gamma_i=\pm 1} \sum_{\lambda_i\in\{0,1\}} C_{\lambda_i,\nu_i,\gamma_i}(\sigma_i)\ \theta(\gamma_i x_i)\ e^{i\theta_{\nu_i}(x_i,\sigma_i,t_i) + 2\pi i\nu_i\lambda_i \int_{sgn(x_i)\infty}^{x_i} \rho_s(-y_i,\sigma_i,t_i)\ dy_i} \tag{3.16}$$

This 'non-standard harmonic analysis' is an alternative to the usual one invoked while using g-ology methods which is valid for translationally invariant systems and half lines whereas the harmonic analysis in equation (3.16) is valid for systems considered in this chapter. Current algebra, point splitting constraints, etc. continue to be obeyed by this new Fermi-Bose correspondence (see chapter 7).

An analogy with the anharmonic oscillator problem in undergraduate quantum mechanics may be useful. One could either study this problem in the the translationally invariant plane

wave basis or more conveniently in a basis closer to the real ground state of the system viz. the states of the simple harmonic oscillator. While technically there is nothing wrong with using the plane wave basis, this really makes the problem quite complicated. Using equation (3.14) to study the problem of fermions in presence of barriers and wells is somewhat like using the plane wave basis to study the anharmonic oscillator. It is much better to use equation (3.16) which is analogous to using the harmonic oscillator basis to study the anharmonic oscillator.

The quantities $C_{\lambda_i,\nu_i,\gamma_i}(\sigma_i)$ are c-numbers and involve cutoffs and such, which, as in the traditional approach, are not obtainable using these techniques (see section 3.4.4 for more about these c-numbers). The only quantities that have absolute meaning are the anomalous exponents i.e., numbers g when the term involved appears as $[(\nu x - \nu^{'} x^{'}) - v_F(t - t^{'})]^g$. The operators that appear in the exponent in equation (3.16) are the ones that are really crucial in this approach since they provide the right anomalous exponents. The crucial new ingredient in the modified formula in equation (3.16) is the term involving $\rho_s(-y_i, \sigma_i, t_i)$ that ensures that the effects of backscattering from the external potentials are automatically and naturally taken into account so that the mandated trivial exponents are obtained when equation (3.16) is used to compute the N-point functions in the sense of the RPA. The addition of these new terms does not spoil fermion commutation rules since there is a prefactor of $2\pi i\nu_i$ next to it which ensure that fermion commutation relations of the fields are respected. These new terms also do not spoil the point-splitting constraints for the Fermi bilinears, which is an opaque way of saying that when equation (3.16) is used to infer the currents and densities - as the latter two are, after all, bilinears of the Fermi fields - the resulting expressions are in accordance with expectations.

In order to extract the anomalous exponents of the system with mutual interactions, two things remain. One is to generalize equation (3.13) to include mutual interactions. The other is to derive a prescription for choosing the values of the crucial parameters $\lambda_i = 0, 1$ which indicates when the traditional form of the field needs modification. It simply involves making sure that the prescription (which is unique) leads to N-point functions of the system (without mutual interactions) identical to what is given by Wick's theorem. This is done subsequently below. In addition to these $\lambda_i^{'}s$, auto-correlation functions of the slowly varying parts of the density when mutual interactions are present are needed.

Again in the spirit of the RPA, the density density correlation functions given in equation (3.13) are modified to include mutual interactions and the following formula may be obtained ($\rho_h(x,t) = \rho_s(x,\uparrow,t) + \rho_s(x,\downarrow,t)$ is the "holon" density and $\rho_n(x,t) = \rho_s(x,\uparrow,t) - \rho_s(x,\downarrow,t)$ is the "spinon" density and $a = h$ for holon and $a = n$ for spinon, see Appendix C for details)

$$\langle T\ \rho_a(x_1,t_1)\rho_a(x_2,t_2)\rangle = \frac{v_F}{2\pi^2 v_a}\sum_{\nu=\pm 1}\left(\frac{-1}{(x_1 - x_2 + \nu v_a(t_1 - t_2))^2} - \frac{\frac{v_F}{v_a}\ \mathrm{sgn}(x_1)\mathrm{sgn}(x_2)\ Z_a}{(|x_1| + |x_2| + \nu v_a(t_1 - t_2))^2}\right) \tag{3.17}$$

where $a = n$ (spinon) or h (holon) and,

$$Z_a = \frac{|R|^2}{\left(1 - \delta_{a,h}\frac{(v_h - v_F)}{v_h}|R|^2\right)} \tag{3.18}$$

Here the spinon velocity is just the Fermi velocity since it is the total density that couples to the short-range potential: $v_n = v_F$, but the holon velocity is modified by interactions, $v_h = \sqrt{v_F^2 + 2v_F v_0/\pi}$ where the interaction between fermions is the two-body short-range forward scattering potential which just means the potential between two particles at x and $x^{'}$ is $V(x - x^{'}) = \frac{1}{L}\sum_{|q|<\Lambda} v_0 \ \exp\left[-iq(x - x^{'})\right]$, where Λ is held fixed as the RPA limit is taken. Finally, $\langle T\ \rho_n(x_1, t_1)\rho_h(x_2, t_2)\rangle \equiv 0$. It can be shown that an expansion of equation (3.17) in powers of v_0 matches with the corresponding series obtained by standard perturbation theory so long as one retains only the most singular terms.

3.4 Full two-point Green's function

The two-point (single-particle) Green's function may be written down using the correspondence in equation (3.16). Only the anomalous exponents which refer to the constants g that appear in terms of the form $[\nu_1 x_1 - \nu_2 x_2 - v_F(t_1 - t_2)]^g$ that emerge from this calculation are of interest here. These g's are uniquely pinned down once a prescription for deciding which of the $\lambda_i^{'}s$ are zero or one and under what circumstances is given. This prescription follows unambiguously by requiring that an evaluation (of the 2M-point function) in the Gaussian (and RPA) sense leads to trivial exponents when mutual interactions between fermions are absent. Of lesser importance are the coefficients $C^{'}s$ which depend on the details of the potentials and cutoffs and other such non-universal features, as is also the case in the conventional approach. The prescription for obtaining the $\lambda_i^{'}s$ are simple. Consider a general 2M-point function. Imagine mentally pairing up one annihilation operator with one creation operator and create M such pairs. This is simply a mental activity since this pairing (Wick's theorem) is not valid when mutual interactions are present. Consider one such pair and let the two λ's of this pair be (λ_m, λ_k) where $k > m$. The constraints are as follows:

$$\lambda_m = \begin{cases} \lambda_k & \text{if } (\nu_m, \nu_k) = (\gamma_m, \gamma_k) \text{ or } (\nu_m, \nu_k) = (-\gamma_m, -\gamma_k) \\ 1 - \lambda_k & \text{if } (\nu_m, \nu_k) = (-\gamma_m, \gamma_k) \text{ or } (\nu_m, \nu_k) = (\gamma_m, -\gamma_k) \end{cases} \tag{3.19}$$

This (unique) prescription guarantees the right trivial exponents in the right places when mutual interactions are turned off. The full Green's function in presence of interactions are as follows (**Notation:** $X_i \equiv (x_i, \sigma_i, t_i)$, also, in order to remove ambiguities associated with cutoff dependent quantities in translationally non-invariant systems, the notion of weak equality denoted by $A[X_1, X_2] \sim B[X_1, X_2]$ is introduced which really means

$\partial_{t_1} Log[A[X_1, X_2]] = \partial_{t_1} Log[B[X_1, X_2]]$ assuming of course, A and B do not vanish identically. Furthermore the finite temperature versions of the formulas below are obtained by replacing $Log[Z]$ by $Log[\frac{\beta v_F}{\pi} Sinh[\frac{\pi Z}{\beta v_F}]]$ where $Z \sim [(\nu x_1 - \nu^{'} x_2) - v_a(t_1 - t_2)]$ and singular cutoffs ubiquitous in this subject are suppressed in this notation for brevity - they have to be understood to be present. The notion of weak equality is unable to pin down possible prefactors in the Green functions that may even be spatially inhomogeneous (but time independent) in addition to being singular. The inhomogeneous prefactors are nothing but terms such as $e^{\frac{1}{2}\langle A^2 \rangle}$ and $e^{\frac{1}{2}\langle B^2 \rangle}$ that come about when when evaluating $\langle e^A e^B \rangle = e^{\frac{1}{2}\langle A^2 \rangle} e^{\frac{1}{2}\langle B^2 \rangle} e^{\langle AB \rangle}$ where $\langle AB \rangle \propto Log[(\nu x_1 - \nu^{'} x_2) - v_a(t_1 - t_2)]$. It must be stressed that these inhomogeneous prefactors are important for extracting the exponents associated with tunneling conductance and the local dynamical density of states. Here $\tau_{12} = t_1 - t_2$):

Case I : x_1 and x_2 on the same side of the origin

$$\Big\langle T\ \psi_R(X_1)\psi_R^{\dagger}(X_2)\Big\rangle$$
$$\sim \frac{(4x_1x_2)^{\gamma_1}}{(x_1 - x_2 - v_h\tau_{12})^P(-x_1 + x_2 - v_h\tau_{12})^Q(x_1 + x_2 - v_h\tau_{12})^X(-x_1 - x_2 - v_h\tau_{12})^X(x_1 - x_2 - v_F\tau_{12})^{0.5}}$$
$$\Big\langle T\ \psi_L(X_1)\psi_L^{\dagger}(X_2)\Big\rangle$$
$$\sim \frac{(4x_1x_2)^{\gamma_1}}{(x_1 - x_2 - v_h\tau_{12})^Q(-x_1 + x_2 - v_h\tau_{12})^P(x_1 + x_2 - v_h\tau_{12})^X(-x_1 - x_2 - v_h\tau_{12})^X(-x_1 + x_2 - v_F\tau_{12})^{0.5}}$$
$$\Big\langle T\ \psi_R(X_1)\psi_L^{\dagger}(X_2)\Big\rangle$$
$$\sim \frac{(2x_1)^{1+\gamma_2}(2x_2)^{\gamma_1}}{2(x_1 - x_2 - v_h\tau_{12})^S(-x_1 + x_2 - v_h\tau_{12})^S(x_1 + x_2 - v_h\tau_{12})^Y(-x_1 - x_2 - v_h\tau_{12})^Z(x_1 + x_2 - v_F\tau_{12})^{0.5}}$$
$$+ \frac{(2x_1)^{\gamma_1}(2x_2)^{1+\gamma_2}}{2(x_1 - x_2 - v_h\tau_{12})^S(-x_1 + x_2 - v_h\tau_{12})^S(x_1 + x_2 - v_h\tau_{12})^Y(-x_1 - x_2 - v_h\tau_{12})^Z(x_1 + x_2 - v_F\tau_{12})^{0.5}}$$
$$\Big\langle T\ \psi_L(X_1)\psi_R^{\dagger}(X_2)\Big\rangle$$
$$\sim \frac{(2x_1)^{1+\gamma_2}(2x_2)^{\gamma_1}}{2(x_1 - x_2 - v_h\tau_{12})^S(-x_1 + x_2 - v_h\tau_{12})^S(x_1 + x_2 - v_h\tau_{12})^Z(-x_1 - x_2 - v_h\tau_{12})^Y(-x_1 - x_2 - v_F\tau_{12})^{0.5}}$$
$$+ \frac{(2x_1)^{\gamma_1}(2x_2)^{1+\gamma_2}}{2(x_1 - x_2 - v_h\tau_{12})^S(-x_1 + x_2 - v_h\tau_{12})^S(x_1 + x_2 - v_h\tau_{12})^Z(-x_1 - x_2 - v_h\tau_{12})^Y(-x_1 - x_2 - v_F\tau_{12})^{0.5}}$$

(3.20)

Case II : x_1 and x_2 on opposite sides of the origin

$$\Big\langle T\ \psi_R(X_1)\psi_R^{\dagger}(X_2)\Big\rangle$$
$$\sim \frac{(2x_1)^{1+\gamma_2}(2x_2)^{\gamma_1}(x_1 + x_2)^{-1}(x_1 + x_2 + v_F\tau_{12})^{0.5}}{2(x_1 - x_2 - v_h\tau_{12})^A(-x_1 + x_2 - v_h\tau_{12})^B(x_1 + x_2 - v_h\tau_{12})^C(-x_1 - x_2 - v_h\tau_{12})^D(x_1 - x_2 - v_F\tau_{12})^{0.5}}$$
$$+ \frac{(2x_1)^{\gamma_1}(2x_2)^{1+\gamma_2}(x_1 + x_2)^{-1}(x_1 + x_2 - v_F\tau_{12})^{0.5}}{2(x_1 - x_2 - v_h\tau_{12})^A(-x_1 + x_2 - v_h\tau_{12})^B(x_1 + x_2 - v_h\tau_{12})^D(-x_1 - x_2 - v_h\tau_{12})^C(x_1 - x_2 - v_F\tau_{12})^{0.5}}$$

$$
\begin{aligned}
&\Big\langle T\ \psi_L(X_1)\psi_L^\dagger(X_2)\Big\rangle \\
&\quad\sim \frac{(2x_1)^{1+\gamma_2}(2x_2)^{\gamma_1}(x_1+x_2)^{-1}(x_1+x_2-v_F\tau_{12})^{0.5}}{2(x_1-x_2-v_h\tau_{12})^{B}(-x_1+x_2-v_h\tau_{12})^{A}(x_1+x_2-v_h\tau_{12})^{D}(-x_1-x_2-v_h\tau_{12})^{C}(-x_1+x_2-v_F\tau_{12})^{0.5}} \\
&\quad+\frac{(2x_1)^{\gamma_1}(2x_2)^{1+\gamma_2}(x_1+x_2)^{-1}(x_1+x_2+v_F\tau_{12})^{0.5}}{2(x_1-x_2-v_h\tau_{12})^{B}(-x_1+x_2-v_h\tau_{12})^{A}(x_1+x_2-v_h\tau_{12})^{C}(-x_1-x_2-v_h\tau_{12})^{D}(-x_1+x_2-v_F\tau_{12})^{0.5}} \\
&\Big\langle T\ \psi_R(X_1)\psi_L^\dagger(X_2)\Big\rangle \sim\ 0 \\
&\Big\langle T\ \psi_L(X_1)\psi_R^\dagger(X_2)\Big\rangle \sim\ 0
\end{aligned}
\tag{3.21}
$$

The analytical expressions of the anomalous exponents in equation (3.20) and equation (3.21) are listed in section 3.4.1. The highlight of this work are the formulas described in Case II above. It is easy to see that even after setting $|R| = 0$, these Green functions do not correspond to the translationally invariant Luttinger liquid. This implies that even a small reflection coefficient changes the properties of the system drastically when the two points are on opposite sides of the origin. The two-point functions in equation (3.20) and equation (3.21) obey the Schwinger-Dyson equation and they agree to those obtained by standard fermionic perturbation theory [101].

3.4.1 Anomalous exponents

The explicit expressions of the anomalous exponents that appeared in equation (3.20) and equation (3.21) are listed below.

$$
Q = \frac{(v_h - v_F)^2}{8v_h v_F}\ ;\ X = \frac{|R|^2(v_h - v_F)(v_h + v_F)}{8v_h(v_h - |R|^2(v_h - v_F))}\ ;\ C = \frac{v_h - v_F}{4v_h} \tag{3.22}
$$

The other exponents can be expressed in terms of the above exponents.

$$
\begin{aligned}
&P = \frac{1}{2} + Q\ ; \qquad S = \frac{Q}{C}(\frac{1}{2} - C)\ ; \qquad Y = \frac{1}{2} + X - C; \\
&Z = X - C\ ; \qquad A = \frac{1}{2} + Q - X\ ; \qquad B = Q - X\ ; \\
&D = -\frac{1}{2} + C\ ; \qquad \gamma_1 = X\ ; \qquad \gamma_2 = -1 + X + 2C;
\end{aligned}
\tag{3.23}
$$

All the anomalous exponents are plotted versus the interaction parameter v_0 and the barrier strength V_0 for a single delta function potential in figure 3.3. The figure 3.3 (a-c) displays the anomalous exponents (for holons) of the two-point functions as a function of the interaction parameter v_0 of a system with a single delta potential, the plots (a) and (b) showing those for both the points x_1 and x_2 on the same side of the origin while the plot (c) showing the same for the points on opposite sides. On the other hand, the anomalous exponents for spinons are either 0 or ± 0.5. For the two points on the same side of origin, only one combination out of

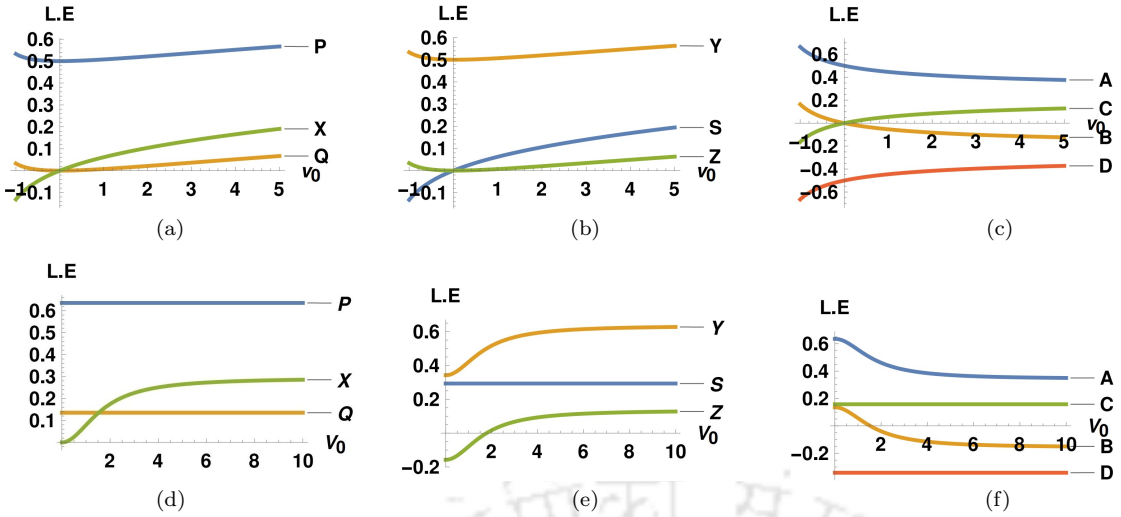

FIGURE 3.3: Plots of anomalous exponents (L.E.) : (a) Exponents for $\langle\psi_R(X_1)\psi_R^\dagger(X_2)\rangle$ on the same side vs v_0 (b) Exponents for $\langle\psi_R(X_1)\psi_L^\dagger(X_2)\rangle$ on the same side vs v_0 (c) Exponents for $\langle\psi_R(X_1)\psi_R^\dagger(X_2)\rangle$ on opposite sides vs v_0 (d) Exponents for $\langle\psi_R(X_1)\psi_R^\dagger(X_2)\rangle$ on the same side vs V_0 (e) Exponents for $\langle\psi_R(X_1)\psi_L^\dagger(X_2)\rangle$ on the same side vs V_0 (f) Exponents for $\langle\psi_R(X_1)\psi_R^\dagger(X_2)\rangle$ on opposite sides vs V_0. Here v_0 is interaction strength and V_0 is impurity strength.

the four $[(\nu_1 x_1 - \nu_2 x_2) - v(t_1 - t_2)]$ survives when $v_0 = 0$ which is expected. But for points on opposite sides of the origin, the rule for choosing λ_i in equation (3.19) causes two such independent terms to be present in the final form of the two-point function in an additive fashion, the denominator being the same in both. When mutual interactions are absent, the numerators add up in such a way as to become time independent which can then be modified by adjusting the c-numbers coefficients (which are both cutoff dependent as well as spatially inhomogeneous) to obtain the proper form of the Green function known from elementary considerations.

When mutual interactions are absent, this Green function becomes the translationally invariant one when $|R| = 0$. But when mutual interactions are present, this Green function does not reduce to the translationally invariant one when $|R|$ is made smaller and smaller implying that when both $v_0 \neq 0$ and $|R| \neq 0$, the most singular part of the asymptotic Green function is discontinuous in $|R|$ near $|R| = 0$. This anomaly is the present work's version of the metaphor introduced by Kane and Fisher [31] who suggested that a $v_0 > 0$ will "cut the wire" when $|R| > 0$. They arrive at their conclusions in a rather convoluted manner by invoking renormalization group methods and so on, but the closed formulas of the present work are more compelling.

The figure 3.3 (d-f) shows the variation of the anomalous exponents for a single impurity as a function of the strength of the impurity V_0 , the interaction parameter v_0 being held constant. When V_0 is made zero, the exponents take standard values of translationally invariant systems that are obtained using conventional bosonization for the two points on the same side of the origin (see Giamarchi [5]).

Many who work in this field are puzzled by two features of our approach and results. The first is that the Luttinger exponents depend on the reflection coefficient ($|R|$) of the cluster of barriers and wells. The other is the fact we continue to use the bare reflection and transmission coefficients in the final formulas whereas in other approaches these are scale dependent. The first puzzle is easier to clear up. Physically speaking, the Green functions for a homogeneous LL ($|R| = 0$) will only contain translational terms $[\pm(x_1 - x_2) - v(t_1 - t_2)]$ and no reflectional terms $[\pm(x_1 + x_2) - v(t_1 - t_2)]$. But for a half line ($|R| = 1$) both types will be present. It is the $|R|$ dependence of the Luttinger exponents which will tune this accordingly.

With regard to the reflection coefficients being the bare ones in our approach we have to point out that the scale dependence in the conventional approaches comes about either because the starting point is far removed from the actual situation or because curvature effects, etc. in the free fermion dispersion are not neglected. The former case is when one tries to study a LL in presence of impurity by treating the impurity as a perturbation or study it by treating it as a weak coupling between two half lines. In both cases the various parameters are likely to be scale dependent due to the poor choice of the starting situation in comparison with the actual situation. To give an analogy, if one tries to study the harmonic oscillator Green function using perturbative RG where the spring constant is a perturbation (analogous to treating impurity as a perturbation), it is naturally going to be scale dependent as it is a relevant perturbation. Conversely if one tries to model this as a sequence of particle in a box with weak coupling between boxes (analogous to a weak link between two half-lines), here too the couplings are going to flow. The present work on the other hand, treats the impurity exactly and strictly neglects the curvature of the free fermion energy dispersion. We also restrict ourselves to forward scattering interaction between fermions. Even with all these qualifications and caveats our results are only able to provide the most singular part (see section 3.4.4) of the asymptotic Green functions in a closed form in terms of elementary functions of positions and times. This is the most important physics that is of interest and it is gratifying that it may be obtained exactly.

3.4.2 Limiting case checks

No interaction. The obvious limiting check is to switch off the inter-particle interactions between particles ($v_0 = 0$) and then compare with the respective single particle Green functions obtained using Fermi algebra. In such a case, the holon velocity is equal to the Fermi velocity ($v_h \to v_F$) and equation (3.20) and equation (3.21) will be identical to equation (3.5)

No impurity. In absence of any impurity, there is no reflection ($|R| = 0$) and no concept of opposite sides as its a homogeneous case. There will be no reflectional terms like $\langle \psi_R \psi_L^\dagger \rangle$ and $\langle \psi_L \psi_R^\dagger \rangle$ which is obvious from table 3.1. The only non zero terms are the translational

terms $\langle\psi_R\psi_R^\dagger\rangle$ and $\langle\psi_L\psi_L^\dagger\rangle$ whose exponents takes the following form.

$$P = \frac{(v_h + v_F)^2}{8v_h v_F};\ Q = \frac{(v_h - v_F)^2}{8v_h v_F};\ X = \gamma_1 = 0;$$

Using the above, one obtains the precise Green functions of the standard homogeneous Luttinger liquid as given in books by Giamarchi [5].

No tunneling. In this case, $R = -1$ (half-line) and hence there is no need to consider the two points to be on the opposite sides. The Green functions take the form that of an infinite barrier for the points on the same side and vanishes when one of the points is at the location of the impurity. The Green functions of a half line are calculated by Mattsson et al. [40] for small values of interaction parameter which are in conformity with those obtained using NCBT subjected to the same conditions.

Far from impurity. It can be observed that when both the points are on the same side of the impurity but far away from it, then the translational terms $\langle\psi_R\psi_R^\dagger\rangle$ and $\langle\psi_L\psi_L^\dagger\rangle$ are immune to the presence of impurity and takes the form of the homogeneous case. But the reflectional terms $\langle\psi_R\psi_L^\dagger\rangle$ and $\langle\psi_L\psi_R^\dagger\rangle$ will certainly not be immune to the presence of the impurity since in these cases the region where the impurity is present needs to be traversed.

3.4.3 Spinless case

The Green functions in equation (3.20) and (3.21) can be easily converted to the corresponding spinless case. All one needs to do is to double all the holon exponents, viz., P to 2P, Q to 2Q, γ_1 to $2\gamma_1$, $(1+\gamma_2)$ to $2(1+\gamma_2)$, etc. and let all the spinon exponents vanish (0.5, 0, -0.5, etc. are set to zero). Thus there will be only one modified velocity given by $v_h = \sqrt{v_F^2 + v_F v_0/\pi}$ indicating no spin-charge separation.

3.4.4 Technical clarification

C-numbers :

While using the modified Fermi Bose correspondence in equation (3.16) to write down the general N-point function, care must be taken in handling the c-numbers. For example, while computing the two-point function one encounters c-numbers which are of the type $\left\langle C_{\lambda_1,\nu_1,\gamma_1}(\sigma_1)C^*_{\lambda_2,\nu_2,\gamma_2}(\sigma_1)\right\rangle$. Rather than thinking of these as products of complex numbers C and its complex conjugate C^*, one is required to think of them as one single object as $F_2(\lambda_1,\nu_1,\gamma_1;\lambda_2,\nu_2,\gamma_2)$.

Most singular part :

While evaluating the Green functions using the Fermi Bose correspondence in equation (3.16) we have used the Gaussian approximation as given in equation (2.25).

$$< \psi_R(x,\sigma,t)\psi_R^{\dagger}(x',\sigma,t') > \quad \sim \quad e^{\frac{1}{2}<(i\theta_R(x,\sigma,t))^2>} e^{\frac{1}{2}<(-i\theta_R(x',\sigma,t'))^2>} e^{<(i\theta_R(x,\sigma,t))(-i\theta_R(x',\sigma,t'))>}$$

Here 'θ_R' is the local phase given by equation (3.15) which linearly depends on the densities. Using the Gaussian approximation means that the higher moments of density fluctuations are ignored. Although $\langle T\ \rho_s(x_1,t_1)\rho_s(x_2,t_2)\rho_s(x_3,t_3)\rangle = 0$, but the fourth order of density fluctuation is not zero.

$$\langle T\ \rho_s(x_1,t_1)\rho_s(x_2,t_2)\rho_s(x_3,t_3)\rho_s(x_4,t_4)\rangle - \langle T\ \rho_s(x_1,t_1)\rho_s(x_2,t_2)\rangle \langle T\ \rho_s(x_3,t_3)\rho_s(x_4,t_4)\rangle -$$
$$\langle T\rho_s(x_1,t_1)\rho_s(x_3,t_3)\rangle \langle T\rho_s(x_2,t_2)\rho_s(x_4,t_4)\rangle - \langle T\rho_s(x_1,t_1)\rho_s(x_4,t_4)\rangle \langle T\rho_s(x_2,t_2)\rho_s(x_3,t_3)\rangle \neq 0$$

However the above term is less singular compared to the density fluctuation of the second order viz. $\langle T\ \rho_s(x_1,t_1)\rho_s(x_2,t_2)\rangle - \langle\rho_s(x_1,t_1)\rangle \langle\rho_s(x_2,t_2)\rangle$. Similarly all the higher even order terms are less singular compared to the second order density fluctuation terms while the odd orders are zeros. In other words, using the Gaussian approximation means that we are calculating the most singular part of the Green functions using the non chiral bosonization technique.

3.5 Four-point functions (Friedel oscillations)

The prescription of equation (3.19) for pinning down the form of λ_i in equation (3.16) leads to the correct general four-point functions when mutual interactions are absent. However, the general expressions for four-point functions with mutual interactions are quite formidable. Fortunately, there is a special case viz. the density-density correlation function which is much simpler and also more important physically. Friedel oscillations are the rapid spatial variation ($\sim\ e^{2ik_Fx}$) of the otherwise homogeneous density profile in a Luttinger liquid in response to a spatially localized impurity. In the Kubo formalism it is given as the density-density correlation function [102, 103]. Egger and Grabert have studied Friedel oscillations in a Luttinger liquid with arbitrary interactions and arbitrary strengths of impurities [91].

Consider the slow part of the density density correlation functions given in equation (3.5). This slow part of the DDCF can be used to obtain the fast part of the DDCF which corresponds to Friedel oscillations, which is nothing but a term which oscillates with wavenumber $2k_F$ such as $e^{2ik_F(x-x')} < T\ \rho_f(x,\sigma,t)\rho_f^*(x',\sigma',t') >$. This can be done using a non standard harmonic analysis suited to study inhomogeneous Luttinger liquids like the one under study.

$$\rho_f(x,\sigma,t) \sim e^{2i\pi \int_{-\infty}^{x}(\rho_s(y,\sigma,t)+\lambda\rho_s(-y,\sigma,t))dy} \tag{3.24}$$

The above equation is the basis of the NCBT using which equation (3.16) is derived. The λ is the same as that of equation (3.16) taking values 0 or 1 and setting $\lambda = 0$ yields the standard harmonic analysis of Haldane. The value of λ is first decided by calculating the non-interacting DDCF using equation (3.24) and comparing with the same DDCF obtained using Fermi algebra. After that, similar to the calculation of the two-point functions, the non interacting DDCF in equation (3.5) is to be replaced by the interacting DDCF in equation (3.17) to obtain the required four-point functions in presence of mutual interactions.

Define $\tilde{\rho}_f \equiv \rho_f - < \rho_f >$. The prescription for choosing λ_i in equation (3.24) as discussed in equation (3.19) leads to the unambiguous conclusion that $\lambda_1 = 1 - \lambda_2$ (where λ_1 and λ_2 corresponds to the points x_1 and x_2 respectively) and the fast parts of the DDCF corresponding to Friedel oscillations are obtained as follows.

$$\begin{aligned}
\Big\langle T\ \tilde{\rho}_f(X_1)\tilde{\rho}_f(X_2)\Big\rangle &\sim (Exp[\sum_{\substack{\nu,\nu^{'}=\pm 1\\ a=h,n}} \Gamma(\nu,\nu^{'};a)\ Log[(\nu x_1 - \nu^{'} x_2) - v_a(t_1 - t_2)]] - 1) \\
\Big\langle T\ \tilde{\rho}_f(X_1)\tilde{\rho}^{*}_f(X_2)\Big\rangle &\sim (Exp[-\sum_{\substack{\nu,\nu^{'}=\pm 1\\ a=h,n}} \Gamma(\nu,\nu^{'};a)\ Log[(\nu x_1 - \nu^{'} x_2) - v_a(t_1 - t_2)]] - 1)
\end{aligned} \tag{3.25}$$

One should remember that this really means the time derivative of the logarithms of both sides are equal to each other. The values of the anomalous scaling exponents $\Gamma(\nu,\nu^{'};a)$ can be obtained from the expression below.

$$\Gamma(\nu,\nu^{'};a) = \left(\frac{v_F}{2v_h}\,\delta_{a,h} + \frac{1}{2}\,\delta_{a,n}\right)\ (\delta_{\nu,\nu'} - \delta_{\nu,-\nu'}) \tag{3.26}$$

As mentioned in equation (3.12), the full density is given as follows.

$$\rho(x,t) = \rho_s(x,t) + e^{2ik_F x}\ \rho_f(x,t) + e^{-2ik_F x}\ \rho^{*}_f(x,t)$$

Now ρ_f is the envelope of the rapidly varying part of the density profile which oscillates with a wave-vector $2k_F$. Using equations (3.25) and (3.26), one can write

$$\begin{aligned}
\Big\langle T\ \rho_f(x_1,\sigma,t_1)\rho_f(x_2,\sigma,t_2)\Big\rangle \sim &\left(\frac{[(x_1-x_2)-v_h(t_1-t_2)][-(x_1-x_2)-v_h(t_1-t_2)]}{[(x_1+x_2)-v_h(t_1-t_2)][-(x_1+x_2)-v_h(t_1-t_2)]}\right)^{\frac{v_F}{2v_h}} \\
&\left(\frac{[(x_1-x_2)-v_F(t_1-t_2)][-(x_1-x_2)-v_F(t_1-t_2)]}{[(x_1+x_2)-v_F(t_1-t_2)][-(x_1+x_2)-v_F(t_1-t_2)]}\right)^{\frac{1}{2}}
\end{aligned}$$

Substituting $x_1 = x, x_2 = x + \epsilon$ (to avoid infinities/zeros) and $t_1 = t_2 = t$ we obtain

$$\left\langle \rho_f(x)\rho_f(x) \right\rangle \sim \left(\frac{(-\epsilon)(\epsilon)}{[2x][-2x]} \right)^{\frac{v_F}{2v_h}} \left(\frac{(-\epsilon)(\epsilon)}{[2x][-2x]} \right)^{\frac{1}{2}} \sim (x^2)^{-\frac{v_F}{2v_h}-\frac{1}{2}}$$

Now, $\frac{v_F}{v_h} = g$ is the well known Luttinger liquid interaction parameter and thus we can write

$$\langle \rho_f(x)\rho_f(x) \rangle \sim (x^2)^{-(1+g)/2}$$

Since for a non interacting system, the average density goes as the inverse of length $< \rho(x) > \sim \frac{1}{x}$ while the average of the density density correlation function goes as $< \rho(x)\rho(x) > \sim \frac{1}{x^2}$, hence using the same argument one can write from the above relation for systems with forward scattering interactions as follows.

$$\langle \rho_f(x) \rangle \sim (x)^{-(1+g)/2} \tag{3.27}$$

This is precisely the relation obtained by Egger et al. [91] for the envelope of the oscillatory part of the density which oscillates with a frequency $2k_F$.

3.6 Dynamical density of states

In this section the results for the dynamical density of states (DDOS) $D_x(\omega)$ at location x is presented. Physically, $D_x(\omega)d\omega$ is the number of quasiparticle states per unit length with energy between $\hbar\omega$ and $\hbar(\omega + d\omega)$ relative to the Fermi energy. The idea of density of states is generalized to interacting many body systems as follows:

$$D_{\mathbf{x}}(\omega) = \int_{-\infty}^{\infty} \frac{dt}{2\pi}\, e^{it(\omega+E_F)} \langle \{\psi(\mathbf{x},t), \psi^\dagger(\mathbf{x},0)\} \rangle \tag{3.28}$$

The above local density of states can be related to the single particle Green function formulas derived earlier to obtain a closed formula for $D_x(\omega)$ (see Appendix E for details) especially in interesting limits viz. when x is far away from the cluster of barriers and wells and also when x is near or at the location of barriers and wells. The final results are discussed below. The detailed plots that help in visualizing these results are relegated to figure 3.4. First a dimensionless parameter proportional to the location x is defined viz. $\xi = \frac{2\omega|x|}{v_h}$. The results for DDOS at zero temperature may be written in general as (the static - i.e. at the Fermi level - local density of states at *finite* temperature is obtained by simply replacing ω below by k_BT viz. the temperature),

$$D_\xi(\omega) \sim \omega^{\alpha(\xi)} \tag{3.29}$$

where $\alpha(0 < \xi \ll 1) \approx 2Q + 2X$ (Q and X are given in equation (3.22)) and $\alpha(\xi \gg 1) \approx \frac{(v_h - v_F)^2}{4v_F v_h} = 2Q = \frac{1}{4}(K_\rho + \frac{1}{K_\rho} - 2)$ which is precisely the exponent found in the textbooks for

fermions with spin (Giamarchi [5], equation (7.27)). In the case of the half line, Kane and Fisher [31] have remarked that for spinless fermions the density of states is $\rho_{end}(\epsilon) \sim \epsilon^{\frac{1}{g}-1}$ where $g = \frac{v_F}{v_h}$. For fermions with spin the exponent may be inferred as half of this as done earlier viz. $D_{half-line}(\omega) \sim \omega^{\frac{1}{2}(\frac{1}{K_\rho}-1)}$. Setting $|R| = 1$ for half-line, $\alpha(\xi \equiv 0) = \frac{(v_h - v_F)}{2v_F} = \frac{1}{2}(\frac{1}{K_\rho} - 1)$ since $K_\rho = \frac{v_F}{v_h}$. For repulsive interactions, $v_h > v_F$ the exponent $\alpha(0 < \xi \ll 1) > 0$. But for attractive interactions, $v_h < v_F$ and the exponent can take both positive as well as negative values. Define a constant R_{c1} such that when $|R|^2 = |R_{c1}|^2 = \frac{v_F - v_h}{3v_F - v_h}$, the exponent vanishes. Now, for $|R| < |R_{c1}|$ the exponent $\alpha(0 < \xi \ll 1) > 0$ and for $|R| > |R_{c1}|$ the exponent $\alpha(0 < \xi \ll 1) < 0$.

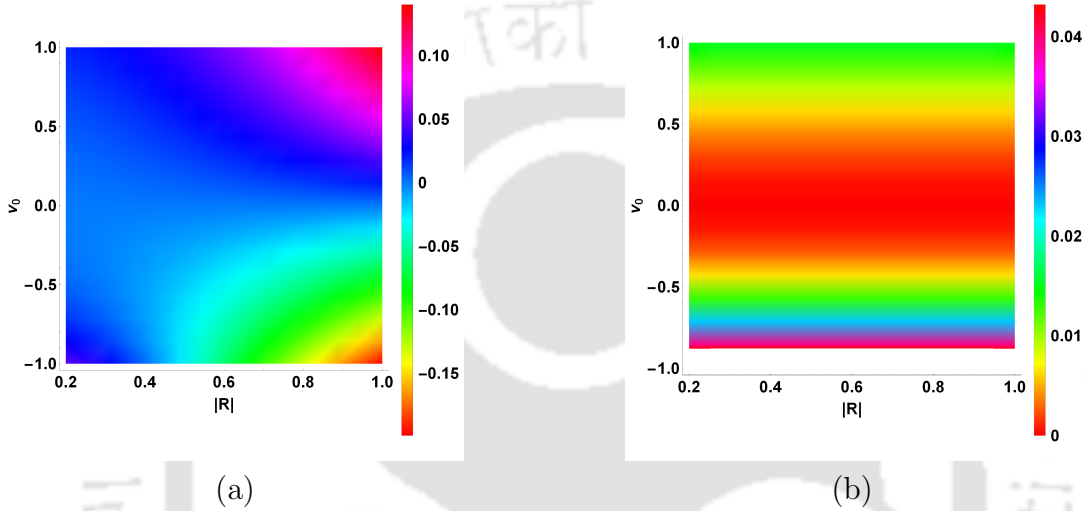

(a) (b)

FIGURE 3.4: (a) Density of state exponents($0 < \xi \ll 1$) as a function of the interaction parameter v_0 for various values of reflection amplitudes $|R|$ given in parenthesis. (b) Density of state exponents($\xi \gg 1$) as a function of the interaction parameter v_0.($v_F = 1$)

For the spinless case and strong impurity, the density of states has been exactly calculated by Delft et al. [72] for the specific case of $K_\rho = \frac{1}{2}$ and obtained to be $D(\omega) \sim \omega$. Redoing the above for the spinless case and strong impurity, NCBT yields $D(\omega) \sim \omega^\alpha$ where $\alpha = \frac{1}{K_\rho} - 1$ and for $K_\rho = \frac{1}{2}$, we have $D(\omega) \sim \omega$ which is in agreement with Von Delft et.al. [72], Fabrizio & Gogolin [104], etc. The main advancement of the present work is being able to provide simple analytical expressions for exponents such as these that interpolate between the no-barrier and strong barrier cases. The novel technical framework that abandons the g-ology framework in favor of a non-chiral bosonization method with non-standard harmonic analysis of the field operator enables an exact treatment of free fermions plus impurity problem.

The exponent near the impurity becomes negative in some regions (see Appendix E) signifying that the density of states diverges at low energies near the impurity i.e. the impurity together with attractive interactions effectively brings back low-energy quasiparticles which ought not to be there in a Luttinger liquid ("healing the chain" [31]). Note that contributions that are analogous to Friedel oscillations (rapidly oscillating terms) have been ignored in the DDOS calculations.

3.7 Summary

In this work, the non-chiral bosonization technique (NCBT) is used to obtain the most singular parts of the asymptotically exact Green functions of a luttinger liquid with a cluster of impurities around an origin. These formulas interpolate between the weak barrier and weak link extreme cases that are studied in the literature. Unlike the competing methods that can only study these extreme limits reliably, the present approach is able to connect the two regimes using analytical means. The formalism is used to calculate the rapidly oscillating parts of the density density correlation functions, also called Friedel oscillation terms, which arises because of the presence of a localized impurity in an otherwise homogeneous Luttinger liquid. The two-point functions obtained using the same technique are used to express the local dynamical density of states as a power law and a closed analytical expression of the exponent is obtained as a function of the strength of impurities and that of mutual interactions. The interesting limits of far away from the impurity as well as near or at the position of impurity is also discussed. A comparison is made with the existing literature for the dynamical density of states in the special case of g=1/2 and an exact match is observed.

भारतीय प्रौद्योगिकी संस्थान गुवाहाटी
Indian Institute of Technology Guwahati

Chapter 4

Transport properties

One of the most important physical phenomena studied in condensed matter systems is the transport of electrons, especially when they are restricted to move in one dimension. This is because of the unique nature of the inter-particle interactions in one dimension which leads to interesting physics which is substantially different from that of the higher dimensions. Secondly, the emergence of advanced technologies has made possible, the realization of one dimensional systems that have unusual properties that hold a promising future - carbon nanotubes [42], semiconducting quantum wires [97, 105] and so on. Most of the physical phenomena of such systems can be systematically studied provided one has analytical forms of the correlation functions - to obtain these is the stated goal in quantum many body physics. In one dimension, this goal is typically achieved using bosonization methods where a fermion field operator is expressed as the exponential of a bosonic field [72]. This operator approach to bosonization [5], is used to compute the N-point Green functions of a clean Luttinger liquid. But in presence of impurities, the conventional method fails and one has to switch to Non chiral bosonization technique which can successfully compute the Green functions of such inhomogeneous systems. Possession of Green functions enables the study of different physical phenomena and attributes of these systems, such as Friedel oscillations [91], temperature dependence of conductance [92, 93], Kondo effect [94, 95], resonant tunneling [32, 106], etc.

The seminal work of Kane and Fisher [31] has shown how impurities can lead to drastic effects on the conductance of the system at low temperatures which can be as severe as 'cutting the chain' by even a small scatterer. Since then, the study of transport phenomena in a Luttinger liquid with impurities has interested a number of researchers [107–110]. The conductance of a narrow quantum wire with non-interacting electrons moving ballistically is given by e^2/h. This conductance is renormalized for a Luttinger liquid with no leads to a value, $g\,e^2/\mathrm{h}$, where g is the Luttinger liquid parameter that depends on the mutual interaction strength of the particles [31, 108, 111]. But no renormalization of the universal conductance is required when leads are present if the electrons have a free behavior in the source and drain reservoirs [110, 112]. Matveev et al. used a simple renormalization group method to calculate the conductance of a

weakly interacting electron gas in presence of a single scatterer [34]. Ogata and Anderson [113] used Green's functions to study conductivity of a Luttinger liquid and showed that if spin-charge separation is taken into account, the resistivity has a linear temperature dependence. Besides conductance, resonant tunneling is yet another important phenomenon studied in a Luttinger liquid with double barriers [32, 106, 114, 115]. Kane and Fisher studied resonant tunneling in a single channel interacting electron gas through a double barrier and found that the width of the resonance vanishes as a power of temperature, in the zero-temperature limit [32, 114]. Furusaki and Nagaosa studied the same for spinless fermions and calculated the conductance as a function of temperature and gate voltage [106]. In another work, Furusaki studied resonant tunneling in a quantum dot weakly coupled to Luttinger liquids [116] and a few years later, this model was supported by experimental evidence [97]. More recently conductance has been studied using numerical methods like Monte Carlo simulations [62, 82] as well as quantum simulations [117]. Aseev et al. [118] recently studied how the combined effect of multi-electron interaction and applied magnetic field leads to a gap in the spectrum, which in turn affects the temperature dependence of fractional conductance of a quantum wire. Other works on transport properties in 1D systems include study of long range disorder [119], short range disorder [120, 121], thermal transport [122–124], spin dependent transport [125], frequency dependent transport [126] and so on.

In this chapter [127, 128], the conductance of a Luttinger liquid in presence of a cluster of impurities is calculated using the correlation functions obtained using NCBT - both in the Kubo formalism as well as when it is treated as an outcome of a tunneling experiment. It is stressed that these two are qualitatively different notions, despite carrying the same name viz. 'conductance' - the former being related to 4-point functions and the latter to 2-point functions. All the necessary limiting cases like Landauer's formula, conductance of a clean Luttinger liquid, half-line, etc. are obtained. From the tunneling conductance, the well-known concepts of 'cutting the chain' and 'healing the chain' are elucidated. The finite-bandwidth conductance of a Luttinger liquid (LL) with a cluster of impurities is also studied and its variation with respect to temperature is shown. The results are compared with those obtained by Matveev, Yue and Glazman [34] who deal with a weakly interacting LL. By contrast, NCBT correctly provides the conductance for all values of the interaction strength (as well as the sign). The condition of resonant tunneling for a double impurity system is obtained and the behavior of the correlation function exponents near its vicinity is explained.

4.1 Conductance

In this section, the conductance of a Luttinger liquid with an infinite bandwidth is discussed while the subsequent section discusses the same with a finite bandwidth. The systems under study remains the same as that of the previous chapter - a cluster of impurities in a Luttinger

liquid. Let us recall the Hamiltonian given by equation (3.1) as

$$H = \int_{-\infty}^{\infty} dx\ \psi^{\dagger}(x) \left(-\frac{1}{2m}\partial_x^2 + V(x) \right) \psi(x) + \frac{1}{2} \int_{-\infty}^{\infty} dx \int_{-\infty}^{\infty} dx^{'}\ v(x - x^{'})\ \rho(x)\rho(x^{'}) \tag{4.1}$$

The first two terms represent the kinetic energy and the external potential energy respectively. The third term is the mutual interaction term where $v(x - x^{'}) = \frac{1}{L}\sum_q v_q \exp\left[-iq(x - x^{'})\right]$ (where $v_q = 0$ if $|q| > \Lambda$ for some fixed bandwidth $\Lambda \ll k_F$ and $v_q = v_0$ is a constant otherwise) is the forward scattering mutual interaction. First we consider infinite bandwidth of the system which effectively means that the temperature is much less than the bandwidth, $T \ll \Lambda v_F$.

The following sequence is maintained in each subsection. Firstly the method adopted is briefly discussed with a mention of the starting equations. This is followed by a display of the main results while the computational details are relegated to Appendix F. The next part will be a discussion of the results and finally a comparison is made with well-known results in the literature.

4.1.1 Kubo conductance

The general formula for the conductance of a quantum wire (obtained from Kubo's formula that relates it to current-current correlations) without leads but with electrons experiencing forward scattering short-range mutual interactions and in the presence of a finite number of barriers and wells clustered around an origin is obtained. Consider an electric field $E(x,t) = \frac{V_g}{L}$ between $-\frac{L}{2} < x < \frac{L}{2}$ and $E(x,t) = 0$ for $|x| > \frac{L}{2}$. Here V_g is the voltage between two extreme points. Thus a d.c. situation is being considered right from the start. This corresponds to a vector potential,

$$A(x,t) = \begin{cases} -\frac{V_g}{L}(ct), & -\frac{L}{2} < x < \frac{L}{2}\ ; \\ 0, & \text{otherwise.} \end{cases} \tag{4.2}$$

Here c is the speed of light. This means the average current can be written as (e is the electronic charge),

$$< j(x,\sigma,t) > = \frac{ie}{c} \sum_{\sigma^{'}} \int_{-L/2}^{L/2} dx^{'} \int_{-\infty}^{t} dt^{'}\ \frac{V_g}{L}(ct') < [j(x,\sigma,t), j(x^{'},\sigma^{'},t^{'})] >_{LL} \tag{4.3}$$

Using the Green functions obtained in an earlier work [90], the current current correlation functions are derived (see Appendix F) and they are used in turn to obtain the formula for conductance (in proper units) as follows,

$$G = \frac{e^2}{h}\frac{v_F}{v_h} \left(1 - \frac{v_F}{v_h}\ \frac{|R|^2}{1 - \frac{(v_h - v_F)}{v_h}|R|^2} \right) \tag{4.4}$$

Here v_F is the Fermi velocity, $v_h = \sqrt{v_F^2 + 2v_F v_0/\pi}$ is the holon velocity and v_0 is the strength of interaction between fermions. The Kubo conductance formula obtained in equation (4.4) is plotted in figure 4.1 as a function of the absolute value of the reflection amplitude $|R|$ (square of this is the reflection coefficient) and the interaction strength v_0. It can be seen that when the reflection coefficient becomes unity ($|R| = 1$), then the conductance vanishes irrespective of the interaction parameter. On the one hand, for any fixed value of $|R|$, the conductance increases as the mutual interaction becomes more and more attractive (negative v_0) and decreases as the interaction becomes more and more repulsive (positive v_0). On the other hand for a fixed value of interaction parameter, the conductance decreases with increase in the reflection strength. This is the most general version of the Kubo conductance of a Luttinger liquid with arbitrary strength of interactions as well as that of impurities. The literature mostly consists of the limiting cases of these results which, as discussed below, are all in favor of this result.

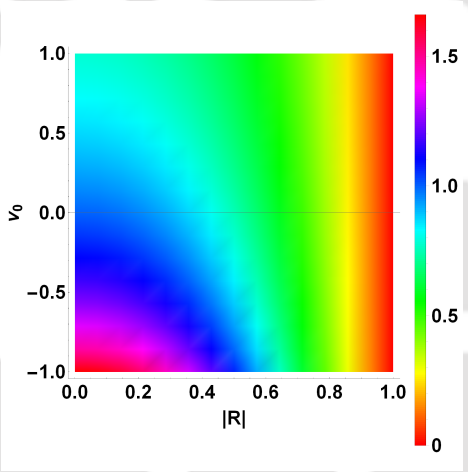

FIGURE 4.1: Conductance as a function of the absolute value of the reflection amplitude $|R|$ as well the interaction parameter v_0 ($v_F = 1$)

4.1.1.1 Limiting cases.

No interaction. In absence of interactions $v_0 = 0$ and hence $v_h = v_F$ and thus from equation (4.4),

$$G = \frac{e^2}{h}(1 - |R|^2) = \frac{e^2}{h}|T|^2$$

which is the Landauer's formula for conductance.

No impurity. In this case, there is no reflection and hence $|R| = 0$ and thus from equation (4.4),

$$G = \frac{e^2}{h}\frac{v_F}{v_h} = \frac{e^2}{h}g$$

which the renormalized conductance of an infinite Luttinger liquid (with parameter g).

Infinite barrier. In the case of a half line, $|R| = 1$ and thus from equation (4.4),

$$G = 0$$

irrespective of the value of holon velocity v_h.

4.1.2 Tunneling conductance

The Kubo conductance is the linear response to external potentials and is therefore related to four-point correlation functions of fermions. Alternatively, conductance may also be thought of as the outcome of a tunneling experiment [31]. Here fermions are injected from one end and collected from the other end. In this sense, the conductance is related to the two-point function or the single particle Green function. Thus we expect these two notions to be qualitatively different from each other, even though both are called "conductance". From this point of view, the tunneling conductance is,

$$G \sim \frac{e^2}{h} |v_F \int_{-\infty}^{\infty} dt \ < \{\psi_R(-\frac{L}{2}, \sigma, 0), \psi_R^\dagger(\frac{L}{2}, \sigma, t)\} > | \tag{4.5}$$

This identification of the tunneling conductance with a properly defined effective tunneling amplitude (when mutual interactions are included) is essentially the same as the approach followed in the important work by Matveev et al. [34].

Now $< \psi_R(-\frac{L}{2}, \sigma, 0)\psi_R^\dagger(\frac{L}{2}, \sigma, t) >$ is the probability amplitude of a particle being annihilated at the extreme left as a right mover and being created at the extreme right also as a right mover after time t, thus tunneling through the cluster of impurities situated at the origin. Since the two points are on the opposite sides of the origin, the Green functions from equation (3.21) have to be used. To avoid infinities in the term $(x_1 + x_2)^{-1}$ one has to set $x_1 = -\frac{L}{2}$ and $x_2 = \frac{L}{2} + \epsilon$ and then taking the limit $\epsilon \to 0$ while performing the summation of the two terms in the Green function. Finally all the exponents associated with the length parameter L that emerges while evaluating equation (4.5) are collected together to obtain the tunneling conductance exponent. The length L has to be scaled by a cutoff $L_\omega = \frac{v_F}{k_B T}$ to preserve the dimensionality of the conductance G since the exponents are some general non-integer quantities. The final result (derived in Appendix F) is as follows.

$$G \sim \left(\frac{L}{L_\omega}\right)^{4X-2Q} \tag{4.6}$$

In this case the results depend on the length of the wire L and a cutoff L_ω that may be regarded either as inverse temperature or inverse frequency (in case of a.c. conductance). Here X and Q are obtained from equation (3.22). It is important to stress that the present work has carefully defined tunneling conductance and it is not simply related to the dynamical

density of states of either the bulk or the half line. The dynamical density of states is equal-space and unequal time Green function. For tunneling, an electron is injected at $x = -L/2$ and collected at $x^{'} = +L/2$ as is the case here which is unequal-space unequal-time Green function, i.e., the Green function of the electron traversing the impurity. Of particular interest is the weak link limit where $|R| \to 1$. The limiting case of the weak link are two semi-infinite wires. In this case,

$$G_{weak-link} \sim \left(\frac{L}{L_\omega}\right)^{\frac{(v_h+v_F)^2-4v_F^2}{4v_h v_F}} \tag{4.7}$$

Hence the d.c. conductance scales as $G_{weak-link} \sim (k_B T)^{\frac{(v_h+v_F)^2-4v_F^2}{4v_h v_F}}$. This formula is consistent with the assertions of Kane and Fisher [31] that show that at low temperatures ($k_B T \to 0$) and for a fixed L, the conductance vanishes as a power law in the temperature if the interaction between the fermions is repulsive ($v_h > v_F > 0$) and diverges as a power law if the interactions between the fermions is attractive ($v_F > v_h > 0$). Their result is applicable to spinless fermions without leads $G_{weak-link-nospin} \sim (k_B T)^{\frac{2}{K}-2}$. In order to compare with the result of the present work, this exponent has to be halved $G_{weak-link-with-spin} \sim (k_B T)^{\frac{1}{K_\rho}-1}$. This exponent is the same as the exponent of the present work so long as $|v_h - v_F| \ll v_F$ i.e. $\frac{(v_h+v_F)^2-4v_F^2}{4v_h v_F} \approx \frac{1}{K_\rho} - 1$ since $K_\rho = \frac{v_F}{v_h}$. In general, the claim of the present work is that the

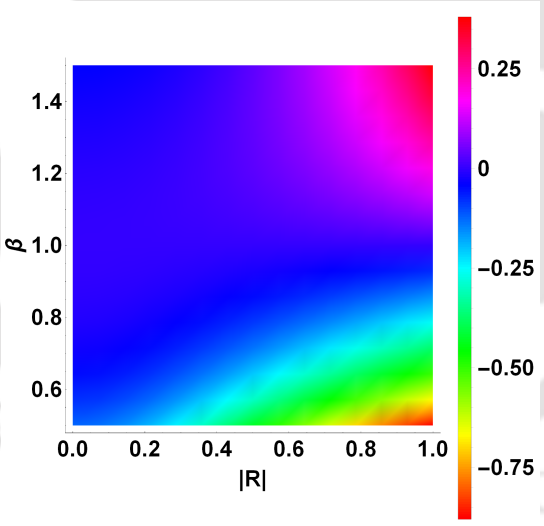

FIGURE 4.2: Conductance exponent η as a function of the absolute value of the reflection amplitude $|R|$ and the ratio $\beta = \frac{v_h}{v_F}$.

temperature dependence of the tunneling d.c. conductance of a wire with no leads and in the presence of barriers and wells and mutual interaction between particles (forward scattering, infinite bandwidth i.e. $k_F \gg \Lambda_b \to \infty$) is,

$$G \sim (k_B T)^\eta; \tag{4.8}$$

and the exponent η is given by

$$\eta = 4X - 2Q = \frac{(g-1)(\tau_0 - g - 3g^2(1-\tau_0))}{4g(\tau_0 + g(1-\tau_0))} \tag{4.9}$$

Here $g = \frac{v_F}{v_h}$ is the Luttinger liquid parameter and $\tau_0 = 1 - |R_0|^2 = |T_0|^2$ is the bare tunneling coefficient. When $\eta > 0$ the conductance vanishes at low temperatures as a power law - characteristic of a weak link. However when $\eta < 0$ the conductance diverges [1] at low temperature as a power law - characteristic of a clean quantum wire. Of special interest is the situation $\eta = 0$ where the conductance is independent of temperature. This crossover from a conductance that vanishes as a power law at low temperatures to one that diverges as a power law occurs at reflection coefficient $|R|^2 = |R_{c2}|^2 \equiv \frac{v_h(v_h - v_F)}{3v_F^2 + v_h^2}$ which is valid only for repulsive interactions $v_h > v_F$. For attractive interactions, $\eta < 0$ for any $|R|^2$ which means the conductance always diverges as a power law at low temperatures. This means attractive interactions heal the chain for all reflection coefficients including in the extreme weak link case. On the other hand for repulsive interactions, for $|R| > |R_{c2}|$, $\eta > 0$ the chain is broken (conductance vanishes) at low temperatures. For $|R| < |R_{c2}|$, $\eta < 0$ and even though the interactions are repulsive the chain is healed (conductance diverges).

4.1.2.1 Derivation of RG equation for the tunneling conductance

In the well-cited work of Matveev et al. [34], the RG equation for the tunneling conductance is derived which is valid for weak mutual interaction between fermions (they consider both forward scattering as well as backward scattering but in the present work we consider only forward scattering between fermions but of arbitrary strength and sign subject to the limitation that the holon velocity be real). Both in their work and in the present work the transmission amplitude of free fermions can vary continuously between zero and unity i.e. it is not constrained in any way. Note that we have chosen an infinite bandwidth to derive the power-law conductance in equation (4.8). Had we chosen a finite bandwidth while calculating equation (4.5), the resulting expressions would be considerably more complicated as Matveev et al. have also found. But for now we look at equation (8) of their paper rather than equation (12) since we are interested in the large bandwidth case only for now. Since $G \sim \mathcal{T}$ in their notation, we may expand the conductance exponent $4X - 2Q$ in powers of v_0, the forward scattering mutual interaction between fermions, to the leading order as follows (in the notation of Matveev et al. this is $V(0)$ and $V(2k_F) \equiv 0$ in the present work),

$$\frac{\delta\mathcal{T}}{\mathcal{T}_0} \approx 4X \ \log(\omega) \approx \mathcal{R}_0 \frac{v_0}{\pi v_F} \ \log(\omega) \tag{4.10}$$

Here $|v_0| \ll v_F$, $\mathcal{R}_0 = 1 - \mathcal{T}_0$ (in the notation of the present work this would be $|R|^2 = 1 - |T|^2$) and $\omega \to |k - k_F|d \sim k_B T$ (where d is the characteristic spatial scale of the interaction

[1] A more careful study shows it saturates to a high value.

potential in Matveev's article). The equation (4.10) is precisely equation (8) of Matveev et al. Thus mutually interacting fermions renormalize the impurities but isolated impurities do not renormalize the homogeneous Luttinger parameters such as $K = \frac{v_F}{v_h}$. Note that our results for the conductance equation (4.8) is the *end result* of properly taking into account the renormalizations to all orders in the infinite-bandwidth-forward-scattering fermion-fermion interactions with no restriction on the bare transmission coefficient of free fermions plus impurity. The final answers of equation (4.8) involve only the bare transmission and reflection coefficients for the same reason why eg. the zero point energy of the harmonic oscillator derived properly using Hermite polynomials (rather than using perturbative RG around free particle, say) involves the bare spring constant (ie. $\frac{1}{2}\hbar\sqrt{\frac{k}{m}}$). Incidentally, even the final answers of Matveev et al. such as their equation (13) involve the bare parameters only since this formula is the *end result* of taking into account all the renormalization properly.

It is hard to overstate the importance of these results. They show that it is possible to analytically interpolate between the weak barrier and weak link limits without involving RG techniques, explicitly. It also shows that NCBT is nothing but non-perturbative RG in disguise.

4.2 Finite bandwidth conductance

The proper way of studying the finite bandwidth conductance would be to re-derive the single particle Green function for finite bandwidth. Also it is important to introduce a bias and calculate the current flowing as a function the bias, temperature, bandwidth etc. and extract the conductance as a linear response coefficient. This has proved to be formidable. However, an alternative is to take the point of view that the transmission and reflection coefficients that appear in η are not the non-interacting temperature independent values but the interacting temperature-dependent values. This amounts to asserting that the equation (4.8) which is strictly speaking valid only for temperatures small compared to the bandwidth is now valid in general since η has now been reinterpreted as being temperature and interaction dependent.

Therefore, for electrons with a finite bandwidth D_0, the tunneling conductance τ is given by a transcendental equation viz.

$$\tau = \tau_0 \left(\frac{k_B T}{D_0}\right)^{\eta(\tau)} \tag{4.11}$$

where τ_0 is the tunneling conductance in absence of interactions and the exponents η is a function of the conductance τ and is obtained by replacing the τ_0 in equation (4.9) by τ.

$$\eta(\tau) = \frac{(g-1)(\tau - g - 3g^2(1-\tau))}{4g(\tau + g(1-\tau))} \tag{4.12}$$

As before, g is the Luttinger parameter given by $\frac{v_F}{v_h}$ which is greater than unity for attractive interactions and less than unity for repulsive interactions. τ_0, being the transmission coefficient

of the non-interacting system, can be obtained from elementary quantum mechanics and its value ranges from 0 to 1. An exact analytical solution of equation (4.11) can't be obtained due to its transcendental nature. However, numerical solutions and approximate analytical solutions are possible, which are described in the subsequent sub-sections.

4.2.1 Numerical solution

The equation (4.11) for tunneling conductance may be solved numerically using appropriate empirical values of the remaining parameters. Based on the transmission coefficient τ_0 and Luttinger liquid parameter g, there are four cases as follows.

(a) Weak barrier and weak interactions: For a weak barrier, there is maximum transmission and hence τ_0 is close to unity. Also for weak interactions, the holon velocity v_h is close to Fermi velocity v_F and hence the following empirical values are chosen: $\tau_0 = 0.9$; $g = 1.1$ for attractive and $g = 0.9$ for repulsive interactions. For $\frac{k_B T}{D_0}$ ranging from 0.1 to 2, equation (4.11) is numerically solved and the obtained values of conductance τ is plotted as a function of temperature ($\frac{k_B T}{D_0}$) and the graph in figure 4.3 is obtained.

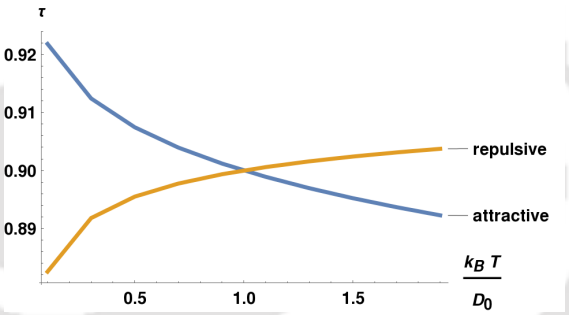

FIGURE 4.3: Conductance as a function of dimensionless temperature ($\frac{k_B T}{D_0}$) for a weak barrier ($\tau_0 = 0.9$) and weak interactions ($g = 0.9$ for repulsive and $g = 1.1$ for attractive).

From the figure 4.3 it can be seen that near zero temperature, the conductance is close to unity for attractive interactions while it tends to vanish for repulsive interactions. This is the signature of 'cutting the chain' by even a small scatterer in case of repulsively interacting particles [31]. As the temperature increases, the conductance decreases from its maximum value for attractive interactions while it increases from its minimum value for repulsive interactions. One more observation is that for $k_B T < D_0$, the conductance is larger in the case of attractive interactions while for $k_B T > D_0$, the conductance is larger in the case of repulsive interactions, the transition taking place at the point when $k_B T = D_0$.

(b) Strong barrier and weak interactions: For a strong barrier, there is minimum transmission and hence τ_0 is close to zero. The following empirical values are chosen: $\tau_0 = 0.1$; $g = 1.1$ for attractive and $g = 0.9$ for repulsive interactions as in the earlier case. For

$\frac{k_BT}{D_0}$ ranging from 0.1 to 2, equation (4.11) is numerically solved and the obtained value of conductance τ is plotted as a function of temperature ($\frac{k_BT}{D_0}$) and the graph in figure 4.4 is obtained.

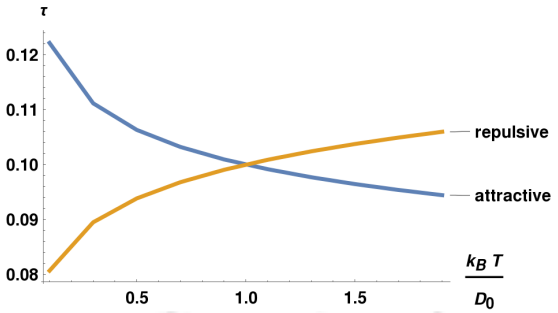

FIGURE 4.4: Conductance as a function of dimensionless temperature ($\frac{k_BT}{D_0}$) for a strong barrier ($\tau_0 = 0.1$) and weak interactions ($g = 0.9$ for repulsive and $g = 1.1$ for attractive).

Similar observations are made in figure 4.4 as in the earlier case, the only difference being that for strong barriers, conductance is less than that for weak barriers.

(c) Strong barrier and strong interactions: When interactions are strong, the holon velocity v_h is quite different from the Fermi velocity v_F and hence the following empirical values are chosen: $\tau_0 = 0.1$; $g = 10$ for attractive and $g = 0.1$ for repulsive interactions. Using these values the graph in figure 4.5 is obtained.

Figure 4.5 clearly signifies the 'healing the chain' phenomenon of Kane and Fisher [31]. It shows that particles with strong attractive forces between them can tunnel through even the strongest of barriers. This conductance however decreases sharply with an increase in the temperature.

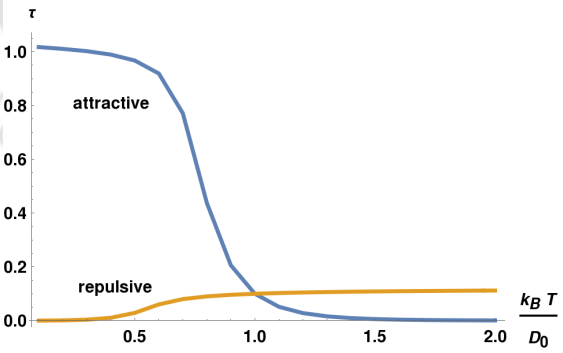

FIGURE 4.5: Conductance as a function of dimensionless temperature ($\frac{k_BT}{D_0}$) for a strong barrier ($\tau_0 = 0.1$) and strong interactions ($g = 0.1$ for repulsive and $g = 10$ for attractive).

(d) Weak barrier and strong interactions: The following empirical values are used as a representative of this case: $\tau_0 = 0.9$; $g = 5$ for attractive and $g = 0.5$ for repulsive interactions. For $\frac{k_BT}{D_0}$ ranging from 0.3 to 2, equation (4.11) is numerically solved and the obtained values of conductance τ is plotted as a function of temperature ($\frac{k_BT}{D_0}$) and the graph in figure 4.6 is obtained.

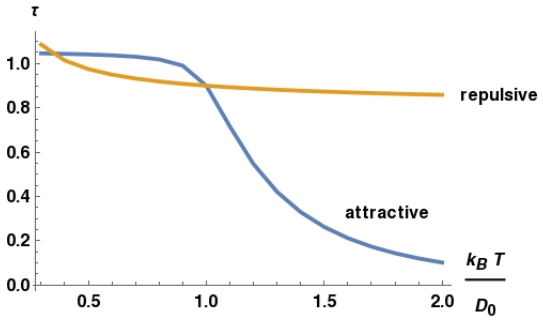

FIGURE 4.6: Conductance as a function of dimensionless temperature ($\frac{k_B T}{D_0}$) for a weak barrier ($\tau_0 = 0.9$) and strong interactions ($g = 0.5$ for repulsive and $g = 5$ for attractive).

The plot in this case shows interesting results in the form of high conductance even for repulsive interactions at lower temperatures. It is well known that for a non homogeneous system, the conductance vanishes at temperatures small compared to bandwidth if the particles are repulsive even if the impurity strength is low, as in the case (a) above. This is believed to be due to a conspiracy between the impurity and mutual interactions which tends to break the chain. But from figure 4.6, it is clear that if the interactions are too strong compared to the strength of the barrier, the system tends to exhibit high conductance at low temperatures rather than exhibiting the well known 'cutting the chain' phenomenon discussed by Kane and Fisher [31]. However at higher temperatures, they are similar to the earlier cases.

For a weak barrier, the transition from low conductance to high conductance at low temperatures as we increase the strength of repulsions is shown in figure 4.7. This can be understood using an analogy of the conductance of a diode. If one applies a reverse bias to a diode, the conductivity is very less, but if one goes on increasing the reverse bias voltage, at one point it enters into the breakdown region and there is a high flow of current in the reverse direction. Similarly in this case, when there is weak repulsion, the weak barrier behaves like a weak link with low tunneling across it. However, when the strength of repulsion is increased, it reaches a stage when conductance increases greatly, as with the case with homogeneous LL.

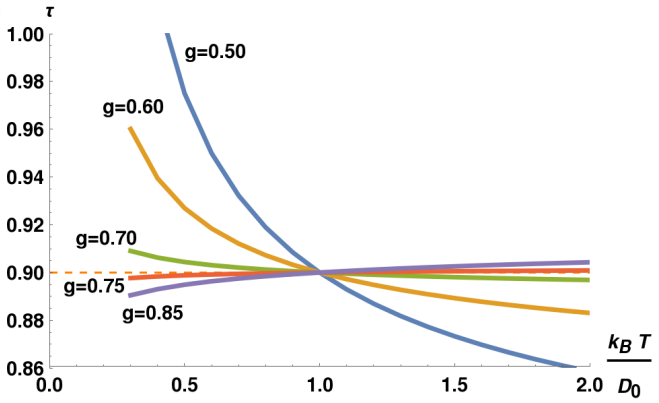

FIGURE 4.7: Conductance as a function of dimensionless temperature ($\frac{k_B T}{D_0}$) for a weak barrier ($\tau_0 = 0.9$) and various strength of repulsive interactions ($g = 0.5$ to 0.85).

4.2.2 Comparison with the results of Matveev et al.

The finite bandwidth calculation of conductance as a function of temperature is calculated by Matveev et al. [34] and is given in equation (14) of their paper as follows (setting $e^2/h = 1$ to tally with our results).

$$G(T) = \frac{\tau_0 \left(\frac{k_B T}{D_0}\right)^{2\alpha}}{1 - \tau_0 + \tau_0 \left(\frac{k_B T}{D_0}\right)^{2\alpha}} \tag{4.13}$$

and using their terminology for forward scattering interactions only, we have

$$2\alpha = \frac{v_0}{\pi v_F} \tag{4.14}$$

Expressing α in terms of the Luttinger parameter g used in this work, $2\alpha = \frac{1}{2}\left(\frac{1}{g^2} - 1\right)$. The formula in the equation (4.13) is valid only for weak interactions, as claimed by the authors [34]. So the comparison is done only for weak interactions and hence the empirical values of Luttinger parameter g is chosen to be 0.9 for repulsive interactions and 1.1 for attractive interactions. The conductance obtained for both strong barrier ($\tau_0 = 0.1$) and weak barrier ($\tau_0 = 0.9$) obtained using the analytical formula in equation (4.13) and that obtained using numerical solution of our results are plotted as a function of temperature ($\frac{k_B T}{D_0}$) in figure 4.8.

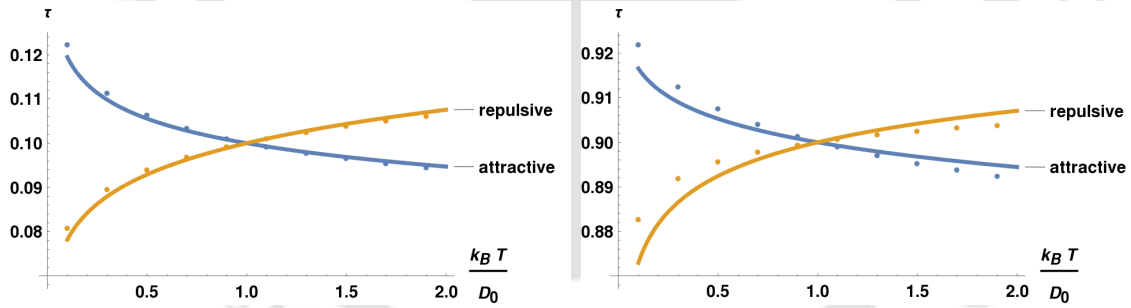

FIGURE 4.8: Conductance as a function of dimensionless temperature ($\frac{k_B T}{D_0}$) for weak interactions ($g = 0.9$ for repulsive and $g = 1.1$ for attractive). The dots are numerically exact solution of the transcendental equation obtained from NCBT and the solid lines represent the analytical formula of Matveev et al. (a) strong barrier ($\tau_0 = 0.1$) (b) weak barrier ($\tau_0 = 0.9$).

In figure 4.8, the continuous lines are obtained from the analytical formulas of conductance by Matveev et al. while the dots represents the numerical solution of the conductance obtained in the present work. It is seen that they are in good agreement with each other. For temperature very close to zero ($\frac{k_B T}{D_0} = 0.01$), the values of conductance obtained by both the methods (Matveev et al. and NCBT) are also in good agreement with each other. The following empirical values are chosen: τ_0 is 0.9 for weak barrier and 0.1 for strong barrier while g is 1.1 for attractive and 0.9 for repulsive interactions. The comparison is shown in the table 4.1.

TABLE 4.1: Values of conductance τ for weak interactions as obtained by Matveev et al. and NCBT for temperature very close to zero ($\frac{k_BT}{D_0} = 0.01$).

Case	Matveev et al.	NCBT	% difference
Weak barrier + attraction	0.930	0.937	0.75
Weak barrier + repulsion	0.840	0.854	1.64
Strong barrier + attraction	0.142	0.148	4.05
Strong barrier + repulsion	0.061	0.064	4.69

On the other hand, for temperatures much greater than the bandwidth ($\frac{k_BT}{D_0} = 50$), the values of conductance obtained by both the methods (Matveev et al. and NCBT) are again in good agreement with each other. The same empirical values are chosen: τ_0 is 0.9 for weak barrier and 0.1 for strong barrier while g is 1.1 for attractive and 0.9 for repulsive interactions. The comparison is shown in the table 4.2. As temperature is further increased the strength of interactions has to be decreased for a more favorable comparison.

TABLE 4.2: Values of conductance τ for weak interactions as obtained by Matveev et al. and NCBT for temperature much greater than bandwidth ($\frac{k_BT}{D_0} = 50$).

Case	Matveev et al.	NCBT	% difference
Weak barrier + attraction	0.865	0.834	3.72
Weak barrier + repulsion	0.934	0.918	1.74
Strong barrier + attraction	0.073	0.070	4.29
Strong barrier + repulsion	0.150	0.140	7.14

The central equation of finite bandwidth conductance of Matveev et al. valid for weak interactions as given by equation (4.13) can actually be obtained by considering the weak interaction limit of the transcendental equation (4.11) obtained using NCBT which is valid for any strength of interactions. Setting $y = \frac{k_BT}{D_0}$, equation (4.11) reads as follows.

$$\tau = \tau_0 \; y^{\eta(\tau)}$$

Differentiating with respect to y,

$$\frac{d\tau}{dy} = \tau_0 \; \eta(\tau) \; y^{\eta(\tau)-1} + \tau_0 \; \log[y] \; y^{\eta(\tau)} \frac{d\eta(\tau)}{dy}$$

For weak interactions, $\eta(\tau) = \frac{v_0}{\pi v_F}(1-\tau) = 2\alpha(1-\tau)$,

$$\frac{d\tau}{dy} = 2\alpha(1-\tau)\frac{\tau}{y} - \tau \; \log[y] \; 2\alpha \frac{d\tau}{dy}$$

For weak interactions, 2α is very small and hence one can write,

$$\frac{d\tau}{dy} = \frac{\tau(1-\tau)}{y}\frac{2\alpha}{(1+2\alpha\ \tau\ \log[y]\ )} \approx 2\alpha\ \frac{\tau(1-\tau)}{y}$$

Using appropriate limits of integration,

$$\log\left(\frac{\tau}{1-\tau}\right)\Big|_{\tau_0}^{\tau} = 2\alpha\log(y)\Big|_1^y$$

which gives,

$$\frac{\tau(1-\tau_0)}{\tau_0(1-\tau)} = y^{2\alpha}$$

which may be easily solved for τ (replacing y by $\frac{k_BT}{D_0}$),

$$\tau = \frac{\tau_0\left(\frac{k_BT}{D_0}\right)^{2\alpha}}{1-\tau_0+\tau_0\left(\frac{k_BT}{D_0}\right)^{2\alpha}} \tag{4.15}$$

which is precisely equation (4.13) obtained by Matveev et al. [34] in their work.

As claimed by Matveev et al. [34], the formula as given in equation (4.13) is valid for weak interactions. The breakdown of the Matveev et al.'s formula for conductance at strong interactions can be seen from figure 4.9. Choosing empirical values for a strong barrier ($\tau_0 = 0.1$) and strong interactions ($g = 0.1$ for repulsive and $g = 10$ for attractive), the conductance is plotted as a function of temperature and the graphs in figure 4.9 are obtained. In the case (c) of the previous subsection, it has been shown how NCBT conductance, for the exact same case as above, supports the healing the chain phenomenon for attractive interactions. But the figure 4.9 somewhat violates the cutting the chain phenomenon for strong repulsive interactions, that too with a strong barrier.

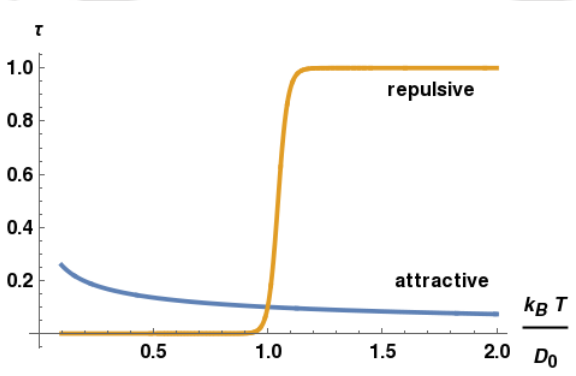

FIGURE 4.9: Conductance as a function of dimensionless temperature ($\frac{k_BT}{D_0}$) for a strong barrier ($\tau_0 = 0.1$) and strong interactions ($g = 0.1$ for repulsive and $g = 10$ for attractive) using Matveev et al.'s formula.

4.2.3 Anomalous conductance

It has been observed from the earlier plots that with an increase in temperature, conductance typically decreases for attractive interactions and increases for repulsive interactions. This is because the exponent η in equation (4.11) is typically positive for repulsive cases and negative for attractive cases. But in absence of interactions (g =1), the exponent η vanishes and the conductance becomes independent of temperature and is given by

$$\tau_{\eta=0} = \tau_0$$

However $g = 1$ is not the only condition for which η vanishes, the other condition being

$$g_0 = \frac{-1 \pm \sqrt{1 + 12\tau_0 - 12\tau_0^2}}{6(1 - \tau_0)}$$

Since $0 \leq \tau_0 \leq 1$, hence $\sqrt{1 + 12\tau_0 - 12\tau_0^2} \geq 1$. But since g can't be negative ($g = v_F/v_h$), the only admissible value of g for $\eta = 0$ is

$$g_0 = \frac{-1 + \sqrt{1 + 12\tau_0 - 12\tau_0^2}}{6(1 - \tau_0)}$$

Here g_0 is the value of g for which η vanishes. In presence of a strong barrier ($\tau_0 = 0.1$) the conductance becomes temperature independent ($\eta = 0$) for $g_0 = 0.08$ which indicates very strong repulsion. On the other hand, for a weak barrier ($\tau_0 = 0.9$) this happens for $g_0 = 0.74$, which is also repulsive but less stronger. This can be thought of as a conspiracy between the impurity and the repulsive interactions to give rise to a state that is similar to the non-interacting one. In figure 4.10, the conductance is shown as a function of temperature for values of g near g_0. It can be seen that as g approaches g_0, the temperature dependence of conductance becomes weaker and weaker (the graph flattens) and finally becomes independent (constant graph) for $g = g_0$.

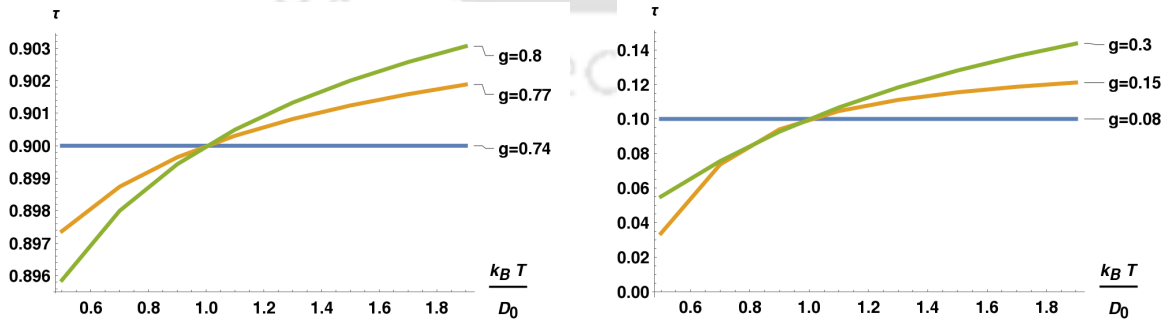

(a) (b)

FIGURE 4.10: Conductance as a function of dimensionless temperature ($\frac{k_B T}{D_0}$) for values of g near g_0 where conductance exponent η vanishes: (a) weak barrier ($\tau_0 = 0.9$) with $g_0 = 0.74$. (a) strong barrier ($\tau_0 = 0.1$) with $g_0 = 0.08$

4.2.4 Analytical solution

Equation (4.11) being transcendental in nature can't be solved analytically. However using the fact that the tunneling conductance τ is less than unity, the RHS of the equation can be expanded in powers of τ and truncated after a certain order. Smaller the value of τ, sooner can the series be truncated. Ignoring the third and higher powers of the series and solving the rest of the equation, the following expression of tunneling conductance is obtained.

$$\tau = \frac{-4g^2(\frac{k_BT}{D_0})^{\frac{1}{4}(2+\frac{1}{g})}\tau_0}{(g^2-1)(\frac{k_BT}{D_0})^{\frac{1}{4}(2+\frac{1}{g})}\tau_0\log(\frac{k_BT}{D_0}) - g^2(\frac{k_BT}{D_0})^{\frac{3g}{4}}(2+\sqrt{C})} \tag{4.16}$$

where

$$\begin{aligned} C =& 4 - 4(\frac{k_BT}{D_0})^{\frac{1}{4}(2+\frac{1}{g}-3g)}\tau_0\log(\frac{k_BT}{D_0})(1-\frac{1}{g^2}) \\ & - \frac{1}{g^4}\Big((1-g)^2(1+g)(\frac{k_BT}{D_0})^{\frac{1}{4}(2+\frac{1}{g}-3g)}\tau_0^2\log(\frac{k_BT}{D_0})(8g+(1+g)\log(\frac{k_BT}{D_0}))\Big) \end{aligned}$$

Using the analytical expression in equation (4.16) for weak interactions ($g = 0.9,\ 1.1$) the conductance is plotted as a function of temperature ($\frac{k_BT}{D_0}$) for both weak ($\tau_0 = 0.9$) and strong ($\tau_0 = 0.1$) barriers in figures 4.11(a) and 4.11(b) respectively and they are in close agreement with those obtained for the results of Matveev et al. depicted in figures 4.8(a) and 4.8(b) respectively.

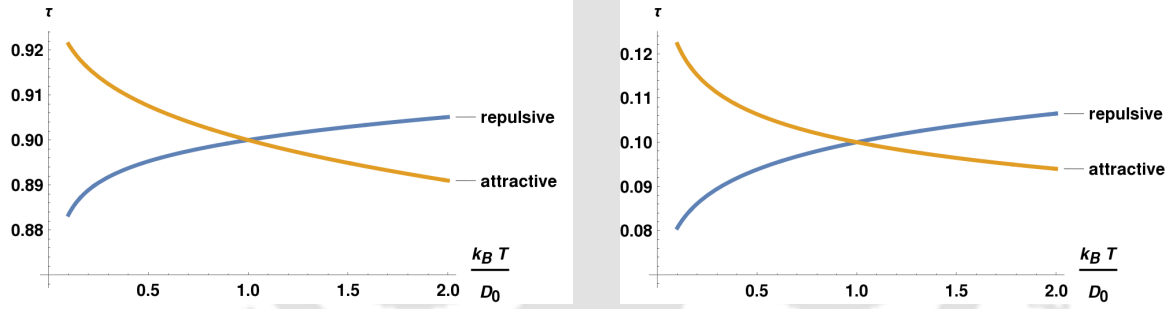

(a) (b)

FIGURE 4.11: Conductance from analytical expression as a function of dimensionless temperature ($\frac{k_BT}{D_0}$) for weak interactions (g = 0.9 for repulsive and $g = 1.1$ for attractive): (a) weak barrier ($\tau_0 = 0.9$) (b) strong barrier ($\tau_0 = 0.1$).

The conductance equation of Matveev et al. given by equation (4.13) may be expanded in powers of the interaction parameter, retaining the terms up to the first order (since it is for weak interactions). On the other hand, the analytical expression of conductance from NCBT given by equation (4.16) can also be expanded in terms of the interaction parameter and terms up to the first order may be retained. In both cases, the following is obtained which is an exact match for finite temperature conductance for weak interactions ($g \sim 1$).

$$\tau = \tau_0 + \frac{(1-g^2)\tau_0(1-\tau_0)\log(\frac{k_BT}{D_0})}{2g^2}$$

4.2.5 Comparison of analytical and numerical solution

The analytical solution using the second order approximation to the conductance and the numerical solution of the exact transcendental equation has to be compared so that one can estimate how good the approximation is for various cases. Choosing the empirical values of $g = 0.9,\ 1.1$ for weak interactions, $g = 0.3,\ 3$ for strong interactions and τ_0 to be 0.1 for strong barrier and 0.9 for weak barriers, the values of conductance are compared for different combinations of g's and τ_0's for the case $\frac{k_B T}{D_0} = 0.5$ and the results are tabulated in table 4.3.

TABLE 4.3: Comparison of the values of conductance τ obtained numerically and analytically for $\frac{k_B T}{D_0} = 0.5$

Case	Numerical	Analytical	% difference
Strong barrier + strong attraction	0.285	0.285	0
Strong barrier + weak attraction	0.106	0.106	0
Strong barrier + strong repulsion	0.055	0.055	0
Strong barrier + weak repulsion	0.094	0.094	0
Weak barrier + strong attraction	1.032	1.183	12.76
Weak barrier + weak attraction	0.907	0.908	0.11
Weak barrier + strong repulsion	1.288	1.024	25.78
Weak barrier + weak repulsion	0.895	0.895	0

From table 4.3 it can be observed that for strong barrier ($\tau_0 \sim 0$), the numerical and analytical values are precisely matching as ignoring the higher powers of τ_0 is a much better approximation in this case. For weak barriers ($\tau_0 \sim 1$) ignoring the higher powers of τ_0 is less accurate, especially for attractive interactions which tends to mitigate the effect of the barrier (healing the chain phenomenon as described by Kane and Fisher [31]) and make τ_0 approach unity. Thus there is a minor mismatch between the analytical and the numerical values for weak attractions and a little more for strong attractions. On the other hand repulsive interactions aggravate the effect of the barrier (cutting the chain phenomenon of Kane and Fisher [31]) and minimize the tunneling. Thus for weak repulsion, there is an exact match between the two values inspite of weak barriers. However for strong repulsions and weak barrier, there is some anomalous behavior as also depicted in figure 4.6 above, where the value of conductance tends towards unity and hence the second order approximation is not a very good one for this case.

4.2.6 Both forward and backward scattering

The transcendental equation given by the equation (4.11) and expression of the exponent $\eta(\tau)$ given by equation (4.12) remains the same upon inclusion of backward scattering interactions between fermions. The difference comes in the expression of the holon velocity v_h (note that

$g = v_F/v_h$), which is now modified to include the effect of backward scattering. Considering v_0 is the strength of forward scattering interactions as discussed in equation (7.2), the holon velocity is given by $v_h = v_F\sqrt{1+\frac{2v_0}{\pi v_F}}$. In presence of backward scattering (of strength v_1) the v_0 is replaced by an effective v_0 given by (in this work we only deal with fermions with spin)

$$v_{0,eff} = g_2(T) - 2g_1(T) \tag{4.17}$$

where g_1 and g_2 are the renormalized values of backward and forward scattering interaction strengths that can be derived using Parquet's approximation [28] and are given by

$$\begin{aligned} g_1(T) =& \frac{v_1}{1+\frac{v_1}{\pi v_F}\log\left[\frac{D_0}{k_B T}\right]} \\ g_2(T) =& v_0 - \frac{v_1}{2} + \frac{v_1}{2(1+\frac{v_1}{\pi v_F}\log\left[\frac{D_0}{k_B T}\right])} \end{aligned} \tag{4.18}$$

Hence the Luttinger parameter g used in equation (4.12) can be written for small values of interactions as follows.

$$g = \frac{1}{\sqrt{1+\frac{2v_{0,eff}}{\pi v_F}}} \approx 1 - \frac{v_{0,eff}}{\pi v_F} \tag{4.19}$$

Setting $y = \frac{k_B T}{D_0}$, equation (4.11) reads as follows.

$$\tau = \tau_0\ y^{\eta(\tau)}$$

Differentiating with respect to y,

$$\frac{d\tau}{dy} = \tau_0\ \eta(\tau)\ y^{\eta(\tau)-1} + \tau_0\ \log[y]\ y^{\eta(\tau)}\frac{d\eta(\tau)}{dy}$$

For weak interactions, $\eta(\tau) = \frac{v_{0,eff}}{\pi v_F}(1-\tau)$. Setting $\frac{v_{0,eff}}{\pi v_F} = 2\alpha_{eff}$,

$$\frac{d\tau}{dy} = 2\alpha_{eff}(1-\tau)\frac{\tau}{y} - \tau\ \log[y]\ 2\alpha_{eff}\frac{d\tau}{dy}$$

For weak interactions, $2\alpha_{eff}$ is very small and hence one can write,

$$\frac{d\tau}{dy} = \frac{\tau(1-\tau)}{y}\frac{2\alpha_{eff}}{(1+2\alpha_{eff}\ \tau\ \log[y]\ )} \approx 2\alpha_{eff}\ \frac{\tau(1-\tau)}{y}$$

Using equations (4.17) and (4.18),

$$\alpha_{eff} = \alpha_2 + \alpha_1\left(-\frac{1}{2} - \frac{3}{2-4\alpha_1\log[y]}\right)$$

Hence the differential equation takes the form

$$\frac{d\tau}{dy} = 2\left(\alpha_2 + \alpha_1\left(-\frac{1}{2} - \frac{3}{2 - 4\alpha_1 \log[y]}\right)\right)\ \frac{\tau(1-\tau)}{y}$$

which is solved and using appropriate limits of integration,

$$\tau = \frac{\tau_0\left(1 + 2\alpha_1 \log\left(\frac{D_0}{k_B T}\right)\right)^{\frac{3}{2}}\left(\frac{k_B T}{D_0}\right)^{2\alpha_2 - \alpha_1}}{1 - \tau_0 + \tau_0\left(1 + 2\alpha_1 \log\left(\frac{D_0}{k_B T}\right)\right)^{\frac{3}{2}}\left(\frac{k_B T}{D_0}\right)^{2\alpha_2 - \alpha_1}}$$

which is the conductance for weakly interacting electrons with both backward and forward scattering as also given by equation (21) of Matveev et al. [34].

It is interesting to see the interplay between the forward and backward scattering interactions. For weak or no backward scattering, the conductance shows a monotonic behavior with respect to temperature. When backward scattering is increased gradually, the conductance starts showing a non-monotonic behavior such that with an increase in temperature, the conductance first increases, reaches a maximum and then decreases. This is shown in figure 4.12 by numerically solving the transcendental equation (4.11) for the empirical values of $\tau_0 = 0.3$, $v_F = 1$, $v_0 = 0.02$ and $v_1 = 0.01$. The solution (depicted by the dots) is in good agreement with that of Matveev et al. (continuous line).

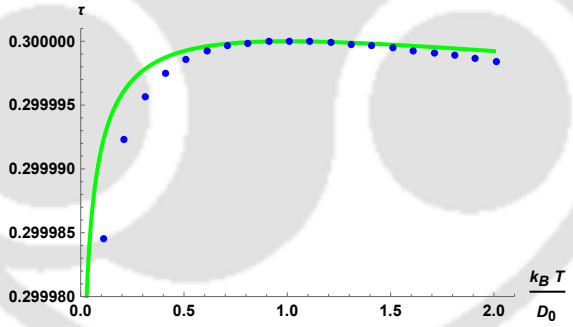

FIGURE 4.12: Conductance as a function of dimensionless temperature ($\frac{k_B T}{D_0}$) for weak interactions ($v_F = 1$, $v_0 = 0.02$ and $v_1 = 0.01$) and a barrier of strength $\tau_0 = 0.3$. The dots represent the NCBT numerical solution and the continuous line represents the analytical solution of Matveev et al.

4.2.7 Comparison with Monte Carlo results

The conductance of Luttinger liquids with impurities has been studied using numerical methods like Monte Carlo simulations [62, 82, 83]. In the work by Hamamoto et al. [62], where path integral Monte Carlo methods are used, it has been found that the d.c. conductance increases monotonically for $K_\rho > 1.025$ ($K_\rho = g$ in our notation and hence weakly attractive) with a decrease in temperature. Whereas for $K_\rho < 0.975$ (weakly repulsive) it decreases monotonically with a decrease in temperature. This is in good agreement with the plots in

figures 4.3 and 4.4 which are also for weak interactions ($g = 1.1$ for attractive and $g = 0.9$ for repulsive). Similar trends were earlier obtained by Leung et al. [83] for repulsive interactions with $g = 1/3$ and $g = 1/6$.

4.3 Resonant tunneling across a double barrier

Resonant tunneling is well-known in elementary quantum mechanics. Typically, this phenomenon is studied in a double-barrier system. When the Fermi wavenumber bears a special relation with the inter-barrier separation and height, the reflection coefficient becomes zero and the Green functions of the system behave as if they are those of a translationally invariant system. Consider a symmetric double delta-function with strength V_0 and separation d. Define, $\xi_0 = k_F d$. The resonance condition in this case is well-known to be,

$$V_0 \sin[\xi_0] + v_F \cos[\xi_0] = 0 \tag{4.20}$$

Resonant tunneling is studied for a square double barrier potential in one dimensions by Xiao et al. [129]. After taking the limiting cases of the square barriers tending to delta potentials and imposing the RPA limit, equation (4.20) is obtained.

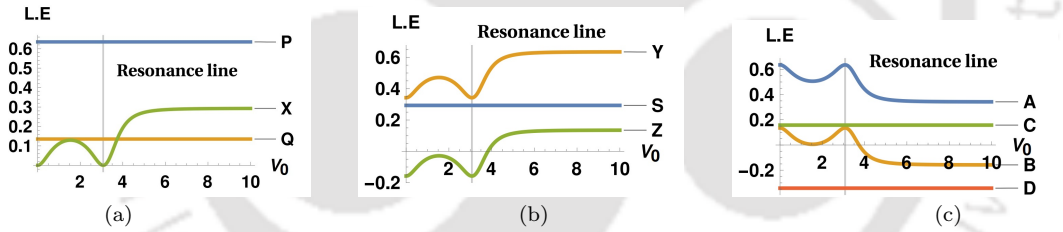

FIGURE 4.13: Anomalous exponents (L.E) vs impurity strength V_0 for symmetric double barrier: (a) Exponents of $\langle \psi_R(X_1)\psi_R^\dagger(X_2)\rangle$ on the same side (b) Exponents of $\langle \psi_R(X_1)\psi_L^\dagger(X_2)\rangle$ on the same side (c) Exponents of $\langle \psi_R(X_1)\psi_R^\dagger(X_2)\rangle$ on opposite sides. Explicit expressions of the exponents are given in equations (3.22) and (3.23)

.

The anomalous exponents of the correlation functions given in equations (3.22) and (3.23) are plotted in figure 4.13 in the vicinity of resonance to see the signatures of resonance tunneling on the Luttinger liquid Green function of a symmetric double delta potential. It may be seen that when the system is at resonance (depicted by the vertical line), all the anomalous exponents take exactly the same values that they take when there is no barrier at all.

For an asymmetric double delta system, $V(x) = V_1\delta(x + a) + V_2\delta(x - a)$, the anomalous exponents can also be calculated using NCBT. The form of the exponents are the same as

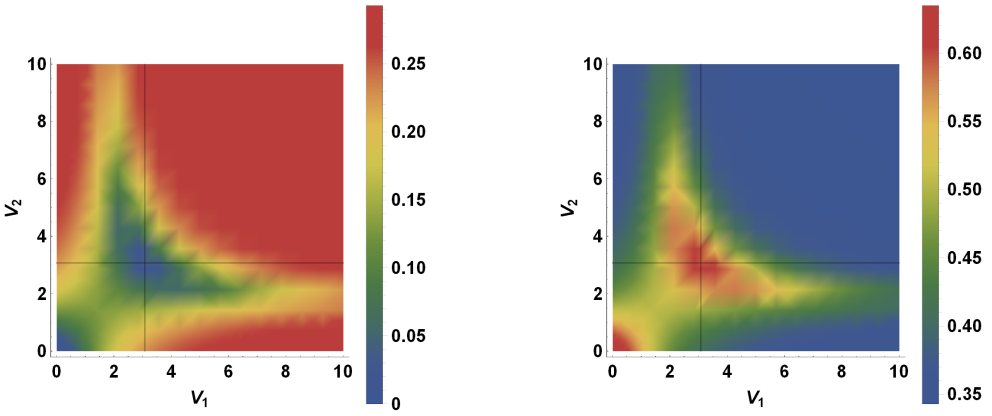

(a) (b)

FIGURE 4.14: Anomalous exponents for double barrier: The anomalous exponents (a) X and (b) A as functions of impurity strength V_1 and V_2 for an asymmetric double delta potential. Near resonance (the point of intersection of the cross lines), the system has the same colour it has when both V_1 and V_2 are zero.

given in equations (3.22) and (3.23) but the expression of the reflection amplitude is now different and is given by (here $\xi_0 = 2k_F a$) [90].

$$R = -\frac{2i\frac{V_1V_2}{v_F^2}\sin[\xi_0] + \frac{2i}{v_F}\left(\frac{V_1e^{i\xi_0}+V_2e^{-i\xi_0}}{2}\right)}{\left(1 + i\frac{V_1+V_2}{v_F} + \frac{i^2V_1V_2}{v_F^2}\right) + \frac{V_1V_2}{v_F^2}e^{2i\xi_0}} \tag{4.21}$$

In this case eg., resonance is achieved when both V_1 and V_2 becomes equal ($V_1 = V_2 = V_0$) and V_0 obeys the same condition in equation (4.20). Two of the anomalous exponents X and A (expressions given in equations (3.22), (3.23) and (4.21)) for the asymmetric double delta system are plotted in figure 4.14. The point of intersection of the cross lines is the condition for resonance and it can easily be seen that the exponent takes the same value (color) at resonance point as it takes for the no-impurity system ($V_1 = V_2 = 0$).

4.4 Summary

In this work, the correlation functions of a Luttinger liquid with a cluster of impurities around an origin obtained using the non-chiral bosonization technique (NCBT) are used to study temperature dependence of tunneling conductance. This temperature dependence is shown to be a simple power law when the forward-scattering mutual interaction between fermions is short-ranged and has a large bandwidth (relative to temperature). Special attention is paid to the nature of the exponent in this power law for situations close to resonant tunneling (eg. in case of double barrier). A distinction is made between Kubo conductance which is related to current-current correlation (a four-point function) and the tunneling conductance which is the outcome of a tunneling experiment (related to two-point functions). In both

the cases, closed analytical expressions for conductance are calculated at temperatures small compared to the bandwidth and a number of interesting physical properties are discussed, besides presenting a favorable comparison with existing literature. The novelty of this work are the closed analytical formulas for the conductance exponents for arbitrary strengths of impurities and mutual interaction between fermions.

The finite-bandwidth conductance of a Luttinger liquid (LL) with a cluster of impurities is studied and its variation with respect to temperature is shown. The results are compared with those obtained by Matveev et al. [34] who deal with a weakly interacting LL. By contrast, NCBT correctly provides the conductance for all values of the interaction strength (as well as the sign). In addition to finding perfect agreement with the results of Matveev et al. for both weakly repulsive and weakly attractive mutual interactions, we are also able to probe novel physics seen when the repulsion is strong - in the form of a weakly temperature dependent conductance when there is a definite relationship between the transmission amplitude of the non-interacting system and the holon velocity. Secondly, an unusual high conductance for strongly repulsive mutual interactions is observed for a weak barrier at low temperatures. Lastly, inclusion of backward scattering leads to the non-monotonic temperature dependence of conductance when dealing with fermions with spin, which can be called as a deviation from the usual Luttinger liquid behavior.

Chapter 5

The one step fermionic ladder

In the previous chapters it has been shown how a modification of the field operator used in standard bosonization can correctly produce the correlation functions of a Luttinger liquid with a cluster of impurities, which are later used to study various physical properties. A variant of this system is the one-step ladder, i.e., Luttinger Liquids (two 'poles'/'legs' of the ladder) lying close to each other with a non-zero hopping probability from one pole to another at a specific location on each pole. In the present work, the same approach, known as the 'Non Chiral Bosonization technique' or NCBT, has been employed to obtain the Green functions for the well-studied one-step fermionic ladder. The system under consideration is described in Fig. 5.1 in the form of a caricature.

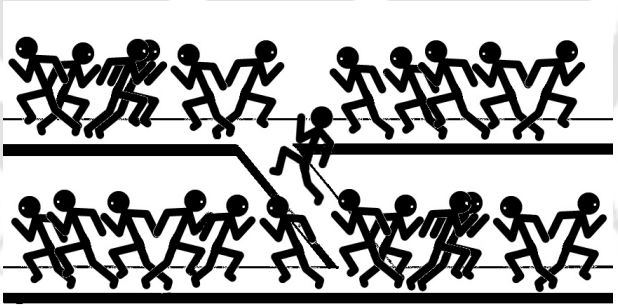

FIGURE 5.1: The one step fermionic ladder: The two parallel tracks representing the two Luttinger liquids, the athletes representing electrons moving in both the directions, with the fastest athlete possessing the Fermi momentum, while rubbing shoulders against each other representing forward scattering interactions. One athlete running between the tracks represents the hopping of electrons between the Luttinger Liquids.

There have been numerous attempts made to compute the correlation functions of fermionic ladder both numerically [130, 131] and analytically [132–135]. H. J. Schulz investigated the phase diagram and excitation spectrum of two parallel Luttinger liquids coupled by single-particle hopping [136]. Patrick et al. applied the Lieb-Schultz-Mattis theorem to spinful electrons interacting on a ladder which allowed them to obtain a generalized Luttinger theorem for such systems [137]. D.G. Clarke et al. demonstrated that there is no coherent single

particle hopping between two spin-charge separated Luttinger Liquids for hopping parameter below a critical value and in such situations, the two Luttinger liquids will not exhibit split Fermi surfaces [138]. S. Das et al. studied the transport of quasiparticles between two edges of Quantum hall liquid via an anti-dot providing the local scattering [139].

In this chapter [140], we obtain the power law behavior of the correlation functions of the one step ladder in the presence of forward scattering interaction among the particles. This happens to be the most singular part of the asymptotic forms of the correlation functions under study. This enables various studies including Friedel oscillations in the density correlation functions and the finite temperature d.c. conductance of such systems.

5.1 Problem overview

Consider the one step ladder where two Luttinger Liquids are placed parallel to each other such that there is a finite probability of hopping at $x = 0$. The Hamiltonian of the system may be written as follows:

$$H = \sum_{k} \sum_{j=1,2} \epsilon_k c_{kj}^{\dagger} c_{kj} + \frac{w}{L} \sum_{k,k'} c_{k1}^{\dagger} c_{k'2} + \frac{w}{L} \sum_{k,k'} c_{k'2}^{\dagger} c_{k1} + \frac{1}{2} \int_{-\infty}^{\infty} dx \int_{-\infty}^{\infty} dx^{'} \; v(x - x^{'}) \; \rho(x) \rho(x^{'}) \tag{5.1}$$

where $v(x-x^{'}) = \frac{1}{L} \sum_q e^{-iq(x-x^{'})} v_q$ (where $v_q = 0$ if $|q| > \Lambda$ for some fixed $\Lambda \ll k_F$ and $v_q = v_0$ is a constant, otherwise) is the forward scattering mutual interaction. 'L' is the length of the system and 'w' is the hopping parameter which determines the probability of an electron to jump from one pole to another along the $x = 0$ line.

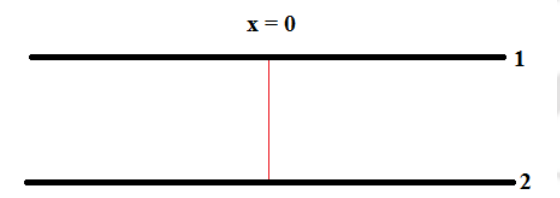

FIGURE 5.2: The one step ladder: Two Luttinger Liquids (1 and 2) placed parallel to each other with a finite probability of hopping at x=0.

The study is carried out in the RPA (Random Phase Approximation) limit, which is a pre-requisite in order to obtain closed expressions of the Green functions, and which means allowing the the Fermi momentum and the mass of the fermion to diverge in such a way that their ratio is finite (i.e. $k_F, m \to \infty$ but $\frac{k_F}{m} = v_F < \infty$) and thus linearizing the energy momentum dispersion near the Fermi surface. Units are chosen such that $\hbar = 1$, so that k_F is both the Fermi momentum as well as a wavenumber.

5.2 Green's functions of free fermions

The full two-point Green function (also known as single-particle Green's function) of the system before taking the RPA limit (i.e. with parabolic energy momentum relation) is denoted as $< T\ \psi(x,\sigma,t)\psi^{\dagger}(x',\sigma',t') >$. The time ordering decides whether it is particle or hole Green's function that is being studied and σ is the spin projection of the individual fermions. In terms of this, the asymptotic or RPA Green function is defined by "smearing out" the positions and times over the scale of the Fermi wavelength and Fermi times as follows,

$$\langle T\ \psi_{\nu}(x,\sigma,t)\psi^{\dagger}_{\nu'}(x',\sigma',t')\rangle = \lim_{m\to\infty} \ll \langle T\psi(y,\sigma,\tau)\psi^{\dagger}(y',\sigma',\tau')\rangle e^{-ik_F(\nu y-\nu' y')}e^{iE_F(\tau-\tau')} \gg \tag{5.2}$$

where,

$$\begin{aligned} \ll f(t) \gg &= \frac{1}{2T_F}\int_{t-T_F}^{t+T_F} d\tau\ f(\tau) \\ \ll g(x) \gg &= \frac{1}{2\lambda_F}\int_{x-\lambda_F}^{x+\lambda_F} dy\ g(y) \end{aligned} \tag{5.3}$$

with $\lambda_F = 2\pi/k_F$ and $T_F = 2\pi/E_F$, $k_F = mv_F$ and $E_F = (1/2)mv_F^2$ with $v_F < \infty$ being held fixed. Also, here $\nu, \nu' = \pm 1$ correspond to the right and left Fermi points. When mutual interactions between the fermions are absent it is easy to show that the two-point function has the form (at zero temperature in the RPA sense) shown below (here 'i' and 'j' in the subscript denote the pole number),

$$\begin{aligned} &< T\ \psi_i(x,t)\psi^{\dagger}_j(x',t') >_0 \\ &= e^{ik_F(x-x')}\ \frac{i}{2\pi}\ \frac{\delta_{i,j}}{(x-x')-v_F(t-t')} + e^{-ik_F(x-x')}\ \frac{i}{2\pi}\ \frac{\delta_{i,j}}{-(x-x')-v_F(t-t')} \\ &+\frac{w}{2\pi}\frac{(v_F\delta_{\bar{i},j}+iw\ \delta_{i,j})}{(v_F^2+w^2)}\ \frac{e^{-ik_F(|x|+|x'|)}}{|x|+|x'|+v_F(t-t')} + \frac{w}{2\pi}\frac{(v_F\delta_{\bar{i},j}-iw\ \delta_{i,j})}{(v_F^2+w^2)}\ \frac{e^{ik_F(|x|+|x'|)}}{|x|+|x'|-v_F(t-t')} \end{aligned} \tag{5.4}$$

Note that in equation (5.4), the term $[(\nu x-\nu' x')-v_F(t-t')]$ (where $\nu=\pm1$) appears in the denominator. In general, when mutual interactions are incorporated into the Luttinger liquid, this term appears with a non-trivial system dependent exponent viz. $[(\nu x-\nu' x')-v_F(t-t')]^g$. Listing these g's and other similar exponents has been one of the main goals of the NCBT since $g=1$ is only when mutual interaction between fermions are absent. It is easy to generalize these results to finite temperature since for this a simple replacement viz. $\frac{1}{X}\to\frac{\pi}{\beta v_F}\ csch[\frac{\pi X}{\beta v_F}]$ is sufficient where e.g. $X \equiv [(\nu x-\nu' x')-v_F(t-t')]$ and β is inverse temperature.

5.2.1 Density density correlation function

In the RPA sense, the density $\rho(x,t)$ may be harmonically analyzed as follows.

$$\rho^i(x,t) = \rho^i_s(x,t) + e^{2ik_F x}\ \rho^i_f(x,t) + e^{-2ik_F x}\ \rho^{i*}_f(x,t) \tag{5.5}$$

The slowly varying part of the density ρ_s (the average density is subtracted out, so this is really the deviation) has an auto-correlation function which when mutual interactions are absent, may be written down using Wick's theorem as follows,

$$\begin{aligned} < T\ \rho_s^i(x,t)\rho_s^j(x^{'},t^{'}) >_0 \ &= -\frac{\delta_{i,j}}{4\pi^2}\sum_{\nu=\pm 1}\frac{1}{((x-x^{'})-\nu v_F(t-t^{'}))^2}\theta(xx^{\prime}) \\ &-\frac{w^2(v_F^2\delta_{\bar{i},j}+w^2\delta_{i,j})}{4\pi^2(v_F^2+w^2)^2}\sum_{\nu=\pm 1}\frac{1}{((x+x^{'})-\nu v_F(t-t^{'}))^2}\theta(xx^{\prime}) \\ &-\frac{v_F^2(v_F^2\delta_{i,j}+w^2\delta_{\bar{i},j})}{4\pi^2(v_F^2+w^2)^2}\sum_{\nu=\pm 1}\frac{1}{((x-x^{'})-\nu v_F(t-t^{'}))^2}\theta(-xx^{\prime}) \end{aligned} \tag{5.6}$$

5.3 Bosonized version of the two point Green functions

The inversion of the defining relation between currents and densities in the standard bosonization scheme that goes by the name g-ology (see the book by Giamarchi [5]) yields the following relation between $\psi_\nu(x,\sigma,t)$ (where $\nu = R(+1)\ or\ L(-1)$) and the slowly varying part of the density (this is a mnemonic for generating the N-point functions),

$$\psi_\nu(x,\sigma,t) \sim e^{i\theta_\nu(x,\sigma,t)} \tag{5.7}$$

with the local phase given by the formula,

$$\theta_\nu(x,\sigma,t) = \pi\int_{sgn(x)\infty}^{x} dy\Big(\nu\ \rho_s(y,\sigma,t) - \int_{sgn(y)\infty}^{y} dy^{'}\ \partial_{v_F t}\ \rho_s(y^{'},\sigma,t)\Big) \tag{5.8}$$

It has been argued in the previous chapters that the prescription in equation (5.7) is merely a mnemonic valid only for nearly homogeneous systems and may not be thought of as an operator identity and should not be used to generate Hamiltonians of systems with strongly inhomogeneous external potentials. In order to validate the computation of N-point function for a cluster of impurities in a Luttinger Liquid, it is necessary to slightly modify the above prescription as follows [90],

$$\psi_{\nu_i}(x_i,\sigma_i,t_i) \rightarrow \sum_{\gamma_i=\pm 1}\sum_{\lambda_i\in\{0,1\}} C_{\lambda_i,\nu_i,\gamma_i}(\sigma_i)\ \theta(\gamma_i x_i)\ e^{i\theta_{\nu_i}(x_i,\sigma_i,t_i)+2\pi i\nu_i\lambda_i\int_{sgn(x_i)\infty}^{x_i}\rho_s(-y_i,\sigma_i,t_i)\ dy_i} \tag{5.9}$$

For two Luttinger liquids with a finite probability of hopping at one point, the pole index 'i' (to which Luttinger liquid the field operator belongs to) also comes into the picture and the prescription is given as follows.

$$\begin{aligned} \psi_{\nu_i}^i(x_i,\sigma_i,t_i) \rightarrow e^{-iX_{\sigma_i}}e^{-iX^i}\sum_{\gamma_i=\pm 1}\sum_{\lambda_i\in\{0,1\}} C^i_{\lambda_i,\nu_i,\gamma_i}(\sigma_i)\ \theta(\gamma_i x_i)\ \ e^{i\theta^i_{\nu_i}(x_i,\sigma_i,t_i)}\ \ e^{i\pi\sum_{\sigma>\sigma_i}N_\sigma} \\ e^{i\pi\sum_{j>i}N^j}\ \ e^{2\pi i\nu_i\lambda_i\int_{sgn(x_i)\infty}^{x_i}\left(\rho_s^{\bar{i}}(y_i,\sigma_i,t_i)+\sum_{i=i,\bar{i}}\rho_s^i(-y_i,\sigma_i,t_i)\right)\ dy_i} \end{aligned} \tag{5.10}$$

where $\lambda_i = 0, 1$ only. Here N^i is the total number of fermions (all spins combined) on the i-th pole of the ladder and N_σ is the total number of fermions with spin projection σ on both the poles combined. Also $[X_{\sigma_i}, N_{\sigma_j}] = i\delta_{\sigma_i,\sigma_j}$ and $[X^i, N^j] = i\delta_{i,j}$, $[X^i, X^j] = 0$ and $[X_{\sigma_i}, X_{\sigma_j}] = 0$ are canonical conjugates. These additional global quantities ensure that the up spin field anticommutes with the down spin field and different poles also anti-commute. All these global quantities commute with the local operators in the exponent. Fortunately, as far as practical calculations go, nothing is lost by treating these global objects as c-numbers since doing so enables the correct correlation functions to be reproduced.

The quantities $C^i_{\lambda_i,\nu_i,\gamma_i}(\sigma_i)$ are c-numbers which involves cut-offs, etc. and are as such not obtainable using these techniques. They are fixed by a comparison with the non-interacting N-point functions obtained using Fermi algebra. The term $\rho^i_s(-y_i, \sigma_i, t_i)$, which is the signature of NCBT [90] ensures that trivial exponents are obtained when equation (5.10) is used to compute the N-point functions in the sense of RPA and in absence of interactions.

The first task is to derive a prescription for choosing the λ's which would lead to the N-point functions of the system (without mutual interactions) identical to what is given by Wick's theorem. The next task is to generalize the slow part of the density density correlation functions in equation (5.6) to include mutual interactions, which when done in the spirit of RPA gives the following results.

$$
\begin{aligned}
&< \rho^1_s(x_1,t_1,\sigma_1)\rho^1_s(x_2,t_2,\sigma_2) > \\
&\quad = -\frac{1}{4\pi^2}\sum_{\nu=\pm1}\Bigg[\frac{v_F}{2v_h}\left(\frac{1}{[|x_1-x_2|-\nu v_h(t_1-t_2)]^2}\right) + \sigma_1\sigma_2\frac{1}{2}\left(\frac{1}{[|x_1-x_2|-\nu v_F(t_1-t_2)]^2}\right) \\
&\qquad + \left(\frac{v_F w^2\ \mathrm{sgn}(x_1x_2)}{2v_h(v_Fv_h+w^2)} - \frac{v_F^2w^2}{2(v_F^4+2v_Fv_hw^2+w^4)}\right)\left(\frac{1}{[|x_1|+|x_2|-\nu v_h(t_1-t_2)]^2}\right) \\
&\qquad + \sigma_1\sigma_2\left(\frac{w^2\ \mathrm{sgn}(x_1x_2)}{2(w^2+v_F^2)} - \frac{w^2v_F^2}{2(w^2+v_F^2)^2}\right)\left(\frac{1}{[|x_1|+|x_2|-\nu v_F(t_1-t_2)]^2}\right)\Bigg]
\end{aligned}
\tag{5.11}
$$

$$
\begin{aligned}
< \rho^1_s(x_1,t_1,\sigma_1)\rho^2_s(x_2,t_2,\sigma_2) > = -\frac{1}{4\pi^2}\sum_{\nu=\pm1}\Bigg[&\sigma_1\sigma_2\frac{w^2v_F^2}{2(w^2+v_F^2)^2}\left(\frac{1}{[|x_1|+|x_2|-\nu v_F(t_1-t_2)]^2}\right) \\
&+\frac{v_F^2w^2}{2(v_F^4+2v_Fv_hw^2+w^4)}\left(\frac{1}{[|x_1|+|x_2|+v_h(t_1-t_2)]^2}\right)\Bigg]
\end{aligned}
\tag{5.12}
$$

Here $v_h = \sqrt{v_F^2 + \frac{2v_Fv_0}{\pi}}$ is the holon velocity whereas the spinon velocity is just the Fermi velocity since it is the total density that couples to the short range potential: $v_n = v_F$. The interaction between fermions is the two-body short range forward scattering potential which just means the potential between two particles at x and x' is $V(x-x') = \frac{1}{L}\sum_{|q|<\Lambda} e^{-iq(x-x')}\, v_0$, where Λ is the bandwidth which is held fixed as the RPA limit is taken. Also the correlation of holon density with spinon density is zero.

$$\langle T\ \rho_n(x_1,t_1)\rho_h(x_2,t_2)\rangle \equiv 0$$

Equation (5.11) and equation (5.12) boil down to the density density correlation functions of a clean Luttinger liquid when the hopping parameter 'w' is zero. It is easy to show that equation (5.11) and equation(5.12) are the outcomes of a re-summation of the most singular parts of the RPA terms in a perturbation series in powers of the mutual interaction v_0 carried out using Fermi algebra.

The notion of "the most singular part" of an expression such as the ones shown above may be made sense of in the following manner. Think of these as function of the time difference $\tau = t_1 - t_2$ (which they are). In the formulas that are encountered while expanding in powers of the coupling, there are going to be terms of the form (e.g.)

$$\frac{A\,\tau}{(\tau - a)^2} + \frac{B}{(\tau - a_1)(\tau - a_2)} \tag{5.13}$$

The first term is regarded as more singular than the second (if $a_1 \neq a_2$) since the former is a second order pole whereas the latter when partial fraction expanded are a sum of two first order poles. In the perturbative expansion of the slow part of the density density correlations, pretending that Wick's theorem applies at the level of the density fluctuations is tantamount to retaining second order poles and discarding poles of a lower order. The same rule applies when deciding what to retain and what to discard in the perturbation expansion of the single-particle Green function. The density density correlation functions as mentioned in equations (5.11) and (5.12) is perturbatively expanded in powers of the interaction parameter v_0. The zeroth order term has an exact match with that of the non interacting density density correlation function as mentioned in equation (5.6) of the main text. The most singular part of the first order term of the density density correlation functions obtained from conventional perturbation theory are as follows:

Case I : x_1 and x_2 are on the same pole and same side of the origin

$$\delta < \rho_1(x_1,t_1)\rho_1(x_2,t_2) > = \frac{1}{4\pi^3}\Bigg(\frac{(t_1-t_2)}{(|x_1-x_2| + v_F(t_1-t_2))^3} - \frac{(t_1-t_2)}{(|x_1-x_2| - v_F(t_1-t_2))^3} + \frac{w^4}{(w^2+v_F^2)^2}\Big(\frac{(t_1-t_2)}{(x_1+x_2+v_F(t_1-t_2))^3} - \frac{(t_1-t_2)}{(x_1+x_2-v_F(t_1-t_2))^3}\Big)\Bigg)$$

Case II : x_1 and x_2 are on same pole and opposite sides of the origin

$$\delta <\rho_1(x_1,t_1)\rho_1(x_2,t_2) >= \frac{v_F^4}{4\pi^3(w^2+v_F^2)^2}\left(\frac{(t_1-t_2)}{(x_1-x_2+v_F(t_1-t_2))^3} - \frac{(t_1-t_2)}{(x_1-x_2-v_F(t_1-t_2))^3}\right)$$

Case III : x_1 and x_2 are on opposite poles and same of the origin

$$\delta <\rho_1(x_1,t_1)\rho_2(x_2,t_2) >= \frac{v_F^2w^2}{4\pi^3(w^2+v_F^2)^2}\left(\frac{(t_1-t_2)}{(x_1+x_2+v_F(t_1-t_2))^3} - \frac{(t_1-t_2)}{(x_1+x_2-v_F(t_1-t_2))^3}\right)$$

Case IV : x_1 and x_2 are on opposite poles and opposite sides of the origin

$$\delta <\rho_1(x_1,t_1)\rho_2(x_2,t_2) >= \frac{v_F^2w^2}{4\pi^3(w^2+v_F^2)^2}\left(\frac{(t_1-t_2)}{(x_1-x_2+v_F(t_1-t_2))^3} - \frac{(t_1-t_2)}{(x_1-x_2-v_F(t_1-t_2))^3}\right)$$

It is easy to see that these are identical to the corresponding expansions of (5.11) and (5.12).

5.4 Full two-point Green's function

The two point (single-particle) Green function, in the sense of RPA, may be written down using the correspondence in equation (5.10). The main focus is on the anomalous exponents which refer to the constants g that appear in terms of the form $[\nu_1 x_1 - \nu_2 x_2 - v_F(t_1 - t_2)]^g$ that emerge from this calculation. The necessary step here is to formulate a prescription for deciding which of the $\lambda_i's$ are zeros and which are ones and under what circumstances, after which the g's may be uniquely pinned down. This prescription follows unambiguously from the condition that an evaluation (of the 2M-point function) in the Gaussian (and RPA) sense leads to trivial exponents when mutual interactions between fermions are absent. The coefficients $C's$ which depend on the details of the potentials and cutoffs and other such non-universal features are of lesser importance, as is also the case in the conventional approach. The prescription for obtaining the $\lambda_i's$ are simple. One needs to consider a general 2M-point function and then mentally pair up one annihilation operator with one creation operator and create M such pairs. This is merely a mental activity since this pairing (Wick's theorem) is not valid when mutual interactions are present. Consider one such pair and let the two λ's of this pair be (λ_m, λ_k) where $k > m$. The constraints are as follows:

$$\lambda_m = \begin{cases} \lambda_k & \text{if } (\nu_m, \nu_k) = (\gamma_m, \gamma_k) \text{ or } (\nu_m, \nu_k) = (-\gamma_m, -\gamma_k) \\ 1 - \lambda_k & \text{if } (\nu_m, \nu_k) = (-\gamma_m, \gamma_k) \text{ or } (\nu_m, \nu_k) = (\gamma_m, -\gamma_k) \end{cases} \tag{5.14}$$

This (unique) prescription guarantees the right trivial exponents in the right places when mutual interactions are turned off. The full Green function in presence of interactions are as follows (Notation: $X_i \equiv (x_i, \sigma_i, t_i)$. Furthermore the finite temperature versions of the formulas below are obtained by replacing $Log[Z]$ by $Log[\frac{\beta v_F}{\pi}\ Sinh[\frac{\pi Z}{\beta v_F}]]$ where $Z \sim [(\nu x_1 - \nu^{'} x_2) - v_a(t_1 - t_2)]$ and singular cutoffs ubiquitous in this subject are suppressed in this notation for brevity - they have to be understood to be present).

Case I : x_1 and x_2 on the same side of the origin and on the same pole

$$\begin{aligned}
\Big\langle T\ \psi_R(X_1)\psi_R^{\dagger}(X_2)\Big\rangle &= \frac{i}{2\pi} e^{\gamma_1 \log[4x_1x_2]} Exp[-\sum_{\substack{\nu,\nu^{'}=\pm 1 \\ a=h,n}} Q_{1,1}(\nu,\nu^{'};a)\ Log[(\nu x_1 - \nu^{'} x_2) - v_a(t_1 - t_2)]] \\
\Big\langle T\ \psi_L(X_1)\psi_L^{\dagger}(X_2)\Big\rangle &= \frac{i}{2\pi} e^{\gamma_1 \log[4x_1x_2]} Exp[-\sum_{\substack{\nu,\nu^{'}=\pm 1 \\ a=h,n}} Q_{-1,-1}(\nu,\nu^{'};a)\ Log[(\nu x_1 - \nu^{'} x_2) - v_a(t_1 - t_2)]] \\
\Big\langle T\ \psi_R(X_1)\psi_L^{\dagger}(X_2)\Big\rangle &= \frac{i}{2\pi} \frac{w^2}{w^2 + v_F^2} \frac{1}{2}(e^{\gamma_1 \log[2x_1]} e^{(3+\gamma_2)\log[2x_2]} + e^{(3+\gamma_2)\log[2x_1]} e^{\gamma_1 \log[2x_2]}) \\
&\quad Exp[-\sum_{\substack{\nu,\nu^{'}=\pm 1 \\ a=h,n}} Q_{1,-1}(\nu,\nu^{'};a)\ Log[(\nu x_1 - \nu^{'} x_2) - v_a(t_1 - t_2)]] \\
\Big\langle T\ \psi_L(X_1)\psi_R^{\dagger}(X_2)\Big\rangle &= \frac{i}{2\pi} \frac{w^2}{w^2 + v_F^2} \frac{1}{2}(e^{\gamma_1 \log[2x_1]} e^{(3+\gamma_2)\log[2x_2]} + e^{(3+\gamma_2)\log[2x_1]} e^{\gamma_1 \log[2x_2]}) \\
&\quad Exp[-\sum_{\substack{\nu,\nu^{'}=\pm 1 \\ a=h,n}} Q_{-1,1}(\nu,\nu^{'};a)\ Log[(\nu x_1 - \nu^{'} x_2) - v_a(t_1 - t_2)]]
\end{aligned} \tag{5.15}$$

The values of the exponents 'Q' are mentioned in Table 5.1.

Case II : x_1 and x_2 on the same side of the origin and on opposite poles

$$
\begin{aligned}
&< T\ \psi_R(X_1)\psi_R^{\dagger}(X_2) > \ = \ 0 \\
&< T\ \psi_L(X_1)\psi_L^{\dagger}(X_2) > \ = \ 0 \\
&< T\ \psi_R(X_1)\psi_L^{\dagger}(X_2) > \\
&\quad = \frac{1}{2\pi^2}\frac{wv_F}{w^2+v_F^2}\frac{e^{\gamma_1 \log[2x_1]}e^{(3+\gamma_2)\log[2x_2]}}{2(x_1-x_2)}\ Exp[-\sum_{\substack{\nu,\nu^{'}=\pm 1\\ a=h,n}} S_{1,1}(\nu,\nu^{'};a;1)\ \ Log[(\nu x_1-\nu^{'}x_2)-v_a(t_1-t_2)]] \\
&\quad + \frac{1}{2\pi^2}\frac{wv_F}{w^2+v_F^2}\frac{e^{(3+\gamma_2)\log[2x_1]}e^{\gamma_1 \log[2x_2]}}{2(x_1-x_2)}\ Exp[-\sum_{\substack{\nu,\nu^{'}=\pm 1\\ a=h,n}} S_{1,1}(\nu,\nu^{'};a;2)\ \ Log[(\nu x_1-\nu^{'}x_2)-v_a(t_1-t_2)]] \\
&< T\ \psi_L(X_1)\psi_R^{\dagger}(X_2) > \\
&\quad = \frac{1}{2\pi^2}\frac{wv_F}{w^2+v_F^2}\frac{e^{\gamma_1 \log[2x_1]}e^{(3+\gamma_2)\log[2x_2]}}{2(x_1-x_2)}\ Exp[-\sum_{\substack{\nu,\nu^{'}=\pm 1\\ a=h,n}} S_{-1,-1}(\nu,\nu^{'};a;1)\ Log[(\nu x_1-\nu^{'}x_2)-v_a(t_1-t_2)]] \\
&\quad + \frac{1}{2\pi^2}\frac{wv_F}{w^2+v_F^2}\frac{e^{(3+\gamma_2)\log[2x_1]}e^{\gamma_1 \log[2x_2]}}{2(x_1-x_2)}\ Exp[-\sum_{\substack{\nu,\nu^{'}=\pm 1\\ a=h,n}} S_{-1,-1}(\nu,\nu^{'};a;2)\ Log[(\nu x_1-\nu^{'}x_2)-v_a(t_1-t_2)]]
\end{aligned}
\tag{5.16}
$$

The values of the exponents 'S' are mentioned in Table 5.2.

Case III : x_1 and x_2 on opposite sides of the origin and on the same pole

$$
\begin{aligned}
&< T\ \psi_R(X_1)\psi_R^{\dagger}(X_2) > \\
&\quad = \frac{i}{2\pi^2}\frac{v_F^2}{w^2+v_F^2}\frac{e^{\gamma_1 \log[2x_1]}e^{(3+\gamma_2)\log[2x_2]}}{2(x_1+x_2)}\ Exp[-\sum_{\substack{\nu,\nu^{'}=\pm 1\\ a=h,n}} U_{1,1}(\nu,\nu^{'};a;1)\ \ Log[(\nu x_1-\nu^{'}x_2)-v_a(t_1-t_2)]] \\
&\quad + \frac{i}{2\pi^2}\frac{v_F^2}{w^2+v_F^2}\frac{e^{(3+\gamma_2)\log[2x_1]}e^{\gamma_1 \log[2x_2]}}{2(x_1+x_2)}\ Exp[-\sum_{\substack{\nu,\nu^{'}=\pm 1\\ a=h,n}} U_{1,1}(\nu,\nu^{'};a;2)\ \ Log[(\nu x_1-\nu^{'}x_2)-v_a(t_1-t_2)]] \\
&< T\ \psi_L(X_1)\psi_L^{\dagger}(X_2) > \\
&\quad = \frac{i}{2\pi^2}\frac{v_F^2}{w^2+v_F^2}\frac{e^{\gamma_1 \log[2x_1]}e^{(3+\gamma_2)\log[2x_2]}}{2(x_1+x_2)}\ Exp[-\sum_{\substack{\nu,\nu^{'}=\pm 1\\ a=h,n}} U_{-1,-1}(\nu,\nu^{'};a;1)\ Log[(\nu x_1-\nu^{'}x_2)-v_a(t_1-t_2)]] \\
&\quad + \frac{i}{2\pi^2}\frac{v_F^2}{w^2+v_F^2}\frac{e^{(3+\gamma_2)\log[2x_1]}e^{\gamma_1 \log[2x_2]}}{2(x_1+x_2)}\ Exp[-\sum_{\substack{\nu,\nu^{'}=\pm 1\\ a=h,n}} U_{-1,-1}(\nu,\nu^{'};a;2)\ Log[(\nu x_1-\nu^{'}x_2)-v_a(t_1-t_2)]]
\end{aligned}
$$

$$
\begin{aligned}
&< T\ \psi_R(X_1)\psi_L^{\dagger}(X_2) > \ = \ 0 \\
&< T\ \psi_L(X_1)\psi_R^{\dagger}(X_2) > \ = \ 0
\end{aligned}
\tag{5.17}
$$

The values of the exponents 'U' are mentioned in Table 5.3.

Case IV : x_1 and x_2 on opposite sides of the origin and on different poles

$$
\begin{aligned}
&< T\ \psi_R(X_1)\psi_R^{\dagger}(X_2) > \\
&= \frac{1}{2\pi^2}\frac{wv_F}{w^2+v_F^2}\frac{e^{\gamma_1 \log[2x_1]}e^{(3+\gamma_2)\log[2x_2]}}{2(x_1+x_2)}\ Exp[-\sum_{\substack{\nu,\nu'=\pm 1\\ a=h,n}} W_{1,1}(\nu,\nu';a;1)\ \ Log[(\nu x_1-\nu' x_2)-v_a(t_1-t_2)]] \\
&+ \frac{1}{2\pi^2}\frac{wv_F}{w^2+v_F^2}\frac{e^{(3+\gamma_2)\log[2x_1]}e^{\gamma_1 \log[2x_2]}}{2(x_1+x_2)}\ Exp[-\sum_{\substack{\nu,\nu'=\pm 1\\ a=h,n}} W_{1,1}(\nu,\nu';a;2)\ \ Log[(\nu x_1-\nu' x_2)-v_a(t_1-t_2)]] \\
&< T\ \psi_L(X_1)\psi_L^{\dagger}(X_2) > \\
&= \frac{1}{2\pi^2}\frac{wv_F}{w^2+v_F^2}\frac{e^{\gamma_1 \log[2x_1]}e^{(3+\gamma_2)\log[2x_2]}}{2(x_1+x_2)}\ Exp[-\sum_{\substack{\nu,\nu'=\pm 1\\ a=h,n}} W_{-1,-1}(\nu,\nu';a;1)\ Log[(\nu x_1-\nu' x_2)-v_a(t_1-t_2)]] \\
&+ \frac{1}{2\pi^2}\frac{wv_F}{w^2+v_F^2}\frac{e^{(3+\gamma_2)\log[2x_1]}e^{\gamma_1 \log[2x_2]}}{2(x_1+x_2)}\ Exp[-\sum_{\substack{\nu,\nu'=\pm 1\\ a=h,n}} W_{-1,-1}(\nu,\nu';a;2)\ Log[(\nu x_1-\nu' x_2)-v_a(t_1-t_2)]] \\
&< T\ \psi_R(X_1)\psi_L^{\dagger}(X_2) > \ = \ 0 \\
&< T\ \psi_L(X_1)\psi_R^{\dagger}(X_2) > \ = \ 0
\end{aligned}
\tag{5.18}
$$

The values of the exponents 'W' are mentioned in Table 5.4.

TABLE 5.1: Luttinger exponents $Q_{\nu_1,\nu_2}(\nu,\nu';a)$ for x_1 and x_2 on the same side of the origin and on the same pole. Explicit expressions are given in section 5.4.1.

$Q_{\nu_1,\nu_2}(\nu,\nu';a)$	ν=1 ; ν'=1	ν=−1 ; ν'=−1	ν=1 ; ν'=−1	ν=−1 ; ν'=1
ν_1=1,ν_2=1;a=h	P	Q	X	X
ν_1=1 , ν_2=1 ; a=n	0.5	0	0	0
ν_1=−1 , ν_2=−1 ; a=h	Q	P	X	X
ν_1=−1 , ν_2=−1 ; a=n	0	0.5	0	0
ν_1=1 , ν_2=−1 ; a=h	S	S	Y	Z
ν_1=1, , ν_2=−1 ; a=n	0	0	0.5	0
ν_1=−1 , ν_2=1 ; a=h	S	S	Z	Y
ν_1=−1 , ν_2=1 ; a=n	0	0	0	0.5

TABLE 5.2: Luttinger exponents $S_{\nu_1,\nu_2}(\nu,\nu';a;j)$ for x_1 and x_2 on the same side of the origin and on different poles. Explicit expressions are given in section 5.4.1.

$S_{\nu_1,\nu_2}(\nu,\nu';a;j)$	ν=1 ; ν'=1	ν=−1 ; ν'=−1	ν=1 ; ν'=−1	ν=−1 ; ν'=1
ν_1=1 , ν_2=1 ; a=h , j=1	A_1	B_1	C_1	D_1
ν_1=1 , ν_2=1 ; a=n , j=1	-0.5	0	0.5	0
ν_1=1 , ν_2=1 ; a=h , j=2	B_1	A_1	C_1	D_1
ν_1=1 , ν_2=1 ; a=n , j=2	0	-0.5	0.5	0
ν_1=−1 , ν_2=−1 ; a=h , j=1	A_1	B_1	D_1	C_1
ν_1=−1 , ν_2=−1 ; a=n , j=1	-0.5	0	0	0.5
ν_1=−1 , ν_2=−1 ; a=h , j=2	B_1	A_1	D_1	C_1
ν_1=−1 , ν_2=−1 ; a=n , j=2	0	−0.5	0	0.5

TABLE 5.3: Luttinger exponents $U_{\nu_1,\nu_2}(\nu,\nu';a;j)$ for x_1 and x_2 on opposite sides of the origin and on the same pole. Explicit expressions are given in section 5.4.1.

$U_{\nu_1,\nu_2}(\nu,\nu';a;j)$	ν=1 ; ν'=1	ν=−1 ; ν'=−1	ν=1 ; ν'=−1	ν=−1 ; ν'=1
ν_1=1 , ν_2=1 ; a=h , j=1	A_2	B_2	C_2	D_2
ν_1=1 , ν_2=1 ; a=n , j=1	0.5	0	−0.5	0
ν_1=1 , ν_2=1 ; a=h , j=2	A_2	B_2	D_2	C_2
ν_1=1 , ν_2=1 ; a=n , j=2	0.5	0	0	−0.5
ν_1=−1 , ν_2=−1 ; a=h , j=1	B_2	A_2	C_2	D_2
ν_1=−1 , ν_2=−1 ; a=n , j=1	0	0.5	−0.5	0
ν_1=−1 , ν_2=−1 ; a=h , j=2	B_2	A_2	D_2	C_2
ν_1=−1 , ν_2=−1 ; a=n , j=2	0	0.5	0	−0.5

TABLE 5.4: Luttinger exponents $W_{\nu_1,\nu_2}(\nu,\nu';a;j)$ for x_1 and x_2 on opposite sides of the origin and on different poles. Explicit expressions are given in section 5.4.1.

$W_{\nu_1,\nu_2}(\nu,\nu';a;j)$	ν=1 ; ν'=1	ν=−1 ; ν'=−1	ν=1 ; ν'=−1	ν=−1 ; ν'=1
ν_1=1 , ν_2=1 ; a=h , j=1	A_3	B_3	C_3	D_3
ν_1=1 , ν_2=1 ; a=n , j=1	0.5	0	−0.5	0
ν_1=1 , ν_2=1 ; a=h , j=2	A_3	B_3	D_3	C_3
ν_1=1 , ν_2=1 ; a=n , j=2	0.5	0	0	−0.5
ν_1=−1 , ν_2=−1 ; a=h , j=1	B_3	A_3	C_3	D_3
ν_1=−1 , ν_2=−1 ; a=n , j=1	0	0.5	−0.5	0
ν_1=−1 , ν_2=−1 ; a=h , j=2	B_3	A_3	D_3	C_3
ν_1=−1 , ν_2=−1 ; a=n , j=2	0	0.5	0	−0.5

5.4.1 Anomalous exponents

The explicit expressions of the anomalous exponents mentioned in Table 5.1, Table 5.2, Table 5.3, and Table 5.4 are listed below. For compactness, all the other exponents are written in

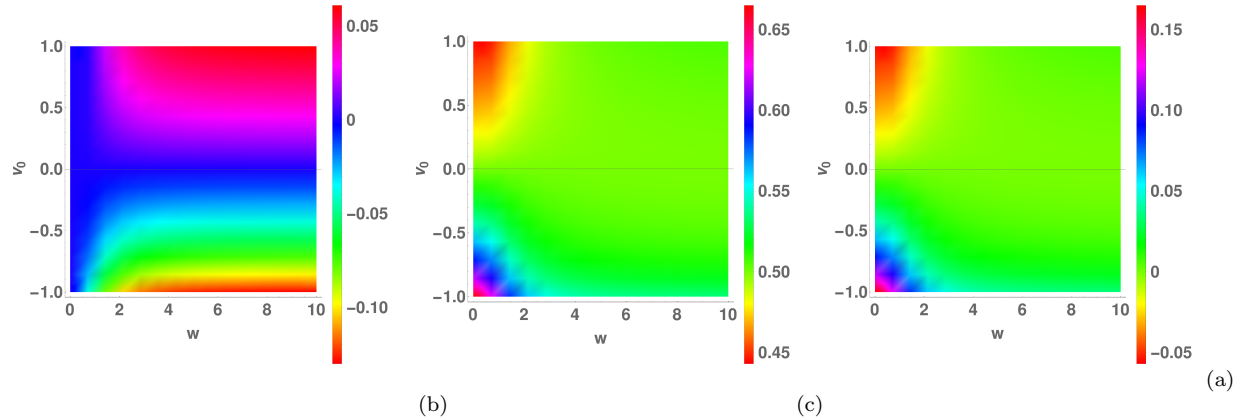

(b) (c) (a)

FIGURE 5.3: Anomalous exponents vs hopping parameter w and interaction strength v_0 for a step ladder ($v_F = 1$) with the points on the same pole and same side of the origin (a) X (b) Y (c) Z. The other exponents are independent of the hopping parameter.

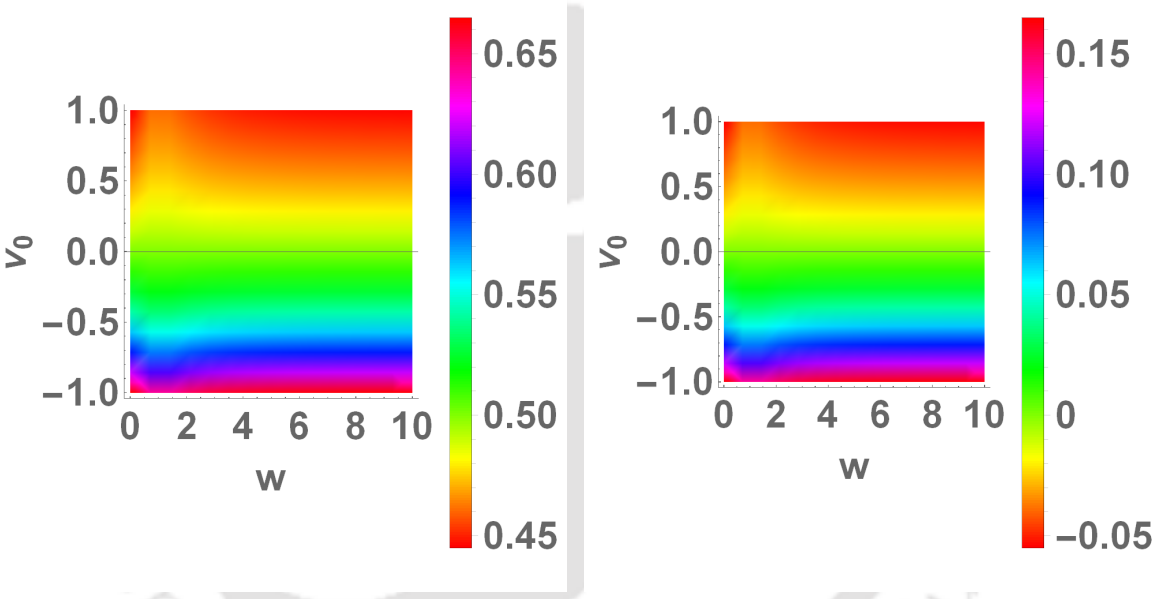

(a) (b)

FIGURE 5.4: Anomalous exponents vs hopping parameter w and interaction strength v_0 for a step ladder ($v_F = 1$) with the points on different poles and same side of the origin (a) C_1 (b) D_1. The other exponents are independent of the hopping parameter.

terms of the following five exponents.

$$
\begin{aligned}
Q =& \frac{(v_F - v_h)^2}{8 v_F v_h} \; ; \; B_1 = \frac{v_h - v_F}{4 v_h} \\
X =& -\frac{(v_F - v_h)(v_F + v_h) w^2 (v_F^4 - v_F^2 v_h^2 + v_F v_h w^2 + w^4)}{8 v_F v_h (v_F v_h + w^2)(v_F^4 + 2 v_F v_h w^2 + w^4)} \\
C_1 =& \frac{(v_h + v_F)(2 v_F^4 + v_h (3 v_F + v_h) w^2 + 2 w^4)}{8 v_h (v_F^4 + 2 v_F v_h w^2 + w^4)} \; ; \\
A_2 =& -\frac{(v_h + v_F)}{8} \left(-\frac{2}{v_h} - \frac{(v_h - v_F)}{v_F v_h + w^2} + \frac{w^2 (v_h - v_F)}{v_F^4 + 2 v_F v_h w^2 + w^4} \right)
\end{aligned}
\tag{5.19}
$$

Homogeneous Exponents

$$
\gamma_1 = X \; ; \quad \gamma_2 = X + 6 B_1 - 3 \tag{5.20}
$$

Case I : x_1 and x_2 on the same side of the origin and same pole

$$P = Q + \frac{1}{2} \; ; \; S = \frac{Q}{B_1}\left(\frac{1}{2} - B_1\right) ; \; Y = X - B_1 + \frac{1}{2} \; ; \; Z = X - B_1 \tag{5.21}$$

Case II : x_1 and x_2 on same side of the origin and different pole

$$A_1 = B_1 - \frac{1}{2} \; ; \; D_1 = C_1 - \frac{1}{2} \; ; \tag{5.22}$$

Case III : x_1 and x_2 on the opposite sides of the origin and on the same pole

$$B_2 = A_2 - \frac{1}{2} \; ; \; C_2 = B_1 - \frac{1}{2} \; ; \; D_2 = B_1 \tag{5.23}$$

Case IV : x_1 and x_2 on the opposite sides of the origin and on different poles

$$A_3 = C_1 \; ; \; B_3 = C_1 - \frac{1}{2} \; ; \; C_3 = B_1 - \frac{1}{2} \; ; \; D_3 = B_1 \; ; \tag{5.24}$$

Some of the anomalous exponents are plotted as a function of hopping parameter and interaction parameter (taking empirical value of v_F to be 1) in the Figures 5.3, 5.4, 5.5 and 5.6. Only those exponents which have a dependence on both the hopping parameter and mutual interaction strength are plotted. Thus the exponents for spinons are omitted as they take only trivial values even in presence of interactions as it is the total density which couples to

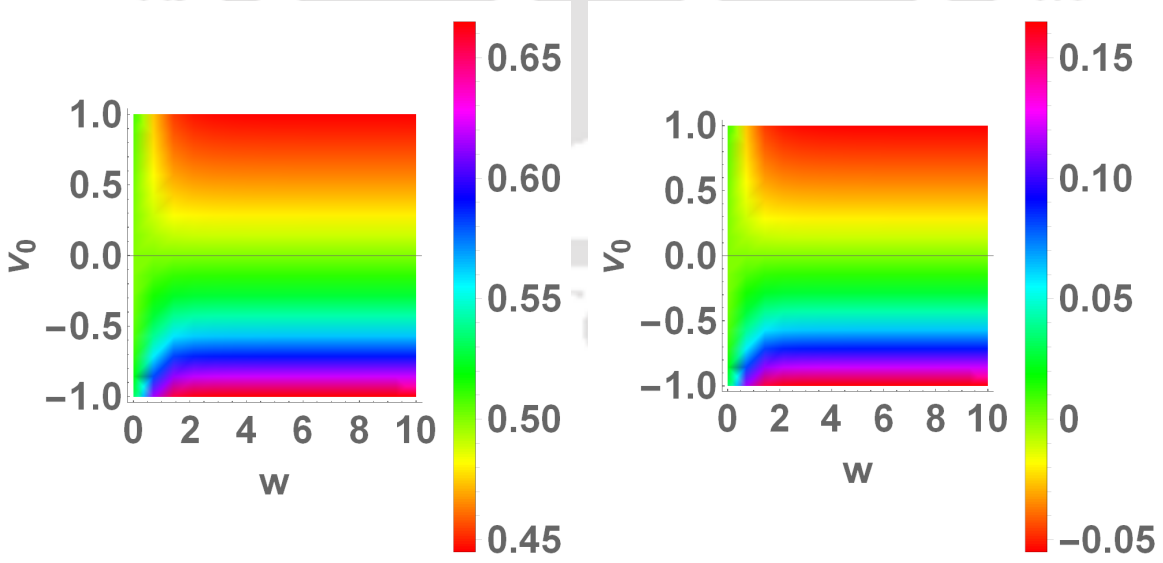

(a) (b)

FIGURE 5.5: Anomalous exponents vs hopping parameter w and interaction strength v_0 for a step ladder ($v_F = 1$) with the points on the same pole and different sides of the origin (a) A_2 (b) B_2. The other exponents are independent of the hopping parameter.

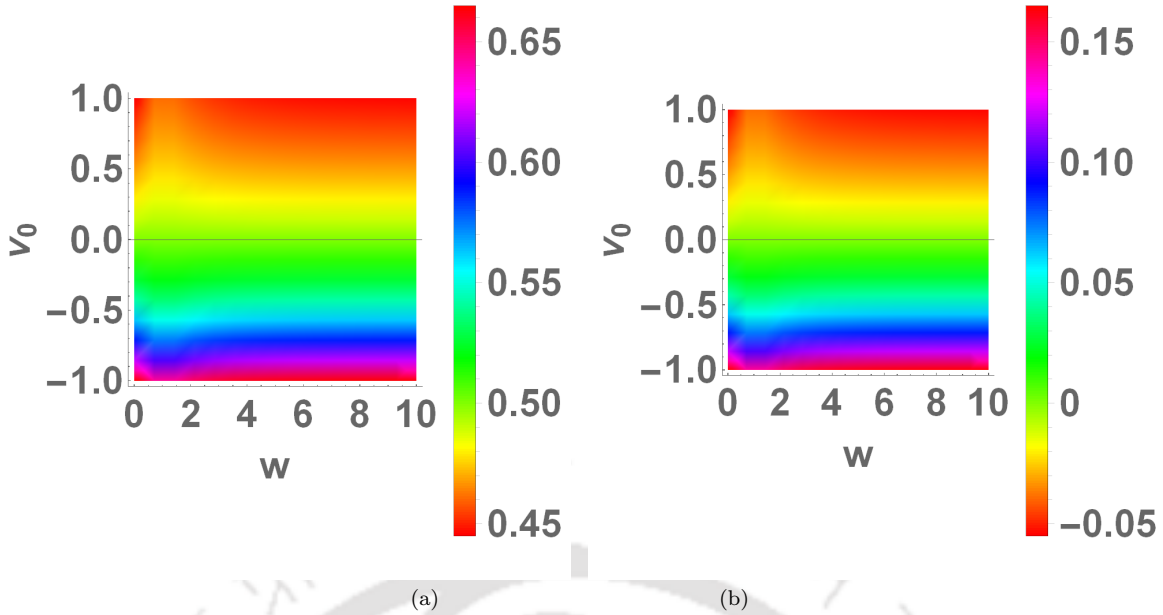

(a) (b)

FIGURE 5.6: Anomalous exponents vs hopping parameter w and interaction strength v_0 for a step ladder ($v_F = 1$) with the points on opposite poles and different sides of the origin (a) A_3 (b) B_3. The other exponents are independent of the hopping parameter.

the short range mutual interactions. The key observations from the plots may be summarized as follows. When both interactions and hopping are absent, all the exponents take on trivial values of zero or half (the other half comes from spinons to make the exponent unity). When hopping is absent but interactions are present, the exponents take the exact values as that of the standard (homogeneous) Luttinger liquid (see section 5.7).

5.5 Conductance

Conductance may be thought of as the outcome of a tunneling experiment [31]. In this case, the results depend on the length of the wire L and a cutoff $L_\omega = \frac{v_F}{k_B T}$ that may be regarded either as inverse temperature or inverse frequency (former in case of d.c. conductance at finite temperature and latter in case of a.c. conductance at zero temperature). The result is expressed as a power law with a system dependent exponent η.

$$G \sim \left(\frac{L}{L_\omega}\right)^\eta \tag{5.25}$$

In case of the quantum steeplechase, the electrons were injected from one end and collected from the other end and the tunneling conductance was measured as the probability of this tunneling. But in this case, as shown in figure 5.7, for a beam of electrons incident from the left extreme of pole 1, electrons can be collected from the other three ends, and accordingly, we have three varieties of tunneling conductance which are derived below.

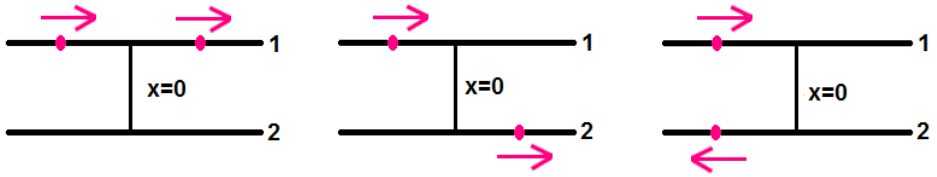

(a) (b) (c)

FIGURE 5.7: Conductance measured across different ends of the ladder.

Conductance measured across the same pole but opposite sides of the origin

Consider the general Green function derived earlier for $x_1 x_2 < 0$ and same pole (equation (5.17)). From that it is possible to conclude ($W = \frac{i}{2\pi}\frac{v_F^2}{w^2+v_F^2}$),

$$
\begin{aligned}
&< T\psi_R(x_1,\sigma_1,t_1)\psi_R^\dagger(x_2,\sigma_2,t_2) > \\
&= \frac{e^{\gamma_1 \log[2x_1]} e^{(3+\gamma_2)\log[2x_2]}}{2(x_1+x_2)}\, W\, e^{-\frac{1}{2}\log[(x_1-x_2)-v_F(t_1-t_2)]} e^{\frac{1}{2}\log[(x_1+x_2)-v_F(t_1-t_2)]} \\
&\quad e^{-A_2\log[(x_1-x_2)-v_h(t_1-t_2)]} e^{-B_2\log[(x_1-x_2)+v_h(t_1-t_2)]} \\
&\quad e^{-C_2\log[(x_1+x_2)-v_h(t_1-t_2)]} e^{-D_2\log[(x_1+x_2)+v_h(t_1-t_2)]} \\
&+ \frac{e^{(3+\gamma_2)\log[2x_1]} e^{\gamma_1\log[2x_2]}}{2(x_1+x_2)}\, W\, e^{-\frac{1}{2}\log[(x_1-x_2)-v_F(t_1-t_2)]} e^{\frac{1}{2}\log[(x_1+x_2)+v_F(t_1-t_2)]} \\
&\quad e^{-A_2\log[(x_1-x_2)-v_h(t_1-t_2)]} e^{-B_2\log[(x_1-x_2)+v_h(t_1-t_2)]} \\
&\quad e^{-D_2\log[(x_1+x_2)-v_h(t_1-t_2)]} e^{-C_2\log[(x_1+x_2)+v_h(t_1-t_2)]}
\end{aligned}
$$

Setting $x = \frac{L}{2}+\epsilon$ and $x' = -\frac{L}{2}$ so that $x - x' = L$ and $x + x' = \epsilon \to 0$ is small and also $t_1 = t$ and $t_2 = 0$,

$$
\begin{aligned}
&< T\psi_R(\frac{L}{2},\sigma,t)\psi_R^\dagger(-\frac{L}{2},\sigma,0) > = \frac{e^{\gamma_1\log[L]} e^{(3+\gamma_2)\log[L]}}{2\epsilon} g^{1,1}_{1,-1}(1,1) e^{-\frac{1}{2}\log[L-v_F t]} e^{\frac{1}{2}\log[\epsilon-v_F t]} \\
&\quad e^{-A_2\log[L-v_h t]} e^{-B_2\log[L+v_h t]} e^{-C_2\log[\epsilon-v_h t]} e^{-D_2\log[\epsilon+v_h t]} \\
&\quad + \frac{e^{(3+\gamma_2)\log[L]} e^{\gamma_1\log[L]}}{2\epsilon}\, g^{1,1}_{1,-1}(1,1) e^{-\frac{1}{2}\log[L-v_F t]} e^{\frac{1}{2}\log[\epsilon+v_F t]} \\
&\quad e^{-A_2\log[L-v_h t]} e^{-B_2\log[L+v_h t]} e^{-D_2\log[\epsilon-v_h t]} e^{-C_2\log[\epsilon+v_h t]} \\
&= \frac{e^{(3+\gamma_1+\gamma_2)\log[L]}}{2\epsilon}\, g^{1,1}_{1,-1}(1,1)\; e^{-\frac{1}{2}\log[L-v_F t]}\; e^{\frac{1}{2}\log[\epsilon-v_F t]} \\
&\quad e^{(B_2-A_2)\log[L-v_h t]} e^{(D_2-C_2)\log[\epsilon-v_h t]} e^{-B_2\log[L^2-(v_h t)^2]} e^{-D_2\log[\epsilon^2-(v_h t)^2]} \\
&\quad + \frac{e^{(3+\gamma_1+\gamma_2)\log[L]}}{2\epsilon}\, g^{1,1}_{1,-1}(1,1)\; e^{-\frac{1}{2}\log[L-v_F t]}\; e^{\frac{1}{2}\log[\epsilon+v_F t]} \\
&\quad e^{(B_2-A_2)\log[L-v_h t]} e^{(D_2-C_2)\log[\epsilon+v_h t]} e^{-B_2\log[L^2-(v_h t)^2]} e^{-D_2\log[\epsilon^2-(v_h t)^2]}
\end{aligned}
$$

Now, $D_2 - C_2 = \frac{1}{2}$

$$< T\psi_R(\frac{L}{2},\sigma,t)\psi_R^\dagger(-\frac{L}{2},\sigma,0) >= \frac{e^{(3+\gamma_1+\gamma_2)\log[L]}}{2\epsilon} g_{1,-1}(1,1) e^{-\frac{1}{2}\log[L-v_F t]} e^{(B_2-A_2)\log[L-v_h t]} e^{\frac{1}{2}\log[\epsilon-v_F t]} e^{\frac{1}{2}\log[\epsilon-v_h t]} e^{-B_2\log[L^2-(v_h t)^2]} e^{-D_2\log[\epsilon^2-(v_h t)^2]} + \frac{e^{(3+\gamma_1+\gamma_2)\log[L]}}{2\epsilon} g_{1,-1}(1,1) e^{-\frac{1}{2}\log[L-v_F t]} e^{(B_2-A_2)\log[L-v_h t]} e^{\frac{1}{2}\log[\epsilon+v_F t]} e^{\frac{1}{2}\log[\epsilon+v_h t]} e^{-B_2\log[L^2-(v_h t)^2]} e^{-D_2\log[\epsilon^2-(v_h t)^2]}$$

$$\lim_{\epsilon\to 0} \frac{1}{2\epsilon}\left[e^{\frac{1}{2}\log[\epsilon-v_h t]} e^{\frac{1}{2}\log[\epsilon-v_F t]} + e^{\frac{1}{2}\log[\epsilon+v_h t]} e^{\frac{1}{2}\log[\epsilon+v_F t]} \right] \rightarrow \frac{v_F+v_h}{2\sqrt{v_F v_h}}. \tag{5.26}$$

$$< T\psi_R(\frac{L}{2},\sigma,t)\psi_R^\dagger(-\frac{L}{2},\sigma,0) > = \frac{v_F+v_h}{2\sqrt{v_F v_h}} e^{(3+\gamma_1+\gamma_2)\log[L]} g_{1,-1}(1,1) e^{-\frac{1}{2}\log[L-v_F t]} e^{(B_2-A_2)\log[L-v_h t]} e^{-B_2\log[L^2-(v_h t)^2]} e^{-D_2\log[-(v_h t)^2]}$$

Since $G \sim |v_F \int_{-\infty}^{\infty} dt < \{\psi_R(\frac{L}{2},\sigma,t), \psi_R^\dagger(-\frac{L}{2},\sigma,0)\} >|^2$ it is possible to read off the conductance exponent as follows,

$$G \sim \left(\frac{L}{L_\omega}\right)^{2(4+\gamma_1+\gamma_2-A_2-B_2-2D_2-\frac{1}{2})} \tag{5.27}$$

Conductance measured across the different poles and on opposite sides of the origin

In a very similar fashion as described above, the conductance exponent for this case can be obtained as the following (using the two point functions from equation (5.18)).

$$G \sim \left(\frac{L}{L_\omega}\right)^{2(4+\gamma_1+\gamma_2-A_3-B_3-2D_3-\frac{1}{2})} \tag{5.28}$$

Conductance measured across the different poles but same side of the origin

Consider the general Green function derived earlier for $x_1 x_2 > 0$ and different poles (equation 5.16). From that it is possible to conclude ($W = \frac{i}{2\pi}\frac{w v_F}{w^2+v_F^2}$),

$$< T\psi_R(x_1,\sigma_1,t_1)\psi_L^{\dagger}(x_2,\sigma_2,t_2) >$$
$$=\frac{e^{\gamma_1 \log[2x_1]}e^{(3+\gamma_2)\log[2x_2]}}{2(x_1-x_2)}\ W\ e^{-\frac{1}{2}\log[(x_1+x_2)-v_F(t_1-t_2)]}e^{\frac{1}{2}\log[(x_1-x_2)-v_F(t_1-t_2)]}$$
$$e^{-A_1\log[(x_1-x_2)-v_h(t_1-t_2)]}e^{-B_1\log[(x_1-x_2)+v_h(t_1-t_2)]}$$
$$e^{-C_1\log[(x_1+x_2)-v_h(t_1-t_2)]}e^{-D_1\log[(x_1+x_2)+v_h(t_1-t_2)]}$$
$$+\frac{e^{(3+\gamma_2)\log[2x_1]}e^{\gamma_1\log[2x_2]}}{2(x_1-x_2)}W\ e^{-\frac{1}{2}\log[(x_1+x_2)-v_F(t_1-t_2)]}e^{\frac{1}{2}\log[(x_1-x_2)+v_F(t_1-t_2)]}$$
$$e^{-B_1\log[(x_1-x_2)-v_h(t_1-t_2)]}e^{-A_1\log[(x_1-x_2)+v_h(t_1-t_2)]}$$
$$e^{-C_1\log[(x_1+x_2)-v_h(t_1-t_2)]}e^{-D_1\log[(x_1+x_2)+v_h(t_1-t_2)]}$$

Putting $x=-\frac{L}{2}+\epsilon$ and $x^{'}=-\frac{L}{2}$ so that $x+x^{'}=-L$ and $x-x^{'}=\epsilon\to 0$ is small and also $t_1=t$ and $t_2=0$,

$$< T\psi_R(-\frac{L}{2},\sigma,t)\psi_L^{\dagger}(-\frac{L}{2},\sigma,0) >=\frac{e^{\gamma_1\log[L]}e^{(3+\gamma_2)\log[L]}}{2\epsilon}\ W\ e^{-\frac{1}{2}\log[-L-v_Ft]}e^{\frac{1}{2}\log[\epsilon-v_Ft]}$$
$$e^{-A_1\log[\epsilon-v_ht]}e^{-B_1\log[\epsilon+v_ht]}e^{-C_1\log[-L-v_ht]}e^{-D_1\log[-L+v_ht]}$$
$$+\frac{e^{(3+\gamma_2)\log[L]}e^{\gamma_1\log[L]}}{2\epsilon}\ W\ e^{-\frac{1}{2}\log[-L-v_Ft]}e^{\frac{1}{2}\log[\epsilon+v_Ft]}$$
$$e^{-A_1\log[\epsilon+v_ht]}e^{-B_1\log[\epsilon-v_ht]}e^{-C_1\log[-L-v_ht]}e^{-D_1\log[-L+v_ht]}$$

$$< T\psi_R(-\frac{L}{2},\sigma,t)\psi_L^{\dagger}(-\frac{L}{2},\sigma,0) >=\frac{e^{(3+\gamma_1+\gamma_2)\log[L]}}{2\epsilon}\ W\ e^{-\frac{1}{2}\log[-L-v_Ft]}e^{\frac{1}{2}\log[\epsilon-v_ht]}$$
$$e^{(B_1-A_1)\log[\epsilon-v_ht]}e^{(C_1-D_1)\log[-L+v_ht]}e^{-B_1\log[\epsilon^2-(v_ht)^2]}e^{-C_1\log[L^2-(v_ht)^2]}$$
$$+\frac{e^{(3+\gamma_1+\gamma_2)\log[L]}}{2\epsilon}\ W\ e^{-\frac{1}{2}\log[-L-v_Ft]}e^{\frac{1}{2}\log[\epsilon+v_ht]}$$
$$e^{(B_1-A_1)\log[\epsilon+v_ht]}e^{(C_1-D_1)\log[-L+v_ht]}e^{-B_1\log[\epsilon^2-(v_ht)^2]}e^{-C_1\log[L^2-(v_ht)^2]}$$

Now, $B_1-A_1=\frac{1}{2}$

$$< T\psi_R(-\frac{L}{2},\sigma,t)\psi_L^{\dagger}(-\frac{L}{2},\sigma,0) >=\frac{e^{(3+\gamma_1+\gamma_2)\log[L]}}{2\epsilon}W\ e^{-\frac{1}{2}\log[-L-v_Ft]}e^{(C_1-D_1)\log[-L+v_ht]}$$
$$e^{\frac{1}{2}\log[\epsilon-v_Ft]}e^{\frac{1}{2}\log[\epsilon-v_ht]}e^{-B_1\log[\epsilon^2-(v_ht)^2]}e^{-C_1\log[L^2-(v_ht)^2]}$$
$$+\frac{e^{(3+\gamma_1+\gamma_2)\log[L]}}{2\epsilon}W\ e^{-\frac{1}{2}\log[L-v_Ft]}e^{(C_1-D_1)\log[-L+v_ht]}$$
$$e^{\frac{1}{2}\log[\epsilon+v_Ft]}e^{\frac{1}{2}\log[\epsilon+v_ht]}e^{-B_1\log[\epsilon^2-(v_ht)^2]}e^{-C_1\log[L^2-(v_ht)^2]}$$

Using equation (5.26) for $\epsilon\to 0$,

$$< T\psi_R(-\frac{L}{2},\sigma,t)\psi_R^{\dagger}(-\frac{L}{2},\sigma,0) >=\frac{v_F+v_h}{2\sqrt{v_Fv_h}}\ e^{(3+\gamma_1+\gamma_2)\log[L]}\ g^{1,2}_{-1,-1}(1,-1)\ e^{-\frac{1}{2}\log[L-v_Ft]}$$
$$e^{(C_1-D_1)\log[-L+v_ht]}e^{-C_1\log[L^2-(v_ht)^2]}e^{-B_1\log[\epsilon^2-(v_ht)^2]}$$

Since $G \sim |v_F \int_{-\infty}^{\infty} dt < \{\psi_R(-\frac{L}{2}, \sigma, t), \psi_L^{\dagger}(-\frac{L}{2}, \sigma, 0)\} > |^2$ it is possible to read off the conductance exponent as follows,

$$G \sim \left(\frac{L}{L_\omega}\right)^{2(4+\gamma_1+\gamma_2-2B_1-C_1-D_1-\frac{1}{2})} \tag{5.29}$$

The explicit values of A's, B's, etc. are given in section 5.4.1. It is to be noted that $\eta_2 = \eta_3$ (see Fig. 5.9 for a diagrammatic explanation). Fig. 5.8 shows the variation of the conductance exponent as a function of the hopping parameter and the strength of mutual interaction. It is seen that for attractive interactions ($v_0 < 0$), the conductance exponents are negative ($\eta < 0$) indicating that the conductance diverges at low temperature as a power law. On the other hand, for repulsive interactions ($v_0 > 0$), the conductance exponents are positive ($\eta > 0$) and thus conductance vanishes as a power law at low temperature. When mutual interactions are absent ($v_0 = 0$), then the conductance exponent vanishes ($\eta = 0$) which indicates that in such cases, the conductance is independent of temperature.

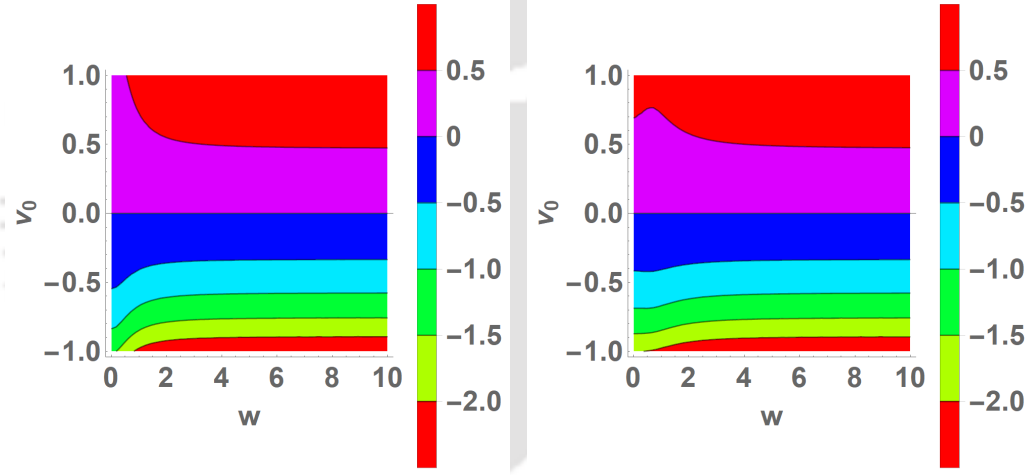

FIGURE 5.8: Contour plot showing the variation of the conductance exponent as a function of the hopping parameter 'w' and the strength of mutual interaction 'v_0' ($v_F = 1$). (a) For η_1 .(b) For $\eta_2 (= \eta_3)$.

5.6 Friedel Oscillations

The presence of a localized impurity that weakly couples to the fermions causes Friedel oscillations, which are the rapid spatial variation ($\sim e^{2ik_F x}$) of the otherwise homogeneous density profile in a Luttinger liquid. In the Kubo formalism, it is given as the density-density correlation function [102, 103]. In chapter 3, the expression for the rapidly oscillating part of the DDCF was calculated for a luttinger liquid with a cluster of impurities. In a similar fashion,

using a non standard harmonic analysis for the one step ladder, we write the fast part of the density operator as follows:

$$\rho^i_f(x,\sigma,t) \equiv \psi^\dagger_{L,i}(x,\sigma,t)\psi_{R,i}(x,\sigma,t) = \sum_{\lambda=0,1}\sum_{\gamma=\pm 1} \theta(\gamma x)\ R^i_{\lambda,\gamma}(\sigma)\ e^{2\pi i \int_{sgn(x)\infty}^{x} dy\ \rho^i_s(y,\sigma,t)} \\ e^{2\pi i\lambda_i \int_{sgn(x)\infty}^{x} dy\ (\rho^{\bar{i}}_s(y,\sigma,t)+\rho^1_s(-y,\sigma,t)+\rho^2_s(-y,\sigma,t))} \tag{5.30}$$

The prescription for choosing λ_i in equation (5.10) leads to the unambiguous conclusion that,

$$\begin{aligned} \left\langle T\ \tilde{\rho}^i_f(X_1)\tilde{\rho}^j_f(X_2)\right\rangle &\sim\ (Exp[\sum_{\substack{\nu,\nu^{'}=\pm 1\\ a=h,n}} \Gamma(\nu,\nu^{'};a)\ Log[(\nu x_1 - \nu^{'} x_2) - v_a(t_1-t_2)]] - 1) \\ \left\langle T\ \tilde{\rho}^i_f(X_1)\tilde{\rho}^{j*}_f(X_2)\right\rangle &\sim\ (Exp[-\sum_{\substack{\nu,\nu^{'}=\pm 1\\ a=h,n}} \Gamma(\nu,\nu^{'};a)\ Log[(\nu x_1 - \nu^{'} x_2) - v_a(t_1-t_2)]] - 1) \end{aligned} \tag{5.31}$$

One should remember that this (use of tilde "$\sim$") really means that the time derivative of the logarithms of both sides are equal to each other. The values of the anomalous scaling exponents $\Gamma(\nu,\nu^{'};a)$ can be obtained from the expression below.

$$\Gamma(\nu,\nu^{'};a) = \left(\frac{v_F}{2v_h}\ \delta_{a,h} + \frac{1}{2}\ \delta_{a,n}\right)\ (\delta_{\nu,\nu'} - \delta_{\nu,-\nu'}) \tag{5.32}$$

5.7 Limiting checks

5.7.1 Non-interacting case

The obvious limiting check is to switch off the inter-particle interactions ($v_0 = 0$) and then compare with the respective single particle Green functions obtained using Fermi algebra. In such a case, the holon velocity is equal to the Fermi velocity ($v_h = v_F$) and all the exponents takes values as follows.

Homogeneous Exponents

$$\gamma_1 := 0; \quad \gamma_2 := -3 \tag{5.33}$$

Case I : x_1 and x_2 on the same side of the origin and same pole

$$P = \frac{1}{2}\ ;\ Q = 0\ ;\ S = 0\ ;\ X = 0\ ;\ Z = 0\ ;\ Y = \frac{1}{2} \tag{5.34}$$

Case II : x_1 and x_2 on same side of the origin and different pole

$$A_1 = -\frac{1}{2}\ ;\ B_1 = 0\ ;\ D_1 = 0\ ;\ C_1 = \frac{1}{2} \tag{5.35}$$

Case III : x_1 and x_2 on the opposite sides of the origin and on the same pole

$$C_2 = -\frac{1}{2}\ ;\ D_2 = 0\ ;\ B_2 = 0\ \ A_2 = \frac{1}{2} \tag{5.36}$$

Case IV : x_1 and x_2 on the opposite sides of the origin and on different poles

$$C_3 = -\frac{1}{2}\ ;\ D_3 = 0\ ;\ B_3 = 0\ ;\ A_3 = \frac{1}{2} \tag{5.37}$$

Using the above exponents in all the subcases of the interacting two point functions in equations (5.15, 5.16, 5.17, 5.18), one recovers the non-interacting Green functions as given by equation (5.4). For example, one of the subcases (same side and same pole as in equation (5.15)) is explicitly shown.

$$\begin{aligned}
\Big\langle T\psi_R(x_1,\sigma_1,t_1)\psi_R^\dagger(x_2,\sigma_2,t_2)\Big\rangle &= \frac{i}{2\pi}\ e^{\gamma_1 \log[4x_1x_2]}e^{-\frac{1}{2}\log[(x_1-x_2)-v_F(t_1-t_2)]}e^{-P\log[(x_1-x_2)-v_h(t_1-t_2)]} \\
&\quad e^{-Q\log[-(x_1-x_2)-v_h(t_1-t_2)]}e^{-X\log[(x_1+x_2)-v_h(t_1-t_2)]}e^{-X\log[-(x_1+x_2)-v_h(t_1-t_2)]} \\
&= \frac{i}{2\pi}\ e^{-\log[(x_1-x_2)-v_F(t_1-t_2)]} \\
&= \frac{i}{2\pi}\ \frac{1}{(x_1-x_2)-v_F(t_1-t_2)}
\end{aligned}$$

$$\begin{aligned}
\Big\langle T\psi_L(x_1,\sigma_1,t_1)\psi_L^\dagger(x_2,\sigma_2,t_2)\Big\rangle &= \frac{i}{2\pi}\ e^{\gamma_1 \log[4x_1x_2]|}e^{-\frac{1}{2}\log[-(x_1-x_2)-v_F(t_1-t_2)]}e^{-Q\log[(x_1-x_2)-v_h(t_1-t_2)]} \\
&\quad e^{-P\log[-(x_1-x_2)-v_h(t_1-t_2)]}e^{-X\log[(x_1+x_2)-v_h(t_1-t_2)]}e^{-X\log[-(x_1+x_2)-v_h(t_1-t_2)]} \\
&= \frac{i}{2\pi}\ e^{-\log[-(x_1-x_2)-v_F(t_1-t_2)]} \\
&= \frac{i}{2\pi}\ \frac{1}{-(x_1-x_2)-v_F(t_1-t_2)}
\end{aligned}$$

$$\begin{aligned}
\Big\langle T\psi_R(x_1,\sigma_1,t_1)\psi_L^\dagger(x_2,\sigma_2,t_2)\Big\rangle &= \frac{i}{2\pi}\frac{w^2}{w^2+v_F^2}\frac{e^{\gamma_1\log[2x_1]|}e^{(3+\gamma_2)\log[2x_2]|}+e^{(1+\gamma_3)\log[2x_1]|}e^{\gamma_1\log[2x_2]|}}{2} \\
&\quad e^{-\frac{1}{2}\log[(x_1+x_2)-v_F(t_1-t_2)]}e^{-S\log[(x_1-x_2)-v_h(t_1-t_2)]}e^{-S\log[-(x_1-x_2)-v_h(t_1-t_2)]} \\
&\quad e^{-Y\log[(x_1+x_2)-v_h(t_1-t_2)]}e^{-Z\log[-(x_1+x_2)-v_h(t_1-t_2)]} \\
&= \frac{i}{2\pi}\frac{w^2}{w^2+v_F^2}\ e^{-\log[(x_1+x_2)-v_F(t_1-t_2)]} \\
&= \frac{i}{2\pi}\frac{w^2}{w^2+v_F^2}\ \frac{1}{(x_1+x_2)-v_F(t_1-t_2)}
\end{aligned}$$

$$\begin{aligned}
\Big\langle T\psi_L(x_1,\sigma_1,t_1)\psi_R^\dagger(x_2,\sigma_2,t_2)\Big\rangle &= \frac{i}{2\pi}\frac{w^2}{w^2+v_F^2}\frac{e^{\gamma_1\log[2x_1]|}e^{(3+\gamma_2)\log[2x_2]|}+e^{(1+\gamma_3)\log[2x_1]|}e^{\gamma_1\log[2x_2]|}}{2} \\
&\quad e^{-\frac{1}{2}\log[-(x_1+x_2)-v_F(t_1-t_2)]}e^{-S\log[(x_1-x_2)-v_h(t_1-t_2)]}e^{-S\log[-(x_1-x_2)-v_h(t_1-t_2)]} \\
&\quad e^{-Z\log[(x_1+x_2)-v_h(t_1-t_2)]}e^{-Y\log[-(x_1+x_2)-v_h(t_1-t_2)]} \\
&= \frac{i}{2\pi}\frac{w^2}{w^2+v_F^2}\ e^{-\log[-(x_1+x_2)-v_F(t_1-t_2)]} \ = \ \frac{i}{2\pi}\frac{w^2}{w^2+v_F^2}\ \frac{1}{-(x_1+x_2)-v_F(t_1-t_2)}
\end{aligned}$$

Similarly, switching off interactions in the interacting version of the DDCF (equations (5.11) and (5.12)) leads to the the non interacting density density correlation functions as given by equation (5.6).

5.7.2 No hopping

When the hopping parameter vanishes ($w = 0$) then from equation (5.15), it is obvious that

$$< T\ \psi_R(x_1,t_1)\psi_L^\dagger(x_2,t_2) >=< T\ \psi_L(x_1,t_1)\psi_R^\dagger(x_2,t_2) >= 0$$

Moreover, in this situation,

$$P = \frac{(v_h+v_F)^2}{8v_hv_F}\ ; \quad Q = \frac{(v_h-v_F)^2}{8v_hv_F}\ ; \quad X = 0\ ; \quad \gamma_1 = 0$$

Hence the only non-vanishing parts of the NCBT two-point function for points on the same side the origin are,

$$\begin{aligned}\left\langle T\psi_R(x_1,\sigma_1,t_1)\psi_R^\dagger(x_2,\sigma_2,t_2)\right\rangle &= \frac{i}{2\pi}\ e^{-\frac{1}{2}\log\left[(x_1-x_2)-v_F(t_1-t_2)\right]} \\ &\quad e^{-\frac{(v_h+v_F)^2}{8v_hv_F}\log\left[(x_1-x_2)-v_h(t_1-t_2)\right]}e^{-\frac{(v_h-v_F)^2}{8v_hv_F}\log\left[-(x_1-x_2)-v_h(t_1-t_2)\right]} \\ \left\langle T\psi_L(x_1,\sigma_1,t_1)\psi_L^\dagger(x_2,\sigma_2,t_2)\right\rangle &= \frac{i}{2\pi}\ e^{-\frac{1}{2}\log\left[-(x_1-x_2)-v_F(t_1-t_2)\right]} \\ &\quad e^{-\frac{(v_h-v_F)^2}{8v_hv_F}\log\left[(x_1-x_2)-v_h(t_1-t_2)\right]}e^{-\frac{(v_h+v_F)^2}{8v_hv_F}\log\left[-(x_1-x_2)-v_h(t_1-t_2)\right]}\end{aligned} \tag{5.38}$$

These are precisely the standard Luttinger liquid two-point functions of a translationally invariant system. For points on the opposite sides of the origin, the most singular forms of the asymptotic Green functions have a discontinuous dependence on the hopping parameter w at $w = 0$ when mutual interactions between fermions are present.

5.7.3 Mandatory hopping

The other extreme limit is to allow the hopping parameter tend to infinity ($w \to \infty$), so that the particle compulsorily travels through the connecting link without going to the other side of the same pole. In such case, the two point functions of the 'case III: Same pole opposite sides' (equation (5.17)) vanishes. Furthermore,

$$\begin{aligned}A_1 = C_3 &= -\frac{v_h+v_F}{4v_h}; \quad B_1 = D_3 = \frac{v_h-v_F}{4v_h} \\ C_1 = A_3 &= \frac{v_h+v_F}{4v_h}; \quad D_1 = B_3 = -\frac{v_h-v_F}{4v_h}\end{aligned}$$

Therefore from equation (5.16) and (5.18) we have the following (see Fig. 5.9):

$$\left\langle T\ \psi_R^1(x_1,t_1,\sigma_1)\psi_R^{2\dagger}(x_2,t_2,\sigma_2)\right\rangle_{\text{opposite sides}} = \left\langle T\ \psi_R^1(x_1,t_1,\sigma_1)\psi_L^{2\dagger}(-x_2,t_2,\sigma_2)\right\rangle_{\text{same side}}$$

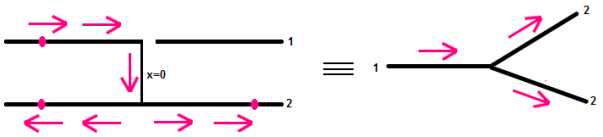

FIGURE 5.9: An electron after hopping from pole 1 when just reaches pole 2 has equal probabilities going to either sides due to identical environments.

5.7.4 Far away from hopping site

Consider the situation when $x_1 > 0,\ x_2 > 0$. Set $R_{cm} = (x_1 + x_2)/2$ and $y = x_1 - x_2$. This means $x_1 = R_{cm} + \frac{y}{2}$ and $x_2 = R_{cm} - \frac{y}{2}$. If y is held fixed and $R_{cm} \to \infty$, then this depicts the region far away from the hopping site. In such a situation, it is expected that Green's functions such as $< T\ \psi_R(x_1,t_1)\psi_R^\dagger(x_2,t_2) >$ and $< T\ \psi_L(x_1,t_1)\psi_L^\dagger(x_2,t_2) >$ to be immune to the presence or absence of the hopping sites. However the parts $< T\ \psi_R(x_1,t_1)\psi_L^\dagger(x_2,t_2) >$ and $< T\ \psi_L(x_1,t_1)\psi_R^\dagger(x_2,t_2) >$, that are non-zero only because of the hopping site, have no such restriction. In passing, it is noted that while the opposite choice viz. holding R_{cm} fixed while making $y \to \infty$ also makes the two points far from the impurity, since the region where the impurity is present has to be traversed, this Green function certainly will not be immune to the presence of the impurity.

$$\begin{aligned}
\Big\langle T\psi_R(x_1,\sigma_1,t_1)\psi_R^\dagger(x_2,\sigma_2,t_2)\Big\rangle &\sim e^{\gamma_1 \log[4R_{cm}^2 - y^2]} e^{-\frac{1}{2}\log[y - v_F(t_1-t_2)]} \\
&\quad e^{-P\log[y-v_h(t_1-t_2)]} e^{-Q\log[-y-v_h(t_1-t_2)]} e^{-X\log[2R_{cm}-v_h(t_1-t_2)]} e^{-X\log[-2R_{cm}-v_h(t_1-t_2)]} \\
\Big\langle T\psi_L(x_1,\sigma_1,t_1)\psi_L^\dagger(x_2,\sigma_2,t_2)\Big\rangle &\sim e^{\gamma_1 \log[4R_{cm}^2 - y^2]} e^{-\frac{1}{2}\log[-y - v_F(t_1-t_2)]} \\
&\quad e^{-Q\log[y-v_h(t-t_2)]} e^{-P\log[-y-v_h(t_1-t_2)]} e^{-X\log[2R_{cm}-v_h(t_1-t_2)]} e^{-X\log[-2R_{cm}-v_h(t_1-t_2)]}
\end{aligned} \tag{5.39}$$

where,

$$\begin{aligned}
P &= \frac{(v_F+v_h)^2}{8v_Fv_h}; \quad Q = \frac{(v_F-v_h)^2}{8v_Fv_h}; \quad \gamma_1 = X; \\
X &= -\frac{(v_F-v_h)(v_F+v_h)w^2(v_F^4 - v_F^2v_h^2 + v_Fv_hw^2 + w^4)}{8v_Fv_h(v_Fv_h+w^2)(v_F^4 + 2v_Fv_hw^2 + w^4)}
\end{aligned}$$

Now we have $P - Q = \frac{1}{2}$ and $\gamma_1 = X$. Performing the said limit $R_{cm} \to \infty$ and holding everything else fixed reduces equation (5.39) to,

$$\begin{aligned}
&\Big\langle T\psi_R(x_1,\sigma_1,t_1)\psi_R^\dagger(x_2,\sigma_2,t_2)\Big\rangle \\
&\quad \sim e^{-\frac{1}{2}\log[y-v_F(t_1-t_2)]} e^{-\frac{1}{2}\log[y-v_h(t_1-t_2)]} e^{-Q\log[y-v_h(t_1-t_2)]} e^{-Q\log[-y-v_h(t_1-t_2)]} \\
&\Big\langle T\psi_L(x_1,\sigma_1,t_1)\psi_L^\dagger(x_2,\sigma_2,t_2)\Big\rangle \\
&\quad \sim e^{-\frac{1}{2}\log[-y-v_F(t_1-t_2)]} e^{-\frac{1}{2}\log[-y-v_h(t_1-t_2)]} e^{-Q\log[-y-v_h(t_1-t_2)]} e^{-Q\log[y-v_h(t_1-t_2)]}
\end{aligned} \tag{5.40}$$

Since $Q = \frac{(v_h - v_F)^2}{8 v_h v_F}$, equation (5.40) is precisely the Green function of a homogeneous Luttinger liquid. In other words, these Green's functions are immune to the presence of the impurity.

5.8 Summary

The "non-chiral" bosonization technique, which is based on a non-standard harmonic analysis of the rapidly varying parts of the density fields, is used to obtain closed analytical formulas for the two-point function and four point functions relevant to Friedel oscillations of a one step fermionic ladder. Unlike g-ology based methods, the present approach treats the source of inhomogeneities exactly. The analytical expressions for the correlation functions written down are nothing but the re-summation of the most singular parts of the RPA terms in an expansion in powers of the mutual interaction using Fermi algebra. To further validate the results, various limiting cases are cross checked. Finally, the tunneling conductance of the system is calculated across different ends of the ladder.

Chapter 6

Ponderous impurities in a Luttinger liquid

Impurities in solid state systems are commonly immobile and are considered as static perturbations. On the other hand, mobile impurities are more typically studied in fluidic systems [141]. The well-known example in this regard would be the motion of a heavy particle in a three dimensional quantum fluid [142, 143]. The presence of an impurity can bring drastic changes to interacting systems, especially if the systems are one dimensional [31], whose physics is quite different from higher dimensional systems, described in the previous chapters. But the external potentials described till now, eg. single delta potential, finite barrier, one step ladder, etc., are all static. In this chapter we take into account a potential which has a time dependence. It physically resembles a mobile impurity in a Luttinger liquid.

More recently, the study of mobile impurities in one dimensional quantum liquids has been an active area of research [144–149]. Neto and Fisher [144] studied the dynamics of a heavy particle in a Luttinger liquid with repulsive interactions, besides analyzing the temperature dependence of the mobility of the particle. Caldeira and Neto computed the damping constant of a heavy particle, coupled to fermionic and bosonic environments in 1D [145]. Tsukamoto et al. obtained the exact critical exponents of various correlation functions of a TL liquid with a mobile impurity as functions of the impurity mass and momentum [146]. Fukuhara et al. studied the quantum dynamics of a spin impurity as it propagates in a 1D lattice [147]. Astrakharchik and Pitaevskii [148] predicted a power-law dependence of the drag force on a moving heavy impurity within Luttinger liquid on its velocity for small velocities. Girardeau and Minguzzi studied the problem of a moving impurity of finite mass in a 1D gas of hardcore bosons, also known as the TG (Tonks-Girardeau) gas [150]. In the work done by Mathy et al. [149], a phenomenon called quantum flutter was described for an impurity injected with finite momentum into a 1D quantum liquid. Schecter et al. realized that a constant force acting on an impurity in a 1D liquid leads to Bloch oscillations of the impurity around a fixed point, followed by energy release in the form of phonons [151]. Lychkovskiy studied mobile

impurities in a 1D quantum fluid at zero temperature and concluded that the velocity of the impurity at infinite time does not vanish at zero temperature, which is not the case at finite temperature [152, 153].

FIGURE 6.1: Ponderous impurity in a Luttinger liquid: The huge athlete walking towards right, representing the heavy particle, and the short athletes, representing electrons, running in both directions while rubbing shoulders representing forward scattering interactions.

In this chapter [154], the Green functions of a Luttinger liquid in presence of a slowly moving heavy particle (or a pair of them) is calculated using a combination of perturbative approaches and the Non chiral bosonization method [90, 140]. Using the Green function, the force acting on the heavy particle is calculated in terms of its terminal velocity, both in the linear and non-linear regime. Mobility is calculated for the linear regime, shedding light on temperature dependence and mutual interaction strength between the fermions. Our results are qualitatively consistent with the highly cited work on the subject [144] both at low and high temperatures. Our findings are also consistent with the impenetrable impurity moving ballistically (mobility diverges) at low temperatures so long as the fermions are mutually repelling. At higher temperatures small compared to the Fermi energy the mobility saturates to a constant value.

6.1 System description and method of solution

Consider a Luttinger liquid in one dimension with forward scattering short range mutual interactions [5] in the presence of a heavy particle (classical impurity) moving with speed small compared with the Fermi velocity v_F. The full generic-Hamiltonian of the system(s) under study (before approaching the RPA limit) is (are),

$$H = \int_{-\infty}^{\infty} dx\ \psi^{\dagger}(x) \left(-\frac{1}{2m}\partial_x^2 + V_0\delta(x - X(t)) \right) \psi(x) + \frac{1}{2}\int_{-\infty}^{\infty} dx \int_{-\infty}^{\infty} dx^{'}\ v(x - x^{'})\ \rho(x)\rho(x^{'}) \tag{6.1}$$

where $V_0\delta(x - X(t))$ is the potential due to the impurity at position X(t) and $v(x - x^{'}) = \frac{1}{L}\sum_q e^{-iq(x-x^{'})}v_q$ (where $v_q = 0$ if $|q| > \Lambda$ for some fixed $\Lambda \ll k_F$ and $v_q = v_0$ is a constant, otherwise) is the forward scattering mutual interaction. It is necessary to confine the study to the so-called RPA limit which means, among other things, working in the limit where the Fermi momentum and the mass of the fermion diverge in such a way that their ratio is finite (i.e. $k_F, m \to \infty$ but $k_F/m = v_F < \infty$: units that make $\hbar = 1$, so that k_F is both the

Fermi momentum as well as a wavenumber, are used). This amounts to linearizing the energy momentum dispersion near the Fermi surface and thereby leading to a feasible analytical solution.

The obvious method for studying this system is to observe that a mobile impurity moving with a speed much lower than the Fermi velocity may be regarded as being stationary to the lowest order approximation. The fermion Green function (with or without mutual interactions between fermions) is computed with this assumption. In order to incorporate the effects of the non-zero speed of the impurity, an iteration of the relevant equations is performed wherein the zeroth order stationary Green functions are employed in order to compute leading corrections due to the finite speed of the impurity. The general Dyson's equation for the full Green function denoted by $G(x,x';t,t') \equiv< T\ \psi(x,t)\psi^{\dagger}(x',t') >$ in terms of its counterpart $G_{SCh}(x,x';t,t')$ that assumes the impurity(s) is(are) stationary at (near) the origin is (the subscript SCh stands for steeplechase which represents the static impurity discussed in chapter 3),

$$G(x,x';t,t') = G_{SCh}(x,x';t-t') + V_0 \int_C dt^{''} \Big(G_{SCh}(x,X(t^{''});t-t^{''}) G(X(t^{''}),x';t^{''},t') - G_{SCh}(x,0;t-t^{''}) G(0,x';t^{''},t') \Big) \tag{6.2}$$

Here C is the Keldysh contour. Keeping in mind that the speed of the mobile impurity is small compared to the Fermi velocity, the leading approximation to the above full Green function would be,

$$G(x,x';t,t') \approx G_{SCh}(x,x';t-t') + V_0 \int_C dt^{''} \times \Big(G_{SCh}(x,X(t^{''});t-t^{''}) G_{SCh}(X(t^{''}),x';t^{''},t') - G_{SCh}(x,0;t-t^{''}) G_{SCh}(0,x';t^{''},t') \Big) \tag{6.3}$$

Having obtained this, the force acting on the impurity may be computed as follows,

$$F_X = -\,V_0 \left(\frac{d}{dx}\right)_{x=X(t)} < \rho(x,t) > \;\; = \;\; V_0 \left(\frac{d}{dx}\right)_{x=X(t)} G_{<}(x,x;t,t) \tag{6.4}$$

where $G_{>}$ and $G_{<}$ are the advanced and retarded Green functions respectively and

$$G(x,x',t,t') = \theta(t-t')\langle \psi(x,t)\psi^{\dagger}(x',t') \rangle - \theta(t'-t)\langle \psi^{\dagger}(x',t')\psi(x,t) \rangle$$

The RPA Green function with and without mutual forward scattering interactions between fermions with stationary impurities has been computed in an earlier chapter using the non chiral bosonization technique [90].

6.2 Analysis and computations

The analytical expressions for the Green functions of a Luttinger liquid in presence of one and two scalar impurities obtained in the cited central work [90] is heavily relied upon in the present work. The technique of non-chiral bosonization used in this work provides an analytical expression for the most singular part of the RPA Green function of such systems which also happens to exhibit power law behavior analogous to homogeneous Luttinger liquids.

In the RPA limit, the assertion is: $X(t) \to 0$ even as $k_F \to \infty$ so that $|k_F X(t)| < \infty$. Hence quantities such as $e^{ik_F X(t)}$ that appear repeatedly in the calculations now make sense. The ansatz that amounts to asserting that the impurity executes a simple harmonic motion about the origin $X(t) = \frac{v_X}{\omega} sin(\omega t)$ is used where v_X is the maximum drift (steady state) velocity of the particle in response to an weak external force that is applied on it. The frequency ω could represent one of two things - a) if the applied force is sinusoidal in time, it is the frequency of the applied force b) if the force is independent of time, then $|\hbar\omega| \sim T$ which is the temperature of the system. When the particle is moving very slowly i.e. $|k_F X(t)| \ll 1$ in other words $\frac{k_F v_X}{T} \ll 1$, calculations are done using the approximation $e^{ik_F X(t'')} \approx 1 + ik_F X(t'')$ which is inserted into the right hand side of equation (6.3). This shows that the terminal speed is proportional to the applied force and the coefficient of proportionality is a power law in the dominant energy scale in this problem viz. temperature T, in this case.

When the particle is not moving slowly i.e. $\frac{k_F v_X}{T} \gg 1$, it is not possible to expand in this fashion, but since $e^{ik_F X(t'')} = e^{i\frac{k_F v_X}{T} sin(Tt'')}$ where T is temperature in frequency units, this term rapidly oscillates and averages out to zero unless $t'' \ll \frac{2\pi}{T}$. In this case we may write, $e^{ik_F X(t'')} \sim e^{ik_F v_X t''}$ and rescaling t'' while performing the integral means the integrals in equation (6.3) are going to be a power-law in the dominant energy scale in the problem which is now $k_F v_X$ rather than temperature. This is the reason for the nonlinear power-law dependence of the force on the terminal velocity when $k_F v_X \gg T$.

6.2.1 Single impurity

For a single mobile impurity, the externally applied force F_X on the impurity may be related to the drift velocity v_X quite easily. Using equations (6.4) and (6.3), the force can be related to the Green functions of the static impurity, which are given in Appendix B. When fermions are not mutually interacting with one another, the force takes the following form.

$$F_X = \frac{2V_0^2 k_F^2}{\pi (V_0^2 + v_F^2)} v_X \tag{6.5}$$

where V_0 is the strength of the coupling between the heavy particle and the fermions. Mobility μ is defined as the ratio between the terminal velocity of the impurity and the force acting

on it so that,

$$\mu = \frac{\pi\,(V_0^2 + v_F^2)}{2V_0^2 k_F^2} \tag{6.6}$$

The mobility diverges when the coupling between the impurity and the fermions vanishes ($V_0 \to 0$), implying ballistic motion of the impurity, i.e., the impurity accelerates in response to the external force rather than reaching a terminal velocity. Conversely, when the coupling diverges - which means no tunneling of fermions through the impurity is permitted ($V_0 \to \infty$), the mobility saturates to its minimum value of $\mu_0 = \frac{\pi}{2k_F^2}$ [144].

6.2.2 Two identical impurities

Two mobile impurities may be studied by observing that since both are slowly moving, the leading approximation would have only one of them moving and the other fixed so that the applied force would be proportional to the drift velocity of the moving impurity. In general it may be surmised that $F = const.v_X + const.v_X^2$ where the second term is the small correction to the mobility of one of the moving impurity in response to the motion of the second impurity which may be neglected. The mobility of a moving impurity in presence of another at a distance $a = \frac{\xi_0}{k_F}$ (where ξ_0 is a tunable dimensionless parameter) is (using equations (6.4), (6.3) and the Green functions of two impurity system mentioned in Appendix B),

$$\mu = \mu_0 \frac{v_F^2\left((2V_0^2\sin^2[\xi_0] - v_F^2)^2 + 4V_0^2(V_0\sin(\xi_0)\cos(\xi_0) + v_F)^2\right)}{V_0^2(2V_0^2\sin^2[\xi_0] - v_F^2)^2} \tag{6.7}$$

where $\mu \geq \mu_0 \frac{v_F^2}{V_0^2}$ and the fermions are not mutually interacting.

In presence of a finite number of identical impurities, the reflection and transmission amplitudes of fermions may be parametrized as follows: $R = \sin(\theta)e^{i\phi}$ and $T = i\cos(\theta)e^{i\phi}$ which is consistent with known identities such as $|T|^2 + |R|^2 = 1$ and $RT^* = -R^*T$. The mobility

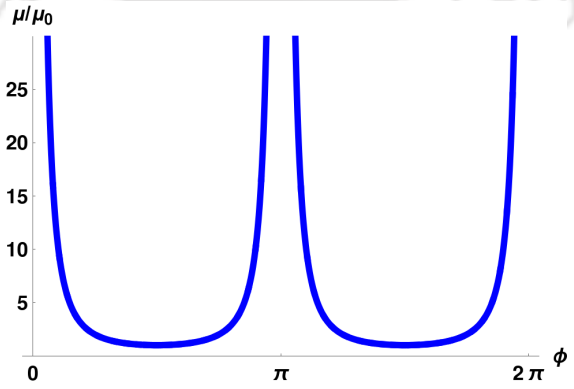

FIGURE 6.2: Plot of the mobility vs phase ϕ for the general case of a finite number of heavy particles.

then evaluates to a simple expression (μ_0 has been defined previously),

$$\mu = \mu_0 \csc^2 \phi \tag{6.8}$$

The dependence of the mobility on the phase (ϕ) is depicted in figure 6.2. The minimum mobility is μ_0 which corresponds to the situation where no tunneling across the impurities is allowed. The maximum mobility is infinite which corresponds to the ballistic motion of the impurity which happens in the trivial situation when the coupling between the impurity and the fermions vanishes. The interesting question is, does it also happen when there are appropriate resonances? In the two impurity case, an examination of the formula in equation (6.7) suggests that ballistic motion of the impurities in response to an applied force may be expected to be seen when $V_0 = \frac{v_F}{\sqrt{2}|\sin(\xi_0)|}$, in which case the mobility diverges, but for the most part, the motion of the impurities is heavily damped by the fermions in the background. Also, when $sin(\xi_0) = 0$, the two-impurity system resembles the single impurity system where there is no possibility of ballistic motion of impurities for non-zero V_0. The other extreme is when the strength of the impurities tends to infinity ($V_0 \to \infty$) when the mobility tends to a non-zero minimum value of $\frac{\pi}{2k_F^2}$ for a single impurity. Of special interest is the double impurity system where the mobility vanishes when $V_0 \to \infty$, provided $\sin(\xi_0) \neq 0$ as may be seen from equation (6.7). This means that when tunneling through the impurities is forbidden, their mobilities vanish except when the distance between them is an integral multiple of half a Fermi wavelength.

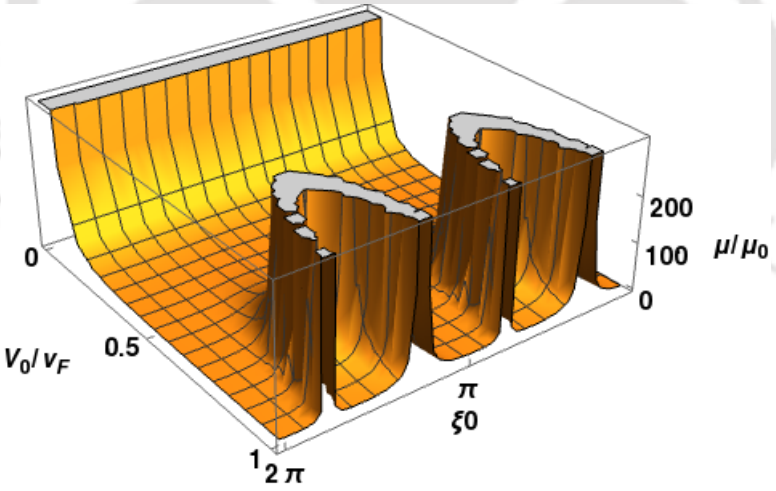

FIGURE 6.3: $\frac{\mu}{\mu_0}$ versus $\frac{V_0}{v_F}$ and ξ_0 for a two-impurity system

Since the dependence of the phase angle ϕ on V_0 and ξ_0 in the two-impurity case is complicated, it is better to visualize the dependence of the mobility on these variables more directly through the following 3D plot in figure 6.3. The explicit dependence of the phase angle ϕ on V_0 and ξ_0 for a two impurity system may be expressed as follows.

$$\sin^2(\phi) = \frac{(2V_0^2 \sin^2(\xi_0) - v_F^2)^2}{(v_F^4 + 4V_0^2(v_F \cos(\xi_0) + V_0 \sin(\xi_0))^2)}$$

6.3 Mobility of a single and two-impurity system in a Luttinger liquid

When mutual interactions between fermions are absent, it is well known that the mobility is infinite (ballistic motion) for a homogeneous system. Upon introducing an impurity, the mobility gradually diminishes with increasing strength of the impurity and saturates to minimum non-zero value when tunneling across the impurity is forbidden. The NCBT is able to interpolate between these two extremes. The interesting question is how these expectations are modified upon inclusion of mutual interactions between fermions. It is well-known that the low temperature properties of the interacting systems are qualitatively different from those of free fermions. They form what is known as a Luttinger liquid. In earlier works [90, 140], it have been shown that the most singular part of the RPA Green function of Luttinger liquids in presence of barriers or wells is a discontinuous function of the height of the barriers for small barrier heights. Thus the limit of small barriers (large tunneling amplitudes) may not be usefully studied by the traditional approaches that invoke a perturbation theory around the homogeneous Luttinger liquid starting point. In fact, the present approach which is based on a non-standard harmonic analysis of the fast part of the density fluctuations is uniquely suited to study impurity systems as it allows for an analytical interpolation between the weak link and the weak barrier extreme limits unlike the traditional approaches that fall well short of providing explicit expressions for the exponents associated with the mobility in the general cases and instead rely on tentative renormalization flow analyses.

It suffices to state that the analytical expressions for the Green functions for Luttinger liquids in presence of barriers and wells derived in a recent work [90] are borrowed and used as input to compute the mobility of one and two impurities using the algorithm outlined in section 6.1 of the present work. This leads to the following formula for the external force acting on the impurity F_X in terms of the drift velocity v_X.

$$F_X \sim \mu_*^{-1}\ \omega^{\alpha}\ v_X$$

where μ_* is the mobility of the corresponding system with no mutual interactions between fermions. The notion of weak equality ($\sim$) is used because the force is actually a linear combination of terms ($F = const\ \omega^{\alpha_1} + const\ \omega^{\alpha_2}$). Now the energy scale ω being rescaled by some cut-off (bandwidth Λv_F which is very large) to become dimensionless and magnitude much less than unity and thus the leading order term will be the one with the smallest exponent. Hence,

$$\alpha = \mathrm{Min}(\alpha_1, \alpha_2)$$

The explicit values of α_1 and α_2 both for single impurity are as follows.

$$\alpha_1 = \frac{(v_h - v_F)(2V_0^2 + v_F(v_h - v_F))}{2v_F(V_0^2 + v_h v_F)}; \alpha_2 = \frac{v_h^2 - v_F^2}{2(V_0^2 + v_h v_F)}$$

where $v_h = v_F\sqrt{1+\frac{2v_0}{\pi v_F}}$, V_0 is the strength of the impurity and v_0 is the strength of forward scattering interactions such that $v_0 < 0$ for attractive interactions and $v_0 > 0$ for repulsive ones. For two identical impurities with strength V_0, the values of α_1 and α_2 are given below.

$$\begin{aligned}\alpha_1 =& \frac{v_h - v_F}{v_F} + \frac{v_F^2(v_F^2 - v_h^2)}{2(4V_0^2(V_0\sin(\xi_0) + v_F\cos(\xi_0))^2 + v_F^3 v_h)}\\ \alpha_2 =& \frac{v_F^2(v_h^2 - v_F^2)}{2(4V_0^2(V_0\sin(\xi_0) + v_F\cos(\xi_0))^2 + v_F^3 v_h)}\end{aligned}$$

with $\xi_0 = k_F a$ where a is the distance between the two impurities and k_F is the Fermi momentum. In both the cases, α_1 is the dynamical density of states (DDOS) exponent at the origin when the two (spatial) points of the two-point function are assumed to merge with the origin from the same side while α_2 is that from the opposite sides. Both these appear in the analysis since in the defining equation for the Green function viz. equation (6.3), even if $x = x'$, the heavy particle can be found on either side of $x = x'$.

As pointed out earlier, ω is the dominant energy scale that corresponds to temperature as long as $\frac{k_F v_X}{T} \ll 1$ but ω would correspond to the energy scale set by the drift velocity viz. $v_X k_F$ if $\frac{k_F v_X}{T} \gg 1$. Roughly speaking, it should not matter whether the drift velocity or the externally applied force is used to pin down the second energy scale (other than temperature), these two notions are interchangeable as long as $|\alpha| \ll 1$. The present study is limited to regions where this condition is obeyed. Thus the force acting on the heavy particle is explicitly expressed as follows.

$$F_X = \mu_*^{-1}\left[Max\left(\frac{k_F v_X}{v_F\Lambda}, \frac{T}{v_F\Lambda}\right)\right]^{Min(\alpha_1,\alpha_2)} v_X \tag{6.9}$$

Here v_X is the drift velocity of the heavy particle(s) when acted upon by a force F_X. The cross-over speed which provides a scale that separates the regime of linear dependence on the applied force and the nonlinear regime is clearly, $v_{X_c} = \frac{T}{k_F}$. The force on the particle moving with this cross-over speed is the cross-over force

$$F_{X_c} = \mu_*^{-1}\left[\frac{T}{v_F\Lambda}\right]^{Min(\alpha_1,\alpha_2)} v_{X_c}$$

where Λv_F is the band-width mentioned earlier. Figure 6.4 shows the variation of the force on the heavy particle as a function of the drift velocity (rescaled appropriately to make them both, dimensionless). From figure 6.4, it is clear that when $v_X \ll v_{X_c} = \frac{T}{k_F}$, the force varies linearly with drift velocity, the ratio being the inverse of mobility. On the other hand, when $v_X \gg v_{X_c}$, the force varies non-linearly with the drift velocity and the curvature is decided by the sign of the exponent α.

The dependence of the cross-over scales themselves on temperature may also be studied. Consider the dimensionless quantities $\frac{k_F v_{X_c}}{\Lambda v_F}$ and $\frac{k_F F_{X_c}}{\Lambda F_{v_F}}$ where F_{v_F} is the hypothetical force extrapolated from the above formulas which would naively correspond to the force acting on a heavy particle whose drift velocity is the Fermi velocity v_F (there is no valid physics here -

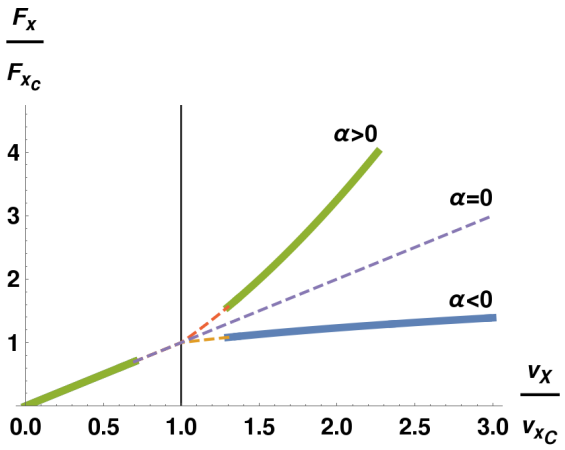

FIGURE 6.4: Plot of $\frac{F_X}{F_{X_c}}$ vs $\frac{v_X}{v_{X_c}}$ where $v_{X_c} = \frac{T}{k_F}$ is constant for a given temperature. The dotted lines signify regions that interpolate between regimes that are easily amenable to analytical approaches.

this is just a scale to render dimensional quantities, dimensionless). It is pertinent to examine the dependence of these quantities on the dimensionless temperature $g = \frac{T}{\Lambda v_F}$. From the above formulas it is clear that,

$$\frac{k_F F_{X_c}}{\Lambda F_{v_F}} = g^{1+\alpha}; \qquad \frac{k_F v_{X_c}}{\Lambda v_F} = g \tag{6.10}$$

These formulas may also be described diagrammatically as in figure 6.5. An examination of

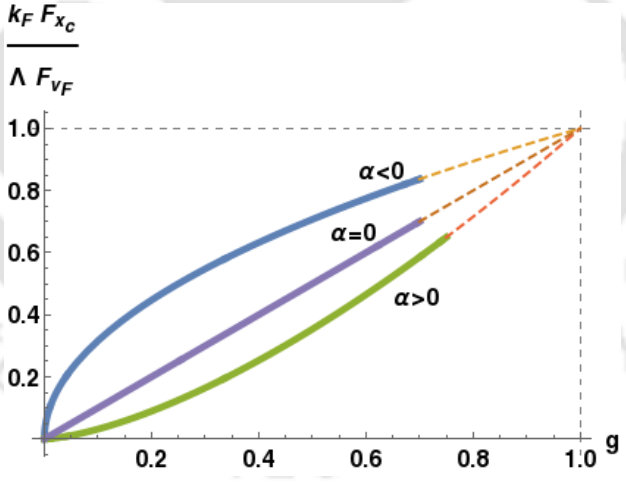

FIGURE 6.5: Variation of the cross-over force scale on temperature for different choices of the sign of α.

figure 6.6 shows that for negative values of α, the mobility decreases from a maximum value with an increase in temperature while for positive values of α, it increases from a minimum value with an increase in temperature, while both of them tend to converge to the value of the non-interacting case. As mentioned earlier, the force acting on the heavy particle is expressed as a power-law in terms of the energy scale 'ω' which is expressed in units of the bandwidth Λv_F such that $\frac{\omega}{\Lambda v_F}$ is dimensionless and is always less than unity. The expression for force obtained from the Green function is originally a linear combination of terms with

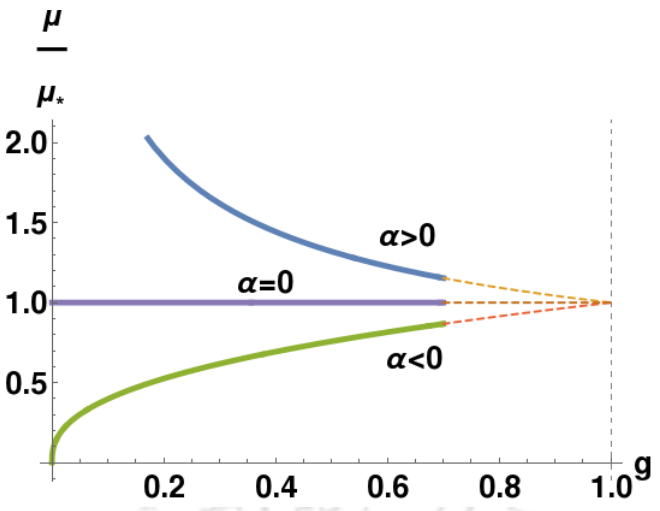

FIGURE 6.6: Ratio of mobility in the linear regime in presence of interactions to that without interactions vs g (temperature).

different powers of $\frac{\omega}{\Lambda v_F}$ and thus the dominant term is the one with the smallest exponent, which explains the choice of α as the minimum of α_1 and α_2 in equation (6.9).

It is important to analyze the exponent α since earlier plots show that the sign of α is quite important in determining the qualitative behavior of the applied force versus terminal velocity. In general, α can be positive or negative or even vanish altogether while its absolute value is sufficiently less than unity. From the plots in figure 6.7 it is observed that both for single and double impurity, α tends to take positive values for repulsive interactions and thus the mobility, as observed from figure 6.6, decreases with an increase in temperature which is consistent with the literature [144, 155]. On the other hand for attractive interactions, α

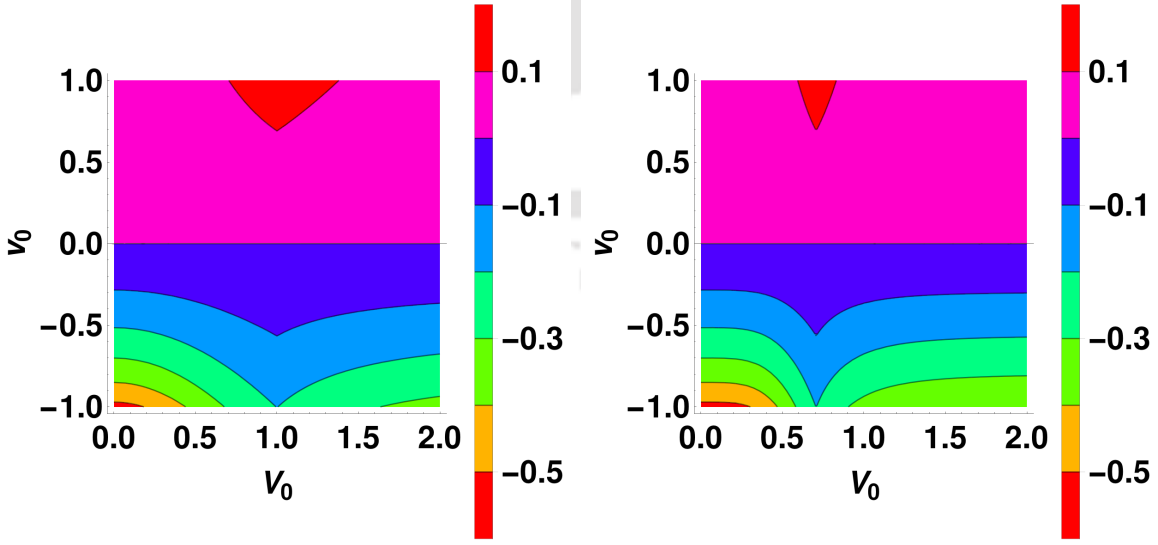

(a) (b)

FIGURE 6.7: Plots of the exponent α for (a) Single impurity system and (b) Two-impurity system as a function of the impurity strenth V_0 and the strength of the mutual interactions v_0 (setting $v_F = 1$ and $\xi_0 = \pi/2 + n\pi$ for two impurity case where n is an integer).

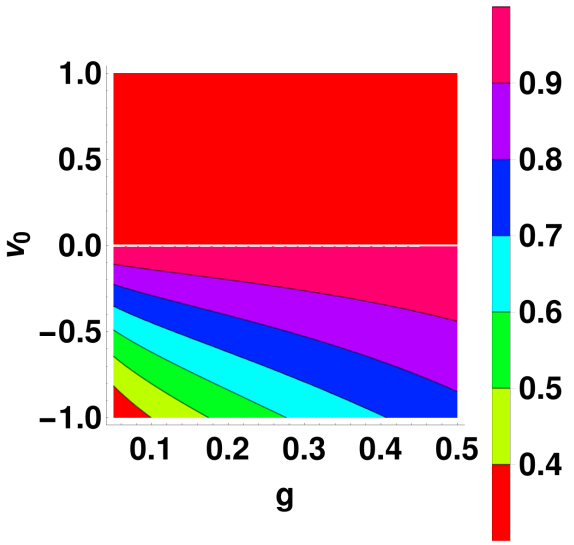

FIGURE 6.8: Ratio of mobility in the linear regime in presence of interactions to that without interactions vs g (temperature) and the strength of the mutual interactions v_0 when the strength of impurities diverge (no-tunneling case).

takes negative values which indicates an increase in mobility with an increase in temperature. The two-impurity system shows some interesting physics in the behavior of the exponents as well. The plot in figure 6.7 b is given for $\xi_0 = \pi/2$ but it is observed that the exact same plot is obtained for $\xi = \pi/2 + n\pi$ where n is an integer. This indicates that the mobility oscillates as a function of ξ_0 with a period of π.

Finally the mobility is studied when tunneling through the impurities is forbidden ($V_0 \to \infty$). In this case the exponent α vanishes for repulsive interactions and becomes equal to $(v_h - v_F)/v_F$ for attractive interactions both for the double and the single impurity. The double impurity is of lesser importance here because, as already discussed earlier, the mobility vanishes for double impurity in this situation except when $\xi_0 = n\pi$. The variation of mobility is shown in figure 6.8 as a function of the forward scattering strength v_0 and temperature g $(= \frac{kT}{\Lambda v_F})$.

Generally, fermions that are mutually attracting tend to mitigate the effect of an impurity [31] ("heal the chain"). A weak impurity in turn implies a tendency toward ballistic mobility or at least increased mobility. At higher temperatures, attractive fermions become better at mitigating the effect of the impurity hence the mobility increases when temperature increases.

Conversely for fermions that are mutually repelling, there is a tendency to aggravate the effect of the impurity [31] ("cut the chain"). However, when the impurity strength is already strong enough to prevent tunneling through the impurity, the mutual repulsion of the fermions do not do anything to the mobility as it is already the minimum value it can be. Hence in this situation the mobility is independent of temperature. When tunneling is allowed in the repulsive case, mobility decreases with increasing temperature as it would have done had the barrier strength increased instead.

6.4 Comparison with existing studies

The highly cited work on the subject by Castro Neto et al. [144] considers a.c. mobility. When the applied force is a.c., the terminal velocity is also a.c. and proportional to the applied force right down to absolute-zero temperature. This is not the case in the present work where we consider a d.c. applied force. At temperatures small compared to the Fermi energy when fermion-fermion interactions are ignored, it is well-known that the mobility of a heavy particle is temperature independent. This is clearly stated in [144], and their μ_0 is the same as ours - indeed we simply borrowed this well-known result. At very low temperatures the main prediction of [144] is that the a.c. mobility (d.c. limit of a.c. mobility is not the same as d.c. mobility: this is clearly stated in [144]. We have calculated d.c. mobility and not the d.c. limit of a.c. mobility) diverges as the 4-th power of temperature whereas at high temperatures it is approximately independent of temperature as long as the heavy particle is impenetrable by the mutually repelling fermions. In order to study this limit as best as we can using our manifestly d.c. formulas, we first observe that the terminal velocity v_X is related to applied d.c. force F_X at very low temperatures in the following nonlinear way:

$$F_X = \mu_*^{-1} v_X^{1+c}$$

where $c = (v_h^2 - v_F^2)/(2V_0^2)$ for $v_h > v_F$ (repulsion between fermions) and $c = (v_h - v_F)/v_F$ for $v_h < v_F$ (attraction between fermions), both for an impenetrable impurity ($V_0 \to \infty$). Now the differential mobility is

$$\mu = \frac{dv_X}{dF_X} = (1+c)^{-1} \mu_* v_X^{-c}$$

The linear mobility is defined as the $v_X \to 0$ limit of the differential mobility.

$$\mu_{diff} = \lim_{v_X \to 0} (1+c)^{-1} \mu_* v_X^{-c} = \infty \text{ since } c > 0 \ (repulsion)$$

This is consistent with [144] which says that at very low temperatures the mobility of an impenetrable heavy particle with mutually repelling fermions diverges (motion is ballistic). Conversely at high temperatures, both [144] and our results predicts a roughly temperature independent linear mobility as long as the impurity is impenetrable by the mutually repelling fermions. The particular result of [144] namely the T^{-4} law is derived by them by treating the time-dependent spatially inhomogeneous impurity potential as a small perturbation around the homogeneous Luttinger liquid background. This is because their RG equations show that at low temperature the impurity behaves effectively as if it were much lighter and much more penetrable. Since our formalism is identical to theirs for the homogeneous system, discussing this T^{-4} law would be a simple duplication of their analysis. Our results are only valid for a fully d.c. externally applied force and hence this is qualitatively different from the situation they consider in the latter half of their paper. Even so, our results also confirm their conclusions namely that the impurity tends to be much more mobile at low temperatures when

fermions are mutually repelling than when they are non-interacting.

6.5 Summary

In this chapter, the Green function of slowly moving impurities in a Luttinger liquid is obtained using a combination of perturbative approach and the non-chiral bosonization technique. The force acting on the heavy particle is calculated as a function of the drift velocity for the non-interacting case and the expression for mobility is calculated. Both the linear and non-linear dependence of the force on the drift velocity has been analytically obtained for systems with forward scattering interactions between the fermions with one or two mobile impurities. Peculiar resonances that are seen in the two-impurity system have been mapped out. The unique feature of this work is the analytical closed expressions for the exponents in terms of the coupling strengths in the problem that interpolate between the ballistic regime on the one hand and the no-tunneling regime on the other.

Chapter 7

Validating Non chiral bosonization technique

Any novel technique needs validation. A usual way of doing this is to compare its results with those obtained using well established techniques. But the very fact that the same results can be obtained using other techniques would lessen the importance of a novel approach. In this regard, as already mentioned, the standard g-ology method is unable to produce the two-point functions of even free fermions with an impurity without resorting to renormalization methods. Another validation route would be to adopt a perturbative approach and calculate the Green functions up to a certain order of the interaction term and compare with conventional fermionic perturbation theory. But the most convincing validation would be to insert the putative best Green functions obtained by any technique into the Schwinger-Dyson equation [156, 157] which are the equations of motion of the Green functions and show that the result is an identity. This route is much more convincing than any other analytical or numerical comparison.

There is an alternative to the operator method of bosonization, which we also briefly discuss here is based on the idea that the Green functions of systems with mutual interaction between fermions may be expressed as functional averages of the Green functions of free fermions interacting with arbitrary external potentials. The averages are performed by treating the external potentials as Gaussian random variables with a mean determined by the actual external potentials present in the problem and the standard deviations related to the forward scattering strength of the short-range interaction between fermions. This approach, originally suggested by Fogedby [158], was elaborated by Lee and Chen [30]. This approach was further expanded in [46] and [159] where it was used to deal with impurities in a Luttinger liquid.

When it comes to numerical validation, the obvious tools that springs to mind are density-matrix renormalization group (DMRG) [160], finite-size scaling, etc. But performing numerical validation of an analytical result is somewhat like asking a high-school pupil to prove the analytical formulas for the solution of a quadratic equation by solving the latter numerically.

The pupil would rightly argue that it is much more convincing and easier to simply insert the putative analytical solution back into the defining equation and show that the result is an identity. This is precisely what Schwinger Dyson validation does. Moreover for gapless systems such as the ones under consideration in the work, DMRG has its own shortcomings which is discussed in a later section.

In this chapter [101], it has been emphasized that inserting the Green functions into the Schwinger-Dyson equation and checking for an identity is superior to any other methods of validation. Section 7.1 describes the systems under study and their respective Green functions. Section 7.2 illustrates the necessary validation checks the Green functions must obey. In section 7.3, the perturbative comparison is discussed whereas section 7.4 elaborates the Schwinger Dyson validation. The subsequent sections briefly describes the functional bosonization method and the DMRG method as to why they are not suitable in this regard.

7.1 System description and Green functions

The Green functions for the homogeneous Luttinger liquid have been calculated by Mattis and Lieb [3] and are explained for example, in the textbook by Giamarchi [5]. On the other hand, those of strongly inhomogeneous Luttinger liquids such as a cluster of impurities around a fixed point are calculated by the recently developed Non chiral bosonization technique [90]. In this chapter, the procedure to validate these Green functions has been illustrated. It is, of course, redundant to validate the well-established results of homogeneous LL. However this is done to demonstrate the validation method itself which is then used for the results obtained by the recently developed approach to bosonization - the NCBT. Consider once again the generic Hamiltonian for Luttinger liquid with short ranged forward scattering mutual interactions between the fermions.

$$H = \int_{-\infty}^{\infty} dx\ \psi^{\dagger}(x) \left(-\frac{1}{2m}\partial_x^2 + V(x) \right) \psi(x) + \frac{1}{2} \int_{-\infty}^{\infty} dx \int_{-\infty}^{\infty} dx^{'}\ v(x - x^{'})\ \rho(x)\rho(x^{'}) \tag{7.1}$$

The first term represents the kinetic energy while the second term represents the potential energy which is set to zero for homogeneous systems. For strongly inhomogeneous systems, it can be modeled as a finite sequence of barriers and wells clustered around a point (taken to be the origin, $x = 0$) as discussed in chapter 3. The last term represents the forward scattering mutual interaction and can be written as

$$v(x - x^{'}) = \frac{1}{L} \sum_{q} v_q\ e^{-iq(x-x^{'})} \tag{7.2}$$

where $v_q = 0$ if $|q| > \Lambda$ for some fixed bandwidth $\Lambda \ll k_F$ and $v_q = v_0$ is a constant, otherwise.

Now the Green functions of these systems are obtained using bosonization, where a fermionic field is represented as an exponential of a bosonic field. This involves inverting the defining formulas for current and number densities viz. $j(x) = Im[\psi^\dagger(x)\partial_x\psi(x)]$ and $\rho(x) = \psi^\dagger(x)\psi(x)$ and rewriting $\psi(x)$ in terms of j and ρ. Then the continuity equation $\partial_t\rho + \partial_x j = 0$ is invoked and $\psi(x)$ is written purely as a (non-local) function of ρ and $\partial_t\rho$. Thus the N-point function is some combination of the correlations of the density field with itself.

The inversion of the defining relation between current and densities in the standard bosonization scheme that goes by the name g-ology [5] yields the following relation between $\psi_\nu(x,\sigma,t)$ (where ν = R(+1) or L(-1) for right and left movers respectively) and the slowly varying part of the density (this is a mnemonic for generating the N-point functions),

$$\psi_\nu(x,\sigma,t) \sim e^{i\theta_\nu(x,\sigma,t)} \tag{7.3}$$

with the local phase given by the formula,

$$\theta_\nu(x,\sigma,t) = \pi \int_{sgn(x)\infty}^{x} dy \Big(\nu\ \rho_s(y,\sigma,t) - \int_{sgn(y)\infty}^{y} dy^{'}\ \partial_{v_F t}\ \rho_s(y^{'},\sigma,t) \Big) \tag{7.4}$$

Here ρ_s is the slow part of the density operator ρ which can be harmonically analyzed as shown in equation (7.13). The prescription in equation (7.3) is valid only for homogeneous systems and for a half line (no tunneling across the barrier) and the Green functions in both cases are provided in Appendix A.

Analogous to conventional bosonization schemes [5], the fermionic field operator in NCBT is also expressed in terms of currents and densities. But in NCBT, the field operator is modified to include the effect of back-scattering by impurities making it suitable to study translationally non-invariant systems such as the ones mentioned in the last section. The modified field operator of NCBT may be written as follows [90].

$$\psi_\nu(x,\sigma,t) \sim C_{\lambda,\nu,\gamma}\ e^{i\theta_\nu(x,\sigma,t) + 2\pi i\lambda\nu \int_{sgn(x)\infty}^{x}\ \rho_s(-y,\sigma,t)dy} \tag{7.5}$$

Here θ_ν is the familiar local phase given by equation (7.4). NCBT differs by the addition of the optional term $\rho_s(-y,\sigma,t)$ to this local phase that ensures the necessary trivial exponents for the single particle Green functions for a system of otherwise free fermions with impurities (which may also be obtained using standard Fermi algebra). The adjustable parameter λ can take values either 0 or 1, which decides the presence or absence of the new term. In other words, setting $\lambda = 0$ reduces the NCBT operator to standard bosonization operator given in equation (7.3). The factor $2\pi i$ ensures that the field operator obeys the necessary fermion commutation rules since this term does not change the statistics of the field operator. $C_{\lambda,\nu,\gamma}$ are pre-factors which are fixed by comparison using the non-interacting Green functions obtained from Fermi algebra. The field operator as given in equation (7.5) is to be treated as a mnemonic to obtain the Green functions rather than an operator identity, which avoids the necessity of the Klein factors that are conventionally used. The field operator (annihilation) is

clubbed together with another such field operator (creation) and after fixing the C's and λ's, one obtains the non-interacting two-point functions in terms of density-density correlation functions of the system. Lastly, these density correlation functions are replaced by their interacting versions to obtain the many-body Green functions for the strongly inhomogeneous LL under study are given in Appendix B. The details are described in an earlier work [90] (chapter 3).

7.2 Necessary validation checks

First let us examine the necessary rules which the Fermi Bose correspondence used and the Green functions obtained must satisfy. However, these are not sufficient to declare them as correct. The next section describes some cross-checks which can conclusively declare the correctness of the results.

7.2.1 Commutation rules

The Green functions under consideration in the present chapter have been obtained using standard g-ology methods [5] and the recently developed NCBT [90] both of which are a field-theoretic approach to bosonization. In both these approaches, the fermion field operator is expressed as a function of currents and densities. It is necessary that these operators obey the necessary commutation rules, which is the first mandatory step in validating the results.

7.2.1.1 Fermi Language

Fermi fields: Let there be N species of fermions $\psi_j(x)$ where $j = 1, 2, ..., N$. By definition we have,

$$\{\psi_j(x,t), \psi_k(x^{'},t)\} = 0 \ ; \ \{\psi_j(x,t), \psi_k^{\dagger}(x^{'},t)\} = \delta_{j,k} \ \delta(x - x^{'}) \tag{7.6}$$

Forward relation: The currents and the densities are defined in terms of the fields as follows (no point splitting etc. are needed in this general approach which makes no approximations at the outset of any sort - RPA or otherwise).

$$j_k(x,t) = Im[\psi_k^{\dagger}(x,t)\partial_x\psi_k(x,t)] \ ; \ \rho_k(x,t) = \psi_k^{\dagger}(x,t)\psi_k(x,t) \tag{7.7}$$

Current Algebra: The densities and the currents obey current algebra.

$$\begin{aligned}
&[\rho_k(x,t), \rho_l(x^{'},t)] = 0 \\
&[\rho_k(x,t), j_l(x^{'},t)] = i \ \delta_{l,k} \ \rho_l(x^{'},t)\partial_{x^{'}}\delta(x - x^{'}) \\
&[j_k(x,t), j_l(x^{'},t)] = -i \ \delta_{k,l} \ j_l(x^{'},t)\partial_x\delta(x - x^{'}) + i \ \delta_{k,l} \ j_k(x,t)\partial_{x^{'}}\delta(x - x^{'})
\end{aligned} \tag{7.8}$$

Field-Current/Density commutators: The fields and the currents/densities obey the following equal-time commutation rules.

$$\begin{aligned}&[\psi_k(x,t),\rho_l(x^{'},t)] = \delta_{k,l}\ \delta(x-x^{'})\ \psi_k(x,t);\\ &[\psi_k(x,t),j_l(x^{'},t)] = \frac{1}{2i}(\delta_{k,l}\delta(x-x^{'})\ (\partial_{x'}\psi_l(x^{'},t)) - \delta_{k,l}(\partial_{x'}\delta(x-x^{'}))\psi_l(x^{'},t))\end{aligned} \tag{7.9}$$

7.2.1.2 Bose Language

Boson Fields: Define self adjoint $\pi_j(x,t)$ and $\rho_j(x,t)$, $j = 1,2,3,...,N$ obeying canonical commutation rules.

$$.[\rho_j(x,t),\rho_k(x^{'},t)] = 0\ \ ;\ [\pi_j(x,t),\pi_k(x^{'},t)] = 0\ ;\ [\pi_j(x,t),\rho_k(x^{'},t)] = i\delta_{j,k}\ \delta(x-x^{'}) \tag{7.10}$$

Forward relation:

$$j_k(x,t) = -\rho_k(x,t)\partial_x\pi_k(x,t) \tag{7.11}$$

Equation (7.11) together with equation (7.8) implies equation (7.10) provided $\rho_k(x,t)$ does not vanish anywhere since division by this quantity is needed.

Conjecture: Fermi-Bose Correspondence:

$$\psi_k(x,t) = e^{i\pi\sum_{l<k}\int_{-\infty}^{\infty}dy\ \rho_l(y,t)}\frac{1}{\sqrt{N^0}}\sum_p n_F(p)\ e^{i\xi(p)}\ e^{i\pi sgn(p)\int_{sgn(x)\infty}^{x}dy\ \rho_k(y,t)}e^{-i\pi_k(x,t)}\ \sqrt{\rho_k(x,t)} \tag{7.12}$$

where $n_F(p) = \theta(k_F - |p|)$ and $N^0 = \sum_p n_F(p)$. The equation (7.12) inserted into equation (7.7) leads to an identity together with equation (7.11) provided the following identification is made, $e^{i\xi(p)}\ e^{-i\xi(p^{'})} = \delta_{p,p'}$, which can be justified as follows. Imagine, for example, $\xi(p) \neq \xi(p')$ when $p \neq p'$ to be a real quantity that tends to infinity for all p. This means that we can write

$$e^{i\xi(p)} = \lim_{\lambda\to\infty}\ e^{i\lambda\phi(p)}$$

where $\phi(p)$ is a finite function of p. Thus we can also write

$$e^{i\xi(p)}e^{-i\xi(p')} = \lim_{\lambda\to\infty}\ e^{i\lambda(\phi(p)-\phi(p'))} = \lim_{\lambda\to\infty}\ e^{i\lambda\theta}$$

where $\theta = \phi(p) - \phi(p')$ and thus when $p = p'$ then $\theta = 0$. Now we define the following.

$$\text{“ } e^{i\lambda\theta}\text{ ”} = \begin{cases} \frac{1}{\Delta\theta}\int_{\theta-\frac{\Delta\theta}{2}}^{\theta+\frac{\Delta\theta}{2}} e^{i\lambda\theta'}d\theta' & \theta \neq 0 \\ 1 & \theta = 0 \end{cases}$$

Now.

$$\frac{1}{\Delta\theta}\int_{\theta-\frac{\Delta\theta}{2}}^{\theta+\frac{\Delta\theta}{2}} e^{i\lambda\theta'}d\theta' = \frac{1}{i\lambda\Delta\theta}\left(e^{i\lambda(\theta+\frac{\Delta\theta}{2})} - e^{i\lambda(\theta-\frac{\Delta\theta}{2})}\right) = e^{i\lambda\theta}\,\frac{\sin\left(\lambda\frac{\Delta\theta}{2}\right)}{\left(\lambda\frac{\Delta\theta}{2}\right)}$$

Now when we use the limit $\lambda \to \infty$, the numerator is bounded but the denominator diverges and hence for $\theta \neq 0$ (and $\Delta\theta \neq 0$), which implies $p \neq p'$, we have the following.

$$\lim_{\lambda\to\infty} \text{“}e^{i\lambda\theta}\text{”} = 0$$

Hence the assertion that $e^{i\xi(p)}e^{-i\xi(p')} = \delta_{p,p'}$.

Theorem: The conjecture in equation (7.12) obeys fermion commutation rules in equation (7.6) in conjunction with equation (7.10) and $e^{i\xi(p)}\ e^{-i\xi(p^{'})} = \delta_{p,p'}$.

The proof of the above theorem is given in Appendix D. The central NCBT relation between the slow part of the Fermi field and current/densities viz. equation (7.5) may be obtained from the conjecture in equation (7.12) using harmonic analysis of the density operator, which goes as follows.

$$\rho(x,\sigma,t) = \rho_0 + \rho_s(x,\sigma,t) + e^{2ik_Fx}\ \rho_f(x,\sigma,t) + e^{-2ik_Fx}\ \rho_f^*(x,\sigma,t) \tag{7.13}$$

Here ρ_s is the slow part and ρ_f is the oscillating part of the density. According to Haldane's harmonic analysis [4], the fast part can be expressed in terms of the slow part as follows.

$$\rho_f(x,\sigma,t) \sim e^{2i\pi\int_{-\infty}^{x}\rho_s(y,\sigma,t)dy} \tag{7.14}$$

Using Haldane's harmonic analysis in equation (7.13) and inserting to the conjecture in equation (7.12) and extracting the slow part, one can obtain the expression of the field operator used in standard bosonization, given by equation (7.3). On the other hand, NCBT uses a non-standard harmonic analysis which is ideally suited to study systems with a cluster of impurities [90]. Non-standard harmonic analysis means the replacement,

$$\rho_f(x,\sigma,t) \sim e^{2i\pi\int_{-\infty}^{x}(\rho_s(y,\sigma,t)+\lambda\rho_s(-y,\sigma,t))dy} \tag{7.15}$$

Using this non-standard harmonic analysis in equation (7.13) and inserting it to the conjecture in equation (7.12) and extracting the slow part, one can obtain the expression of the field operator used in non chiral bosonization, given by equation (7.5). Note that the variable λ in equation (7.15) can take values only 0 or 1, as also discussed in the last section and the the non-standard harmonic analysis reduces to the standard one when $\lambda = 0$.

Field-Current/Density commutators: Lastly, the identities in equation (7.16) below are obeyed regardless of whether these commutators are evaluated in the usual Fermi language or using the conjecture equation (7.12) and the canonical commutators equation (7.10). However, division by $\rho_k(x)$ should be permissible to prove the same.

$$\begin{aligned}
&[\psi_k(x,t), \rho_l(x^{'},t)] = \delta_{k,l}\ \delta(x-x^{'})\ \psi_k(x,t);\\
&[\psi_k(x,t), j_l(x^{'},t)] = \frac{1}{2i}(\delta_{k,l}\delta(x-x^{'})\ (\partial_{x^{'}}\psi_l(x^{'},t)) - \delta_{k,l}(\partial_{x^{'}}\delta(x-x^{'}))\psi_l(x^{'},t))
\end{aligned} \tag{7.16}$$

It must be stressed that the addition of the extra term $\rho_s(-y,\sigma,t)$ in equation (7.5) of the NCBT scheme does not violate any of the commutation rules above because of the constant '$2\pi i$' in it and the integration of the density is just a natural number. It is also to be noted that there are some additional global quantities that are needed to be incorporated into the C-numbers in equation (7.5) to make sure the up-spin field anti-commutes with the down spin field, the left leg of the ladder anti-commutes with the right leg (in case of a one step fermionic ladder) and so on. They are described in an earlier work [140].

7.2.2 Limiting case checks

Another necessary criterion to be obeyed by the correlation functions are the limiting case checks. For the homogeneous case, there is just one limiting case, viz., switching off mutual interactions between the particles. Under this condition the LL Green functions must reduce to the free particle Green functions. In absence of interactions, the holon velocity becomes equal to the Fermi velocity ($v_h \to v_F$) and thus the Green functions in equation (A.2) takes the form of that of a free particle.

$$\begin{aligned}
\Big\langle T\ \psi_R(x_1,\sigma,t_1)\psi_R^{\dagger}(x_2,\sigma,t_2)\Big\rangle &\sim \frac{1}{(x_1-x_2-v_F(t_1-t_2))}\\
\Big\langle T\ \psi_L(x_1,\sigma,t_1)\psi_L^{\dagger}(x_2,\sigma,t_2)\Big\rangle &\sim \frac{1}{(-x_1+x_2-v_F(t_1-t_2))}
\end{aligned}$$

On the other hand, for the strongly inhomogeneous systems, the Green functions obtained using NCBT can be subjected to various limiting cases as follows.

No interaction. By switching off the inter-particle interactions between particles ($v_0 = 0$), one obtains the Green functions for free fermions plus impurities which can also be obtained using Fermi algebra. In such a case, the holon velocity is equal to the Fermi velocity ($v_h \to v_F$) and equation (B.2) and equation (B.3) will take the form of single particle Green functions of such inhomogeneous systems.

No impurity. In absence of any impurity, there is no reflection ($|R| = 0$) and there is no concept of opposite sides of the origin as it is a homogeneous case. There will be no reflection

terms such as $\langle\psi_R\psi_L^\dagger\rangle$ and $\langle\psi_L\psi_R^\dagger\rangle$ in this case. The only non-zero terms are the transmission propagators $\langle\psi_R\psi_R^\dagger\rangle$ and $\langle\psi_L\psi_L^\dagger\rangle$ whose exponents takes the following form:

$$P = \frac{(v_h + v_F)^2}{8v_h v_F};\ Q = \frac{(v_h - v_F)^2}{8v_h v_F};\ X = \gamma_1 = 0;$$

Using the above, one obtains the precise Green functions of the standard homogeneous Luttinger liquid as given in equation (A.2).

No tunneling. For an infinite barrier ($|R| = 1$), there is no need to consider the two points to be on the opposite sides of the impurity. While the Green functions for points on the same side of the origin as given in equation (B.2) takes the form that of a half line as given in equation (A.7). Also in this case, the full Green function vanishes when one of the points is at the location of the infinite barrier.

Far from impurity. Lastly it can be observed that when both the points are situated far away from the impurity and on the same side of it, then the transmission propagators $\langle\psi_R\psi_R^\dagger\rangle$ and $\langle\psi_L\psi_L^\dagger\rangle$ become immune to the presence of impurities and takes the form of the homogeneous case (equation (A.2)). But the reflection terms viz. $\langle\psi_R\psi_L^\dagger\rangle$ and $\langle\psi_L\psi_R^\dagger\rangle$ continue to be affected by the presence of the impurity since in these cases the region where the impurity is present needs to be traversed (in order for reflection to take place).

7.2.3 Point splitting constraint

It is mandatory that the field operators as in equation (7.3) and equation (7.5) do not violate the point splitting constraints, which is a crucial self-consistency check. Point splitting constraint is the assertion that the NCBT Green functions are consistent with current algebra. The use of the non-local expression for the field gives back the currents and densities which were used to exponentiate the commutation rules and write down the non-local expression in the first place.

$$\begin{aligned}\lim_{a\to 0}\ (\psi_\nu^\dagger(x,\sigma,t)\psi_\nu(x+a,\sigma,t) - <\psi_\nu^\dagger(x,\sigma,t)\psi_\nu(x+a,\sigma,t)>) \\ = \frac{1}{2\nu}(\nu\ \rho_s(x,\sigma,t) - \int_{sgn(x)\infty}^{x} dy^{'}\partial_{v_F t}\rho_s(y^{'},\sigma,t))\end{aligned} \tag{7.17}$$

Here the subscript ν represents a right mover or a left mover and takes values 1 and -1 respectively. It may be seen below that it leads to constraints on the form for the product of the coefficient $C_{\lambda,\nu,\gamma}$ in equation (7.5) and its complex conjugate which is to be regarded as one single object rather than a product of two complex numbers as the non-local expression for the field is merely a mnemonic - not be be taken literally. After some straightforward

algebra which is given briefly below, the following constraints emerge from equation (7.17) (here $C_{\lambda,\nu}(x,\sigma) \equiv \sum_{\gamma=\pm1} \theta(\gamma x) C_{\lambda,\nu,\gamma}(\sigma)$),

$$\lim_{a\to 0} \sum_{\lambda,\lambda^{'}\in\{0,1\}} < C^{\dagger}_{\lambda^{'},\nu}(x,\sigma) C_{\lambda,\nu}(x+a,\sigma) > e^{\frac{1}{2}[Q_\nu(x,\sigma;\lambda^{'}),-Q_\nu(x+a,\sigma;\lambda)]} \times \left(e^{Q_\nu(x,\sigma;\lambda^{'})-Q_\nu(x+a,\sigma;\lambda)} - < e^{Q_\nu(x,\sigma;\lambda^{'})-Q_\nu(x+a,\sigma;\lambda)} > \right) = \frac{1}{2\nu}(\nu\ \rho_s(x,\sigma,t) - \int_{sgn(x)\infty}^{x} dy^{'} \partial_{v_F t} \rho_s(y^{'},\sigma,t))$$

where $Q_\nu(x,\sigma;\lambda^{'}) = -i\theta_\nu(x,\sigma,t) - 2\pi i\nu\lambda^{'} \int_{sgn(x)\infty}^{x} \rho_s(-y,\sigma,t)\ dy$.

When λ and $\lambda^{'}$ are unequal,

$$< C^{\dagger}_{1,\nu}(x,\sigma) C_{0,\nu}(x,\sigma) > \lim_{a\to 0}\ e^{\frac{1}{2}[Q_\nu(x,\sigma;1),-Q_\nu(x+a,\sigma;0)]} = < C^{\dagger}_{0,\nu}(x,\sigma) C_{1,\nu}(x,\sigma) > \lim_{a\to 0}\ e^{\frac{1}{2}[Q_\nu(x,\sigma;0),-Q_\nu(x+a,\sigma;1)]}$$

where $[Q_\nu(x,\sigma;\lambda^{'}), -Q_\nu(x+a,\sigma;\lambda)] = -\pi\ \nu i - 2\pi\nu\lambda i\theta(2x+a) + 2\pi\nu\lambda^{'} i\theta(2x+a)$.

When they are equal however, the following results emerge,

$$\lim_{a\to 0} \sum_{\lambda\in\{0,1\}} < C^{\dagger}_{\lambda,\nu}(x,\sigma) C_{\lambda,\nu}(x+a,\sigma) > e^{\frac{1}{2}(-\pi\ \nu i)}\ (-a)\ \partial_x Q_\nu(x,\sigma;\lambda) = \frac{1}{2\nu}(\nu\ \rho_s(x,\sigma,t) - \int_{sgn(x)\infty}^{x} dy^{'} \partial_{v_F t} \rho_s(y^{'},\sigma,t))$$

Note that $\partial_x Q_\nu(x,\sigma;\lambda) = -i\partial_x\theta_\nu(x,\sigma,t) - 2\pi i\nu\lambda\rho_s(-x,\sigma,t)$ hence,

$$\lim_{a\to 0} \sum_{\lambda\in\{0,1\}} < C^{\dagger}_{\lambda,\nu}(x,\sigma) C_{\lambda,\nu}(x+a,\sigma) > e^{\frac{1}{2}(-\pi\ \nu i)}\ (-a)\ (-2\pi i\nu\lambda\rho_s(-x,\sigma,t)) = 0$$

This means,

$$< C^{\dagger}_{0,\nu}(x,\sigma) C_{0,\nu}(x+a,\sigma) > = \frac{e^{\frac{i}{2}\pi\ \nu}}{2\pi i\nu a}$$

Since $\nu = \pm 1$, hence $e^{\frac{i}{2}\pi\nu} = i\ \nu$ and we can write

$$< C^{\dagger}_{0,\nu}(x,\sigma) C_{0,\nu}(x+a,\sigma) > = \frac{1}{2\pi a}$$

and also,

$$< C^{\dagger}_{1,\nu}(x,\sigma) C_{1,\nu}(x+a,\sigma) >= 0$$

These may be compactly written as follows. Define

$$< C^{\dagger}_{\lambda^{'},\nu^{'}}(x^{'},\sigma^{'}) C_{\lambda,\nu}(x,\sigma) > \to C_2(\lambda^{'},\nu^{'},x^{'},\sigma^{'};\lambda,\nu,x,\sigma)$$

so the final point splitting constraints take the following form,

$$\begin{aligned} C_2(0,\nu,x,\sigma;0,\nu,x+a,\sigma) &= \frac{1}{2\pi a} \\ C_2(1,\nu,x,\sigma;0,\nu,x+a,\sigma) &= C_2(0,\nu,x,\sigma;1,\nu,x+a,\sigma) \\ C_2(1,\nu,x,\sigma;1,\nu,x+a,\sigma) &= 0 \end{aligned} \tag{7.18}$$

This is the reason why, in the evaluation of the two-point function, the possibility of both $\lambda = \lambda^{'} = 1$ was never considered (the corresponding C's are zero). Thus the NCBT formulas for the Green functions obey the point splitting constraints (so does standard bosonization).

7.3 Perturbative comparison

The Green functions of a homogeneous Luttinger liquid obtained using g-ology method (given in Appendix A) can be verified by a comparison with those obtained using standard fermionic perturbation. For this, the Green functions are expanded in powers of the interaction parameter v_0 (see equation (7.2)). Note that the holon velocity v_h is related to the Fermi velocity and the interaction parameter v_0 by the relation $v_h = v_F\sqrt{1+2v_0/(\pi v_F)}$. On the other hand, the zeroth and the first order terms of the perturbation series can be calculated as follows (**Notation:** $X_i \equiv (x_i, \sigma_i, t_i)$).

The two point functions in presence of interactions can be written in terms of the non-interacting ones as follows.

$$\langle T\psi_{\nu_1}(X_1)\psi^{\dagger}_{\nu_2}(X_2)\rangle = \frac{\langle TS\ \psi_{\nu_1}(X_1)\psi^{\dagger}_{\nu_2}(X_2)\rangle_0}{\langle TS\rangle_0} \tag{7.19}$$

Here T represents the time ordering and the action S can be written as follows.

$$S = e^{-i\int H_I(t)dt} = 1 - i\int H_I(t)dt + ... \tag{7.20}$$

Hence the zeroth order term is simply $\langle T\psi_{\nu_1}(X_1)\psi^{\dagger}_{\nu_2}(X_2)\rangle_0$ and the first order perturbation term can be written as follows.

$$\delta\langle T\psi_{\nu_1}(X_1)\psi^{\dagger}_{\nu_2}(X_2)\rangle^1 = -i\int\langle TH_I(t_1)\psi_{\nu_1}(X_1)\psi^{\dagger}_{\nu_2}(X_2)\rangle_0 dt_1 \tag{7.21}$$

From equation (7.1) the interacting part of the Hamiltonian can be written as

$$H_I = \frac{1}{2}\int_{-\infty}^{\infty}dx\int_{-\infty}^{\infty}dx^{'}\ v(x-x^{'})\ \rho(x)\rho(x^{'}) \tag{7.22}$$

Hence the terms in the perturbation series up to the first order can be written as follows.

$$\delta\langle T\psi_{\nu_1}(X_1)\psi^\dagger_{\nu_2}(X_2)\rangle^0 = \langle T\psi_{\nu_1}(X_1)\psi^\dagger_{\nu_2}(X_2)\rangle_0$$
$$\delta\langle T\psi_{\nu_1}(X_1)\psi^\dagger_{\nu_2}(X_2)\rangle^1 = -\frac{i}{2}\int d\tau \int dy \int dy' \; v(y-y')\langle T\; \rho_s(y,\tau_+)\rho_s(y',\tau)\psi_{\nu_1}(X_1)\psi^\dagger_{\nu_2}(X_2)\rangle_0 \tag{7.23}$$

Here $v(y-y') = v_0\delta(y-y')$ is the short ranged mutual interaction term, the ν's represent either a right mover ($\nu_i = 1$) or a left mover ($\nu_i = -1$) and $\rho_s = \psi^\dagger_R\psi_R + \psi^\dagger_L\psi_L$ is the slow part of the density function. The symbol $\langle..\rangle_0$ on the RHS indicates single particle functions. Using equation (7.23), the Green functions of a homogeneous LL up to the first order in interaction parameter can be obtained as follows:

$$G_{RR}(x_1,x_2,t_1-t_2) = \frac{i}{2\pi}\frac{1}{(x_1-x_2)-v_F(t_1-t_2)} + \frac{i(t_1-t_2)}{4\pi^2((x_1-x_2)-v_F(t_1-t_2))^2}v_0$$

This is precisely the same as that obtained by expanding equation (A.2) obtained using standard bosonization in powers of v_0 and keeping up to the first order.

The Green functions obtained from NCBT technique (given in Appendix B) are claimed to be the most singular part of the full Green function [90]. Similar to the case above, the Green functions of strongly inhomogeneous systems (with reflection amplitude R and transmission amplitude T) are calculated perturbatively using equation (7.23), while treating the source of inhomogeneities exactly. After retaining the most singular terms in the first order (the zeroth order is a single term), the following results are obtained (the **R** and **T** on the RHS are reflection and transmission amplitudes respectively).

G_{RR} : $x_1, x_2 > 0$

$$G_{RR}(x_1,x_2,t_1-t_2) = \frac{i}{2\pi}\frac{1}{(x_1-x_2)-v_F(t_1-t_2)} + \frac{i(t_1-t_2)}{4\pi^2((x_1-x_2)-v_F(t_1-t_2))^2}v_0$$

G_{RL} : $x_1, x_2 > 0$

$$G_{RL}(x_1,x_2,t_1-t_2) = \frac{i\mathbf{R}}{2\pi}\frac{1}{(x_1+x_2)-v_F(t_1-t_2)} + \frac{i\mathbf{R}(t_1-t_2)}{4\pi^2((x_1+x_2)-v_F(t_1-t_2))^2}v_0$$

G_{RR} : $x_1 > 0, x_2 < 0$

$$G_{RR}(x_1,x_2,t_1-t_2) = \frac{i\mathbf{T}}{2\pi}\frac{1}{(x_1-x_2)-v_F(t_1-t_2)} + \frac{i\mathbf{T}(t_1-t_2)}{4\pi^2((x_1-x_2)-v_F(t_1-t_2))^2}v_0$$

These are precisely the same as those obtained by expanding equation (B.2) and equation (B.3) obtained using NCBT in powers of v_0 and retaining up to the first order and also discarding the less singular terms at this order. The notion of "the most singular part" of an expression may be made sense of in the following manner. Think of these as function of the time difference $\tau = t - t'$ (which they are). In the formulas that are encountered while

expanding in powers of the coupling, there are going to be terms of the form (e.g.)

$$\frac{A\ \tau}{(\tau - a)^2} + \frac{B}{(\tau - a_1)(\tau - a_2)}$$

The first term is regarded as more singular than the second (if $a_1 \neq a_2$) since the former is a second order pole whereas the latter when partial fraction expanded are a sum of two first order poles. In the perturbative expansion of the single-particle Green function, pretending that Wick's theorem applies at the level of the density fluctuations is tantamount to retaining second order poles and discarding poles of a lower order.

7.4 Schwinger-Dyson equation

The Schwinger-Dyson equation relates the two-point Green functions to certain four-point functions as follows:

$$\begin{aligned} G^{full}_{\nu,\nu'}(x,x';t-t') = G^{0}_{\nu,\nu'}(x,x';t-t') - i\sum_{\nu_1}\int dx_1 \int dt_1\ G^{0}_{\nu,\nu_1}(x,x_1;t-t_1) \\ \times \int dy\ v(x_1-y) < T\ \rho(y,t_1)\psi_{\nu_1}(x_1,\sigma,t_1)\psi^{\dagger}_{\nu'}(x',\sigma,t') >_{full} \end{aligned} \tag{7.24}$$

where $\rho(y,t_1) = \rho(y,\uparrow,t_1) + \rho(y,\downarrow,t_1)$ is the total density (sum of up spin and down spin density) and $v(y-y')$ is the mutual interaction. After operating the equation by $(i\partial_t + i\nu v_F\partial_x)$ and $(-i\partial_{t'} - i\nu' v_F\partial_{x'})$ we get (only for $x, x' \neq 0$ and $x \neq \pm x'$ and $t \neq t'$)

$$\begin{aligned} (i\partial_t + i\nu v_F\partial_x)G^{full}_{\nu,\nu'}(x,x';t-t') &= \int dy\ v(x-y)\ \ < T\ \rho(y,t)\psi_{\nu}(x,\sigma,t)\psi^{\dagger}_{\nu'}(x',\sigma,t') >_{full} \\ (-i\partial_{t'} - i\nu' v_F\partial_{x'})G^{full}_{\nu,\nu'}(x,x';t-t') &= \int dy\ v(x'-y)\ \ < T\rho(y,t')\psi_{\nu}(x,\sigma,t)\psi^{\dagger}_{\nu'}(x',\sigma,t') >_{full} \end{aligned} \tag{7.25}$$

The next task is to examine whether the Green functions obtained using g-ology and those obtained using NCBT obey the above set of equations.

7.4.1 Homogeneous case

The Green functions for homogeneous LL can be calculated using the standard bosonization technique (equation (7.3)) where the local phase is given by equation (7.4) as follows.

$$\theta_{\nu}(x,\sigma,t) = \pi \int_{sgn(x)\infty}^{x} dy\ \left(\nu\ \rho_s(y,\sigma,t) - \int_{sgn(y)\infty}^{y} dy'\ \partial_{v_F t}\ \rho_s(y,\sigma,t)\right) \tag{7.26}$$

Using standard bosonization one can write

$$\psi_\nu(x,\sigma,t) \rightarrow e^{i\theta_\nu(x,\sigma,t)} \quad ; \quad \psi_{\nu'}(x',\sigma,t') \rightarrow e^{i\theta_{\nu'}(x',\sigma,t')} \tag{7.27}$$

Now,

$$\lim_{\epsilon\to 0} \frac{e^{\epsilon\rho}-1}{\epsilon} = \rho.$$

Hence the four point function in equation (7.25) can be written as

$$\begin{aligned} <\rho(y,t)\ \psi_\nu(x,\sigma,t)\ \psi^\dagger_{\nu'}(x',\sigma,t')> &= \lim_{\epsilon\to 0} < \frac{e^{\epsilon\rho(y,t)}-1}{\epsilon}\ e^{i\theta_\nu(x,\sigma,t)}\ e^{-i\theta_{\nu'}(x',\sigma,t')} > \\ &= \lim_{\epsilon\to 0} \frac{1}{\epsilon} < e^{\epsilon\rho(y,t)}\ e^{i\theta_\nu(x,\sigma,t)}\ e^{-i\theta_{\nu'}(x',\sigma,t')} - e^{i\theta_\nu(x,\sigma,t)}\ e^{-i\theta_{\nu'}(x',\sigma,t')} > \end{aligned}$$

Choose,

$$\mathcal{A} = \ \epsilon\rho(y,t)\ ;\ \mathcal{B} = i\theta_\nu(x,\sigma,t)\ ;\ \mathcal{C} = -i\theta_{\nu'}(x',\sigma,t')$$

Using Baker-Campbell-Hausdorff formula,

$$< e^{\mathcal{A}} e^{\mathcal{B}} e^{\mathcal{C}} > = e^{\frac{1}{2}\mathcal{A}^2} e^{\frac{1}{2}\mathcal{B}^2} e^{\frac{1}{2}\mathcal{C}^2} e^{<\mathcal{A}\mathcal{B}>} e^{<\mathcal{B}\mathcal{C}>} e^{<\mathcal{A}\mathcal{C}>}$$

Now $e^{\frac{1}{2}\mathcal{B}^2} e^{\frac{1}{2}\mathcal{C}^2} e^{<\mathcal{B}\mathcal{C}>}$ is the Green functions $<\psi_\nu(x,\sigma,t)\ \psi^\dagger_{\nu'}(x',\sigma,t')>$ and $e^{\frac{1}{2}\mathcal{A}^2}$ can be ignored as ϵ is tending to zero. Hence we can write,

$$\begin{aligned} &<\rho(y,t)\ \psi_\nu(x,\sigma,t)\ \psi^\dagger_{\nu'}(x',\sigma,t')> \\ &\quad = \lim_{\epsilon\to 0}\left[e^{<i\epsilon\rho(y,t)\ \theta_\nu(x,\sigma,t)>}\ e^{<-i\epsilon\rho(y,t)\ \theta_{\nu'}(x',\sigma,t')>} - 1\right] \frac{<\psi_\nu(x,\sigma,t)\ \psi^\dagger_{\nu'}(x',\sigma,t')>}{\epsilon} \\ &\quad = \lim_{\epsilon\to 0}\Big[1 + <i\ \epsilon\ \rho(y,t)\theta_\nu(x,\sigma,t)> - <i\ \epsilon\ \rho(y,t)\theta_{\nu'}(x',\sigma,t')> - 1\Big] \\ &\qquad\qquad \times \frac{<\psi_\nu(x,\sigma,t)\ \psi^\dagger_{\nu'}(x',\sigma,t')>}{\epsilon} \\ &\quad = \Big[<i\ \rho(y,t)\theta_\nu(x,\sigma,t)> - <i\ \rho(y,t)\theta_{\nu'}(x',\sigma,t')>\Big] <\psi_\nu(x,\sigma,t)\ \psi^\dagger_{\nu'}(x',\sigma,t')> \end{aligned}$$

Using equation (7.26),

$$\begin{aligned} &<\rho(y,t)\ \psi_\nu(x,\sigma,t)\ \psi^\dagger_{\nu'}(x',\sigma,t')> \\ &= \Big(<i\pi\nu \int_{sgn(x)\infty}^{x} dz\ \rho_h(y,t)\rho_h(z,t) - i\pi \int_{sgn(x)\infty}^{x} dz\ \partial_{v_F t} \int_{sgn(y)\infty}^{z} \rho_h(y,t)\rho_h(z',t)dz' > \\ &- <i\pi\nu' \int_{sgn(x')\infty}^{x'} dz\ \rho_h(y,t)\rho_h(z,t') - i\pi \int_{sgn(x')\infty}^{x'} dz\ \partial_{v_F t'} \int_{sgn(y)\infty}^{z} \rho_h(y,t)\rho_h(z',t')dz' > \Big) \\ &\quad <\psi_\nu(x,\sigma,t)\ \psi^\dagger_{\nu'}(x',\sigma,t')> \end{aligned}$$

Using the density density correlation functions from equation (A.5), the following form of the Schwinger Dyson equation is obtained.

$$(i\partial_t + iv_F\partial_x) < T\ \psi_R(x,\sigma,t)\psi_R^\dagger(x',\sigma,t') > \\ = v_0\frac{i}{4\pi v_h^2}\left(\frac{v_h(v_h-v_F)}{-v_h(t-t')-x+x'} - \frac{v_h(v_F+v_h)}{v_h(t-t')-x+x'}\right) < T\ \psi_R(x,\sigma,t)\psi_R^\dagger(x',\sigma,t') > \tag{7.28}$$

Substituting the two point function from equation (A.2),

$$-i\left(\frac{P(v_h-v_F)}{v_h(t-t')-x+x'} + \frac{Q(v_F+v_h)}{v_h(t-t')+x-x'}\right) \\ = v_0\frac{i}{4\pi v_h^2}\left(\frac{v_h(v_h-v_F)}{-v_h(t-t')-x+x'} - \frac{v_h(v_F+v_h)}{v_h(t-t')-x+x'}\right)$$

Upon inserting the explicit expressions of the anomalous exponents from Eq (A.3) into the above equation, one obtains an identity. Thus the correlation functions obtained by g-ology methods satisfy the exact Schwinger Dyson equation, which is a non-perturbative validation of the same.

7.4.2 Inhomogeneous case

The Green functions of a Luttinger liquid with a cluster of impurities around a point can be calculated using the powerful Non chiral bosonization technique (equation (7.5)) where the familiar local phase undergoes modification and is given by the following ($\lambda = 0, 1$).

$$\Theta_\nu(x,\sigma,t,\lambda) = \pi\int_{sgn(x)\infty}^{x} dy\ \left(\nu\ \rho_s(y,\sigma,t) - \int_{sgn(y)\infty}^{y} dy'\ \partial_{v_F t}\ \rho_s(y,\sigma,t)\right) \\ + 2\pi\nu\lambda\int_{sgn(x)\infty}^{x} dy\ \rho(-y,\sigma,t) \tag{7.29}$$

Similar to the homogeneous case, the four point functions on the RHS of equation (7.25) can be derived as follows.

$$< \rho(y,t)\ \psi_\nu(x,\sigma,t)\ \psi_{\nu'}^\dagger(x',\sigma,t') > = \Bigg(< i\pi\nu\ \int_{sgn(x)\infty}^{x} dz\ \rho_h(y,t)\rho_h(z,t) \\ - i\pi\ \int_{sgn(x)\infty}^{x} dz\ \partial_{v_F t}\int_{sgn(y)\infty}^{z}\rho_h(y,t)\rho_h(z',t)dz'\ + 2\nu\lambda\int_{sgn(x)\infty}^{x} dz\ \rho_h(y,t)\rho_h(-z,t) > \\ - < i\pi\nu'\ \int_{sgn(x')\infty}^{x'} dz\ \rho_h(y,t)\rho_h(z,t') - i\pi\ \int_{sgn(x')\infty}^{x'} dz\ \partial_{v_F t'}\int_{sgn(y)\infty}^{z}\rho_h(y,t)\rho_h(z',t')dz' \\ + 2\nu'\lambda'\int_{sgn(x')\infty}^{x'} dz\ \rho_h(y,t)\rho_h(-z,t') > \Bigg) < \psi_\nu(x,\sigma,t)\ \psi_{\nu'}^\dagger(x',\sigma,t') >$$

Using the density density correlation functions from equation (B.7) and then inserting the above four point function into the RHS of equation (7.25), the necessary Schwinger Dyson

equations are obtained. We take into account three cases, viz. RR same side (of the origin), RL same side and RR opposite sides. The remaining three cases: LL same side, LR same side and LL opposite sides are very similar to the former three cases respectively. The choice of λ, λ' is discussed in an earlier work [90] and also explicitly given in Table 7.1 for the cases discussed.

TABLE 7.1: Choice of λ, λ' for different cases of Green functions.

Green's function part	λ	λ'
RR sameside	0	0
RL_1 sameside	1	0
RL_2 sameside	0	1
RR_1 oppositesides	1	0
RR_2 oppositesides	0	1

7.4.2.1 RR same side

Equation of motion: (here $Z_h = \frac{v_h|R|^2}{v_h - |R|^2(v_h - v_F)}$)

$$\begin{aligned}(i\partial_t + iv_F\partial_x) < T\ \psi_R(x,\sigma,t)\psi_R^\dagger(x',\sigma,t') > \\ = v_0 \frac{i}{4\pi v_h^2}\ (-\frac{2v_F Z_h\left(v_F(x+x') + v_h^2(t'-t)\right)}{(x+x'+v_h(t-t'))(x+x'+v_h(t'-t))} + \frac{v_h(v_h-v_F)}{-v_h(t-t')-x+x'} \\ - \frac{v_h(v_F+v_h)}{v_h(t-t')-x+x'} + \frac{v_F^2 Z_h}{x})\ < T\ \psi_R(x,\sigma,t)\psi_R^\dagger(x',\sigma,t') >\end{aligned} \tag{7.30}$$

Substituting the two point function from equation (B.2),

$$\begin{aligned}-i\left(\frac{P(v_h-v_F)}{v_h(t-t')-x+x'} + \frac{Q(v_F+v_h)}{v_h(t-t')+x-x'} + \frac{X(v_F-v_h)}{-v_h(t-t')+x+x'} + \frac{X(v_F+v_h)}{v_h(t-t')+x+x'} - \frac{\gamma_1 v_F}{x}\right) \\ = v_0 \frac{i}{4\pi v_h^2}\ (-\frac{2v_F Z_h\left(v_F(x+x') + v_h^2(t'-t)\right)}{(x+x'+v_h(t-t'))(x+x'+v_h(t'-t))} + \frac{v_h(v_h-v_F)}{-v_h(t-t')-x+x'} \\ - \frac{v_h(v_F+v_h)}{v_h(t-t')-x+x'} + \frac{v_F^2 Z_h}{x})\end{aligned}$$

Upon inserting the explicit expressions of the anomalous exponents from equations (B.4) and (B.5) into the above equation, one obtains an identity.

7.4.2.2 RL same side

Now for this case we have,

$$< T\ \psi_R(x,\sigma,t)\psi_L^\dagger(x',\sigma,t') > = < T\ \psi_R(x,\sigma,t)\psi_L^\dagger(x',\sigma,t') >_1 + < T\ \psi_R(x,\sigma,t)\psi_L^\dagger(x',\sigma,t') >_2$$

Equations of motion are:

$$
\begin{aligned}
&(-i\partial_{t'}+iv_F\partial_{x'}) < T\ \psi_R(x,\sigma,t)\psi_L^\dagger(x',\sigma,t') >_1 \\
&\quad = v_0\Big(-\frac{iv_F Z_h\left(-v_F(x'+x)-v_h^2(t'-t)\right)}{2\pi v_h^2(-x-x'+v_h(t-t'))(x+x'+v_h(t-t'))}+\frac{iv_F}{2\pi v_h(-v_h(t-t')+x+x')} \\
&\qquad +\frac{iv_F}{2\pi v_h(v_h(t-t')+x+x')}-\frac{i(v_h-v_F)}{4\pi v_h(v_h(t-t')+x-x')} \\
&\qquad -\frac{i(v_h+v_F)}{4\pi v_h(v_h(t-t')-x+x')}+\frac{iv_F^2Z_h}{4\pi v_h^2x'}\Big)\ < T\ \psi_R(x,\sigma,t)\psi_L^\dagger(x',\sigma,t') >_1
\end{aligned}
\tag{7.31}
$$

and

$$
\begin{aligned}
&(i\partial_{t}+iv_F\partial_{x}) < T\ \psi_R(x,\sigma,t)\psi_L^\dagger(x',\sigma,t') >_2 \\
&\quad = v_0\Big(\frac{iv_F Z_h\left(v_F(x'+x)+v_h^2(t'-t)\right)}{2\pi v_h^2(-x-x'+v_h(t-t'))(x+x'+v_h(t-t'))}+\frac{iv_F}{2\pi v_h(v_h(t-t')+x+x')} \\
&\qquad +\frac{iv_F}{2\pi v_h(v_h(t'-t)+x+x')}-\frac{i(v_F+v_h)}{4\pi v_h(v_h(t-t')+x-x')} \\
&\qquad -\frac{i(v_h-v_F)}{4\pi v_h(v_h(t-t')-x+x')}+\frac{iv_F^2Z_h}{4\pi v_h^2x}\Big)\ < T\ \psi_R(x,\sigma,t)\psi_L^\dagger(x',\sigma,t') >_2
\end{aligned}
\tag{7.32}
$$

Substituting the two point functions from equation (B.2),

$$
\begin{aligned}
&i\Big(\frac{-S(v_F+v_h)}{v_h(t-t')-x+x'}+\frac{S(v_F-v_h)}{v_h(t-t')+x-x'}-\frac{Y(v_F-v_h)}{-v_h(t-t')+x+x'}-\frac{Z(v_F+v_h)}{v_h(t-t')+x+x'}+\frac{\gamma_1 v_F}{x'}\Big) \\
&= v_0\Big(-\frac{iv_F Z_h\left(-v_F(x'+x)-v_h^2(t'-t)\right)}{2\pi v_h^2(-x-x'+v_h(t-t'))(x+x'+v_h(t-t'))}+\frac{iv_F^2Z_h}{4\pi v_h^2x'}+\frac{iv_F}{2\pi v_h(-v_h(t-t')+x+x')} \\
&+\frac{iv_F}{2\pi v_h(v_h(t-t')+x+x')}-\frac{i(v_h-v_F)}{4\pi v_h(v_h(t-t')+x-x')}-\frac{i(v_h+v_F)}{4\pi v_h(v_h(t-t')-x+x')}\Big)
\end{aligned}
$$

$$
\begin{aligned}
&i\Big(\frac{S(v_F-v_h)}{v_h(t-t')-x+x'}+\frac{S(v_F+v_h)}{-v_h(t-t')-x+x'}-\frac{Y(v_F-v_h)}{-v_h(t-t')+x+x'}-\frac{Z(v_F+v_h)}{v_h(t-t')+x+x'}+\frac{\gamma_1 v_F}{x}\Big) \\
&= v_0\Big(\frac{iv_F Z_h\left(v_F(x'+x)+v_h^2(t'-t)\right)}{2\pi v_h^2(-x-x'+v_h(t-t'))(x+x'+v_h(t-t'))}+\frac{iv_F^2Z_h}{4\pi v_h^2x}+\frac{iv_F}{2\pi v_h(v_h(t-t')+x+x')} \\
&+\frac{iv_F}{2\pi v_h(v_h(t'-t)+x+x')}-\frac{i(v_F+v_h)}{4\pi v_h(v_h(t-t')+x-x')}-\frac{i(v_h-v_F)}{4\pi v_h(v_h(t-t')-x+x')}\Big)
\end{aligned}
$$

Upon inserting the explicit expressions of the anomalous exponents from equations (B.4) and (B.5), both the above equations are satisfied.

7.4.2.3 RR opposite side

Now for this case we again have,

$$
< T\ \psi_R(x,\sigma,t)\psi_R^\dagger(x',\sigma,t') >=< T\ \psi_R(x,\sigma,t)\psi_R^\dagger(x',\sigma,t') >_1 + < T\ \psi_R(x,\sigma,t)\psi_R^\dagger(x',\sigma,t') >_2
$$

Equations of motion are:

$$
\begin{aligned}
&(-i\partial_{t'} - iv_F\partial_{x'}) < T\ \psi_R(x,\sigma,t)\psi_R^\dagger(x',\sigma,t') >_1 \\
&\quad = v_0\Big(\frac{iv_F Z_h\left(v_F(x-x') - v_h^2(t-t')\right)}{2\pi v_h^2(-x+x'+v_h(t-t'))(-x+x'+v_h(t'-t))} - \frac{i(v_h-v_F)}{4\pi v_h(v_h(t-t')+x-x')} \\
&\qquad - \frac{i(v_F+v_h)}{4\pi v_h(v_h(t-t')-x+x')} + \frac{iv_F}{2\pi v_h(-v_h(t'-t)+x+x')} \\
&\qquad + \frac{iv_F}{2\pi v_h(v_h(t'-t)+x+x')} - \frac{iv_F^2 Z_h}{4\pi v_h^2 x'}\Big) < T\ \psi_R(x,\sigma,t)\psi_R^\dagger(x',\sigma,t') >_1
\end{aligned}
\tag{7.33}
$$

and

$$
\begin{aligned}
&(i\partial_t + iv_F\partial_x) < T\ \psi_R(x,\sigma,t)\psi_R^\dagger(x',\sigma,t') >_2 \\
&\quad = v_0\Big(-\frac{iv_F Z_h\left(v_F(x-x') - v_h^2(t-t')\right)}{2\pi v_h^2(-x+x'+v_h(t-t'))(x-x'+v_h(t-t'))} - \frac{iv_F}{2\pi v_h(-v_h(t-t')+x+x')} \\
&\qquad - \frac{iv_F}{2\pi v_h(v_h(t-t')+x+x')} - \frac{i(v_h-v_F)}{4\pi v_h(v_h(t-t')+x-x')} \\
&\qquad - \frac{i(v_F+v_h)}{4\pi v_h(v_h(t-t')-x+x')} + \frac{iv_F^2 Z_h}{4\pi v_h^2 x}\Big) < T\ \psi_R(x,\sigma,t)\psi_R^\dagger(x',\sigma,t') >_2
\end{aligned}
\tag{7.34}
$$

Substituting the two point functions from equation (B.3),

$$
\begin{aligned}
&i\Big(\frac{A(v_F-v_h)}{v_h(t-t')-x+x'} + \frac{B(v_F+v_h)}{-v_h(t-t')-x+x'} + \frac{C(v_F+v_h)}{-v_h(t-t')+x+x'} + \frac{D(v_F-v_h)}{v_h(t-t')+x+x'} - \frac{\gamma_1 v_F}{x'}\Big) \\
&= v_0\Big(\frac{iv_F Z_h\left(v_F(x-x') - v_h^2(t-t')\right)}{2\pi v_h^2(-x+x'+v_h(t-t'))(-x+x'+v_h(t'-t))} - \frac{iv_F^2 Z_h}{4\pi v_h^2 x'} - \frac{i(v_h-v_F)}{4\pi v_h(v_h(t-t')+x-x')} \\
&- \frac{i(v_F+v_h)}{4\pi v_h(v_h(t-t')-x+x')} + \frac{iv_F}{2\pi v_h(-v_h(t'-t)+x+x')} + \frac{iv_F}{2\pi v_h(v_h(t'-t)+x+x')}\Big)
\end{aligned}
$$

$$
\begin{aligned}
&i\Big(\frac{A(v_F-v_h)}{v_h(t-t')-x+x'} + \frac{B(v_F+v_h)}{-v_h(t-t')-x+x'} - \frac{C(v_F+v_h)}{v_h(t-t')+x+x'} - \frac{D(v_F-v_h)}{-v_h(t-t')+x+x'} + \frac{\gamma_1 v_F}{x}\Big) \\
&= v_0\Big(-\frac{iv_F Z_h\left(v_F(x-x') - v_h^2(t-t')\right)}{2\pi v_h^2(-x+x'+v_h(t-t'))(x-x'+v_h(t-t'))} + \frac{iv_F^2 Z_h}{4\pi v_h^2 x} - \frac{iv_F}{2\pi v_h(-v_h(t-t')+x+x')} \\
&- \frac{iv_F}{2\pi v_h(v_h(t-t')+x+x')} - \frac{i(v_h-v_F)}{4\pi v_h(v_h(t-t')+x-x')} - \frac{i(v_F+v_h)}{4\pi v_h(v_h(t-t')-x+x')}\Big)
\end{aligned}
$$

Upon inserting the explicit expressions of the anomalous exponents from equations (B.4) and (B.5), both the above equations are satisfied. Note that the term $(\frac{1}{x+x'})$ in RR opposite sides (equation (B.3)) belongs to the pre-factors which are treated as constants in both sides of the Dyson equation. This is tantamount to the assertion that prefactors are not correctly given by bosonization - only the exponents are. The prefactors in the present context are spatially dependent and have been adjusted to recover certain limiting behavior - they are to be ignored while one is examining the crucially important Luttinger exponents. A more convincing way of saying this is - one only looks to equate the time derivative of the logarithms of the two sides of the Schwinger-Dyson equations which forces these prefactors to drop out.

There is one puzzling feature of the arguments that has been presented till now that requires clarification. Instead of verifying the Schwinger-Dyson equation (SDE) for the Green function (for RR opposite sides and RL same side) as a whole, we have first written the latter as a sum of two pieces labeled as $< ... >_1$ and $< ... >_2$ and verified the SDE that involves (x,t) derivatives for the piece labeled $< .... >_2$ and verified the SDE that involves (x',t') derivatives for the piece labeled $< .... >_1$. This is the same as asserting that the (x,t) operator (i.e. $i\partial_t + i\nu v_F \partial_x$) acting on $e^{i\theta_\nu(x,t)}$ behaves as expected but not when it is acting on $e^{i\theta_\nu(x,t)+2\pi i\nu \int^x \rho(-y,t)\ dy}$. That is, anomalous extensions of the bosonized fields, mandatory for strongly inhomogeneous systems such as the ones being studied here, do not obey the free field equations. Note that while equating two sides of these equations, the left hand side is purely a power law but for RR opposite sides and RL same side the right hand side has a term of the same functional form as the left hand side plus a term which has a similar but not identical functional form. At the very least we may expect that the two terms whose functional forms match exactly should be equal to each other. It is remarkable that this is indeed the case. Note that for RR and LL same side, the two sides match perfectly without any need for further qualifications. This is important for example to reproduce the dynamical density of states close to the impurity.

It is amply clear and quite remarkable that the explicit formulas for the exponents of the most singular part of the asymptotic Green function of a Luttinger liquid in presence of barriers and wells clustered around an origin as predicted by the non-chiral bosonization method is consistent with the exact Schwinger-Dyson equation of motion for the Green functions. Not only that, the Green functions of NCBT obey the Schwinger-Dyson equation if and only if the anomalous exponents have the precise analytical forms given in equations (B.4) and (B.5). This is a clear vindication of the non-standard harmonic analysis of the density fields and a non-perturbative validation of the NCBT.

7.5 Functional bosonization

In functional bosonization [30, 158], one imagines a slowly varying time dependent external potential of the form $\sum_{q,n} e^{-iqx} e^{-w_n t} u(q,w_n)$ to be present along with the cluster of barriers and wells. When $u(q,w_n) \equiv 0$ and mutual interaction between fermions are absent, the averages are denoted by $< .... >_{SCh}$. It may be shown that the Green function of the system (denoted by $< T\ \psi_\nu(x,t)\psi^\dagger_{\nu'}(x',t') >_{full}$) with barriers and wells and including mutual interaction between fermions but without u , i.e. $u(q,w_n) \equiv 0$ may be obtained by first obtaining the Green function with barriers and wells including u but without mutual interaction between fermions (denoted by $< T\ \psi_\nu(x,t)\psi^\dagger_{\nu'}(x',t') >$) and averaging this Green function over u with a weight $W[u]$ as given below,

$$< T\ \psi_\nu(x,t)\psi^\dagger_{\nu'}(x',t') >_{full} = \int D[u]\ W[u]\ \ < T\ \psi_\nu(x,t)\psi^\dagger_{\nu'}(x',t') > \qquad (7.35)$$

where the weight is,

$$W[u] \equiv \frac{e^{\frac{\beta}{2L}\sum_{q,m}\frac{u(q,w_m)u(-q,-w_m)}{v_q}} < TS_U >_{SCh}}{\int D[u]\; e^{\frac{\beta}{2L}\sum_{q,m}\frac{u(q,w_m)u(-q,-w_m)}{v_q}} < TS_U >_{SCh}} \tag{7.36}$$

and,

$$< TS_U >_{SCh} = < e^{-\frac{\beta}{L}\sum_{q,m} u(q,w_m)\rho_{q,m}} >_{SCh} \tag{7.37}$$

The nonequilibrium free particle Green function may be related to the equilibrium free particle Green function through the following relation,

$$< T\; \psi_\nu(x,t)\psi^\dagger_{\nu'}(x',t') > = \frac{< TS_U\; \psi_\nu(x,t)\psi^\dagger_{\nu'}(x',t') >_{SCh}}{< TS_U >_{SCh}} \tag{7.38}$$

This method, like the g-ology methods works well for systems with translational symmetry and can be used to obtain the Green functions of such systems given in equation (A.2). But when applied to systems with impurities, they gives rise to some anomalous terms of the type $\log\left[\left(\frac{x}{v_h} - \frac{x'}{v_F} - (t-t')\right)\right]$ not seen either in conventional perturbation theory nor in the Schwinger Dyson equation. Therefore Green functions obtained are inconsistent with perturbation theory which makes the study of functional bosonization not suitable for strongly inhomogeneous systems.

7.6 Density matrix renormalization group (DMRG)

Density matrix renormalization has been the method of choice for the numerical studies in 1D systems. When it comes to calculation of the correlation functions, there are some fundamental differences owing to the energy band structures of the systems. For gapped systems, the correlation functions decay exponentially with the distance while correlation functions of gapless models decay algebraically with distance [76]. DMRG is used to optimize the ansatz wavefunctions called as Matrix Product States (MPS) and thus obtaining the correlation functions. But matrix product states are proven useful only for describing the ground states of gapped local Hamiltonians [77–79]. Every ground state of a gapped Hamiltonian in 1D can be approximated by a tensor network state to arbitrary precision [80]. But M. Andersson et al. investigated the convergence of DMRG for gapless systems in thermodynamic limit [81]. They concluded that when DMRG is used to study a gapless systems of free fermions it gives the wrong particle-hole and density density correlation functions. The expected correlation functions must decay algebraically but the ones obtained from DMRG decay exponentially.

The difficulty in studying gapless systems using DMRG is that convergence is tough to achieve. Some remedies such as increasing the number of DMRG sweeps, working with finite sized systems are adopted to mitigate the problems. However even if such problems are taken care of, it is less likely that such numerical methods can capture the most singular part of the Green

functions which NCBT claims to provide. Nevertheless, it will be a challenging problem for researchers working in the field of DMRG and other numerical techniques to verify the results of NCBT, which are already validated analytically using the Schwinger Dyson equation.

7.7 Summary

In this chapter, the correlation functions obtained using standard bosonization (g-ology) techniques for homogeneous systems as well as those obtained using the recently developed non-chiral bosonization technique (NCBT) for strongly inhomogeneous systems are validated. Firstly, it has been shown that the correlation functions obey the necessary requirements like current algebra, limiting cases and point splitting constraints. Secondly, a favorable comparison with the results of standard fermionic perturbation is shown. Thirdly, the Green functions are inserted into the Schwinger-Dyson equation which is the equation of motion of the Green functions resulting in an identity. This serves as a non-perturbative confirmation of these ideas. Lastly, we have discussed that competing analytical approaches such as functional bosonization and numerical ones such as DMRG etc. are not suitable for reproducing the correlation functions obtained easily by NCBT.

Chapter 8

Conclusions

The study of strongly correlated electrons in one dimension fascinates condensed matter physicists due to the unusual nature of the mutual interactions. Well established theories like the Fermi liquid theory or perturbative techniques fails to explain the interactions in such systems where the excitations are of collective nature. The first soluble model in this regard was proposed by Tomonaga [1] who expressed a fermionic Hamiltonian in terms of bosonic operators using the assumption that particle hole excitations in 1D are bosonic in nature. Later, Luttinger [2] proposed a similar model where he assumed two types of fermions (one having energy spectrum $\epsilon = kv_F$ and the other $\epsilon = -kv_F$: linear dispersion relations) and each type being infinite in number. The key idea of these models is that interaction Hamiltonian which is quartic in terms of fermionic operators becomes quadratic in terms of bosonic operators and hence trivial to diagonalize. Mattis and Lieb [3] provided an exact solution to this model after which substantial progress has been made in understanding the properties of the 1D electron systems in the works of Dzyaloshinkii, Larkin, Efetov, etc. [23, 26] and later Haldane in his famous work [4] developed the fundamentals of modern bosonization. In the mean time, with the progress of nano-technology, physical realization of 1D systems was made possible and prominent examples in this regard were carbon nanotubes, semiconducting quantum wire, ultra cold atoms and so on which have fantastic properties. Hence the study of interactions in 1D systems became important both from the theoretical and technological point of view.

The field theoretical approach to bosonization, also known as g-ology, has been widely adopted as it was able to provide explicit expressions for the N-point functions of a homogeneous Luttinger liquid [4] in presence of forward scattering interactions. However, this method fails when the translational symmetry is broken by an impurity and has to rely on other methods like renormalization group, etc. [9, 90], yet are unable to provide closed analytical expressions of the Green functions of such systems. On the other hand, the study of impurities in a quantum system constitutes a major theme in many body physics, and 1D system is no exception [31]. Hence the present work introduces and promulgates a new way of doing

bosonization, which overcomes the shortcomings of the conventional bosonization techniques and is ideally suited to study strongly inhomogeneous systems. This approach, which goes by the name "Non Chiral Bosonization technique (NCBT)", has been successfully applied to yield the most singular part of the Green functions of different categories of systems like a cluster of impurities around an origin [90], one step fermionic ladder [140], one and two slowly moving impurities in a Luttinger liquid [154], etc. The formalism of NCBT is discussed in the second chapter.

The third chapter describes the seminal work done using NCBT, which is metaphorically called as 'the quantum steeplechase' [90]. The system includes a cluster of barriers or wells around a fixed point, which can be as simple as a delta potential or quite complicated as an asymmetric double delta potential. The system is subjected to the RPA (random phase approximation) which linearizes the energy momentum dispersion relations near the Fermi surface which is necessary to obtain analytical expressions of the correlation functions. The NCBT is then used to obtain the most singular part of the Green functions of such systems, which exhibits a power law with non trivial exponents. The results are obtained for the fermions with spin, which exhibits spin charge separation. Moreover, the systematic procedure for going to the spinless case is also elaborated.

The four point functions relevant to the study of Friedel oscillations are also calculated using the non standard harmonic analysis of NCBT [98]. The two-point functions obtained using the same method are used to calculate the dynamical density of states (DDOS), which exhibits a power law in energy and closed analytical expressions for the DDOS exponent is calculated. These results interpolates between the weak barrier and weak link cases which are typically studied in the literature. The dependence of the DDOS on the nature of interactions and the strength of the impurity clusters are highlighted. Finally the special case of the Luttinger parameter g=1/2 is studied and compared with existing results [72].

In the fourth chapter, the transport properties like conductance and resonant tunneling are discussed [127]. Conductance is studied both in the Kubo formalism, which relates it to current-current correlations (four-point functions), as well as the outcome of a tunneling phenomena (two-point functions). Using the correlation functions obtained using NCBT, the Kubo conductance is obtained for arbitrary strengths of mutual interactions as well as that of impurities. On the other hand, the tunneling conductance of a Luttinger liquid with infinite bandwidth is obtained as a power law which throws light into the temperature dependence of conductance. This endorses the well known results of Kane and Fisher [31], viz., 'cutting the chain' and 'healing the chain'. Besides, the tunneling conductance result obtained by Matveev et al. [34] is also derived from the NCBT conductance for infinite bandwidth. The finite bandwidth conductance is also calculated for the same class of systems and its dependence on temperature has been elucidated [128]. A thorough comparison has been done with the results of Matveev et al. which deals only with weakly interacting electrons. But NCBT provides conductance for all values of interaction strength as well as sign. Novel

Physics in the form of a weakly temperature dependent conductance is seen when the mutual repulsion between fermions is large and the holon velocity bears a certain well-defined relation to the bare transmission coefficient of the system. Deviations from the cutting the chain phenomenon is observed for a weak scatterer when the strength of repulsion is strong, leading to an unusual high conductance at lower temperatures, similar to breakdown current in a diode. Upon inclusion of backward scattering, there occurs an interplay between the forward and backward scattering such that the monotonic temperature dependence which dominates for forward scattering starts showing non-monotonic behavior when backward scattering is gradually increased. The condition of resonant tunneling is also obtained and the behavior of the correlation function exponents near resonance is described.

The fifth chapter deals with a one step fermionic ladder - two parallel Luttinger Liquids (poles of the ladder) placed such that there is a finite probability of electrons hopping between the two poles at a pair of opposing points along each of the poles. The many-body Green function for such a system is calculated in presence of forward scattering interactions using NCBT. The Friedel oscillation terms are calculated for the system, which is a special case of four point function. The tunneling conductance in this case is interesting as for a jet of electrons inserted into one end of the ladder can be collected from the other three ends with different probabilities. The dependence of conductance on the temperature and the nature of interactions is described [140].

In the sixth chapter, a Luttinger liquid with one or two mobile impurities (heavy particles) are considered. Using a combination of bosonization and perturbative approaches, the Green functions of these systems are calculated in the RPA limit [154]. The force acting on the heavy particle(s) is studied as a function of its terminal velocity, both in the linear and non-linear regime. Linear mobility (which is valid for impurities moving much slower than a certain cross-over speed) has a power-law temperature dependence whose exponent has a closed algebraic expression in terms of the various parameters in the problem. This expression interpolates between the ballistic regime of no-coupling with the fermions and the no-tunneling regime. When the speed of the impurity is much larger than this cross-over speed, the applied force depends non linearly on the speed and this too is a power-law with a closely related exponent. The results are consistent with the work of Castro Neto et al. [144] which says that at very low temperatures the mobility of an impenetrable heavy particle with mutually repelling fermions diverges (motion is ballistic). Conversely at high temperatures, both [144] and this work predicts a roughly temperature independent linear mobility so long as the impurity is impenetrable by the mutually repelling fermions. The case of two mobile impurities is also studied whose mobility exhibits peculiar resonances when their mutual separation is appropriately chosen.

This seventh chapter discusses the necessary and sufficient cross-checks to validate the NCBT [101]. Firstly the fermion commutation rules are checked for the field operator, followed by all the limiting case checks. It is also checked that NCBT does not violate the point-splitting

constraints. The Green functions obtained using NCBT are then expanded in powers of the interaction parameter and retained up to the first order. The same quantities are obtained using standard fermionic perturbation and compared favorably with those of NCBT, keeping in mind that NCBT provides the most singular part of the full Green functions. Finally the putative Green functions are inserted into the Schwinger-Dyson equation which is the equation of motion of the Green functions. The explicit expressions of Green functions obtained using NCBT indeed satisfy the Schwinger-Dyson equations which is a non-perturbative validation of the same. The functional bosonization method gave rise to some anomalous terms when applied to strongly inhomogeneous systems which are inconsistent with perturbation and hence can't be used to compare with the results of NCBT.

When it comes to a numerical validation, the obvious methods that springs to one's mind are DMRG [160], finite scaling, etc. But this is somewhat like asking a high-school pupil to prove the analytical formulas for the solution of a quadratic equation by solving the latter numerically. The pupil would rightly argue that it is much more convincing and easier to simply insert the putative analytical solution back into the defining equation and show that the result is an identity. This is precisely what Schwinger Dyson validation does. Moreover for gapless systems like the ones under consideration in the work, DMRG has its own shortcomings.

Future direction

Non chiral bosonization is novel way of looking into bosonization and it differs both mathematically and philosophically from the traditional methods. It facilitates the study of diverse systems using bosonization. Besides the ones studied in the present work, one may think of using similar ideas to deal with magnetic impurities like the Kondo model. Besides, the NCBT can also be tested to deal with other static potentials like the potential step, linear potential, harmonic oscillator, etc. The conductance of Luttinger liquids with impurities in presence of a magnetic field can also be studied following Matveev et al. [34]. It would also be interesting to explore whether it can be used to deal with disordered one dimensional systems where Anderson localization occurs, systems with quenched disorder, etc.

It will be challenging task to see how NCBT can be used beyond the low energy limit, where non-linearity becomes essential and one has to go beyond the Luttinger paradigm. Moreover, it will be a challenging job to generalize these ideas to higher dimensions. It is also important to study the same problems using numerical methods.

Appendix A

Correlation functions using conventional bosonization

The conventional bosonization method that goes by the name 'g-ology' can only yield the correlation functions for the extreme cases of homogeneous LL ($|R| = 0$) and half line ($|R| = 1$).

Case I: Green functions for $|R| = 0$.

The full Green function is the sum of all the parts. The notion of weak equality is introduced which is denoted by $A[X_1, X_2] \sim B[X_1, X_2]$. This really means $\partial_{t_1} Log[A[X_1, X_2]] = \partial_{t_1} Log[B[X_1, X_2]]$ assuming that A and B do not vanish identically. **Notation:** $X_i \equiv (x_i, \sigma_i, t_i)$ and $\tau_{12} = t_1 - t_2$.

$$\Big\langle T\ \psi(X_1)\psi^\dagger(X_2)\Big\rangle = \Big\langle T\ \psi_R(X_1)\psi_R^\dagger(X_2)\Big\rangle + \Big\langle T\ \psi_L(X_1)\psi_L^\dagger(X_2)\Big\rangle \tag{A.1}$$

where

$$\begin{aligned}\Big\langle T\ \psi_R(X_1)\psi_R^\dagger(X_2)\Big\rangle &\sim \frac{1}{(x_1 - x_2 - v_h\tau_{12})^P(-x_1 + x_2 - v_h\tau_{12})^Q(x_1 - x_2 - v_F\tau_{12})^{0.5}} \\ \Big\langle T\ \psi_L(X_1)\psi_L^\dagger(X_2)\Big\rangle &\sim \frac{1}{(x_1 - x_2 - v_h\tau_{12})^Q(-x_1 + x_2 - v_h\tau_{12})^P(-x_1 + x_2 - v_F\tau_{12})^{0.5}}\end{aligned} \tag{A.2}$$

and

$$P = \frac{(v_h + v_F)^2}{8v_hv_F}\ ;\ Q = \frac{(v_h - v_F)^2}{8v_hv_F} \tag{A.3}$$

On the other hand, the density-density correlation functions (DDCF) in presence of interactions is given by

$$\langle T\ \rho_s(x_1,\sigma_1,t_1)\rho_s(x_2,\sigma_2,t_2)\rangle = \frac{1}{4}(\langle T\ \rho_h(x_1,t_1)\rho_h(x_2,t_2)\rangle + \sigma_1\sigma_2\langle T\ \rho_n(x_1,t_1)\rho_n(x_2,t_2)\rangle) \tag{A.4}$$

where $\rho_h(x,t) = \rho_s(x,\uparrow,t) + \rho_s(x,\downarrow,t)$ is the "holon" density, while the "spinon" density is given by $\rho_n(x,t) = \rho_s(x,\uparrow,t) - \rho_s(x,\downarrow,t)$. Now,

$$\langle T\rho_a(x_1,t_1)\rho_a(x_2,t_2)\rangle = \frac{v_F}{2\pi^2 v_a}\sum_{\nu=\pm 1}\left(\frac{-1}{(x_1-x_2+\nu v_a(t_1-t_2))^2}\right) \tag{A.5}$$

where $a = n$ (spinon) or h (holon).

Case II: Green functions for $|R| = 1$.

$$\left\langle T\ \psi(X_1)\psi^\dagger(X_2)\right\rangle = \left\langle T\ \psi_R(X_1)\psi_R^\dagger(X_2)\right\rangle + \left\langle T\ \psi_L(X_1)\psi_L^\dagger(X_2)\right\rangle + \left\langle T\ \psi_R(X_1)\psi_L^\dagger(X_2)\right\rangle + \left\langle T\ \psi_L(X_1)\psi_R^\dagger(X_2)\right\rangle \tag{A.6}$$

where

$$\begin{aligned}
\left\langle T\ \psi_R(X_1)\psi_R^\dagger(X_2)\right\rangle &\sim \frac{1}{(x_1-x_2-v_h\tau_{12})^P(-x_1+x_2-v_h\tau_{12})^Q(x_1+x_2-v_h\tau_{12})^X(-x_1-x_2-v_h\tau_{12})^X(x_1-x_2-v_F\tau_{12})^{0.5}}\\
\left\langle T\ \psi_L(X_1)\psi_L^\dagger(X_2)\right\rangle &\sim \frac{1}{(x_1-x_2-v_h\tau_{12})^Q(-x_1+x_2-v_h\tau_{12})^P(x_1+x_2-v_h\tau_{12})^X(-x_1-x_2-v_h\tau_{12})^X(-x_1+x_2-v_F\tau_{12})^{0.5}}\\
\left\langle T\ \psi_R(X_1)\psi_L^\dagger(X_2)\right\rangle &\sim \frac{1}{(x_1-x_2-v_h\tau_{12})^X(-x_1+x_2-v_h\tau_{12})^X(x_1+x_2-v_h\tau_{12})^P(-x_1-x_2-v_h\tau_{12})^Q(x_1+x_2-v_F\tau_{12})^{0.5}}\\
\left\langle T\ \psi_L(X_1)\psi_R^\dagger(X_2)\right\rangle &\sim \frac{1}{(x_1-x_2-v_h\tau_{12})^X(-x_1+x_2-v_h\tau_{12})^X(x_1+x_2-v_h\tau_{12})^Q(-x_1-x_2-v_h\tau_{12})^P(-x_1-x_2-v_F\tau_{12})^{0.5}}
\end{aligned} \tag{A.7}$$

and

$$P = \frac{(v_h+v_F)^2}{8v_hv_F}\ ;\ Q = \frac{(v_h-v_F)^2}{8v_hv_F}\ ;\ X = \frac{(v_h^2-v_F^2)}{8v_hv_F}$$

Appendix B

Correlation functions using NCBT

The full single particle Green function of a Luttinger liquid in presence of impurities of arbitrary strength ($0 < |R| < 1$) has been recently derived using the NCBT [90]. The full Green function is the sum of all the parts. The notion of weak equality is introduced which is denoted by $A[X_1, X_2] \sim B[X_1, X_2]$. This really means $\partial_{t_1} Log[A[X_1, X_2]] = \partial_{t_1} Log[B[X_1, X_2]]$ assuming that A and B do not vanish identically. **Notation:** $X_i \equiv (x_i, \sigma_i, t_i)$ and $\tau_{12} = t_1 - t_2$.

$$\left\langle T\ \psi(X_1)\psi^\dagger(X_2)\right\rangle = \left\langle T\ \psi_R(X_1)\psi_R^\dagger(X_2)\right\rangle + \left\langle T\ \psi_L(X_1)\psi_L^\dagger(X_2)\right\rangle + \left\langle T\ \psi_R(X_1)\psi_L^\dagger(X_2)\right\rangle + \left\langle T\ \psi_L(X_1)\psi_R^\dagger(X_2)\right\rangle \tag{B.1}$$

Case I : x_1 and x_2 on the same side of the origin

$$\begin{aligned}
\left\langle T\ \psi_R(X_1)\psi_R^\dagger(X_2)\right\rangle &\sim \frac{(4x_1x_2)^{\gamma_1}}{(x_1-x_2-v_h\tau_{12})^P(-x_1+x_2-v_h\tau_{12})^Q(x_1+x_2-v_h\tau_{12})^X(-x_1-x_2-v_h\tau_{12})^X(x_1-x_2-v_F\tau_{12})^{0.5}}\\
\left\langle T\ \psi_L(X_1)\psi_L^\dagger(X_2)\right\rangle &\sim \frac{(4x_1x_2)^{\gamma_1}}{(x_1-x_2-v_h\tau_{12})^Q(-x_1+x_2-v_h\tau_{12})^P(x_1+x_2-v_h\tau_{12})^X(-x_1-x_2-v_h\tau_{12})^X(-x_1+x_2-v_F\tau_{12})^{0.5}}\\
\left\langle T\ \psi_R(X_1)\psi_L^\dagger(X_2)\right\rangle &\sim \frac{(2x_1)^{1+\gamma_2}(2x_2)^{\gamma_1}}{2(x_1-x_2-v_h\tau_{12})^S(-x_1+x_2-v_h\tau_{12})^S(x_1+x_2-v_h\tau_{12})^Y(-x_1-x_2-v_h\tau_{12})^Z(x_1+x_2-v_F\tau_{12})^{0.5}}\\
&+ \frac{(2x_1)^{\gamma_1}(2x_2)^{1+\gamma_2}}{2(x_1-x_2-v_h\tau_{12})^S(-x_1+x_2-v_h\tau_{12})^S(x_1+x_2-v_h\tau_{12})^Y(-x_1-x_2-v_h\tau_{12})^Z(x_1+x_2-v_F\tau_{12})^{0.5}}\\
\left\langle T\ \psi_L(X_1)\psi_R^\dagger(X_2)\right\rangle &\sim \frac{(2x_1)^{1+\gamma_2}(2x_2)^{\gamma_1}}{2(x_1-x_2-v_h\tau_{12})^S(-x_1+x_2-v_h\tau_{12})^S(x_1+x_2-v_h\tau_{12})^Z(-x_1-x_2-v_h\tau_{12})^Y(-x_1-x_2-v_F\tau_{12})^{0.5}}\\
&+ \frac{(2x_1)^{\gamma_1}(2x_2)^{1+\gamma_2}}{2(x_1-x_2-v_h\tau_{12})^S(-x_1+x_2-v_h\tau_{12})^S(x_1+x_2-v_h\tau_{12})^Z(-x_1-x_2-v_h\tau_{12})^Y(-x_1-x_2-v_F\tau_{12})^{0.5}}
\end{aligned} \tag{B.2}$$

Case II : x_1 and x_2 on opposite sides of the origin

$$\begin{aligned}
\left\langle T\ \psi_R(X_1)\psi_R^\dagger(X_2)\right\rangle &\sim \frac{(2x_1)^{1+\gamma_2}(2x_2)^{\gamma_1}(x_1+x_2)^{-1}(x_1+x_2+v_F\tau_{12})^{0.5}}{2(x_1-x_2-v_h\tau_{12})^A(-x_1+x_2-v_h\tau_{12})^B(x_1+x_2-v_h\tau_{12})^C(-x_1-x_2-v_h\tau_{12})^D(x_1-x_2-v_F\tau_{12})^{0.5}}\\
&+ \frac{(2x_1)^{\gamma_1}(2x_2)^{1+\gamma_2}(x_1+x_2)^{-1}(x_1+x_2-v_F\tau_{12})^{0.5}}{2(x_1-x_2-v_h\tau_{12})^A(-x_1+x_2-v_h\tau_{12})^B(x_1+x_2-v_h\tau_{12})^D(-x_1-x_2-v_h\tau_{12})^C(x_1-x_2-v_F\tau_{12})^{0.5}}\\
\left\langle T\ \psi_L(X_1)\psi_L^\dagger(X_2)\right\rangle &\sim \frac{(2x_1)^{1+\gamma_2}(2x_2)^{\gamma_1}(x_1+x_2)^{-1}(x_1+x_2-v_F\tau_{12})^{0.5}}{2(x_1-x_2-v_h\tau_{12})^B(-x_1+x_2-v_h\tau_{12})^A(x_1+x_2-v_h\tau_{12})^D(-x_1-x_2-v_h\tau_{12})^C(-x_1+x_2-v_F\tau_{12})^{0.5}}\\
&+ \frac{(2x_1)^{\gamma_1}(2x_2)^{1+\gamma_2}(x_1+x_2)^{-1}(x_1+x_2+v_F\tau_{12})^{0.5}}{2(x_1-x_2-v_h\tau_{12})^B(-x_1+x_2-v_h\tau_{12})^A(x_1+x_2-v_h\tau_{12})^C(-x_1-x_2-v_h\tau_{12})^D(-x_1+x_2-v_F\tau_{12})^{0.5}}\\
\left\langle T\ \psi_R(X_1)\psi_L^\dagger(X_2)\right\rangle &\sim 0\\
\left\langle T\ \psi_L(X_1)\psi_R^\dagger(X_2)\right\rangle &\sim 0
\end{aligned} \tag{B.3}$$

where ($|R|^2$ is the reflection coefficient)

$$Q = \frac{(v_h - v_F)^2}{8v_h v_F} \; ; \; X = \frac{|R|^2(v_h - v_F)(v_h + v_F)}{8v_h(v_h - |R|^2(v_h - v_F))} \; ; \; C = \frac{v_h - v_F}{4v_h} \tag{B.4}$$

The other exponents can be expressed in terms of the above exponents.

$$\begin{aligned} &P = \frac{1}{2} + Q \; ; \qquad S = \frac{Q}{C}(\frac{1}{2} - C) \; ; \qquad Y = \frac{1}{2} + X - C; \\ &Z = X - C \; ; \qquad A = \frac{1}{2} + Q - X \; ; \qquad B = Q - X \; ; \\ &D = -\frac{1}{2} + C \; ; \qquad \gamma_1 = X \; ; \qquad \gamma_2 = -1 + X + 2C; \end{aligned} \tag{B.5}$$

On the other hand, the density density correlation functions (DDCF) in presence of interactions is given by

$$\langle T \; \rho_s(x_1, \sigma_1, t_1)\rho_s(x_2, \sigma_2, t_2)\rangle = \frac{1}{4}(\langle T \; \rho_h(x_1, t_1)\rho_h(x_2, t_2)\rangle + \sigma_1\sigma_2\langle T \; \rho_n(x_1, t_1)\rho_n(x_2, t_2)\rangle) \tag{B.6}$$

where $\rho_h(x,t) = \rho_s(x,\uparrow,t) + \rho_s(x,\downarrow,t)$ is the "holon" density while the "spinon" density is given by $\rho_n(x,t) = \rho_s(x,\uparrow,t) - \rho_s(x,\downarrow,t)$.

$$\begin{aligned} \langle T\rho_a(x_1,t_1)\rho_a(x_2,t_2)\rangle = \frac{v_F}{2\pi^2 v_a} \sum_{\nu=\pm 1} \Bigg(&- \frac{1}{(x_1 - x_2 + \nu v_a(t_1 - t_2))^2} \\ &- \frac{|R|^2}{\left(1 - \delta_{a,h}\frac{(v_h - v_F)}{v_h}|R|^2\right)} \frac{\frac{v_F}{v_a}\,\mathrm{sgn}(x_1)\mathrm{sgn}(x_2)}{(|x_1| + |x_2| + \nu v_a(t_1 - t_2))^2} \Bigg) \end{aligned} \tag{B.7}$$

where $a = n$ (spinon) or h (holon).

Appendix C

DDCF in presence of interactions

The density density correlation functions (DDCF) in absence of mutual interactions is given by equation (3.13) as follows.

$$\langle T\ \rho_s(x_1,\sigma_1,t_1)\rho_s(x_2,\sigma_2,t_2)\rangle_0 = -\delta_{\sigma_1,\sigma_2}\sum_{\gamma,\gamma^{'}=\pm1}\sum_{\nu,\nu^{'}=\pm1}\frac{|g_{\gamma,\gamma^{'}}(\nu,\nu^{'})|^2\ \theta(\gamma x_1)\theta(\gamma^{'}x_2)}{[(\nu x_1-\nu^{'}x_2)-v_F(t_1-t_2)]^2}$$

The space time DDCF is related to the momentum frequency DDCF as follows.

$$< T\ \rho_s(x_1,t_1;\sigma_1)\rho_s(x_2,t_2;\sigma_2) >_0 = \frac{1}{L^2}\sum_{q,q^{'},n} e^{-iqx_1}e^{-iq^{'}x_2}e^{-w_n(t_1-t_2)} < T\ \rho_s(q,n;\sigma_1)\rho_s(q^{'},-n;\sigma_2) >_0$$

From this we can obtain the DDCF in momentum and frequency space as follows (here β is the inverse temperature which comes into the calculation because of converting summation to integration which is allowed in the zero temperature limit: $\sum_n f(z_n) = \frac{\beta}{2\pi}\int f(z)dz$ where $z_n = \frac{2\pi(n+1)}{\beta}$).

$$\begin{aligned} < T\ \rho_s(q,n;\sigma_1)\rho_s(q^{'},-n;\sigma_2) >_0 \ &= \frac{\delta_{\sigma_1,\sigma_2}}{\beta}\frac{(2v_Fq^{'})(2v_Fq)|g_{1,1}(1,-1)|^2|w_n|(2\pi)}{((v_Fq)^2+w_n^2)((v_Fq^{'})^2+w_n^2)} \\ &+\frac{\delta_{\sigma_1,\sigma_2}}{\beta}\frac{2q^2v_F}{w_n^2+(qv_F)^2}\delta_{q+q^{'},0}\frac{L}{(2\pi)} \end{aligned} \tag{C.1}$$

Now the generating function for an auxiliary field U in presence of mutual interactions between particles given by $v(x_1-x_2)$ can be written as

$$Z[U] = \int D[\rho]e^{iS_{eff,0}[\rho]}e^{\sum_{q,n,\sigma}\rho_{q,n,\sigma}U_{q,n,\sigma}}e^{-i\int_0^{-i\beta}dt\int dx_1\int dx_2\frac{1}{2}v(x_1-x_2)\rho(x_1,t_1;.)\rho(x_2,t_1;.)} \tag{C.2}$$

where S_0 is the action of free fermions and

$$\rho(x_1,t_1;.) = \frac{1}{L}\sum_{q,n}e^{-iqx}e^{w_nt}\ \rho_{q,n;.}$$

$$v(x_1 - x_2) = \frac{1}{L}\sum_Q e^{-iQ(x_1-x_2)} v_Q$$

$$\rho(x_1, t_1; .) = \rho(x_1, t_1; \uparrow) + \rho(x_1, t_1; \downarrow)$$

Thus the generating function can be written as follows.

$$Z[U] = \int D[\rho] e^{iS_{eff,0}[\rho]} e^{\sum_{q,n,\sigma} \rho_{q,n,\sigma} U_{q,n,\sigma}} e^{-\sum_{q,n} \frac{\beta v_q}{2L} \rho_{q,n;.} \rho_{-q,-n;.}} \tag{C.3}$$

If one denotes the generating function in absence of interactions as Z_0, then

$$Z_0[U] = \int D[\rho] e^{iS_{eff,0}[\rho]} e^{\sum_{q,n,\sigma} \rho_{q,n,\sigma} U_{q,n,\sigma}}$$

$$\Rightarrow e^{iS_{eff,0}[\rho]} = \int D[U'] e^{-\sum_{q,n,\sigma} \rho_{q,n,\sigma} U'_{q,n,\sigma}} \; Z_0[U']$$

Inserting in equation (C.3),

$$Z[U] = \int D[\rho] \int D[U'] \; Z_0[U'] \; e^{\sum_{q,n,\sigma} \rho_{q,n,\sigma} (U_{q,n,\sigma} - U'_{q,n,\sigma})} e^{-\sum_{q,n} \frac{\beta v_q}{2L} \rho_{q,n;.} \rho_{-q,-n;.}}$$

Set,

$$\rho_{q,n,\sigma} = \frac{1}{2}\rho_{q,n;.} + \frac{1}{2}\sigma \; \sigma_{q,n} \; ; \; U_{q,n,\sigma} = \frac{1}{2}U_{q,n;.} + \frac{1}{2}\sigma \; W_{q,n} \; ; \; U'_{q,n,\sigma} = \frac{1}{2}U'_{q,n;.} + \frac{1}{2}\sigma \; W'_{q,n} \tag{C.4}$$

Using these relations the generating function can be written as

$$Z[U] = \int D[\rho] \int D[U'] \; Z_0[U'] \; e^{\frac{1}{4}\sum_{q,n,\sigma} (\rho_{q,n;.} + \sigma \; \sigma_{q,n})((U_{q,n;.} - U'_{q,n;.}) + \sigma \; (W_{q,n} - W'_{q,n}))}$$
$$\times \; e^{-\sum_{q,n} \frac{\beta v_q}{2L} \rho_{q,n;.} \rho_{-q,-n;.}}$$

where in the RPA sense (for the homogeneous system, this choice corresponds to RPA, for the present steeplechase problem this choice corresponds to the most singular truncation of the RPA generating function)

$$Z_0[U'] = e^{\frac{1}{2}\sum_{q,q',n;\sigma} <\rho_{q,n}\rho_{q',-n}>_0 \; U'_{q,n;\sigma} U'_{q',-n;\sigma}}$$

where $< \rho_{q,n}\rho_{q',-n} >_0$ is equation (C.1) with $\sigma_1 = \sigma_2$. It is to be noted that we have neglected the higher moments of ρ in $Z_0[U']$ beyond the quadratic. The reason for this is the following. The connected parts of the odd moments ρ vanish identically (in the RPA limit) and the fourth moment is much less singular than the second moment, etc. For example, the connected 4-density function,

$$< T\rho(x_1)\rho(x_2)\rho(x_3)\rho(x_4) >_c$$
$$\sim < T\psi(x_1)\psi^*(x_2) >< T\psi(x_2)\psi^*(x_3) >< T\psi(x_3)\psi^*(x_4) >< T\psi(x_4)\psi^*(x_1) >$$
$$+ \text{ permutations}$$

has only first order poles and no second order poles. The NCBT does not claim to provide the asymptotic Green functions of strongly inhomogeneous interacting Fermi systems exactly but it does claim to provide the *most singular part of* the asymptotic Green functions of strongly inhomogeneous interacting Fermi systems exactly. Now,

$$\begin{aligned}
Z[U] &= \int D[\rho] \int D[U^{'}]\ e^{\frac{1}{2}\sum_{q,q^{'},n;\sigma}<\rho_{q,n}\rho_{q^{'},-n}>_0\ \frac{1}{4}(U^{'}_{q,n;.}+\sigma\ W^{'}_{q,n})(U^{'}_{q^{'},-n;.}+\sigma\ W^{'}_{q^{'},-n})} \\
&\quad e^{\frac{1}{4}\sum_{q,n,\sigma}(\rho_{q,n;.}+\sigma\ \sigma_{q,n})((U_{q,n;.}-U^{'}_{q,n;.})+\sigma\ (W_{q,n}-W^{'}_{q,n}))} e^{-\sum_{q,n}\frac{\beta v_q}{2L}\rho_{q,n;.}\rho_{-q,-n;.}} \\
&= \int D[U^{'}]\ e^{\frac{1}{2}\sum_{q,q^{'},n}<\rho_{q,n}\rho_{q^{'},-n}>_0\ \frac{1}{2}(U^{'}_{q,n;.}U^{'}_{q^{'},-n;.}+W^{'}_{q,n}W^{'}_{q^{'},-n})} \\
&\quad \int D[\rho]\ e^{\frac{1}{2}\sum_{q,n}(\rho_{q,n;.}(U_{q,n;.}-U^{'}_{q,n;.})+\sigma_{q,n}(W_{q,n}-W^{'}_{q,n}))} e^{-\sum_{q,n}\frac{\beta v_q}{2L}\rho_{q,n;.}\rho_{-q,-n;.}} \\
&= \int D[U^{'}]\ e^{\frac{1}{4}\sum_{q,q^{'},n}<\rho_{q,n}\rho_{q^{'},-n}>_0\ W_{q,n}W_{q^{'},-n}}\ e^{\frac{1}{4}\sum_{q,q^{'},n}<\rho_{q,n}\rho_{q^{'},-n}>_0\ U^{'}_{q,n;.}U^{'}_{q^{'},-n;.}} \\
&\quad \int D[\rho]\ e^{\frac{1}{2}\sum_{q,n}\rho_{q,n;.}(U_{q,n;.}-U^{'}_{q,n;.})} e^{-\sum_{q,n}\frac{\beta v_q}{2L}\rho_{q,n;.}\rho_{-q,-n;.}}
\end{aligned}$$

Also,

$$\rho_{-q,-n;.} = \frac{L}{2\beta v_q}(U_{q,n;.} - U^{'}_{q,n;.})$$

Thus,

$$\begin{aligned}
Z[U] = \int D[U^{'}]\ & e^{\frac{1}{4}\sum_{q,q^{'},n}<\rho_{q,n}\rho_{q^{'},-n}>_0\ W_{q,n}W_{q^{'},-n}}\ e^{\frac{1}{4}\sum_{q,q^{'},n}<\rho_{q,n}\rho_{q^{'},-n}>_0\ U^{'}_{q,n;.}U^{'}_{q^{'},-n;.}} \\
& e^{\frac{1}{4}\sum_{q,n}\frac{L}{2\beta v_q}(U_{-q,-n;.}-U^{'}_{-q,-n;.})(U_{q,n;.}-U^{'}_{q,n;.})}
\end{aligned}$$

After doing the integration using the saddle point method, we obtain the following form of the partition function,

$$\begin{aligned}
Z[U] =& e^{\frac{1}{4}\sum_{q,q^{'},n}<\rho_{q,n}\rho_{q^{'},-n}>_0\ W_{q,n}W_{q^{'},-n}}\ e^{\sum_{q,n}\frac{L}{8\beta v_q}U_{q,n;.}U_{-q,-n;.}\frac{(qv_h)^2-(qv_F)^2}{w_n^2+(qv_h)^2}} \\
& e^{\sum_{q,n}\frac{L}{8\beta v_q}\frac{1}{L}\sum_{q^{'}}\frac{(2v_Fq^{'})U_{q,n;.}U_{q^{'},-n;.}}{\left(1-\frac{4v_qv_F}{(v_h+v_F)v_h}\ |g_{1,1}(1,-1)|^2(2\pi)\right)\left(w_n^2+(q^{'}v_h)^2\right)}(2v_Fq)\frac{2v_q|g_{1,1}(1,-1)|^2|w_n|(2\pi)}{(w_n^2+(qv_h)^2)}}
\end{aligned} \tag{C.5}$$

Here

$$v_h = \sqrt{v_F^2 + \frac{2v_Fv_q}{\pi}}$$

Since we have,

$$\rho_{q,n;.} = \rho_{q,n;\uparrow} + \rho_{q,n;\downarrow}\ ;\ \sigma_{q,n} = \rho_{q,n;\uparrow} - \rho_{q,n;\downarrow} \tag{C.6}$$

Thus,

$$\begin{aligned}
\frac{1}{4}\ <\rho_{q,n;.}\rho_{q^{'},-n;.}> =& +\delta_{q+q^{'},0}\ \frac{L}{4\beta v_q}\frac{(qv_h)^2-(qv_F)^2}{w_n^2+(qv_h)^2} \\
&+\frac{1}{2\beta}\frac{(2v_Fq)(2v_Fq^{'})|g_{1,1}(1,-1)|^2|w_n|(2\pi)}{\left(1-\frac{4v_qv_F}{(v_h+v_F)v_h}\ |g_{1,1}(1,-1)|^2(2\pi)\right)\left(w_n^2+(q^{'}v_h)^2\right)\left(w_n^2+(qv_h)^2\right)}
\end{aligned} \tag{C.7}$$

$$\frac{1}{4} < \sigma_{q,n}\sigma_{q',-n} > = \frac{(2v_F q')(2v_F q)}{2\beta((v_F q)^2 + w_n^2)((v_F q')^2 + w_n^2)}|g_{1,1}(1,-1)|^2|w_n|(2\pi) + \frac{q^2 v_F L}{2\pi\beta(w_n^2 + (qv_F)^2)}\delta_{q+q',0} \tag{C.8}$$

$$< \sigma_{q,n}\rho_{q',-n;.} > = 0$$

Finally, the full density density correlation functions in momentum frequency space can be written as,

$$< \rho_{q,n,\sigma}\rho_{q',-n,\sigma'} >= \frac{1}{4} < \rho_{q,n;.}\rho_{q',-n;.} > + \frac{1}{4}\sigma\sigma' < \sigma_{q,n}\sigma_{q',-n} > \tag{C.9}$$

Doing an inverse Fourier transform of the above we get the DDCF in real space time.

$$\begin{aligned}
&< T\ \rho_s(x_1,t_1;\sigma)\rho_s(x_2,t_2;\sigma') >= \\
&-\frac{v_F^2}{v_h^4}\ \mathrm{sgn}(x_1)\mathrm{sgn}(x_2)\left(\frac{\beta}{2\pi}\ \frac{1}{[(t_1-t_2)+\frac{|x_1|+|x_2|}{v_h}]^2} + \frac{\beta}{2\pi}\ \frac{1}{[(t_1-t_2)-\frac{|x_1|+|x_2|}{v_h}]^2}\right) \\
&\qquad \times \frac{1}{2\beta}\frac{|g_{1,1}(1,-1)|^2(2\pi)}{\left(1-\frac{4v_q v_F}{(v_h+v_F)v_h}\ |g_{1,1}(1,-1)|^2(2\pi)\right)} \\
&-\frac{\mathrm{sgn}(x_1)\mathrm{sgn}(x_2)}{v_F^2}\left(\frac{\beta}{2\pi}\ \frac{1}{[(t_1-t_2)+\frac{|x_1|+|x_2|}{v_F}]^2} + \frac{\beta}{2\pi}\ \frac{1}{[(t_1-t_2)-\frac{|x_1|+|x_2|}{v_F}]^2}\right)\frac{1}{2\beta}|g_{1,1}(1,-1)|^2(2\pi\sigma\sigma') \\
&-\frac{v_F}{4\pi\beta v_h^3}\left(\frac{\beta}{2\pi}\ \frac{1}{[(t_1-t_2)+\frac{|x_1-x_2|}{v_h}]^2} + \frac{\beta}{2\pi}\ \frac{1}{[(t_1-t_2)-\frac{|x_1-x_2|}{v_h}]^2}\right) \\
&-\frac{\sigma\sigma'}{4\pi\beta v_F^2}\left(\frac{\beta}{2\pi}\ \frac{1}{[(t_1-t_2)+\frac{|x_1-x_2|}{v_F}]^2} + \frac{\beta}{2\pi}\ \frac{1}{[(t_1-t_2)-\frac{|x_1-x_2|}{v_F}]^2}\right)
\end{aligned} \tag{C.10}$$

From this we obtain the equation (3.17) of the main text as follows:

$$\begin{aligned}
\langle T\ \rho_h(x_1,t_1)\rho_h(x_2,t_2)\rangle =& \frac{v_F}{2\pi^2 v_h}\sum_{\nu=\pm1}\left(-\frac{1}{(x_1-x_2+\nu v_h(t_1-t_2))^2}\right. \\
&\left.-\frac{|R|^2}{\left(1-\frac{(v_h-v_F)}{v_h}|R|^2\right)}\frac{\frac{v_F}{v_h}\ \mathrm{sgn}(x_1)\mathrm{sgn}(x_2)}{(|x_1|+|x_2|+\nu v_h(t_1-t_2))^2}\right) \\
\langle T\ \rho_n(x_1,t_1)\rho_n(x_2,t_2)\rangle =& \frac{1}{2\pi^2}\sum_{\nu=\pm1}\left(-\frac{1}{(x_1-x_2+\nu v_F(t_1-t_2))^2} - \frac{\mathrm{sgn}(x_1)\mathrm{sgn}(x_2)\ |R|^2}{(|x_1|+|x_2|+\nu v_F(t_1-t_2))^2}\right)
\end{aligned}$$

The full density density correlation functions is given as follows.

$$\langle T\ \rho_s(x_1,\sigma_1,t_1)\rho_s(x_2,\sigma_2,t_2)\rangle = \frac{1}{4}\left(\langle T\ \rho_h(x_1,t_1)\rho_h(x_2,t_2)\rangle + \sigma_1\sigma_2\langle T\ \rho_n(x_1,t_1)\rho_n(x_2,t_2)\rangle\right) \tag{C.11}$$

Appendix D

Fermi Bose Correspondence

The Fermi Bose correspondence is given by equation (7.12) of the main text as follows.

$$\psi_k(x) = e^{i\pi \sum_{l<k} \int_{-\infty}^{\infty} dy\ \rho_l(y)} \frac{1}{\sqrt{N^0}} \sum_p n_F(p)\ e^{i\xi(p)}\ e^{i\pi sgn(p) \int_{sgn(x)\infty}^{x} dy\ \rho_k(y)} e^{-i\pi_k(x)}\ \sqrt{\rho_k(x)} \quad \text{(D.1)}$$

where $n_F(p) = \theta(k_F - |p|)$ and $N^0 = \sum_p n_F(p)$.

Theorem: The correspondence equation (D.1) is compatible with fermion commutation rules equation (7.6) in conjunction with equation (7.10).

Proof: Observe,

$$\psi_j(x) = e^{i\pi \sum_{l<j} \int_{-\infty}^{\infty} dy\ \rho_l(y)} \frac{1}{\sqrt{N^0}} \sum_p n_F(p)\ e^{i\xi(p)}\ e^{i\pi sgn(p) \int_{sgn(x)\infty}^{x} dy\ \rho_j(y)} e^{-i\pi_j(x)}\ \sqrt{\rho_j(x)}$$

$$\psi_k(x^{'}) = e^{i\pi \sum_{l<k} \int_{-\infty}^{\infty} dy\ \rho_l(y)} \frac{1}{\sqrt{N^0}} \sum_{p^{'}} n_F(p^{'})\ e^{i\xi(p^{'})}\ e^{i\pi sgn(p^{'}) \int_{sgn(x^{'})\infty}^{x^{'}} dy\ \rho_k(y)} e^{-i\pi_k(x^{'})}\ \sqrt{\rho_k(x^{'})}$$

$$\psi_k^{\dagger}(x^{'}) = \sqrt{\rho_k(x^{'})}\ e^{i\pi_k(x^{'})} \frac{1}{\sqrt{N^0}} \sum_{p^{'}} n_F(p^{'})\ e^{-i\xi(p^{'})} e^{-i\pi sgn(p^{'}) \int_{sgn(x^{'})\infty}^{x^{'}} dy\ \rho_k(y)} e^{-i\pi \sum_{l<k} \int_{-\infty}^{\infty} dy\ \rho_l(y)}$$

This means,

$$\psi_j(x)\psi_k(x^{'}) = e^{i\pi \sum_{l<j} \int_{-\infty}^{\infty} dy\ \rho_l(y)} \frac{1}{\sqrt{N^0}} \sum_p n_F(p)\ e^{i\xi(p)}\ e^{i\pi sgn(p) \int_{sgn(x)\infty}^{x} dy\ \rho_j(y)} e^{-i\pi_j(x)}\ \sqrt{\rho_j(x)}$$

$$e^{i\pi \sum_{l<k} \int_{-\infty}^{\infty} dy\ \rho_l(y)} \frac{1}{\sqrt{N^0}} \sum_{p^{'}} n_F(p^{'})\ e^{i\xi(p^{'})}\ e^{i\pi sgn(p^{'}) \int_{sgn(x^{'})\infty}^{x^{'}} dy\ \rho_k(y)} e^{-i\pi_k(x^{'})}\ \sqrt{\rho_k(x^{'})}$$

$$\psi_j(x)\psi_k(x^{'}) = \frac{1}{\sqrt{N^0}}\sum_{p} n_F(p)\ e^{i\xi(p)}\ \frac{1}{\sqrt{N^0}}\sum_{p^{'}} n_F(p^{'})\ e^{i\xi(p^{'})}$$
$$e^{i\pi sgn(p)\int_{sgn(x)\infty}^{x} dy\ \rho_j(y)} e^{i\pi sgn(p^{'})\int_{sgn(x^{'})\infty}^{x^{'}} dy\ \rho_k(y)} e^{i\pi\sum_{l<k}\int_{-\infty}^{\infty} dy\ \rho_l(y)}$$
$$e^{i\pi\sum_{l<j}\int_{-\infty}^{\infty} dy\ \rho_l(y)}\ \sqrt{(\rho_j(x)+\delta(0))(\rho_k(x^{'})+\delta_{j,k}\delta(x-x^{'})+\delta(0))}$$
$$e^{-i\pi_j(x)-i\pi_k(x^{'})}\ e^{i\pi\sum_{l<k}\delta_{j,l}}\ e^{i\pi sgn(p^{'})\ \delta_{j,k}\theta(x^{'}-x)}$$

Also,

$$\psi_k(x^{'})\psi_j(x) = \frac{1}{\sqrt{N^0}}\sum_{p^{'}} n_F(p^{'})\ e^{i\xi(p^{'})}\ \frac{1}{\sqrt{N^0}}\sum_{p} n_F(p)\ e^{i\xi(p)}$$
$$e^{i\pi sgn(p^{'})\int_{sgn(x^{'})\infty}^{x^{'}} dy\ \rho_k(y)} e^{i\pi sgn(p)\int_{sgn(x)\infty}^{x} dy\ \rho_j(y)} e^{i\pi\sum_{l<j}\int_{-\infty}^{\infty} dy\ \rho_l(y)}$$
$$e^{i\pi\sum_{l<k}\int_{-\infty}^{\infty} dy\ \rho_l(y)}\ \sqrt{(\rho_k(x^{'})+\delta(0))(\rho_j(x)+\delta_{j,k}\delta(x-x^{'})+\delta(0))}$$
$$e^{-i\pi_j(x)-i\pi_k(x^{'})}\ e^{i\pi\sum_{l<j}\delta_{k,l}}\ e^{i\pi sgn(p)\ \delta_{j,k}\theta(x-x^{'})}$$

Now,

$$\begin{aligned}(\rho_j(x)+\delta(0))(\rho_k(x^{'})+&\delta_{j,k}\delta(x-x^{'})+\delta(0)) \\ &= (\rho_j(x)+\delta(0))(\rho_k(x^{'})+\delta(0)) + \delta_{j,k}\delta(x-x^{'})(\rho_j(x)+\delta(0)) \\ &= (\rho_k(x^{'})+\delta(0))(\rho_j(x)+\delta_{j,k}\delta(x-x^{'})+\delta(0)) \\ &= (\rho_k(x^{'})+\delta(0))(\rho_j(x)+\delta(0)) + \delta_{j,k}\delta(x-x^{'})(\rho_k(x^{'})+\delta(0))\end{aligned}$$

Hence,

$$\{\psi_j(x),\psi_k(x^{'})\} = \frac{1}{\sqrt{N^0}}\sum_{p^{'}} n_F(p^{'})\ e^{i\xi(p^{'})}\ \frac{1}{\sqrt{N^0}}\sum_{p} n_F(p)\ e^{i\xi(p)}\ e^{i\pi sgn(p^{'})\int_{sgn(x^{'})\infty}^{x^{'}} dy\ \rho_k(y)}$$
$$e^{i\pi sgn(p)\int_{sgn(x)\infty}^{x} dy\ \rho_j(y)} e^{i\pi\sum_{l<j}\int_{-\infty}^{\infty} dy\ \rho_l(y)} e^{i\pi\sum_{l<k}\int_{-\infty}^{\infty} dy\ \rho_l(y)}$$
$$\sqrt{(\rho_k(x^{'})+\delta(0))(\rho_j(x)+\delta_{j,k}\delta(x-x^{'})+\delta(0))}\, e^{-i\pi_j(x)-i\pi_k(x^{'})}$$
$$\left(e^{i\pi\sum_{l<k}\delta_{j,l}}\ e^{i\pi sgn(p^{'})\ \delta_{j,k}\theta(x^{'}-x)} + e^{i\pi\sum_{l<j}\delta_{k,l}}\ e^{i\pi sgn(p)\ \delta_{j,k}\theta(x-x^{'})}\right)$$

But,

$$\left(e^{i\pi\sum_{l<k}\delta_{j,l}}\ e^{i\pi sgn(p^{'})\ \delta_{j,k}\theta(x^{'}-x)} + e^{i\pi\sum_{l<j}\delta_{k,l}}\ e^{i\pi sgn(p)\ \delta_{j,k}\theta(x-x^{'})}\right) = 0$$

always. Hence,

$$\boxed{\{\psi_j(x),\psi_k(x^{'})\} = 0}$$

Now,

$$\psi_j(x)\psi_k^{\dagger}(x^{'}) =$$

$$e^{i\pi\sum_{l<j}\int_{-\infty}^{\infty}dy\ \rho_l(y)}\frac{1}{\sqrt{N^0}}\sum_p n_F(p)\ e^{i\xi(p)}\ e^{i\pi sgn(p)\int_{sgn(x)\infty}^{x}dy\ \rho_j(y)}e^{-i\pi_j(x)}\ \sqrt{\rho_j(x)}$$

$$\times\sqrt{\rho_k(x^{'})}\ e^{i\pi_k(x^{'})}\frac{1}{\sqrt{N^0}}\sum_{p^{'}} n_F(p^{'})\ e^{-i\xi(p^{'})}e^{-i\pi sgn(p^{'})\int_{sgn(x^{'})\infty}^{x^{'}}dy\ \rho_k(y)}e^{-i\pi\sum_{l<k}\int_{-\infty}^{\infty}dy\ \rho_l(y)}$$

$$\psi_k^{\dagger}(x^{'})\psi_j(x) =$$

$$\sqrt{\rho_k(x^{'})}\ e^{i\pi_k(x^{'})}\frac{1}{\sqrt{N^0}}\sum_{p^{'}} n_F(p^{'})\ e^{-i\xi(p^{'})}e^{-i\pi sgn(p^{'})\int_{sgn(x^{'})\infty}^{x^{'}}dy\ \rho_k(y)}e^{-i\pi\sum_{l<k}\int_{-\infty}^{\infty}dy\ \rho_l(y)}$$

$$\times e^{i\pi\sum_{l<j}\int_{-\infty}^{\infty}dy\ \rho_l(y)}\frac{1}{\sqrt{N^0}}\sum_p n_F(p)\ e^{i\xi(p)}\ e^{i\pi sgn(p)\int_{sgn(x)\infty}^{x}dy\ \rho_j(y)}e^{-i\pi_j(x)}\ \sqrt{\rho_j(x)}$$

Or,

$$\psi_j(x)\psi_k^{\dagger}(x^{'}) = e^{-i\pi_j(x)}e^{i\pi\sum_{l<j}\int_{-\infty}^{\infty}dy\ \rho_l(y)}\frac{1}{\sqrt{N^0}}\sum_p n_F(p)\ e^{i\xi(p)}\ e^{i\pi sgn(p)\int_{sgn(x)\infty}^{x}dy\ \rho_j(y)}\ \sqrt{\rho_j(x)}$$

$$\times\sqrt{\rho_k(x^{'})}\ \frac{1}{\sqrt{N^0}}\sum_{p^{'}} n_F(p^{'})\ e^{-i\xi(p^{'})}e^{-i\pi sgn(p^{'})\int_{sgn(x^{'})\infty}^{x^{'}}dy\ \rho_k(y)}e^{-i\pi\sum_{l<k}\int_{-\infty}^{\infty}dy\ \rho_l(y)}e^{i\pi_k(x^{'})}$$

$$\psi_k^{\dagger}(x^{'})\psi_j(x) = e^{-i\pi_j(x)}\sqrt{\rho_k(x^{'})-\delta_{j,k}\delta(x-x^{'})}\ \frac{1}{\sqrt{N^0}}\sum_{p^{'}} n_F(p^{'})\ e^{-i\xi(p^{'})}$$

$$e^{-i\pi sgn(p^{'})\int_{sgn(x^{'})\infty}^{x^{'}}dy\ (\rho_k(y)-\delta_{j,k}\delta(x-y))}e^{-i\pi\sum_{l<k}\int_{-\infty}^{\infty}dy\ (\rho_l(y)-\delta_{j,l}\delta(x-y))}$$

$$e^{i\pi\sum_{l<j}\int_{-\infty}^{\infty}dy\ (\rho_l(y)-\delta_{k,l}\delta(x^{'}-y))}\frac{1}{\sqrt{N^0}}\sum_p n_F(p)\ e^{i\xi(p)}\ e^{i\pi sgn(p)\int_{sgn(x)\infty}^{x}dy\ (\rho_j(y)-\delta_{k,j}\delta(x^{'}-y))}$$

$$\sqrt{(\rho_j(x)-\delta_{k,j}\delta(x^{'}-x))}e^{i\pi_k(x^{'})}$$

Or,

$$\psi_k^{\dagger}(x^{'})\psi_j(x) = e^{-i\pi_j(x)}\frac{1}{N^0}\sum_{p,p^{'}} n_F(p)n_F(p^{'})\ e^{-i\xi(p^{'})}e^{i\xi(p)}\ \sqrt{\rho_k(x^{'})-\delta_{j,k}\delta(x-x^{'})}$$

$$\sqrt{\rho_j(x)-\delta_{k,j}\delta(x^{'}-x)}e^{-i\pi sgn(p^{'})\int_{sgn(x^{'})\infty}^{x^{'}}dy\ \rho_k(y)}e^{-i\pi\sum_{l<k}\int_{-\infty}^{\infty}dy\ \rho_l(y)}$$

$$e^{i\pi\sum_{l<j}\int_{-\infty}^{\infty}dy\ \rho_l(y)}\ e^{i\pi sgn(p)\int_{sgn(x)\infty}^{x}dy\ \rho_j(y)}\ e^{i\pi_k(x^{'})}$$

$$e^{i\pi sgn(p^{'})\ \delta_{j,k}\theta(x^{'}-x)}e^{i\pi\sum_{l<k}\ \delta_{j,l}}e^{-i\pi\sum_{l<j}\ \delta_{k,l}}e^{-i\pi sgn(p)\ \delta_{k,j}\theta(x-x^{'})}$$

$$\psi_j(x)\psi_k^{\dagger}(x^{'}) = e^{-i\pi_j(x)}\frac{1}{N^0}\sum_{p,p^{'}} n_F(p)n_F(p^{'})\ e^{-i\xi(p^{'})}e^{i\xi(p)}\ \sqrt{\rho_j(x)}\sqrt{\rho_k(x^{'})}$$

$$e^{i\pi\sum_{l<j}\int_{-\infty}^{\infty}dy\ \rho_l(y)}e^{i\pi sgn(p)\int_{sgn(x)\infty}^{x}dy\ \rho_j(y)}$$

$$e^{-i\pi sgn(p^{'})\int_{sgn(x^{'})\infty}^{x^{'}}dy\ \rho_k(y)}e^{-i\pi\sum_{l<k}\int_{-\infty}^{\infty}dy\ \rho_l(y)}e^{i\pi_k(x^{'})}$$

After setting $e^{-i\xi(p^{'})}e^{i\xi(p)} = \delta_{p,p'}$ it is possible to conclude that,

$$\boxed{\{\psi_j(x), \psi_k^{\dagger}(x^{'})\} = \delta_{j,k}\delta(x - x^{'})}$$

Appendix E

Dynamical density of states

In elementary physics, the dynamical density of states (DDOS) at zero temperature relative to the Fermi energy is defined through the correspondence,

$$D(\omega) = \frac{1}{V}\sum_{\mathbf{k}} \delta(\omega - \epsilon_{\mathbf{k}} + E_F) \tag{E.1}$$

$D(\omega)d\omega$ is the number of states between ω and $\omega + d\omega$ per unit volume. In one dimension for example, this yields the following result for ω small compared to Fermi energy,

$$D(\omega) = \frac{1}{\pi v_F} \tag{E.2}$$

This is the standard result that the density of states near the Fermi energy is constant for a Fermi liquid. This is also the case in higher dimensions. But for a Luttinger liquid, the DDOS $D(\omega) \sim \omega^{\alpha}$ where α is the density of states exponent. α depends on the forward scattering interaction strength and vanishes when this is zero. To prove this, it is important to generalize the idea of density of states to interacting many body systems. The generalization is given below.

$$D_{\mathbf{x}}(\omega) = \int_{-\infty}^{\infty} \frac{dt}{2\pi}\, e^{it(\omega + E_F)}\, \langle\{\psi(\mathbf{x}, t), \psi^{\dagger}(\mathbf{x}, 0)\}\rangle$$

Thus the density of states for translationally non-invariant systems becomes the local density of states (for fermions with spin, it is calculated for one spin projection and the answer is then doubled). The above local density of states has been successfully related to the single particle Green function formulas for which have been derived earlier. From the main text it may be concluded that (upon inserting the pre-factors back in) for points on the same side of the cluster (choose right side) $(sgn(t_1 - t_2) \equiv \theta(t_1 - t_2) - \theta(t_2 - t_1)$ where the Heaviside step function is involved in the time ordering on the left hand side and Z_h is given in equation (3.18)),

$$\Big\langle T\ \psi_R(X_1)\psi_R^\dagger(X_2)\Big\rangle \ = \frac{i}{2\pi}\ e^{-\sum_{a=n,h}\frac{v_F}{8v_a}\ \sum_{\nu=\pm1}(\frac{\nu v_a}{v_F}-1)^2\ Log(x_1-x_2+\nu v_a(t_1-t_2))}$$
$$e^{-\frac{v_F}{8v_h}\ \sum_{\nu=\pm1}\ Z_h\ Log(x_1+x_2+\nu v_h(t_1-t_2))\left(\frac{v_h}{v_F}-\frac{v_F}{v_h}\right)}\ e^{\frac{v_F}{8v_h}\ Log(4x_1x_2)\ Z_h(\frac{v_h}{v_F}-\frac{v_F}{v_h})}$$

$$\Big\langle T\ \psi_L(X_1)\psi_L^\dagger(X_2)\Big\rangle \ = \frac{i}{2\pi}\ e^{-\sum_{a=n,h}\frac{v_F}{8v_a}\ \sum_{\nu=\pm1}(\frac{\nu v_a}{v_F}-1)^2\ Log(-x_1+x_2+\nu v_a(t_1-t_2))}$$
$$e^{-\frac{v_F}{8v_h}\ \sum_{\nu=\pm1}\ Z_h\ Log(-x_1-x_2+\nu v_h(t_1-t_2))\left(\frac{v_h}{v_F}-\frac{v_F}{v_h}\right)}e^{\frac{v_F}{8v_h}\ Log(4x_1x_2)\ Z_h(\frac{v_h}{v_F}-\frac{v_F}{v_h})}$$

$$\Big\langle T\ \psi_R(X_1)\psi_L^\dagger(X_2)\Big\rangle$$
$$= \Big(e^{Log(2x_1)}\frac{i}{4\pi}R\ e^{\sum_{a=n,h}\frac{v_F}{8v_a}\ Log(2x_1)\ (Z_a(\frac{v_a}{v_F}-\frac{v_F}{v_a})-4)}e^{\frac{v_F}{8v_h}\ Log(2x_2)Z_h\ (\frac{v_h}{v_F}-\frac{v_F}{v_h})}+$$
$$e^{Log(2x_2)}\frac{i}{4\pi}R\ e^{\frac{v_F}{8v_h}\ Log(2x_1)\ Z_h(\frac{v_h}{v_F}-\frac{v_F}{v_h})}e^{\sum_{a=n,h}\frac{v_F}{8v_a}\ Log(2x_2)(Z_a\ (\frac{v_a}{v_F}-\frac{v_F}{v_a})-4)}\Big)$$
$$Exp\Big[-\sum_{a=n,h}\frac{v_F}{8v_a}\sum_{\nu=\pm1}(Z_a(\frac{v_a}{v_F}-\frac{v_F}{v_a})-2\nu\frac{v_a}{v_F}+2)\ Log(x_1+x_2+\nu v_a(t_1-t_2))$$
$$-\frac{v_F}{8v_h}\sum_{\nu=\pm1}[(\frac{\nu v_h}{v_F}-1)(\frac{\nu v_h}{v_F}+1)]\ Log(x_1-x_2+\nu v_h(t_1-t_2))\Big]$$

$$\Big\langle T\ \psi_L(X_1)\psi_R^\dagger(X_2)\Big\rangle$$
$$= \Big(e^{Log(2x_1)}\frac{i}{4\pi}R^*\ e^{\sum_{a=n,h}\frac{v_F}{8v_a}\ Log(2x_1)\ (Z_a(\frac{v_a}{v_F}-\frac{v_F}{v_a})-4)}e^{\frac{v_F}{8v_h}\ Log(2x_2)Z_h\ (\frac{v_h}{v_F}-\frac{v_F}{v_h})}$$
$$+e^{Log(2x_2)}\frac{i}{4\pi}R^*\ e^{\frac{v_F}{8v_h}\ Log(2x_1)\ Z_h(\frac{v_h}{v_F}-\frac{v_F}{v_h})}e^{\sum_{a=n,h}\frac{v_F}{8v_a}\ Log(2x_2)(Z_a\ (\frac{v_a}{v_F}-\frac{v_F}{v_a})-4)}\Big)$$
$$Exp\Big[-\sum_{a=n,h}\frac{v_F}{8v_a}\sum_{\nu=\pm1}(Z_a(\frac{v_a}{v_F}-\frac{v_F}{v_a})-2\nu\frac{v_a}{v_F}+2)\ \ Log(-x_1-x_2+\nu v_a(t_1-t_2))$$
$$-\frac{v_F}{8v_h}\sum_{\nu=\pm1}[(\frac{\nu v_h}{v_F}-1)(\frac{\nu v_h}{v_F}+1)]\ Log(-x_1+x_2+\nu v_h(t_1-t_2))\Big]$$

These are sufficient to extract the local DDOS including terms that corresponding to Friedel oscillations since in the present case,

$$D_x(\omega) = \int_{-\infty}^{\infty}\frac{dt}{2\pi}\ e^{it\omega}\ (\langle\{\psi_R(x,t),\psi_R^\dagger(x,0)\}\rangle + \langle\{\psi_L(x,t),\psi_L^\dagger(x,0)\}\rangle)$$
$$+\int_{-\infty}^{\infty}\frac{dt}{2\pi}\ e^{it\omega}\ (e^{2ik_Fx}\ \langle\{\psi_R(x,t),\psi_L^\dagger(x,0)\}\rangle + e^{-2ik_Fx}\ \langle\{\psi_L(x,t),\psi_R^\dagger(x,0)\}\rangle)$$

In the present work one shall be content at evaluating the slow contributions to the local DDOS. Far from the cluster of barriers and wells these formulas predict, $D_\infty(\omega)\sim\omega^\alpha$ and $\alpha=\frac{(v_F-v_h)^2}{4v_Fv_h}=\frac{1}{2}(K_\rho+\frac{1}{K_\rho}-2)$. This is the same density of states exponent one gets when external potentials are absent which is the standard result predicted by Luttinger liquid theory. Hence an important consistency check has been verified.

Now the important next step is to see how $D_x(\omega)$ depends on x. The parameter that determines this is the dimensionless quantity $\xi=\frac{2\omega|x|}{v_h}$. The limit that has already been studied is $D_{\xi\gg1}(\omega)\approx D_\infty(\omega)$. The other limit of interest is $D_{0<\xi\ll1}(\omega)$ i.e. close to the cluster of barriers and wells. Set $\xi=\frac{2\omega|x|}{v_h}$, $2|x|=\frac{\xi v_h}{\omega}$. From the above propagators it is straightforward

to deduce,

$$D_{0<\xi\ll 1}(\omega) \sim \left(\frac{v_h}{\omega}\right)^{\frac{1}{4}Z_h(-1+\frac{v_F^2}{v_h^2})-\frac{v_F^2+v_h^2}{4v_F v_h}+\frac{1}{2}} \sim \omega^{\alpha}$$

where $\alpha(0<\xi\ll 1) \approx \frac{(v_h-v_F)(v_F Z_h(v_F+v_h)+v_h(v_h-v_F))}{4v_F v_h^2}$ and Z_h is given by

$$Z_h = \frac{v_h|R|^2}{v_h-(v_h-v_F)|R|^2}$$

Appendix F

Conductance

In this section, the conductance of a quantum wire with no leads is obtained first using Kubo's formula and next using the idea that it is the outcome of a tunneling experiment.

Kubo formalism

The electric field is $E(x,t) = \frac{V_g}{L}$ between $-\frac{L}{2} < x < \frac{L}{2}$ and $E(x,t) = 0$ for $|x| > \frac{L}{2}$. Here V_g is the Voltage between two extreme points. Thus a d.c. situation is being considered right from the start. This corresponds to a vector potential (c is the velocity of light),

$$A(x,t) = \begin{cases} -\frac{V_g}{L}(ct), & -\frac{L}{2} < x < \frac{L}{2} \ ; \\ 0, & \text{otherwise.} \end{cases}$$

This means (since $j \approx j_s$, the slow part) ,

$$< j(x,\sigma,t) >= \frac{ie}{c} \sum_{\sigma'} \int_{-L/2}^{L/2} dx' \int_{-\infty}^{t} dt' \frac{V_g}{L}(ct') < [j(x,\sigma,t), j(x',\sigma',t')] >_{LL} \qquad \text{(F.1)}$$

Clean wire: $|R| = 0$ **but** $v_0 \neq 0$

Using the Green function from equation (B.2) and setting $|R| = 0$, the current current commutation relation can be calculated as,

$$< [j_s(x,\sigma,t), j_s(x',\sigma',t')] >= -\frac{v_F^2}{8\pi^2} \sum_{\nu=\pm 1} (2\pi i)\partial_{v_F t'} \left(\delta(x - x' + \nu v_h(t-t')) + \sigma\sigma' \ \delta(x - x' + \nu v_F(t-t'))\right) \qquad \text{(F.2)}$$

Inserting equation (F.2) into equation (F.1), the following is obtained.

$$< j(x,\sigma,t) >= \frac{ie}{c}\sum_{\sigma'}\int_{-\frac{L}{2}}^{\frac{L}{2}} dx' \int_{-\infty}^{t} dt' \ \frac{V_g}{L}(ct')\Big(\frac{-v_F^2}{8\pi^2}\sum_{\nu=\pm 1}(2\pi i)\ \partial_{v_F t'}\Big(\delta(x-x'+\nu v_h(t-t')) + \sigma\sigma'\delta(x-x'+\nu v_F(t-t'))\Big)\Big)$$

Finally,

$$< j(x,\sigma,t) >= -\ V_g \frac{e}{(2\pi)}\frac{v_F}{v_h}$$

or,

$$I = (-e) < j(x,\sigma,t) >= \ V_g \frac{e^2}{(2\pi)}\frac{v_F}{v_h}$$

This gives the formula for the conductance (per spin) for a clean quantum wire with interactions,

$$G = \frac{e^2}{2\pi}\frac{v_F}{v_h}$$

or in proper units,

$$\boxed{G = \frac{e^2}{2\pi\hbar}\ \frac{v_F}{v_h} = \frac{e^2}{h}\ \frac{v_F}{v_h}}$$

A comparison with standard g-ology with the present chosen model gives the following identifications (equation (2.105) of Giamarchi [5]).

$$\begin{aligned}
&g_{1,\perp} = g_{1,\parallel} = 0\\
&g_{2,\perp} = g_{2,\parallel} = g_{4,\perp} = g_{4,\parallel} = v_0\\
&g_\rho = g_{1,\parallel} - g_{2,\parallel} - g_{2,\perp} = 0 - v_0 - v_0 = -2v_0\\
&g_\sigma = g_{1,\parallel} - g_{2,\parallel} + g_{2,\perp} = 0 - v_0 + v_0 = 0\\
&g_{4,\rho} = g_{4,\parallel} + g_{4,\perp} = 2v_0\\
&g_{4,\sigma} = g_{4,\parallel} - g_{4,\perp} = 0\\
&y_\rho = g_\rho/(\pi v_F) = -\frac{2v_0}{\pi v_F}\\
&y_\sigma = g_\sigma/(\pi v_F) = 0\\
&y_{4,\rho} = g_{4,\rho}/(\pi v_F) = g_{4,\rho}/(\pi v_F) = 2v_0/(\pi v_F)\\
&y_{4,\sigma} = g_{4,\sigma}/(\pi v_F) = 0
\end{aligned}$$

$$\begin{aligned}
u_\rho =& v_F\sqrt{(1+y_{4,\rho}/2)^2 - (y_\rho/2)^2}\\
=& v_F\sqrt{1+2v_0/(\pi v_F)} \equiv v_h
\end{aligned}$$

$$K_\rho = \sqrt{\frac{1+y_{4,\rho}/2+y_\rho/2}{1+y_{4,\rho}/2-y_\rho/2}} = \sqrt{\frac{1}{1+2v_0/(\pi v_F)}} = \frac{v_F}{v_h}$$

$$u_\sigma = v_F\sqrt{(1+y_{4,\sigma}/2)^2 - (y_\sigma/2)^2} = v_F$$

$$K_\sigma = \sqrt{\frac{1 + y_{4,\sigma}/2 + y_\sigma/2}{1 + y_{4,\sigma}/2 - y_\sigma/2}} = 1$$

This gives,

$$\boxed{G = \frac{e^2}{h}\,\frac{v_F}{v_h} = \frac{e^2}{h}\,K_\rho}$$

which is the standard result for a clean quantum wire.

The general case: $|R| > 0$ **and** $v_0 \neq 0$

Again, using the Green function from equation (B.2) for general value of $|R|$, the current current commutation relation can be calculated as,

$$\begin{aligned}
&< [j_s(x,\sigma,t), j_s(x',\sigma',t')] > \\
&= -(2\pi i)\frac{v_F v_h^2}{8\pi^2 v_h}\,\partial_{v_h t'} \sum_{\nu=\pm 1}\left(\delta(\nu(x-x') + v_h(t-t')) - \frac{v_F}{v_h}\,Z_h\,\delta(\nu(|x|+|x'|) + v_h(t-t'))\right) \\
&\quad -(2\pi i)\frac{\sigma\sigma' v_F^2}{8\pi^2}\,\partial_{v_F t'} \sum_{\nu=\pm 1}\left(\delta(\nu(x-x') + v_F(t-t')) - |R|^2\delta(\nu(|x|+|x'|) + v_F(t-t'))\right)
\end{aligned}$$

where,

$$Z_h = \frac{|R|^2}{\left(1 - \frac{(v_h - v_F)}{v_h}|R|^2\right)}$$

Thus,

$$\begin{aligned}
< j(x,\sigma,t) > &= ie\sum_{\sigma'}\int_{-L/2}^{L/2} dx' \int_{-\infty}^{t} dt'\,\partial_{v_h t'}\,\frac{V_g}{L}(2\pi i)\frac{v_F}{8\pi^2} \\
&\quad \times \sum_{\nu=\pm 1}\left(\theta(-\nu(x-x') - v_h(t-t')) - \frac{v_F}{v_h}\,Z_h\,\theta(-\nu(|x|+|x'|) - v_h(t-t'))\right)
\end{aligned}$$

therefore,

$$< j(x,\sigma,t) >= \frac{2ie}{v_h} V_g (2\pi i)\frac{v_F}{8\pi^2}\left(1 - \frac{v_F}{v_h}\,Z_h\right)$$

The conductance of a quantum wire without leads but in the presence of barriers and wells is,

$$G = \frac{e^2}{(2\pi)}\frac{v_F}{v_h}\left(1 - \frac{v_F}{v_h}\,Z_h\right)$$

Hence the general formula for the conductance of a quantum wire without leads but with electrons experiencing forward scattering short-range mutual interactions and in the presence

of a finite number of barriers and wells clustered around an origin is (in proper units),

$$\boxed{G = \frac{e^2}{h}\frac{v_F}{v_h}\left(1 - \frac{v_F}{v_h}\, Z_h\right)} \tag{F.3}$$

The above general formula agrees with the three well known limiting cases.

(i) when $v_h = v_F$, Landauer's formula $G = \frac{e^2}{h}\,|T|^2$ is recovered.

(ii) when $|R| = 0$, the formula $G = \frac{e^2}{h}\,K_\rho$ is also recovered.

(iii) when $|R| = 1$, $G = 0$ regardless of what v_h is.

Conductance from a tunneling experiment

If the conduction process is envisaged as a tunneling phenomenon as against the usual Kubo formula based approach which involves relating conductance to current-current correlation, a qualitatively different formula for the conductance is obtained. We regard the tunneling conductance as being proportional to the absolute value of an effective tunneling amplitude $G \sim |T|$. This point of view is also the one advocated by Matveev et al. [34]. Now the single particle Green functions of the system (switching off interaction in equation (B.2) and equation (B.3)) are as follows.

$$\langle T\ \psi_\nu(x,\sigma,t)\psi^\dagger_{\nu'}(x',\sigma',t')\rangle_0 = \sum_{\gamma,\gamma'=\pm1}\frac{\theta(\gamma x)\theta(\gamma' x')\ g_{\gamma,\gamma'}(\nu,\nu')}{(\nu x - \nu' x') - v_F(t-t')}\delta_{\sigma,\sigma'} \tag{F.4}$$

where $g_{\gamma,\gamma'}(\nu,\nu)$ are functions of the reflection (R) and the transmission (T) amplitudes of the system and is given explicitly as follows.

$$\begin{aligned} g_{\gamma_1,\gamma_2}(\nu_1,\nu_2) = \frac{i}{2\pi}\Big[&\delta_{\nu_1,\nu_2}\delta_{\gamma_1,\gamma_2} + (T\delta_{\nu_1,\nu_2} + R\delta_{\nu_1,-\nu_2})\delta_{\gamma_1,\nu_1}\delta_{\gamma_2,-\nu_2} \\ &+ (T^*\delta_{\nu_1,\nu_2} + R^*\delta_{\nu_1,-\nu_2})\delta_{\gamma_1,-\nu_1}\delta_{\gamma_2,\nu_2}\Big] \end{aligned} \tag{F.5}$$

Using equation (F.4) and equation (F.5) the following is obtained

$$\begin{aligned} v_F\int_{-\infty}^{\infty} dt\ &< \{\psi_\nu(x,\sigma,t),\psi^\dagger_\nu(x',\sigma,0)\} >= -(2\pi i)\sum_{\gamma,\gamma'=\pm1}\theta(\gamma x)\theta(\gamma' x')g_{\gamma,\gamma'}(\nu,\nu) \\ \Rightarrow v_F\int_{-\infty}^{\infty} dt\ &< \{\psi_\nu(-\nu\frac{L}{2},\sigma,t),\psi^\dagger_\nu(\nu\frac{L}{2},\sigma,0)\} >= -(2\pi i)g_{-\nu,\nu}(\nu,\nu) \\ \Rightarrow v_F\int_{-\infty}^{\infty} dt\ &< \{\psi_\nu(-\nu\frac{L}{2},\sigma,t),\psi^\dagger_\nu(\nu\frac{L}{2},\sigma,0)\} >= -(2\pi i)\frac{i}{2\pi}T^* = T^* \end{aligned}$$

Setting $\nu = 1$ and taking the absolute value we have

$$|v_F \int_{-\infty}^{\infty} dt \ < \{\psi_R(-\frac{L}{2},\sigma,t), \psi_R^\dagger(\frac{L}{2},\sigma,0)\} > | = |T|$$

Hence conductance can be written as

$$G \sim \frac{e^2}{h} \ |v_F \int_{-\infty}^{\infty} dt \ < \{\psi_R(-\frac{L}{2},\sigma,0), \psi_R^\dagger(\frac{L}{2},\sigma,t)\} > | \tag{F.6}$$

Choosing the tunneling conductance to be proportional to the magnitude of the transmission amplitude allows perfect agreement with the RG equations of Matveev et al. [34] as we have seen in the main text ($|T|$ is the magnitude of the transmission amplitude of free fermions plus impurity).

Homogeneous case

Now using the equation (F.6) we calculate the tunneling conductance of a homogeneous Luttinger liquid. For this the Green functions are taken from equation (B.2) and the reflection coefficient $|R|$ is set to zero (which is equivalent to the homogeneous case).

$$\left\langle T\psi_R(-\frac{L}{2},\sigma,0)\psi_R^\dagger(\frac{L}{2},\sigma,t)\right\rangle = \frac{i}{2\pi} \ e^{-\frac{1}{2}\log[L-v_F t]} e^{-\frac{1}{2}\log[L-v_h t]} e^{-\frac{(v_h-v_F)^2}{8v_h v_F}\log\left|\frac{L^2-(v_h t)^2}{L_\omega^2}\right|}$$

Hence,

$$\left\langle \{\psi_R(-\frac{L}{2},\sigma,0), \psi_R^\dagger(\frac{L}{2},\sigma,t)\}\right\rangle = \frac{i}{2\pi} \ e^{-\frac{1}{2}\log[L-v_F(t-i\epsilon)]} e^{-\frac{1}{2}\log[L-v_h(t-i\epsilon)]} e^{-\frac{(v_h-v_F)^2}{8v_h v_F}\log\left|\frac{L^2-(v_h(t-i\epsilon))^2}{L_\omega^2}\right|}$$
$$- \frac{i}{2\pi} \ e^{-\frac{1}{2}\log[L-v_F(t+i\epsilon)]} e^{-\frac{1}{2}\log[L-v_h(t+i\epsilon)]} e^{-\frac{(v_h-v_F)^2}{8v_h v_F}\log\left|\frac{L^2-(v_h(t+i\epsilon))^2}{L_\omega^2}\right|}$$

while integrating over t the only regions that contribute are $L - v_F t \approx 0$ and $L - v_h t \approx 0$. When $v_h \neq v_F$ these two are different regions. Set $L - v_F t = y$ then $L - v_h t = L - \frac{v_h}{v_F}(L-y)$ and $L + v_h t = L + \frac{v_h}{v_F}(L-y)$. The implication is, integration over t is now integration over y and this is important only when y is close to zero. Next set $L - v_h t = y'$ then $L + v_h t = 2L - y'$ and $L - v_F t = L - \frac{v_F}{v_h}(L-y')$ and the integrals are important only when y' is close to zero. This means,

$$v_F \int_{-\infty}^{\infty} dt \left\langle \{\psi_R(-\frac{L}{2},\sigma,0), \psi_R^\dagger(\frac{L}{2},\sigma,t)\}\right\rangle$$
$$= \int_{-\infty}^{\infty} dy \ \frac{i}{2\pi} \ \left(e^{-\frac{1}{2}\log[y+v_F i\epsilon]} - e^{-\frac{1}{2}\log[y-v_F i\epsilon]}\right) \ e^{-\frac{1}{2}\log[L(1-\frac{v_h}{v_F})+\frac{v_h}{v_F}y]} e^{-\frac{(v_h-v_F)^2}{8v_h v_F}\log\left|\frac{L^2-\frac{v_h^2}{v_F}(L-y)^2}{L_\omega^2}\right|}$$
$$+ \frac{v_F}{v_h}\int_{-\infty}^{\infty} dy' \ \frac{i}{2\pi} \ \left(e^{-\frac{1}{2}\log[y'+v_h i\epsilon]} - e^{-\frac{1}{2}\log[y'-v_h i\epsilon]}\right) e^{-\frac{1}{2}\log[L(1-\frac{v_F}{v_h})+\frac{v_F}{v_h}y']} \ e^{-\frac{(v_h-v_F)^2}{8v_h v_F}\log\left|\frac{y'(2L-y')}{L_\omega^2}\right|}$$

Only the dependence on L is of interest. Write $y = L\ s$ and $y^{'} = L\ s^{'}$. Hence,

$$v_F \int_{-\infty}^{\infty} dt \left\langle \{\psi_R(-\frac{L}{2},\sigma,0), \psi_R^{\dagger}(\frac{L}{2},\sigma,t)\} \right\rangle \sim e^{-\frac{(v_h-v_F)^2}{8v_h v_F}\log\left|\frac{L^2}{L_\omega^2}\right|}$$

This means the tunneling conductance of a clean (no barrier) quantum wire scales as,

$$G_{clean} \sim \frac{e^2}{h}\ \ e^{-\frac{(v_h-v_F)^2}{4v_h v_F}\log\left|\frac{L}{L_\omega}\right|} \sim \ \ \left(\frac{L_\omega}{L}\right)^{\frac{1}{4}(K_\rho+\frac{1}{K_\rho}-2)} \tag{F.7}$$

where $L_\omega = \frac{v_F}{k_B T}$ is the length scale associated with temperature (or frequency since $k_B T$ is interchangeable with ω). It says that at low temperatures, the tunneling d.c. conductance of a clean quantum wire with no leads but with interactions ($v_h \neq v_F$) diverges as a power law with exponent $\frac{1}{4}(K_\rho + \frac{1}{K_\rho} - 2) > 0$.

With the impurities

The homogeneous case is well handled by standard bosonization (g-ology) techniques. But the addition of impurities of arbitrary strength makes this technique inadequate and it has to rely on renormalization or other numerical techniques. But these techniques fall well short of proving closed analytical expressions of the correlation function exponents which, as we can already see, are crucial for the calculation of conductance exponents. On the other hand NCBT provides closed analytical expressions for these exponents for the general case with the barriers and wells. Consider the general Green function for the points on the opposite sides (equation (B.3)).

$$\begin{aligned}
&< T\psi_R(x,\sigma,t)\psi_R{}^{\dagger}(x',\sigma,t') > \\
&\quad = \frac{1}{2(x+x')}\ e^{(X+2C)\log[2x]} e^{X\log[2x']}\ g_{-1,1}(1,1)\ e^{-\frac{1}{2}\log[(x-x')-v_F(t-t')]} e^{\frac{1}{2}\log[(x+x')+v_F(t-t')]} \\
&\qquad\qquad e^{-(\frac{1}{2}+Q-X)\log[(x-x')-v_h(t-t')]} e^{-(Q-X)\log[(x-x')+v_h(t-t')]} \\
&\qquad\qquad e^{-C\log[(x+x')-v_h(t-t')]} e^{-(-\frac{1}{2}+C)\log[(x+x')+v_h(t-t')]} \\
&\quad + \frac{1}{2(x+x')}\ e^{X\log[2x]} e^{(X+2C)\log[2x']}\ g_{-1,1}(1,1)\ e^{-\frac{1}{2}\log[(x-x')-v_F(t-t')]} e^{\frac{1}{2}\log[(x+x')-v_F(t-t')]} \\
&\qquad\qquad e^{-(\frac{1}{2}+Q-X)\log[(x-x')-v_h(t-t')]} e^{-(Q-X)\log[(x-x')+v_h(t-t')]} \\
&\qquad\qquad e^{-(-\frac{1}{2}+C)\log[(x+x')-v_h(t-t')]} e^{-C\log[(x+x')+v_h(t-t')]}
\end{aligned}$$

Hence ($x = -\frac{L}{2}$ and $x^{'} = \frac{L}{2} + \epsilon$ and $x + x^{'} = \epsilon \to 0$ is small),

$$\begin{aligned}
&< T\psi_R(\frac{L}{2},\sigma,t)\psi_R^{\dagger}(-\frac{L}{2},\sigma,0) >= \frac{1}{2\epsilon}\ e^{(X+2C)\log[L]} e^{X\log[L]}\ g_{1,-1}(1,1)\ e^{-\frac{1}{2}\log[L-v_F t]} \\
&\qquad e^{\frac{1}{2}\log[\epsilon+v_F t]} e^{-(\frac{1}{2}+Q-X)\log[L-v_h t]} e^{-(Q-X)\log[L+v_h t]} e^{-C\log[\epsilon-v_h t]} e^{-(-\frac{1}{2}+C)\log[\epsilon+v_h t]}
\end{aligned}$$

$$+\frac{1}{2\epsilon}\; e^{X\log[L]}e^{(X+2C)\log[L]}\; g_{1,-1}(1,1)\; e^{-\frac{1}{2}\log[L-v_Ft]}$$
$$e^{\frac{1}{2}\log[\epsilon-v_Ft]}e^{-(\frac{1}{2}+Q-X)\log[L-v_ht]}e^{-(Q-X)\log[L+v_ht]}e^{-(-\frac{1}{2}+C)\log[\epsilon-v_ht]}e^{-C\log[\epsilon+v_ht]}$$

Hence,

$$< T\psi_R(-\frac{L}{2},\sigma,0)\psi_R^\dagger(\frac{L}{2},\sigma,t) >=\frac{1}{2\epsilon}\; e^{(2X+2C)\log[L]}\; g_{1,-1}(1,1)\; e^{-\frac{1}{2}\log[L-v_Ft]}e^{-\frac{1}{2}\log[L-v_ht]}$$
$$e^{\frac{1}{2}\log[\epsilon+v_Ft]}e^{\frac{1}{2}\log[\epsilon+v_ht]}e^{-(Q-X)\log[L^2-(v_ht)^2]}e^{-C\log[\epsilon^2-(v_ht)^2]}$$
$$+\frac{1}{2\epsilon}\; e^{(2X+2C)\log[L]}\; g_{1,-1}(1,1)\; e^{-\frac{1}{2}\log[L-v_Ft]}e^{-\frac{1}{2}\log[L-v_ht]}$$
$$e^{\frac{1}{2}\log[\epsilon-v_Ft]}e^{\frac{1}{2}\log[\epsilon-v_ht]}e^{-(Q-X)\log[L^2-(v_ht)^2]}e^{-C\log[\epsilon^2-(v_ht)^2]}$$

Taking the limit $\epsilon\to 0$,

$$< T\psi_R(\frac{L}{2},\sigma,t)\psi_R^\dagger(-\frac{L}{2},\sigma,0) >=\frac{v_F+v_h}{2\sqrt{v_Fv_h}}\; g_{1,-1}(1,1)\; e^{(2X+2C)\log[L]}$$
$$e^{-\frac{1}{2}\log[L-v_Ft]}e^{-\frac{1}{2}\log[L-v_ht]}\; e^{-(Q-X)\log[L^2-(v_ht)^2]}e^{-C\log[-(v_ht)^2]}$$

Since $G\sim|v_F\int_{-\infty}^{\infty}dt<\{\psi_R(-\frac{L}{2},\sigma,0),\psi_R^\dagger(\frac{L}{2},\sigma,t)\}>|$ it is possible to read off the conductance exponent as follows,

$$G\sim\left(\frac{L}{L_\omega}\right)^{4X-2Q} \tag{F.8}$$

where $Q=\frac{(v_h-v_F)^2}{8v_hv_F}$ and $X=\frac{|R|^2(v_h-v_F)(v_h+v_F)}{8v_h(v_h-|R|^2(v_h-v_F))}$ as given in equation (3.22). It is easy to see that for a vanishing barrier $|R|\to 0$, the earlier result of the conductance of a clean quantum wire is recovered.

Appendix G

Mathematica commands to verify Schwinger Dyson equations

For verifying any of the Schwinger Dyson equations given in section 7.4, define two variables, say 'LHS' and 'RHS' and type both sides of the equation in Mathematica software as follows:

$$LHS := -i\left(P\frac{(v_h - v_F)}{v_h(t-t') - x + x'} + ...\right)$$
$$RHS := \frac{v_0\ i}{4\pi v_h^2}\left(\frac{v_h(v_h - v_F)}{v_h(t-t') - x + x'} + ...\right)$$

Method I:

Define all the variables.

$$Q := \frac{(v_h - v_F)^2}{8v_h v_F}\ ;\ P := \frac{1}{2} + Q$$

and so on from the section 3.4.1 (Anomalous exponents) in the main text. Check

$$LHS - RHS$$

to get zero.

Method II:

Use the command

$$\text{SolveAlways}[LHS == RHS, \{x, x', t, t'\}]$$

This leads to expressions for the anomalous exponents (denoted by upper case letters of the alphabet) which can then be matched with those in the section 3.4.1 (Anomalous exponents) in the main text.

Appendix H

Derivation of the reflection and transmission amplitudes

(a) Single delta-function Consider a single delta potential at the origin ($V_0\delta(x)$) and a wave propagation towards the right. Then the wavfunction can be written as follows.

$$\psi_R(x) = \begin{cases} A_1 e^{ikx} + B_1 e^{-ikx} & -L/2 < x < 0 \\ A_2 e^{ikx} & 0 < x < L/2 \end{cases}$$

Now using the continuity condition of the wavefunction at the origin, integrating the Schrödinger equation around the delta potential and performing box (of length L) renormalization of the wavefunction, one can fix the three unknowns which are obtained to be the following:

$$A_1 = \sqrt{\frac{1}{L}}\ ; \quad B_1 = \sqrt{\frac{1}{L}}\left(-\frac{\frac{imV_0}{k}}{1+\frac{imV_0}{k}}\right)\ ;\ A_2 = \sqrt{\frac{1}{L}}\left(\frac{1}{1+\frac{imV_0}{k}}\right) \tag{H.1}$$

Under the RPA limit, where $m, k \to \infty$ but $\frac{k}{m} = v_F$ is finite, we have the following.

$$A_1 = \sqrt{\frac{1}{L}}\ ; \quad B_1 = \sqrt{\frac{1}{L}}\left(-\frac{\frac{iV_0}{v_F}}{1+\frac{iV_0}{v_F}}\right)\ ;\ A_2 = \sqrt{\frac{1}{L}}\left(\frac{1}{1+\frac{iV_0}{v_F}}\right) \tag{H.2}$$

Thus we have

$$T = \frac{A_2}{A_1} = \frac{1}{\left(1+V_0\frac{i}{v_F}\right)}\ ;\ R = \frac{B_1}{A_1} = -\frac{iV_0}{v_F\left(1+V_0\frac{i}{v_F}\right)} \tag{H.3}$$

(b) Symmetric double delta-function Consider two delta potentials at distance $\pm a$ from the origin ($V_0(\delta(x-a)+\delta(x+a))$) and a wave propagation towards the right. Then the

wavfunction can be written as follows.

$$\psi_R(x) = \begin{cases} A_1 e^{ikx} + B_1 e^{-ikx} & -L/2 < x < -a \\ A_2 e^{ikx} + B_2 e^{-ikx} & -a < x < a \\ A_3 e^{ikx} & a < x < L/2 \end{cases}$$

Now using the continuity condition of the wavefunction at the points $\pm a$, integrating the Schrödinger equation around the delta potentials and performing box (of length L) renormalization of the wavefunction, one can fix the five unknowns which are obtained to be the following:

$$\begin{aligned} A_1 &= \sqrt{\frac{1}{L}} \\ B_1 &= \sqrt{\frac{1}{L}} \frac{-iz[4k\cos(2ka) + 2z\sin(2ka)]}{4k(k+iz) + z^2(e^{4ika}-1)} \\ A_2 &= \sqrt{\frac{1}{L}} \frac{2ki(-z+2ki)}{4k(k+iz) + z^2(e^{4ika}-1)} \\ B_2 &= \sqrt{\frac{1}{L}} \frac{2ikze^{2ika}}{4k(k+iz) + z^2(e^{4ika}-1)} \\ A_3 &= \sqrt{\frac{1}{L}} \frac{4k^2}{4k(k+iz) + z^2(e^{4ika}-1)} \end{aligned}$$

where,

$$z = \frac{2mV_0}{\hbar^2} \; ; \; k = \frac{\sqrt{2mE}}{\hbar};$$

Under the RPA limit, where $m, k \to \infty$ but $\frac{k}{m} = v_F$ is finite. Also we take the limiting case of $a \to 0$ along with $k \to \infty$ so that the factor $2ka = \xi_0$ is a finite constant. Imposing these limits to the above coefficients we obtain

$$T = \frac{A_3}{A_1} = \frac{1}{\left(1 + V_0 \frac{i}{v_F}\right)^2 - \left(\frac{iV_0}{v_F} e^{i\xi_0}\right)^2} \; ; \; R = \frac{B_1}{A_1} = -\frac{2i\frac{V_0^2}{v_F^2}\sin[\xi_0] + \frac{2iV_0}{v_F}\cos[\xi_0]}{\left(1 + V_0 \frac{i}{v_F}\right)^2 - \left(\frac{iV_0}{v_F} e^{i\xi_0}\right)^2} \tag{H.4}$$

(c) Asymmetric double delta-function Proceeding similar as above we obtain the following for two unequal delta potentials of strengths V_1 and V_2 at position a and $-a$ respectively.

$$T = \frac{1}{\left(1 + i\frac{V_1+V_2}{v_F} + \frac{i^2 V_1 V_2}{v_F^2}\right) + \frac{V_1 V_2}{v_F^2} e^{2i\xi_0}} \; ; \; R = -\frac{2i\frac{V_1 V_2}{v_F^2}\sin[\xi_0] + \frac{2i}{v_F}\left(\frac{V_1 e^{i\xi_0} + V_2 e^{-i\xi_0}}{2}\right)}{\left(1 + i\frac{V_1+V_2}{v_F} + \frac{i^2 V_1 V_2}{v_F^2}\right) + \frac{V_1 V_2}{v_F^2} e^{2i\xi_0}} \tag{H.5}$$

(d) Symmetric triple delta-function Proceeding similar as above we obtain the following for two equal delta potentials of strengths V_1 at position $\pm a$ along with another delta potential

of strength V_0 at the origin.

$$T = \frac{1}{\left(1 - i\frac{V_0V_1^2}{v_F^3} - 2\frac{V_0V_1}{v_F^2} - \frac{V_1^2}{v_F^2} + i\frac{V_0}{v_F} + 2i\frac{V_1}{v_F}\right) + \frac{e^{i\xi_0}}{v_F^2}\left(2i\frac{V_0V_1^2}{v_F} - ie^{i\xi_0}\frac{V_0V_1^2}{v_F} + 2V_0V_1 + e^{i\xi_0}V_1^2\right)}$$

$$R = -\frac{2i\frac{V_0V_1^2}{v_F^3} - 2i\frac{V_0V_1^2}{v_F^3}\cos[\xi_0] + 2i\frac{V_0V_1}{v_F^2}\sin[\xi_0] + 2i\frac{V_1^2}{v_F^2}\sin[\xi_0] + i\frac{V_0}{v_F} + 2i\frac{V_1}{v_F}\cos[\xi_0]}{\left(1 - i\frac{V_0V_1^2}{v_F^3} - 2\frac{V_0V_1}{v_F^2} - \frac{V_1^2}{v_F^2} + i\frac{V_0}{v_F} + 2i\frac{V_1}{v_F}\right) + \frac{e^{i\xi_0}}{v_F^2}\left(2i\frac{V_0V_1^2}{v_F} - ie^{i\xi_0}\frac{V_0V_1^2}{v_F} + 2V_0V_1 + e^{i\xi_0}V_1^2\right)} \tag{H.6}$$

(e) Finite barrier tunneling

Consider a rectangular barrier of height V extending from $x = -a$ to $x = a$ such that the energy of the particle is less that then height of the barrier. The wavefunction is given as follows.

$$\psi_R(x) = \begin{cases} A_1e^{ikx} + B_1e^{-ikx} & -L/2 < x < -a \\ A_2e^{\kappa x} + B_2e^{-\kappa x} & -a < x < a \\ A_3e^{ikx} & a < x < L/2 \end{cases}$$

Using continuity conditions of the wavefunction and its first derivative at points $\pm a$ along with renormalization will yield the following expressions of the coefficients.

$$\begin{aligned} A_1 &= \sqrt{\frac{1}{L}} \\ B_1 &= \sqrt{\frac{1}{L}}\,\frac{e^{-2iak}(e^{4a\kappa} - 1)(k^2 + \kappa^2)}{-(k - i\kappa)^2 + e^{4ak}(k + i\kappa)^2} \\ A_2 &= \sqrt{\frac{1}{L}}\,\frac{-2e^{a(\kappa - ik)}k(k - i\kappa)}{-(k - i\kappa)^2 + e^{4ak}(k + i\kappa)^2} \\ B_2 &= \sqrt{\frac{1}{L}}\,\frac{2e^{-iak + 3a\kappa}k(k + i\kappa)}{-(k - i\kappa)^2 + e^{4ak}(k + i\kappa)^2} \\ A_3 &= \sqrt{\frac{1}{L}}\,\frac{4ie^{2a(-ik + \kappa)}k\kappa}{-(k - i\kappa)^2 + e^{4ak}(k + i\kappa)^2} \\ &where, \\ k &= \frac{\sqrt{2mE}}{\hbar};\ ;\ \kappa = \frac{\sqrt{2m(V - E)}}{\hbar}; \end{aligned}$$

Now take $\lambda = \frac{V}{E_F}$ to be fixed while taking the RPA limit where $E_F = \frac{1}{2}mv_F^2$ is the Fermi energy. $\xi_0 = 2k_Fa$ is finite $k_F \to \infty$ and the width of the barrier $a \to 0$. Under this limit we obtain the following.

$$\begin{aligned} T &= \frac{A_3}{A_1} = \frac{4ie^{-i\xi_0}\sqrt{\lambda - 1}}{4i\sqrt{\lambda - 1}\cosh[\xi_0\sqrt{(\lambda - 1)}] + 2(2 - \lambda)\sinh[\xi_0\sqrt{(\lambda - 1)}]} \\ R &= \frac{B_1}{A_1} = \frac{e^{-i\xi_0}2\lambda\sinh[\xi_0\sqrt{(\lambda - 1)}]}{4i\sqrt{\lambda - 1}\cosh[\xi_0\sqrt{(\lambda - 1)}] + 2(2 - \lambda)\sinh[\xi_0\sqrt{(\lambda - 1)}]} \end{aligned} \tag{H.7}$$

(f) Finite well scattering

Consider a rectangular barrier of depth V extending from $x = -a$ to $x = a$ with the energy of the particle $E > 0$. The wavefunction is given as follows.

$$\psi_R(x) = \begin{cases} A_1 e^{ikx} + B_1 e^{-ikx} & -L/2 < x < -a \\ A_2 e^{ik'x} + B_2 e^{-ik'x} & -a < x < a \\ A_3 e^{ikx} & a < x < L/2 \end{cases}$$

Using continuity conditions of the wavefunction and its first derivative at points $\pm a$ along with renormalization will yield the following expressions of the coefficients.

$$\begin{aligned} A_1 &= \sqrt{\frac{1}{L}} \\ B_1 &= \sqrt{\frac{1}{L}} \frac{e^{-2iak}(e^{4iak'} - 1)(k^2 - k'^2)}{-(k+k')^2 + e^{4iak'}(k-k')^2} \\ A_2 &= \sqrt{\frac{1}{L}} \frac{-2e^{-ia(k-k')}k(k+k')}{-(k+k')^2 + e^{4iak'}(k-k')^2} \\ B_2 &= \sqrt{\frac{1}{L}} \frac{2e^{-ia(k-3k')}k(k-k')}{-(k+k')^2 + e^{4iak'}(k-k')^2} \\ A_3 &= \sqrt{\frac{1}{L}} \frac{-4e^{-2a(k-k')}kk'}{-(k+k')^2 + e^{4iak'}(k-k')^2} \end{aligned}$$

where,

$$k = \frac{\sqrt{2mE}}{\hbar};\ ;\ k' = \frac{\sqrt{2m(V+E)}}{\hbar};$$

Now take $\lambda = \frac{V}{E_F}$ to be fixed while taking the RPA limit where $E_F = \frac{1}{2}mv_F^2$ is the Fermi energy. $\xi_0 = 2k_F a$ is finite $k_F \to \infty$ and the width of the well $a \to 0$. Under this limit we obtain the following.

$$\begin{aligned} T = \frac{A_3}{A_1} &= \frac{4e^{-i\xi_0}\sqrt{\lambda+1}}{4\sqrt{\lambda+1}\cos\left[\xi_0\sqrt{(\lambda+1)}\right] - 2i(2+\lambda)\sin\left[\xi_0\sqrt{(\lambda+1)}\right]} \\ R = \frac{B_1}{A_1} &= \frac{e^{-i\xi_0}2i\lambda\sin\left[\xi_0\sqrt{(\lambda+1)}\right]}{4\sqrt{\lambda+1}\cos\left[\xi_0\sqrt{(\lambda+1)}\right] - 2i(2+\lambda)\sin\left[\xi_0\sqrt{(\lambda+1)}\right]} \end{aligned} \tag{H.8}$$

भारतीय प्रौद्योगिकी संस्थान गुवाहाटी
Indian Institute of Technology Guwahati

Bibliography

[1] Sin-itiro Tomonaga. Remarks on Bloch's method of sound waves applied to many-fermion problems. *Progress of Theoretical Physics*, 5(4):544–569, 1950.

[2] J M Luttinger. An exactly soluble model of a many-fermion system. *Journal of Mathematical Physics*, 4(9):1154–1162, 1963.

[3] Daniel C Mattis and Elliott H Lieb. Exact solution of a many-fermion system and its associated boson field. *Journal of Mathematical Physics*, 6(2):304–312, 1965.

[4] FDM Haldane. 'Luttinger liquid theory' of one-dimensional quantum fluids. i. properties of the Luttinger model and their extension to the general 1d interacting spinless Fermi gas. *Journal of Physics C: Solid State Physics*, 14(19):2585, 1981.

[5] Thierry Giamarchi. *Quantum physics in one dimension*. Clarendon Oxford, 2004.

[6] Gordon E Moore et al. Progress in digital integrated electronics. In *Electron Devices Meeting*, volume 21, pages 11–13, 1975.

[7] LD Landau. The theory of a Fermi liquid. *Soviet Physics Jetp-Ussr*, 3(6):920–925, 1957.

[8] Gerald D Mahan. *Many-particle physics*. Springer Science & Business Media, 2013.

[9] Girish S Setlur. *Dynamics of Classical and Quantum Fields: An Introduction*. Taylor & Francis, 2013.

[10] KD Schotte and U Schotte. Tomonaga's model and the threshold singularity of x-ray spectra of metals. *Physical Review*, 182(2):479, 1969.

[11] A Luther and I Peschel. Single-particle states, Kohn anomaly, and pairing fluctuations in one dimension. *Physical Review B*, 9(7):2911, 1974.

[12] R Heidenreich, B Schroer, R Seiler, and D Uhlenbrock. The sine-gordon equation and the one-dimensional electron gas. *Physics Letters A*, 54(2):119–122, 1975.

[13] FDM Haldane. Coupling between charge and spin degrees of freedom in the one-dimensional fermi gas with backscattering. *Journal of Physics C: Solid State Physics*, 12(22):4791, 1979.

[14] Hiroyoshi Ishii, Hiromichi Kataura, Hidetsugu Shiozawa, Hideo Yoshioka, Hideo Otsubo, Yasuhiro Takayama, Tsuneaki Miyahara, Shinzo Suzuki, Yohji Achiba, Masashi Nakatake, et al. Direct observation of tomonaga-luttinger-liquid state in carbon nanotubes at low temperatures. *Nature*, 426(6966):540–544, 2003.

[15] OM Auslaender, Amir Yacoby, R De Picciotto, KW Baldwin, LN Pfeiffer, and KW West. Tunneling spectroscopy of the elementary excitations in a one-dimensional wire. *Science*, 295(5556):825–828, 2002.

[16] LI Glazman and AI Larkin. New quantum phase in a one-dimensional josephson array. *Physical review letters*, 79(19):3736, 1997.

[17] Xiao-Gang Wen. Chiral luttinger liquid and the edge excitations in the fractional quantum hall states. *Physical Review B*, 41(18):12838, 1990.

[18] Immanuel Bloch, Jean Dalibard, and Wilhelm Zwerger. Many-body physics with ultracold gases. *Reviews of modern physics*, 80(3):885, 2008.

[19] A Schwartz, M Dressel, G Grüner, V Vescoli, L Degiorgi, and T Giamarchi. On-chain electrodynamics of metallic (tmtsf) 2 x salts: Observation of tomonaga-luttinger liquid response. *Physical Review B*, 58(3):1261, 1998.

[20] Elbio Dagotto. Experiments on ladders reveal a complex interplay between a spin-gapped normal state and superconductivity. *Reports on Progress in Physics*, 62(11): 1525, 1999.

[21] Sidney Coleman. Quantum sine-gordon equation as the massive thirring model. *Physical Review D*, 11(8):2088, 1975.

[22] Daniel C Mattis. New wave-operator identity applied to the study of persistent currents in 1d. *Journal of Mathematical Physics*, 15(5):609–612, 1974.

[23] IE Dzyaloshinskii and AI Larkin. Correlation functions for a one-dimensional fermi system with long-range interaction (tomonaga model). *Sov. Phys. JETP*, 38:202, 1974.

[24] PW Anderson. Anderson, pw, 1970, j. phys. c 3, 2346. *J. Phys. C*, 3:2346, 1970.

[25] Jenõ Solyom and A Zawadoswki. Are the scaling laws for the Kondo problem exact? *Journal of Physics F: Metal Physics*, 4(1):80, 1974.

[26] KB Efetov and AI Larkin. Correlation functions in one-dimensional systems with a strong interaction. *Sov. Phys. JETP*, 42(390):11, 1976.

[27] VJ Emery. Highly conducting one-dimensional solids, 1979.

[28] J Solyom. The fermi gas model of one-dimensional conductors. *Advances in Physics*, 28(2):201–303, 1979.

[29] Erik Verlinde and Herman Verlinde. Chiral bosonization, determinants and the string partition function. *Nuclear Physics B*, 288:357–396, 1987.

[30] DKK Lee and Y Chen. Functional bosonisation of the Tomonaga-Luttinger model. *Journal of Physics A: Mathematical and General*, 21(22):4155, 1988.

[31] CL Kane and Matthew PA Fisher. Transport in a one-channel luttinger liquid. *Physical Review Letters*, 68(8):1220, 1992.

[32] CL Kane and Matthew PA Fisher. Resonant tunneling in an interacting one-dimensional electron gas. *Physical Review B*, 46(11):7268, 1992.

[33] Sebastian Eggert and Ian Affleck. Magnetic impurities in half-integer-spin heisenberg antiferromagnetic chains. *Physical Review B*, 46(17):10866, 1992.

[34] KA Matveev, Dongxiao Yue, and LI Glazman. Tunneling in one-dimensional non-luttinger electron liquid. *Physical Review Letters*, 71(20):3351, 1993.

[35] M Fabrizio and Alexander O Gogolin. Interacting one-dimensional electron gas with open boundaries. *Physical Review B*, 51(24):17827, 1995.

[36] A Leclair, F Lesage, and H Saleur. Exact friedel oscillations in the g= 1/2 Luttinger liquid. *Physical Review B*, 54(19):13597, 1996.

[37] Peter Schmitteckert and Ulrich Eckern. Phase coherence in a random one-dimensional system of interacting fermions: A density-matrix renormalization-group study. *Physical Review B*, 53(23):15397, 1996.

[38] Shaojin Qin, Michele Fabrizio, Lu Yu, Masaki Oshikawa, and Ian Affleck. Impurity in a luttinger liquid away from half-filling: A numerical study. *Physical Review B*, 56(15): 9766, 1997.

[39] A Furusaki. Local perturbation in a tomonaga-luttinger liquid at g= 1/2: Orthogonality catastrophe, fermi-edge singularity, and local density of states. *Physical Review B*, 56 (15):9352, 1997.

[40] Ann E Mattsson, Sebastian Eggert, and Henrik Johannesson. Properties of a luttinger liquid with boundaries at finite temperature and size. *Physical Review B*, 56(24):15615, 1997.

[41] Andrei Komnik, Reinhold Egger, and Alexander O Gogolin. Exact fermi-edge singularity exponent in a luttinger liquid. *Physical Review B*, 56(3):1153, 1997.

[42] Marc Bockrath, David H Cobden, Jia Lu, Andrew G Rinzler, Richard E Smalley, Leon Balents, and Paul L McEuen. Luttinger-liquid behaviour in carbon nanotubes. *Nature*, 397(6720):598–601, 1999.

[43] Victoria Fernández, Kang Li, and Carlos Naón. Bosonic description of a tomonaga-luttinger model with impurities. *Physics Letters B*, 452(1):98–102, 1999.

[44] Yu-Liang Liu. Influence of backward scattering on correlation exponents in a one-dimensional system. *Physical Review B*, 62(2):1212, 2000.

[45] K Schönhammer, V Meden, W Metzner, U Schollwöck, and O Gunnarsson. Boundary effects on one-particle spectra of luttinger liquids. *Physical Review B*, 61(7):4393, 2000.

[46] Victoria I Fernández and Carlos M Naón. Friedel oscillations in a luttinger liquid with long-range interactions. *Physical Review B*, 64(3):033402, 2001.

[47] V Meden, W Metzner, U Schollwöck, and K Schönhammer. Scaling behavior of impurities in mesoscopic luttinger liquids. *Physical Review B*, 65(4):045318, 2002.

[48] MA Cazalilla. Low-energy properties of a one-dimensional system of interacting bosons with boundaries. *EPL (Europhysics Letters)*, 59(6):793, 2002.

[49] V Meden, W Metzner, U Schollwöck, and K Schönhammer. A single impurity in a luttinger liquid: How it cuts the chain. *Journal of low temperature physics*, 126(3-4): 1147–1163, 2002.

[50] V Meden, S Andergassen, W Metzner, U Schollwöck, and K Schönhammer. Scaling of the conductance in a quantum wire. *EPL (Europhysics Letters)*, 64(6):769, 2003.

[51] Fabrizio Anfuso and Sebastian Eggert. Luttinger liquid in a finite one-dimensional wire with box-like boundary conditions. *Physical Review B*, 68(24):241301, 2003.

[52] Tobias Stauber. Tomonaga-luttinger model with an impurity for a weak two-body interaction. *Physical Review B*, 67(20):205107, 2003.

[53] S Andergassen, T Enss, V Meden, W Metzner, U Schollwöck, and K Schönhammer. Functional renormalization group for luttinger liquids with impurities. *Physical Review B*, 70(7):075102, 2004.

[54] Alex Grishin, Igor V Yurkevich, and Igor V Lerner. Functional integral bosonization for an impurity in a luttinger liquid. *Physical Review B*, 69(16):165108, 2004.

[55] Satoshi Nishimoto and Eric Jeckelmann. Density-matrix renormalization group approach to quantum impurity problems. *Journal of Physics: Condensed Matter*, 16(4): 613, 2004.

[56] T Enss, V Meden, S Andergassen, X Barnabé-Thériault, W Metzner, and K Schönhammer. Impurity and correlation effects on transport in one-dimensional quantum wires. *Physical Review B*, 71(15):155401, 2005.

[57] V Meden, T Enss, S Andergassen, W Metzner, and K Schönhammer. Correlation effects on resonant tunneling in one-dimensional quantum wires. *Physical Review B*, 71 (4):041302, 2005.

[58] Kenji Kamide, Yuji Tsukada, and Susumu Kurihara. Scaling of a single impurity potential of arbitrary strength in a Tomonaga-Luttinger liquid. In *LOW TEMPERATURE PHYSICS: 24th International Conference on Low Temperature Physics-LT24*, volume 850, pages 1387–1388. AIP Publishing, 2006.

[59] Riccardo Gezzi, Th Pruschke, and V Meden. Functional renormalization group for nonequilibrium quantum many-body problems. *Physical Review B*, 75(4):045324, 2007.

[60] Severin G Jakobs, Volker Meden, and Herbert Schoeller. Nonequilibrium functional renormalization group for interacting quantum systems. *Physical Review letters*, 99 (15):150603, 2007.

[61] Maxim Trushin and AL Chudnovskiy. Tunneling into strongly biased tomonaga-luttinger liquid. *EPL (Europhysics Letters)*, 82(1):17008, 2008.

[62] Yuji Hamamoto, Ken-Ichiro Imura, and Takeo Kato. Numerical study of transport through a single impurity in a spinful Tomonaga–Luttinger liquid. *Physical Review B*, 77(16):165402, 2008.

[63] Kenji Kamide, Takashi Kimura, and Susumu Kurihara. Luttinger liquid renormalized by a single impurity. In *Journal of Physics: Conference Series*, volume 150, page 022031. IOP Publishing, 2009.

[64] DB Gutman, Yuval Gefen, and AD Mirlin. Bosonization of one-dimensional fermions out of equilibrium. *Physical Review B*, 81(8):085436, 2010.

[65] Alexey Galda, Igor V Yurkevich, and Igor V Lerner. Impurity scattering in Luttinger liquid with electron-phonon coupling. In *Journal of Physics: Conference Series*, volume 286, page 012049. IOP Publishing, 2011.

[66] Adilet Imambekov, Thomas L Schmidt, and Leonid I Glazman. One-dimensional quantum liquids: Beyond the Luttinger liquid paradigm. *Reviews of Modern Physics*, 84(3): 1253, 2012.

[67] AV Rozhkov. One-dimensional fermions with neither luttinger-liquid nor fermi-liquid behavior. *Physical Review letters*, 112(10):106403, 2014.

[68] Alexander Altland, Yuval Gefen, and Bernd Rosenow. Incoherent scatterer in a Luttinger liquid: A new paradigmatic limit. *Physical Review letters*, 108(13):136401, 2012.

[69] A Furusaki and KA Matveev. Theory of strong inelastic cotunneling. *Physical Review B*, 52(23):16676, 1995.

[70] Alexander Altland, Yuval Gefen, and Bernd Rosenow. Intermediate fixed point in a luttinger liquid with elastic and dissipative backscattering. *arXiv preprint arXiv:1503.01312*, 2015.

[71] IV Protopopov, DB Gutman, and AD Mirlin. Equilibration in a chiral Luttinger liquid. *Physical Review B*, 91(19):195110, 2015.

[72] Jan Von Delft and Herbert Schoeller. Bosonization for beginnersrefermionization for experts. *Annalen der Physik*, 7(4):225–305, 1998.

[73] Kenneth G Wilson. Renormalization group and critical phenomena. i. renormalization group and the kadanoff scaling picture. *Physical review B*, 4(9):3174, 1971.

[74] Kenneth G Wilson and John Kogut. The renormalization group and the expansion. *Physics Reports*, 12(2):75–199, 1974.

[75] Heinz J Schulz, Gianaurelio Cuniberti, and Pierbiagio Pieri. Fermi liquids and luttinger liquids. In *Field theories for low-dimensional condensed matter systems*, pages 9–81. Springer, 2000.

[76] Jens Eisert. Entanglement and tensor network states. *arXiv preprint arXiv:1308.3318*, 2013.

[77] Nick Bultinck, Dominic J Williamson, Jutho Haegeman, and Frank Verstraete. Fermionic matrix product states and one-dimensional topological phases. *Physical Review B*, 95(7):075108, 2017.

[78] Matthew B Hastings. Entropy and entanglement in quantum ground states. *Physical Review B*, 76(3):035114, 2007.

[79] Frank Verstraete, Valentin Murg, and J Ignacio Cirac. Matrix product states, projected entangled pair states, and variational renormalization group methods for quantum spin systems. *Advances in Physics*, 57(2):143–224, 2008.

[80] Matthew B Hastings. An area law for one-dimensional quantum systems. *Journal of Statistical Mechanics: Theory and Experiment*, 2007(08):P08024, 2007.

[81] Martin Andersson, Magnus Boman, and Stellan Östlund. Density-matrix renormalization group for a gapless system of free fermions. *Physical Review B*, 59(16):10493, 1999.

[82] Denis Morath, Nicholas Sedlmayr, Jesko Sirker, and Sebastian Eggert. Conductance in inhomogeneous quantum wires: Luttinger liquid predictions and quantum monte carlo results. *Physical Review B*, 94(11):115162, 2016.

[83] Kevin Leung, Reinhold Egger, and CH Mak. Dynamical simulation of transport in one-dimensional quantum wires. *Physical review letters*, 75(18):3344, 1995.

[84] Norio Kawakami and Sung-Kil Yang. Finite-size scaling in one-dimensional quantum liquid with long-range interaction. *Physical Review Letters*, 67(18):2493, 1991.

[85] Shaojin Qin, Michele Fabrizio, and Lu Yu. Impurity in a luttinger liquid: A numerical study of the finite-size energy spectrum and of the orthogonality catastrophe exponent. *Physical Review B*, 54(14):R9643, 1996.

[86] Stanley Mandelstam. Soliton operators for the quantized sine-gordon equation. *Physical Review D*, 11(10):3026, 1975.

[87] Michael Stone. *Bosonization*. World Scientific, 1994.

[88] Eleftherios N Economou. *Green's functions in quantum physics*, volume 3. Springer, 1983.

[89] Richard P Feynman and Albert R Hibbs. Quantum mechanics and path integrals. emended edition, 0. emended and with a preface by daniel f. styer, 2010.

[90] Joy Prakash Das and Girish S Setlur. The quantum steeplechase. *International Journal of Modern Physics A*, 33(29): 1850174, 2018.

[91] Reinhold Egger and Hermann Grabert. Friedel oscillations for interacting fermions in one dimension. *Physical Review Letters*, 75(19):3505, 1995.

[92] P Fendley, AWW Ludwig, and H Saleur. Exact conductance through point contacts in the ν= 1/3 fractional quantum hall effect. *Physical Review Letters*, 74(15):3005, 1995.

[93] P Fendley, AWW Ludwig, and H Saleur. Exact nonequilibrium transport through point contacts in quantum wires and fractional quantum hall devices. *Physical Review B*, 52 (12):8934, 1995.

[94] Akira Furusaki and Naoto Nagaosa. Kondo effect in a Tomonaga-Luttinger liquid. *Physical Review Letters*, 72(6):892, 1994.

[95] Avraham Schiller and Kevin Ingersent. Exact results for the Kondo effect in a luttinger liquid. *Physical Review B*, 51(7):4676, 1995.

[96] Reinhold Egger. Luttinger liquid behavior in carbon nanotubes. In *Advances in Solid State Physics 40*, pages 219–231. Springer, 2000.

[97] OM Auslaender, A Yacoby, R De Picciotto, KW Baldwin, LN Pfeiffer, and KW West. Experimental evidence for resonant tunneling in a luttinger liquid. *Physical Review Letters*, 84(8):1764, 2000.

[98] Joy Prakash Das, Chandramouli Chowdhury, and Girish S Setlur. Friedel oscillations and dynamical density of states of an inhomogeneous luttinger liquid. *arXiv preprint arXiv:1811.08173*, 2018.

[99] MAM De Aguiar. Exact greens function for the step and square-barrier potentials. *Physical Review A*, 48(4):2567, 1993.

[100] Fabiano M Andrade. Exact green's function for rectangular potentials and its application to quasi-bound states. *Physics Letters A*, 378(21):1461–1468, 2014.

[101] Joy Prakash Das, Chandramouli Chowdhury, and Girish S Setlur. Non-chiral bosonization of strongly inhomogeneous luttinger liquids. *Theoretical and Mathematical Physics, Springer*, 199(2):736, 2019.

[102] J Friedel. Metallic alloys. *Il Nuovo Cimento (1955-1965)*, 7:287–311, 1958.

[103] I Tüttö and A Zawadowski. Theory of pinning of a spin-density wave by nonmagnetic impurities. *Physical Review Letters*, 60(14):1442, 1988.

[104] Michele Fabrizio and Alexander O Gogolin. Comment on"enhancement of the tunneling density of states in tomonaga-luttinger liquids". *Physical Review Letters*, 78(23):4527, 1997.

[105] A Yacoby, HL Stormer, KW Baldwin, LN Pfeiffer, and KW West. Magneto-transport spectroscopy on a quantum wire. *Solid State Communications*, 101(1):77–81, 1997.

[106] Akira Furusaki and Naoto Nagaosa. Resonant tunneling in a luttinger liquid. *Physical Review B*, 47(7):3827, 1993.

[107] T Giamarchi and AJ Millis. Conductivity of a luttinger liquid. *Physical Review B*, 46 (15):9325, 1992.

[108] Masao Ogata and Hidetoshi Fukuyama. Collapse of quantized conductance in a dirty tomonaga-luttinger liquid. *Physical Review Letters*, 73(3):468, 1994.

[109] Ines Safi. Conductance of a quantum wire: Landauer's approach versus the kubo formula. *Physical Review-Section B-Condensed Matter*, 55(12):7331–7334, 1997.

[110] VV Ponomarenko. Renormalization of the one-dimensional conductance in the luttinger-liquid model. *Physical Review B*, 52(12):R8666, 1995.

[111] W Apel and TM Rice. Combined effect of disorder and interaction on the conductance of a one-dimensional fermion system. *Physical Review B*, 26(12):7063, 1982.

[112] Dmitrii L Maslov and Michael Stone. Landauer conductance of Luttinger liquids with leads. *Physical Review B*, 52(8):R5539, 1995.

[113] Masao Ogata and PW Anderson. Transport properties in the Tomonaga-Luttinger liquid. *Physical Review Letters*, 70(20):3087, 1993.

[114] CL Kane and Matthew PA Fisher. Transmission through barriers and resonant tunneling in an interacting one-dimensional electron gas. *Physical Review B*, 46(23):15233, 1992.

[115] K Moon, H Yi, CL Kane, SM Girvin, and Matthew PA Fisher. Resonant tunneling between quantum hall edge states. *Physical Review Letters*, 71(26):4381, 1993.

[116] A Furusaki. Resonant tunneling through a quantum dot weakly coupled to quantum wires or quantum hall edge states. *Physical Review B*, 57(12):7141, 1998.

[117] A Anthore, Z Iftikhar, E Boulat, FD Parmentier, A Cavanna, A Ouerghi, U Gennser, and F Pierre. Circuit quantum simulation of a Tomonaga-Luttinger liquid with an impurity. *Physical Review X*, 8(3):031075, 2018.

[118] Pavel P Aseev, Daniel Loss, and Jelena Klinovaja. Conductance of fractional luttinger liquids at finite temperatures. *Physical Review B*, 98(4):045416, 2018.

[119] Alex Levchenko, Tobias Micklitz, Jérôme Rech, and KA Matveev. Transport in partially equilibrated inhomogeneous quantum wires. *Physical Review B*, 82(11):115413, 2010.

[120] A Furusaki. A. furusaki and n. nagaosa, phys. rev. b 47, 4631 (1993). *Phys. Rev. B*, 47: 4631, 1993.

[121] T Giamarchi. T. giamarchi and hj schulz, phys. rev. b 37, 325 (1988). *Phys. Rev. B*, 37:325, 1988.

[122] CL Kane and Matthew PA Fisher. Thermal transport in a Luttinger liquid. *Physical review letters*, 76(17):3192, 1996.

[123] IV Krive. Thermal transport through Luttinger liquid constriction. *Low Temperature Physics*, 24(5):377–379, 1998.

[124] Wade DeGottardi and KA Matveev. Electrical and thermal transport in inhomogeneous Luttinger liquids. *Physical Review Letters*, 114(23):236405, 2015.

[125] Leon Balents and Reinhold Egger. Spin-dependent transport in a luttinger liquid. *Physical Review B*, 64(3):035310, 2001.

[126] VV Ponomarenko. Frequency dependences in transport through a tomonaga-luttinger liquid wire. *Physical Review B*, 54(15):10328, 1996.

[127] Joy Prakash Das and Girish S Setlur. Transport properties of a Luttinger liquid with a cluster of impurities. *Physica E: Low-dimensional Systems and Nanostructures*, 110 : 39, 2019.

[128] Joy Prakash Das and Girish S Setlur. Conductance of inhomogeneous Luttinger liquids with a finite bandwidth. *Physics Letters A* 383 (25): 3149, 2019.

[129] Zhi Xiao, Shi-sen Du, and Chun-Xi Zhang. Revisiting 1-dimensional double-barrier tunneling in quantum mechanics. *arXiv preprint arXiv:1210.0970*, 2012.

[130] RM Noack, SR White, and DJ Scalapino. Correlations in a two-chain hubbard model. *Physical review letters*, 73(6):882, 1994.

[131] D. Poilblanc, D. J. Scalapino, and W. Hanke. Spin and charge modes of the t-j ladder. *Phys. Rev. B*, 52:6796–6800, Sep 1995. doi: 10.1103/PhysRevB.52.6796. URL http://link.aps.org/doi/10.1103/PhysRevB.52.6796.

[132] A. M. Finkel'stein and A. I. Larkin. Two coupled chains with tomonaga-luttinger interactions. *Phys. Rev. B*, 47:10461–10473, Apr 1993. doi: 10.1103/PhysRevB.47.10461. URL http://link.aps.org/doi/10.1103/PhysRevB.47.10461.

[133] M. Fabrizio, A. Parola, and E. Tosatti. Strong-coupling phases of two hubbard chains with interchain hopping. *Phys. Rev. B*, 46:3159–3162, Aug 1992. doi: 10.1103/PhysRevB.46.3159. URL http://link.aps.org/doi/10.1103/PhysRevB.46.3159.

[134] D. V. Khveshchenko and T. M. Rice. Spin-gap fixed points in the double-chain problem. *Phys. Rev. B*, 50:252–257, Jul 1994. doi: 10.1103/PhysRevB.50.252. URL http://link.aps.org/doi/10.1103/PhysRevB.50.252.

[135] Leon Balents and Matthew P. A. Fisher. Weak-coupling phase diagram of the two-chain hubbard model. *Phys. Rev. B*, 53:12133–12141, May 1996. doi: 10.1103/PhysRevB.53.12133. URL http://link.aps.org/doi/10.1103/PhysRevB.53.12133.

[136] HJ Schulz. Phases of two coupled luttinger liquids. *Physical Review B*, 53(6):R2959, 1996.

[137] Patrick Gagliardini, Stephan Haas, and TM Rice. Generalization of the luttinger theorem for fermionic ladder systems. *Physical Review B*, 58(15):9603, 1998.

[138] David G Clarke, SP Strong, and PW Anderson. Incoherence of single particle hopping between luttinger liquids. *Physical review letters*, 72(20):3218, 1994.

[139] Sourin Das and Vadim Shpitalnik. Quantum pump for fractional charge. *EPL (Europhysics Letters)*, 83(1):17004, 2008.

[140] Joy Prakash Das and Girish S Setlur. The one step fermionic ladder. *Physica E: Low-dimensional Systems and Nanostructures*, 94: 216–230, 2017.

[141] Gordon Baym and C Ebner. Phonon-quasiparticle interactions in dilute solutions of he 3 in superfluid he 4: I. phonon thermal conductivity and ultrasonic attenuation. *Physical Review*, 164(1):235, 1967.

[142] NV Prokof'ev. Effective masses of ions in superfluid 3 He-b. *Physical review letters*, 74 (14):2748, 1995.

[143] NV Prokofev. Diffusion of a heavy particle in a Fermi-liquid theory. *International Journal of Modern Physics B*, 7(19):3327–3351, 1993.

[144] AH Castro Neto and Matthew PA Fisher. Dynamics of a heavy particle in a Luttinger liquid. *Physical Review B*, 53(15):9713, 1996.

[145] AO Caldeira and AH Castro Neto. Motion of heavy particles coupled to fermionic and bosonic environments in one dimension. *Physical Review B*, 52(6):4198, 1995.

[146] Yasumasa Tsukamoto, Tatsuya Fujii, and Norio Kawakami. Critical behavior of Tomonaga-Luttinger liquids with a mobile impurity. *Physical Review B*, 58(7):3633, 1998.

[147] Takeshi Fukuhara, Adrian Kantian, Manuel Endres, Marc Cheneau, Peter Schauß, Sebastian Hild, David Bellem, Ulrich Schollwöck, Thierry Giamarchi, Christian Gross, et al. Quantum dynamics of a mobile spin impurity. *Nature Physics*, 9(4):235, 2013.

[148] GE Astrakharchik and LP Pitaevskii. Motion of a heavy impurity through a bose-einstein condensate. *Physical Review A*, 70(1):013608, 2004.

[149] Charles JM Mathy, Mikhail B Zvonarev, and Eugene Demler. Quantum flutter of supersonic particles in one-dimensional quantum liquids. *arXiv preprint arXiv:1203.4819*, 2012.

[150] MD Girardeau and A Minguzzi. Motion of an impurity particle in an ultracold quasi-one-dimensional gas of hard-core bosons. *Physical Review A*, 79(3):033610, 2009.

[151] Michael Schecter, DM Gangardt, and Alex Kamenev. Dynamics and bloch oscillations of mobile impurities in one-dimensional quantum liquids. *Annals of Physics*, 327(3): 639–670, 2012.

[152] Oleg Lychkovskiy. Perpetual motion of a mobile impurity in a one-dimensional quantum gas. *Physical Review A*, 89(3):033619, 2014.

[153] Oleg Lychkovskiy. Perpetual motion and driven dynamics of a mobile impurity in a quantum fluid. *Physical Review A*, 91(4):040101, 2015.

[154] Joy Prakash Das and Girish S Setlur. Ponderous impurities in a Luttinger liquid. *EPL (Europhysics Letters)*, 123(2):27002, 2018.

[155] AH Castro Neto and AO Caldeira. Mobility and diffusion of a particle coupled to a luttinger liquid. *Physical Review B*, 50(7):4863, 1994.

[156] Freeman J Dyson. The s matrix in quantum electrodynamics. *Physical Review*, 75(11): 1736, 1949.

[157] Julian Schwinger. On the greens functions of quantized fields. i. *Proceedings of the National Academy of Sciences*, 37(7):452–455, 1951.

[158] Hans Carsten Fogedby. Correlation functions for the tomonaga model. *Journal of Physics C: Solid State Physics*, 9(20):3757, 1976.

[159] Igor V Lerner, Boris L Althsuler, Vladimir I Fal'ko, and Thierry Giamarchi. *Strongly Correlated Fermions and Bosons in Low-Dimensional Disordered Systems*, volume 72. Springer Science & Business Media, 2002.

[160] Ulrich Schollwöck. The density-matrix renormalization group. *Reviews of modern physics*, 77(1):259, 2005.

[161] Osor Slaven Barišić and Peter Prelovšek. Conductivity in a disordered one-dimensional system of interacting fermions. *Physical Review B*, 82(16):161106, 2010.

[162] IL Aleiner, BL Altshuler, and GV Shlyapnikov. A finite-temperature phase transition for disordered weakly interacting bosons in one dimension. *Nature Physics*, 6(11):900, 2010.

[163] Alexander Croy, Philipp Cain, and Michael Schreiber. Anderson localization in 1d systems with correlated disorder. *The European Physical Journal B*, 82(2):107, 2011.

[164] Ian Mondragon-Shem, Mayukh Khan, and Taylor L Hughes. Characterizing disordered fermion systems using the momentum-space entanglement spectrum. *Physical review letters*, 110(4):046806, 2013.

[165] Richard Berkovits. Entanglement properties and quantum phases for a fermionic disordered one-dimensional wire with attractive interactions. *Physical review letters*, 115 (20):206401, 2015.

List of publications

Journal publications:

1. **Joy Prakash Das** and Girish S. Setlur, 'The quantum steeplechase', *International Journal of Modern Physics A*, 33.29, 1850174, **doi**: 10.1142/S0217751X18501749 (2018).
2. **Joy Prakash Das** and Girish S. Setlur, 'The one step fermionic ladder', *Physica E*, 94, 216-230, **doi**: 10.1016/j.physe.2017.07.022 (2017)
3. **Joy Prakash Das** and Girish S. Setlur, 'Ponderous impurities in a Luttinger liquid', *Europhysics letters* , 123.2, 27002, **doi** : 10.1209/0295-5075/123/27002 (2018)
4. **Joy Prakash Das** and Girish S. Setlur, 'Transport properties of a Luttinger liquid with a cluster of impurities', *Physica E*, 110, 39-48, **doi**: 10.1016/j.physe.2019.02.003 (2019)
5. **Joy Prakash Das**, Chandramouli Chowdhury and Girish S. Setlur, 'Non-chiral bosonization of strongly inhomogeneous Luttinger liquids', *Theoretical and Mathematical Physics, Springer*, 199.2, 736-760, **doi**: 10.1134/S0040577919050106 (2019)
6. **Joy Prakash Das** and Girish S. Setlur, 'Conductance of inhomogeneous Luttinger liquids with a finite bandwidth', *Physics Letters A*, 383.25, 3149-3161, **doi**: 10.1016/j.physleta.2019.06.049 (2019)
7. **Joy Prakash Das**, Chandramouli Chowdhury and Girish S. Setlur, 'Friedel oscillations and dynamical density of states of an inhomogeneous Luttinger liquid', *arXiv : 1811.08173* (communicated).

Conferences attended

1. Delivered a talk on the topic "**Effect of impurities on 1D nanostructures**" at the national conference on Nanomaterials Science, Technology and Applications (NAMASTA-2017) held at Dibrugarh University.
2. Presented a poster entitled "**Conductance of inhomogeneous nanowires**" at 5th International Conference on Advanced Nanomaterials and Nanotechnology (ICANN-2017) held at IIT Guwahati and received best poster award.
3. Presented a poster entitled "**The quantum steeplechase**" at PRL conference on condensed matter physics (PRLCCMP) held at Physical Research Laboratory, Ahmedabad during March, 2018.
4. Presented a poster entitled "**The quantum steeplechase**" at the international conference on Recent trends in cold and ultra-cold matter held at IIT Guwahati during March, 2018.
5. Delivered a talk on the topic "**Non chiral bosonization of a Luttinger liquid**" at the National Conference on Hard and Soft Condensed Matter Physics (NCHSCMP-2019) held at Tezpur University and received the best oral presentation award.

Curriculum vitae

Education

2014 - 2019 Ph.D in Physics, IIT Guwahati.
Advisor: Prof. Girish S. Seltur
Thesis title: Non chiral bosonization of a Luttinger liquid.

2019 - 2013 B. Tech in Engineering Physics, IIT Guwahati.
CGPI: 8.65 (Institute silver medalist)

2007 - 2009 Higher secondary, Salt Brook Academy, Dibrugarh.
Percentage: 90.2 (3^{rd} in Assam state board)

2007 High school, Don Bosco school, Dibrugarh.
Percentage: 88.2 (20^{th} in Assam state board)

Academic achievements

2014 CSIR NET (JRF) in Physics.
All India Rank: 89.

2017 CSIR NET (JRF) in Mathematics.
All India Rank: 235.

2015 GATE in Physics.
All India Rank: 112.

2016 GATE in Mathematics.
All India Rank: 91.

2013 GATE in Electronics and communication engineering.
All India Rank: 12450.

2017 Best poster award.
Poster title: Conductance of inhomogeneous nanowires.
Conference: ICANN, IIT Guwahati.

2017 Institute best poster award.
Poster title: The quantum steeplechase.
Conference: Research conclave, IIT Guwahati.

2017 Second best poster award.
Poster title: Escape the quantum maze.
Ocassion: SERB school, IIT Guwahati.

2019 Best oral presentation award.
Title: Non chiral bosonization of a Luttinger liquid.
Ocassion: NCHSCMP, Tezpur University.

2019 Second best oral presentation award.
Title: Non chiral bosonization of a Luttinger liquid.
Ocassion: Research conclave, IIT Guwahati.

2019 Best '3 minute thesis presentation' award.
Thesis title: Non chiral bosonization of a Luttinger liquid.
Ocassion: Research conclave, IIT Guwahati.

Teaching assistantship

2015 General Physics laboratory for M.Sc. students.

2015 Digital electronics laboratory for B.Tech. students.

2016 Basic Physics laboratory for B.Tech. students.

2016 Advanced Physics laboratory for B. Tech. students.

2017 Advanced Physics laboratory for M.Sc. students.

2017 Analog+Digital laboratory for M.Sc. students.

2018 Computing laboratory for Ph.D. students.

भारतीय प्रौद्योगिकी संस्थान गुवाहाटी
Indian Institute of Technology Guwahati